Biogenesis of mitochondrial ATP synthase and its dysfunction leading to diseases

Anna Magdalena Kabala

université de BORDEAUX

INSTITUTE OF BIOCHEMISTRY AND BIOPHYSICS POLISH ACADEMY OF SCIENCES

THÈSE EN COTUTELLE PRÉSENTÉE

POUR OBTENIR LE GRADE DE

DOCTEUR DE

L'UNIVERSITÉ DE BORDEAUX

ET DE L'ACADEMIE POLONAISE DES SCIENCES

ÉCOLE DOCTORALE DE SCIENCES DE LA VIE ET DE LA SANTE, BORDEAUX

ÉCOLE DE BIOLOGIE MOLECULAIRE DU IBB, VARSOVIE

SPÉCIALITÉ BIOCHIMIE

Par

Anna Magdalena KABALA

Biogenesis of mitochondrial ATP synthase and its dysfunction leading to diseases

Sous la direction de Jean-Paul di RAGO et Róża KUCHARCZYK

Soutenue le 18 décembre 2014

Membres du jury :

M. WYSOCKI Robert, Professeur, University of Wrocław	rapporteur
Mme SZCZEPANOWSKA Joanna, PhD, Nencki Institut of Experimental Biology	rapporteur
M. BECKER Hubert, Directeur de recherche CNRS, Université de Strasbourg	rapporteur
M. CHOQUET Yves, Directeur de recherche CNRS, IBPC Paris	rapporteur
M. di RAGO Jean-Paul, Directeur de recherche CNRS, IBGC Bordeaux	co-directeur de thèse
Mme KUCHARCZYK Róża, PhD, IBB Varsovie	co-directrice de thèse

COTUTELLE THESIS PRESENTED TO
OBTAIN THE DEGREE OF

DOCTOR OF

UNIVERSITY OF BORDEAUX
AND POLISH ACADEMY OF SCIENCES

ÉCOLE DOCTORALE DE SCIENCES DE LA VIE ET DE LA SANTE, BORDEAUX
SCHOOL OF MOLECULAR BIOLOGY, IBB WARSAW
SPECIALTY BIOCHEMISTRY

By

Anna Magdalena KABALA

Biogenesis of mitochondrial ATP synthase and its dysfunction leading to diseases

Under direction of Jean-Paul di RAGO and Róża KUCHARCZYK

Defended on 18th of December 2014

Members of commission:

M. WYSOCKI Robert, Professor, University of Wrocław	reviewer
Mme SZCZEPANOWSKA Joanna, PhD, Nencki Institut of Experimental Biology	reviewer
M. BECKER Hubert, Director of research CNRS, University of Strasbourg	reviewer
M. CHOQUET Yves, Director of research CNRS, IBPC Paris	reviewer
M. di RAGO Jean-Paul, Director of research CNRS, IBGC Bordeaux	co-director of thesis
Mme KUCHARCZYK Róża, PhD, IBB Warsaw	co-director of thesis

Biogenese de l'ATP synthase mitochondriale et des dysfonctions générant des maladies

La F_1F_O-ATP synthase mitochondriale produit la majorité de l'énergie cellulaire chez les eucaryotes aérobes sous forme d'ATP par le processus des oxydations phosphorylantes. Chez la plupart des espèces, cette enzyme possède une origine génétique double, nucléaire et mitochondriale. Dans la première partie de ce travail, je décris la construction de modèles de levure de mutations du gène mitochondrial *ATP6* de l'ATP synthase découvertes chez des patients atteints de maladies neurologiques (9185T>C and 9191T>C) ou dans des tumeurs (8716A>G, 8914C>A, 8932C>T, 8953A>G and 9131T>C). Le gène *ATP6* code une sous-unité essentielle (a/6) du domaine F_O de l'ATP synthase. J'ai trouvé que la mutation 9185T>C n'affecte pas l'assemblage de l'ATP synthase, mais conduit à une diminution de la vitesse de synthèse d'ATP d'environ 30%. La mutation 9191T>C empêche presque entièrement l'incorporation de la sous-unité a/6 dans l'ATP synthase. Les cinq mutations identifiées dans les tumeurs ont un effet modeste à nul, indiquant que ces mutations ne favorisent pas la tumorigenèse en affectant le processus énergétique mitochondrial, comme évoqué précédemment. J'ai ensuite étudié la régulation de la synthèse des sous-unités a/6 et 9 dans les mitochondries de levures. La sous-unité 9 est présente sous la forme d'un anneau de 10 copies qui interagit avec la sous-unité 6. Durant la catalyse, la rotation de cet anneau provoque des changements conformationnels favorisant la synthèse d'ATP dans le secteur F_1 de l'ATP synthase. Je montre que la synthèse de ces protéines est couplée à leur assemblage, de manière à ce qu'elles soient produites dans une stœchiométrie adéquate et pour éviter l'accumulation d'intermédiaires d'ATP synthase potentiellement délétères

Mots clés : ATP synthase, syndrome NARP, cancer, biogenese de l'ATP synthase

---

CNRS- UMR5095-IBGC, Institut de Biochimie et Génétique Cellulaires,

1, rue Camille Saint Saëns, CS 61390, 33077 Bordeaux cedex, France

Institute of Biochemistry and Biophysics, Polish Academy of Sciences,

ul. Pawińskiego 5a, 02-106 Warsaw, Poland

Biogenesis of mitochondrial ATP synthase and its dysfunction leading to diseases

Mitochondrial F_1F_O-ATP synthase produces most of the cellular energy in aerobic eukaryotes under the form of ATP in the process of oxidative phosphorylation. This enzyme has in most species a double genetic origin, nuclear and mitochondrial. In the first part of this work, I describe the construction of yeast models of ATP synthase mutations in the mitochondrial *ATP6* gene, that have been found in patients presenting with neurological disorders (9185T>C and 9191T>C) and in tumors (8716A>G, 8914C>A, 8932C>T, 8953A>G and 9131T>C). The *ATP6* gene encodes an essential subunit (called a/6) of the ATP synthase proton-translocating domain (F_O). The 9185T>C mutation had no effect on the assembly of ATP synthase, but reduces the rate of ATP synthesis by 30%. The 9191T>C mutation almost completely prevented incorporation of the subunit a/6 into the ATP synthase. The five mutations found in tumors had modest, if at all, effect, indicating that these mutations probably do not favor tumorigenesis, as was hypothesized. In the second part of my thesis, I studied the regulation of synthesis of subunits a/6 and 9 in yeast mitochondria. The subunit 9 is present in 10 copies forming a ring that interacts with subunit 6. Proton movements through the F_O induce the rotation of the subunit 9-ring, which results in conformational changes that promote ATP synthesis in the catalytic sector (F_1) of ATP synthase. I discovered mechanisms that enable the coupling of the synthesis of these proteins to their assembly, as a means to ensure the production of subunits 6 and 9 in the right stoichiometry and to avoid accumulation of potentially harmful assembly intermediates of the ATP synthase.

Keywords: ATP synthase, NARP syndrome, cancer, biogenesis of ATP synthase

---

CNRS- UMR5095-IBGC, **Institut de Biochimie et Génétique Cellulaires**,

1, rue Camille Saint Saëns, CS 61390, 33077 Bordeaux cedex, France

Institute of Biochemistry and Biophysics, Polish Academy of Sciences,

ul. Pawińskiego 5a, 02-106 Warsaw, Poland

CONTENTS

ABREVIATIONS

aa – amino acids

ADP – adenosine diphosphate

APS – ammonium persulfate

ATP – adenosine triphosphate

BN-PAGE – blue native polyacrylamide gel electrophoresis

CCCP – carbonyl cyanide *m*-chlorophenyl hydrazone

CH – chlorhexidine

$\Delta\Psi$ – membrane potential

DHLA – dihydrolipoic acid

DNA – deoxyribonucleic acid

dNTP – deoxyribonucleotide

DOX – doxycycline

DTT – dithiothreitol

EDTA – ethylenediaminetetraacetic acid

EGTA – ethylene glycol tetraacetic acid

EtBr – ethidium bromide

IM – inner membrane

IMS – intermembrane space

KCN – potassium cyanide

LB – Lysogeny broth

m/v – mass to volume

min – minutes

MOPS – 3-(N-morpholino)propanesulfonic acid

mtDNA – mitochondria deoxyribonucleic acid

NaOH – sodium hydroxide

nDNA – nuclear DNA

NADH – nicotinamide adenine dinucleotide

NARP - neurogenic myopathy, ataxia, retinitis pigmentosa

NH_3Ac – ammonium acetate

OA – oleate

OM – outer membrane

o/n – over night

ORF – open reading frame

PCR – polymerase chain reaction

Pi – inorganic phosphorus

PIPES – piperazine-N,N'-bis(2-ethanesulfonic acid)

ROS – reactive oxygen species

RT – room temperature

SDS – sodium dodecyl sulfate

SDS-PAGE – SDS polyakrylamide gel electrophoresis

sec – seconds

TMPD - N,N,N',N'-tetramethyl-p-phenylenediamine

TCA – trichloroacetic acid

TIM – translocase of the inner membrane

TOM – translocase of the outer membrane

UTR – untranslated region

v/v – volume to volume

WT – wild type

INTRODUCTION

I.1 MITOCHONDRIA

Mitochondria (gr. *mitos* – thread, gr. *chondros* – grain) were described as ubiquitous cytoplasmic structures in 1890 by Altmann. He compared them to bacteria living inside the cell and designated "bioblasts". Investigations of the next century showed that mitochondria are semi-autonomous organelles surrounded with two membranes. They contain their own genome (mitochondrial DNA, mtDNA) which is expressed in the organelle. Mitochondria were shown to contain respiratory chain complexes, the enzymes of the citric acid cycle, fatty acid oxidation and oxidative phosphorylation (Ernster and Schatz 1981). In 1967 Peter Mitchell published his chemiosmotic hypothesis of oxidative phosphorylation (Mitchell 1961; Mitchell 1967a; Mitchell and Moyle 1967b) which brought him a Nobel Prize in 1978. The second Nobel Prize in the mitochondrial area was awarded in 1997 to Paul D. Boyer and John E. Walker for revealing the functioning of F_1F_O-ATP synthase.

The first comparison of mitochondria to bacteria by Altmann was not completely wrong. In 1970 this hypothesis was revived by Lynn Margulis and now we know that mitochondria have originated from once free-living α-proteobacteria from the Rickettsiales order (Gray 2012). Nowadays there are two hypothesis (Fig. 1) describing eukaryogenesis, *i.e.* evolution of eukaryotic cell containing mitochondria (Koonin 2010). The first one, "the archezoan scenario", assumed that an α-proteobacterium was engulfed by a primitive amitochondrial eukaryote called archezoan. In the second one, "the symbiogenesis scenario", an archeal cell took up an α-proteobacterium which resulted in generation of the mitochondria followed by appearance of the nucleus and other components of the cell (Koonin 2010; Gray 2012). For the time being, both hypotheses seem possible.

I.1.1 Mitochondrial structure, morphology and inheritance

Mitochondria are bounded with two membranes. OM (for outer membrane) and IM (for inner membrane). The region between them is referred to as intermembrane space (IMS) (Fig. 2) (Fritz, Rapaport et al. 2001; Logan 2006). The OM is permeable for molecules of the size smaller than 5kDa that can pass easily through a pore channel called the porine and containing a protein importing complex (TOM – Translocase of the Outer Membrane) (Becker, Bottinger et al. 2012; Harbauer, Zahedi et al. 2014)

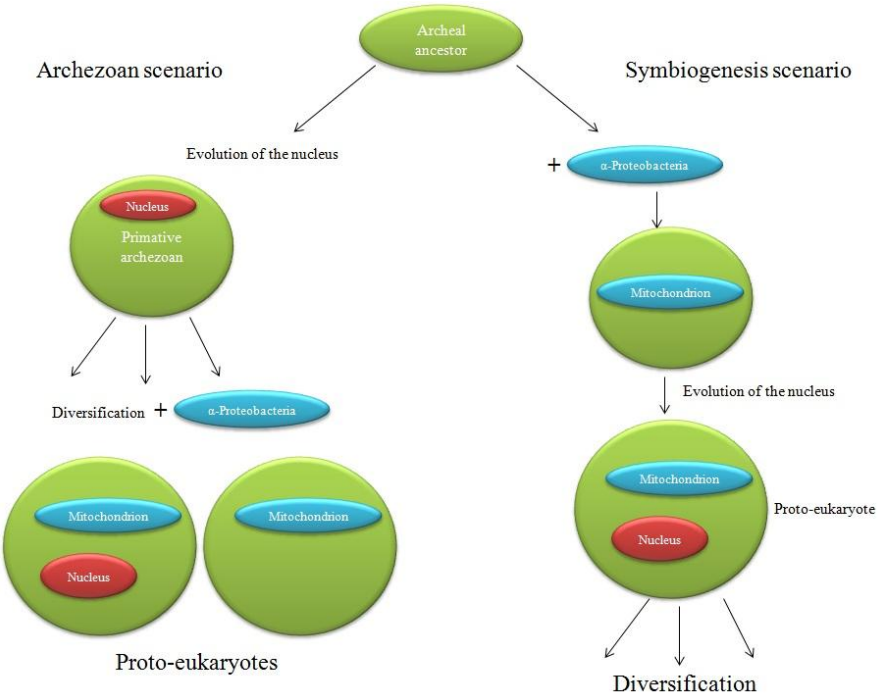

Figure 1 - Two alternatives scenarios of eukaryogenesis. A schema based on Koonin (Koonin 2010).

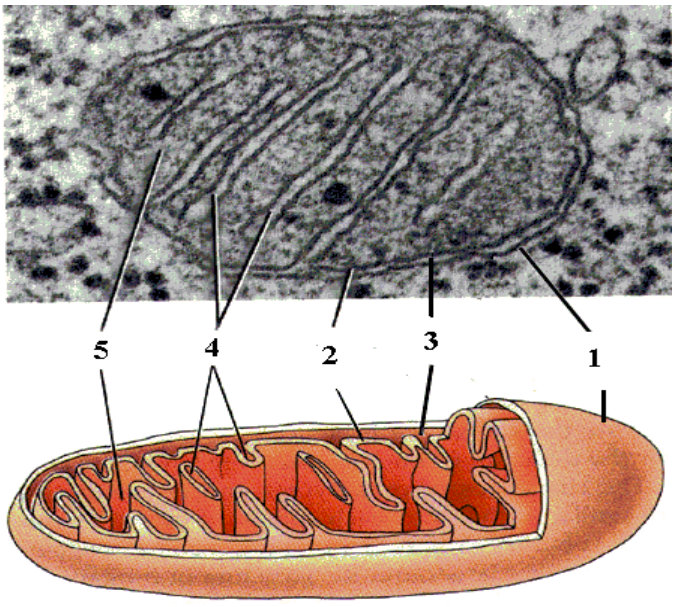

Figure 2 – Structure of a mitochondrion. 1 – outer mitochondrial membrane, 2 – inner mitochondrial membrane, 3 – intermembrane space, 4 - mitochondrial *cristae*, 5 – mitochondria matrix (image from: http://microbewiki.kenyon.edu/images/7/7b/Mito_pic_diagram.gif).

The IM separates mitochondrial matrix from intermembrane space and is largely impermeable. It contains various transporters for metabolites referred to as MCF (Mitochondrial Carrier Family) and protein translocases (TIM – translocase of the inner membrane) (Becker, Bottinger et al. 2012; Harbauer, Zahedi et al. 2014). It is built from about 75% of proteins and 25% of lipids and is enriched with cardiolipin. Its surface is much larger than that of outer membrane because it forms cavities into matrix called *cristae*. The IM contains the complexes of respiratory chain and ATP synthase.

The mitochondrial matrix is an aqueous compartment with high density of proteins (about 270 to 560g/l (Partikian, Olveczky et al. 1998)). It contains particles of mtDNA, proteins needed for its expression and many enzymes participating in metabolic reactions.

Mitochondrial morphology varies between cell types and is dependent on the physiological state of the cell. Mitochondria can be elongated and form a network as the endoplasmic reticulum like in HeLa cells or be more granular like in hepatocytes (Fig. 3A) (Collins, Berridge et al. 2002). They are also very dynamic structures. They move constantly throughout the cytoplasm along actin filaments, change their number, size and shape due to fusion and fission processes (Okamoto and Shaw 2005; Scheffler 2008). In yeast *Saccharomyces cerevisiae* mitochondria form a branched tubular network (Fig. 3B and C) (Okamoto and Shaw 2005) which is constantly changing in response to cellular needs. On a fermentable carbon source yeast cells contain a relatively small number of mitochondria but the network becomes much larger when moved to a non-fermentable carbon source (Westermann 2010). In fission yeast mutants mitochondria form a big tubular network, while in the fusion yeast mutants they are fragmented (Fig. 3C). The processes of fusion and fission play a role in inheritance of mitochondria as they cannot be synthesized *de novo*. Fission occurs before transmission of the mitochondria from the mother to the daughter cell during cell division. In *Saccharomyces cerevisiae* the mitochondria are transported along actin cables to the bud and immobilized there until the end of the bud formation (Fagarasanu and Rachubinski 2007; Westermann 2010). In animals and plants they are transmitted maternally (Logan 2006). The imbalance between fusion and fission may disrupt proper inheritance of mitochondria and mtDNA, and result in development of mitochondrial diseases (Okamoto and Shaw 2005; Westermann 2010; Zhao, Lendahl et al. 2013).

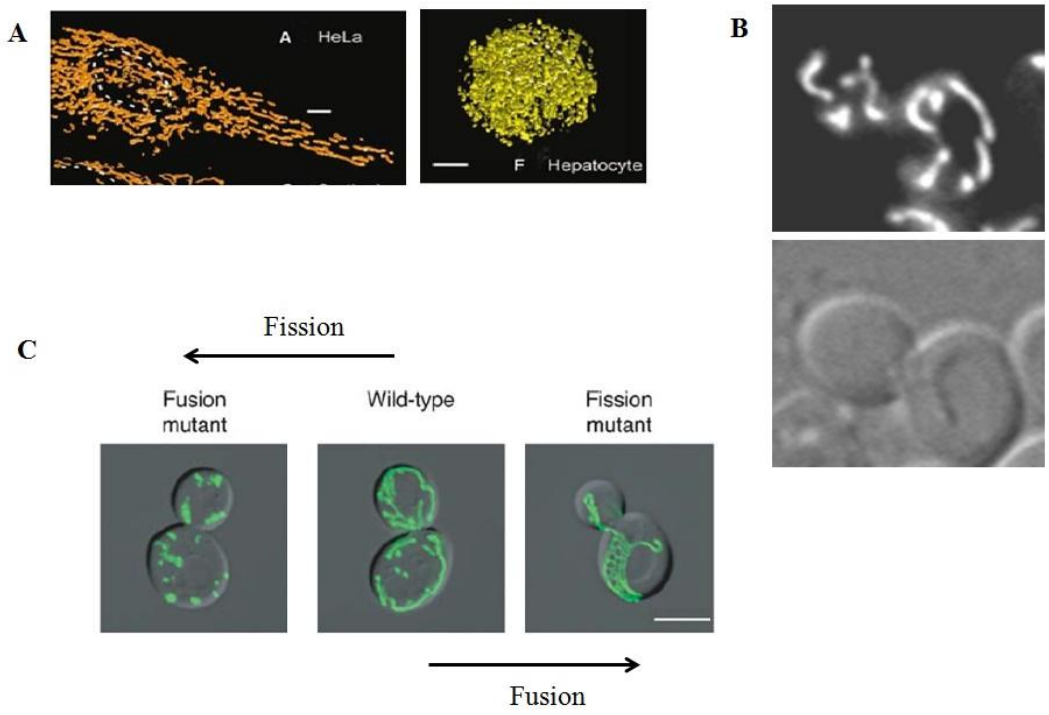

Figure 3 – Mitochondrial morphology, structure and dynamics. A: Three-dimensional reconstructions of cells expressing mito-DsRed1. The dashed circles indicate the position of nuclei. Scale bars, 5µm. Based on (Collins, Berridge et al. 2002). **B:** Mitochondrial network visualized by matrix-targeted GFP in MR6 strain grown on galactose (this work). **C:** Wild-type and mutant cells defective in fusion (*fzo1Δ*) and fission (*dnm1Δ*). Mitochondria are visualized by matrix-targeted GFP. Bar, 5µm. Based on (Okamoto and Shaw 2005).

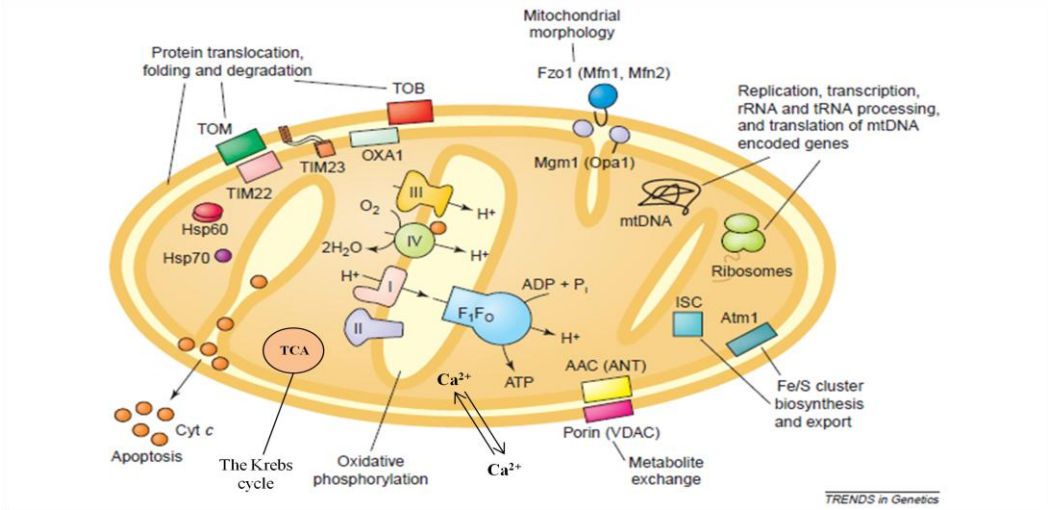

Figure 4 – Functions of mitochondria. A schema representing example proteins with various mitochondrial functions. The processes of: heme synthesis, β-oxidation of fatty acids, the urea cycle, synthesis of amino acids, biosynthesis of lipids and steroidogenesis are not shown. Based on (Reichert and Neupert 2004)

I.1.2 Functions of mitochondria

Many metabolic pathways indispensable for cell life occur in mitochondria (Fig. 4). One of the most important metabolic pathway is the production of cellular energy in the form of ATP by oxidative phosphorylation (the process is described in details later). Mitochondria are the place of β-oxidation of fatty acids where acetyl-CoA is generated. It furnishes the tricarboxylic acid cycle (TCA, known also as the citric acid cycle or the Krebs cycle) where the precursors of other metabolic pathways, such as amino acids or heme synthesis, are produced. Heme synthesis, a part of the urea cycle, biosynthesis of lipids (for example cardiolipin) and steroidogenesis also take place in mitochondria. Another very important metabolic pathway that occurs in mitochondria is the synthesis of iron sulfur centers that serve in such process as electron transfer, redox reactions and iron homeostasis (Scheffler 2008; Galluzzi, Kepp et al. 2012). Mitochondria, together with the endoplasmic reticulum, participate in calcium storage and homeostasis (Pozzan, Magalhaes et al. 2000; Nicholls and Chalmers 2004). They were also shown to trigger the intrinsic pathway of programmed cell death (Galluzzi, Kepp et al. 2012).

I.1.3 The mitochondrial genome

The size of mitochondrial DNA (mtDNA) varies between metazoans, plants and fungi but genetic information is similar for most of them. Human mtDNA is about 16.5 kb. It encodes 2 ribosomal RNAs, 22 tRNAs, 7 subunits of complex I (ND1-6, ND4L), 1 subunit of complex III (cytochrome b), 3 subunits of complex IV (COI, COII, COIII) and 2 subunits of ATP synthase (ATP6, ATP8). It contains also a non-coding "control region" where the origin of replication and promoter sites of transcription are localized (Fig. 5A) (Anderson, Bankier et al. 1981; Scheffler 2008).

The mtDNA of *S. cerevisiae* is about 78 kb. It encodes 2 ribosomal RNAs, Var1p that is a protein of small unit of the ribosome, 24 tRNAs, 9S RNA component of RNase P implicated in tRNA maturation and intron cleavage, 1 subunit of complex III (cytochrome b), 3 subunits of complex IV (*COXI, COXII, COXIII*), 3 subunits of ATP synthase (*ATP6, ATP8, ATP9*) (Fig. 5B). In some yeast strains mtDNA encodes also a subunit of mitochondrial endonuclease (*ENS2*) (de Zamaroczy and Bernardi 1986; Foury, Roganti et al. 1998).

In most organisms sequences of individual mtDNA particles can differ between each other, a state known as heteroplasmy (Chinnery, Thorburn et al. 2000). In *S. cerevisiae*

heteroplasmy is instable and after about 20 generations all particles of mtDNA are the same, *i.e.* in the state of homoplasmy (Berger and Yaffe 2000; Scheffler 2008). Moreover yeast cells, as facultative aerobes, can survive mutations in mtDNA that lead to dysfunction in respiration if they are grown on fermentable carbon sources. Sometimes the mutations cause also mtDNA instability. Yeast cells with point mutations causing a respiration defect are called *mit*$^-$ strains, the ρ^- strains have large deletions (>50%) in mtDNA sequence and ρ^0 strains are totally devoid of mtDNA.

I.1.4 Nuclear DNA-encoded mitochondrial proteins

About 99% of mitochondrial proteins are encoded in the nucleus, synthesized on cytosolic ribosomes and imported into mitochondria (Becker, Bottinger et al. 2012; Harbauer, Zahedi et al. 2014). Most of the mitochondrial proteins are synthesized with a 10 to 60 amino acid pre-sequence that is recognized by the outer membrane transport machinery (the TOM complex) and directed to the inner membrane transport machinery (the TIM23 complex). Active transport into the matrix is driven by the pre-sequence translocase-associated motor (PAM). Once the pre-sequence reaches the matrix, it is cleaved by the mitochondrial processing peptidase (MPP). The protein either is moved into the inner membrane directly, or enters the matrix where it stays, or is directed to the inner membrane by the OXA export machinery (Fig. 6A, from (Harbauer, Zahedi et al. 2014)). The inner membrane proteins synthesized without the pre-sequence bind carrier precursors that are directed to the TOM complex. In the intermembrane space they use small TIM chaperones and TIM22 complex to be inserted into the inner membrane (Fig. 6B, from (Harbauer, Zahedi et al. 2014)). The proteins of the intermembrane space are characterized by cysteine-rich motives and are transported by the TOM complex in a reduced form. In the intermembrane space they are oxidized by the mitochondrial intermembrane space import and assembly (MIA) machinery which traps them inside (Fig.6 C, from (Harbauer, Zahedi et al. 2014)). The outer membrane proteins are β-barrel or contain an α-helical transmembrane segments. The former are transported into the intermembrane space by the TOM complex, and with help of small TIM chaperons are sorted out by the sorting and assembly machinery (the SAM complex) (Fig. 6D, from (Harbauer, Zahedi et al. 2014)). The latter are inserted in the outer membrane directly by the mitochondrial import complex (MIM) (Fig. 6E, from (Harbauer, Zahedi et al. 2014)).

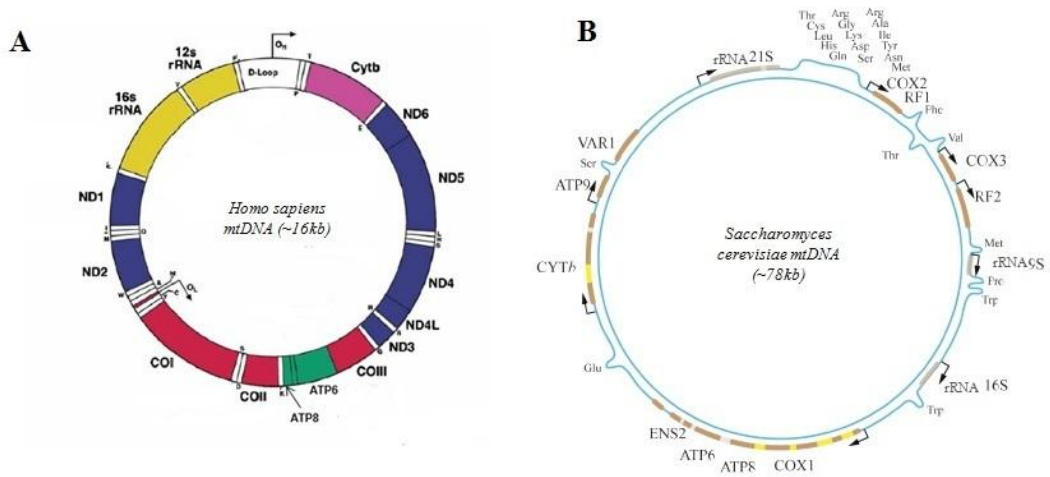

Figure 5 – A schema of mitochondrial genomes. A: A map of a human mitochondrial genome. Genes encoding subunits of respiratory chain complexes and ATP synthase are marked with different colors, tRNAs are marked in white, rRNAs in yellow, O_H and O_L – origins of replication. (The schema made by Małgorzata Rak) **B:** A map of *S. cerevisiae* mitochondrial genome. Brown color represents exons, yellow coding introns and grey non-coding introns. The arrows indicate sites of initiation of transcription (The schema made by François Godard).

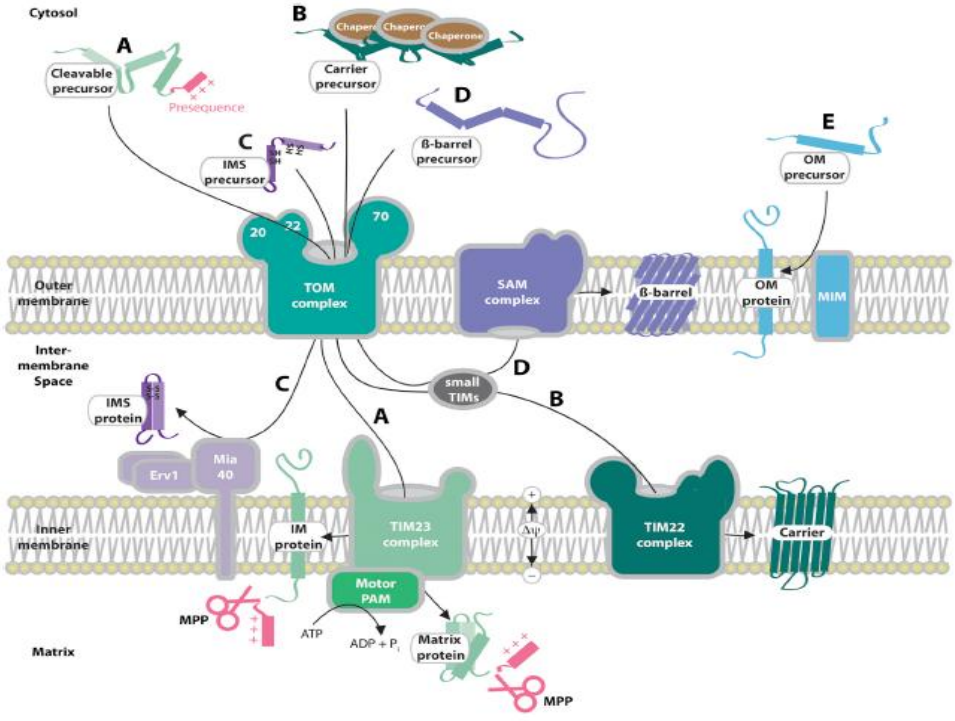

Figure 6 – Protein import pathways of mitochondria (Harbauer, Zahedi et al. 2014).

I.1.5 Respiratory chain and oxidative phosphorylation

The production of cellular energy in the form of ATP by ATP synthase is driven by proton gradient on the IM. The proton gradient is generated by complexes of respiratory chain during electron transfer to oxygen (Fig. 7). Complex I (NADH-ubiquinone oxidoreductase) transfers electrons from NADH to ubiquinone. Complex II (succinate:ubiquinone reductase) oxidizes succinate to fumarate and also uses ubiquinone as an electron acceptor. Electrons from the reduced ubiquinone are transferred to cytochrome *c* by complex III (the bc_1 complex, cytochrome *c* reductase). Complex IV (cytochrome *c* oxidase) catalyzes the final transport of electrons from cytochrome *c* to oxygen. During the electron transport complexes I, III and IV pump protons from the matrix to the intermembrane space, creating a proton gradient (Fig. 7) used by the ATP synthase to synthesize ATP from ADP and Pi (Mitchell 1961; Mitchell and Moyle 1967b). Synthesized ATP is transported out of the mitochondria in exchange for ADP by adenine nucleotide translocator (ANT).

Yeast *S. cerevisiae* does not have complex I but two NADH dehydrogenases, located on the matrix (Ndi1p) and on the intermembrane space (Nde1p) sides of the IM (Fig. 7B). The electron activity of these proteins is not coupled to proton translocation across IM. The yeast's respiratory chain contains also present glycerol-3-phosphate dehydrogenase (Gut2p) which reduces ubiquinone and L-lactate dehydrogenase (LDH), which in turn reduces cytochrome *c* (Fig. 7B) (Rigoulet, Mourier et al. 2010).

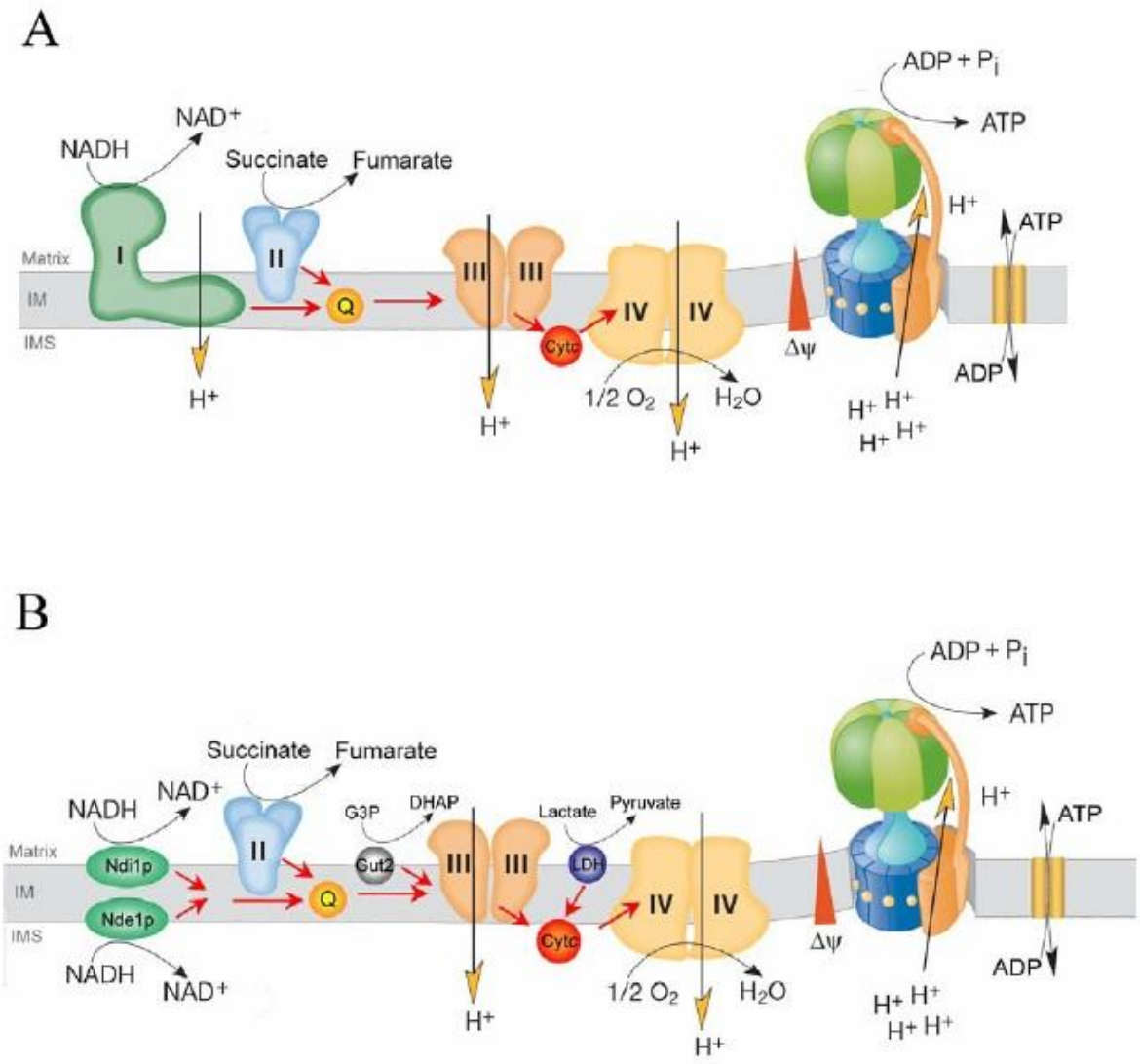

Figure 7 – A schema of the respiratory chain of mammals (A) and *Saccharomyces cerevisiae* (B). The schema made by Małgorzata Rak.

I.2 THE STRUCTURE OF F_1F_O-ATP SYNTHASE

The ATP synthase (Fig. 8) is an energy producing enzyme present in almost all organisms from prokaryotes to eukaryotes and is composed of two functional domains, F_1 and F_O. Its structure is well conserved from the bacteria to humans, however the eukaryotic enzyme has some additional subunits as compared to the prokaryotic one (Ackerman and Tzagoloff 2005; Kucharczyk, Zick et al. 2009c; Jonckheere, Smeitink et al. 2012). The table below (Table 1) presents components of ATP-synthase from bacterium *Escherichia coli*, yeast *Saccharomyces cerevisiae* and humans (*Homo sapiens*).

Domain	**Function**	***E. coli***	***H. sapiens***	***S. cerevisiae***	
				Protein	**Gene**
F_1	Catalytic head	α	α	α	*ATP1*
		β	β	β	*ATP2*
	Central stalk/ rotor	γ	γ	γ	*ATP3*
		ε	δ	δ	*ATP16*
		-	ε	ε	*ATP15*
F_O	Proton channel	a	a	Atp6p	*ATP6*
		c	c	Atp9p	*ATP9*
	Peripheral stalk	δ	OSCP	OSCP	*ATP5*
		b	*b*	Atp4p	*ATP4*
		-	*d*	*d*	*ATP7*
		-	F_6	*h*	*ATP14*
		-	-	*i/j*	*ATP18*
	Stator	-	A6L	Atp8p	*ATP8*
		-	*f*	*f*	*ATP17*
F_O associated proteins	Dimerisation	-	*e*	*e*	*ATP21/TIM11*
		-	*g*	*g*	*ATP20*
		-	-	*k*	*ATP19*
Regulatory proteins	Inhibitors of hydrolytic activity	-	IF1	IF_1/Inh1p	*INH1*
		-	-	Stf1p	*STF1*
		-	-	Stf2p	*STF2*
		-	-	Stf3p	*STF3*

Table 1 – List of ATP synthase subunits from *Escherichia coli*, *Saccharomyces cerevisiae* and *Homo sapiens*. The list is based on (Ackerman and Tzagoloff 2005; Kucharczyk, Zick et al. 2009c; Jonckheere, Smeitink et al. 2012).

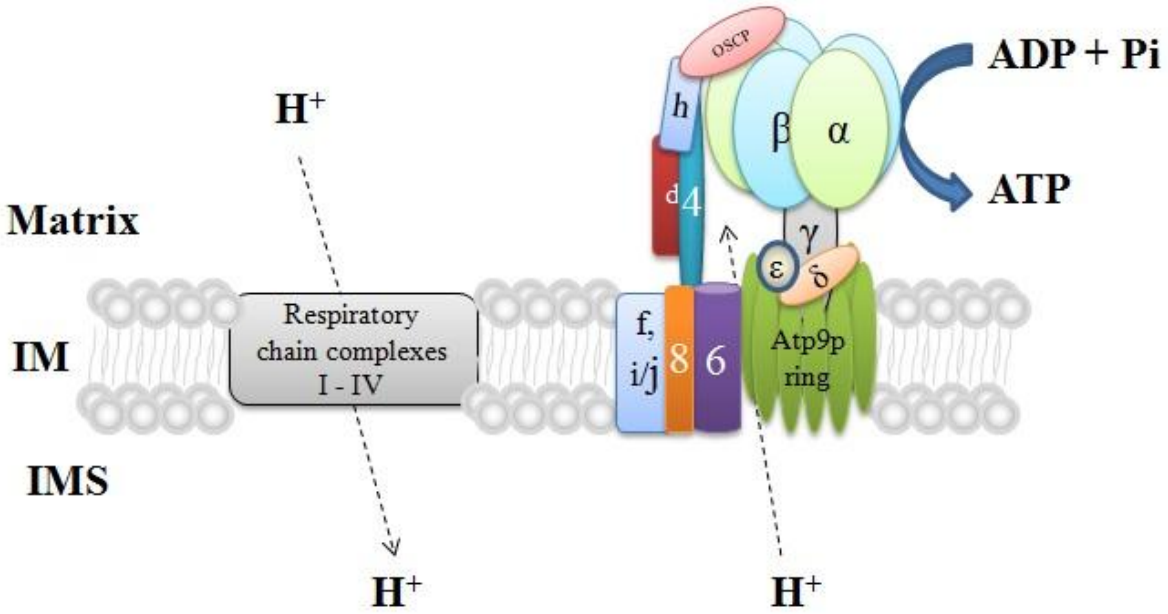

Figure 8 – A schema of F_1F_O-ATP synthase from *Saccharomyces cerevisiae*. IMS – intermembrane space; IM – inner membrane.

I.2.1 The F_1 domain

F_1 domain of ATP synthase is located at matrix side of the inner mitochondrial membrane and contains two functional parts: the α/β hexamer (the catalytic head) and the central stalk (the rotor). The α/β hexamer is built of three α subunits and three β subunits in alternant arrangement. It is the catalytic center of the enzyme. The central stalk is built of subunits γ, δ and ε (Fig. 8). The N- and C-terminal parts of γ subunit protrude into the central cavity of the α/β hexamer while the rest of the protein is in contact with subunits δ and ε, and the Atp9p-ring (Abrahams, Leslie et al. 1994).

The α/β hexamer as a catalytic center contains three nucleotide binding sites in each subunit β, where each subunit is at a different conformational stage in a given moment. Each subunit β changes the conformational states in one cycle of ATP synthesis. The conformational states are: β_E (empty), β_{HC} and β_{DP} (that bind ADP and Pi) ,and β_{TP} (that binds ATP). These conformational changes results in ATP synthesis or ATP hydrolysis (Fig. 9) (Boyer 1993; Gao, Yang et al. 2005). The changes are driven by subunit γ rotation. The rotation of γ is a result of the rotation of the Atp9p-ring which in turn is provoked by proton movement through the proton channel (Stock, Gibbons et al. 2000).

The catalytic head can either synthesize or hydrolyze ATP. The synthesis of ATP requires energy that is produced by the respiratory chain as the proton gradient, whereas hydrolysis does not. Hence, when the respiratory chain is not capable of maintaining the proton gradient, the inhibitory proteins (IF_1/Inh1p and Stf1p in *S. cerevisiae)* fix in the catalytic sites of *α/β* hexamer to block the hydrolysis of ATP, in order to avoid futile consumption of ATP (Schwerzmann and Pedersen 1986; Robinson, Bason et al. 2013).

I.2.2 The F_O domain and the peripheral stalk

F_O domain is composed of subunit 9-ring (10 monomers in *S. cerevisiae*, 8 in mammals), subunits 6, 8, i/j and f (Fig. 8) (Rak, Zeng et al. 2009b; Kucharczyk, Zick et al. 2009c). Subunit 9 has two transmembrane *α*-helices with a connecting loop directed in the matrix. The loops in the ring interact with the central stalk, whereas the membrane part of Atp9 proteins contacts Atp6p. The Atp9p-ring and subunit 6 form the proton channel of ATP synthase. Subunit 6 has five transmembrane *α*-helices with N-terminal directed to the inner membrane space and C-terminal to the matrix. Atp6p is connected with the peripheral stalk with the membrane part of subunit 4 (Rak, Zeng et al. 2009b).

The peripheral stalk (Fig. 8) extends from the inner membrane to the top of the *α/β* hexamer and its function is to stabilize the connection between F_1 and the proton channel during rotation of the motor (the Atp9p-ring and the central stalk). It is built of four subunits: 4, d, h and OSCP (the oligomycin-sensitivity conferring protein). Subunit 4 has two transmembrane domains that anchor it in the inner mitochondrial membrane and make a connection with Atp6p. In the matrix, Atp4p is connected with subunits d, h and OSCP. The last one is located on the top of the catalytic head (Walker and Dickson 2006).

As mentioned before, ATP synthesis/hydrolysis is driven by the rotation of the subunits 9 ring. This rotation is provoked by protonation and deprotonation of Glu^{59} in Atp9p and Arg^{186} in Atp6p (residues in *S. cerevisiae* proteins), which results in the proton translocation through the inner mitochondrial membrane (Stock, Leslie et al. 1999; Stock, Gibbons et al. 2000; Walker 2013). The exact mechanism of this process is still unknown.

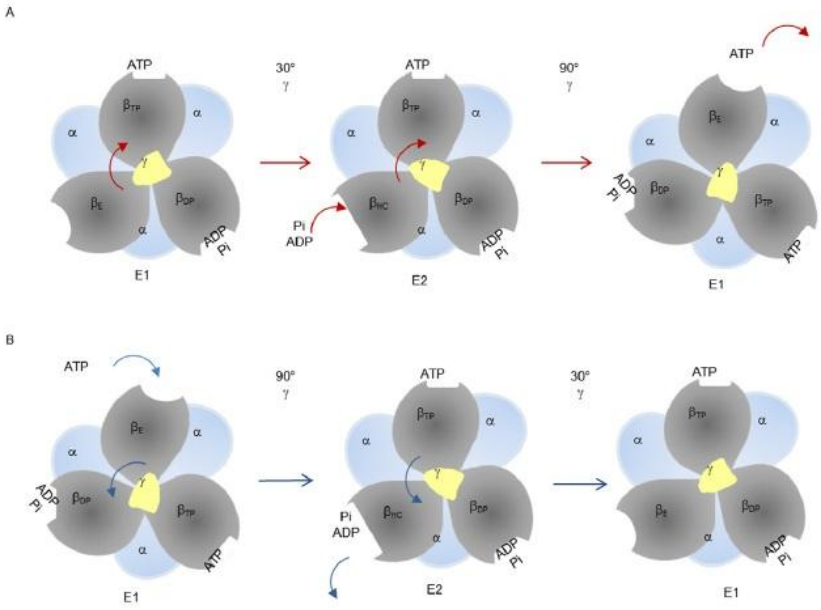

Figure 9 – A schema illustrating ATP synthesis (A) and hydrolysis (B) by the catalytic head of the ATP synthase. The figure shows a 120° rotation of subunit γ, which corresponds to conformational changes in subunit β and synthesis or hydrolysis of ATP. The catalytic binding sites are marked according to their structural descriptions (β_E, β_{HC}, β_{DP} and β_{TP}) (Abrahams, Leslie et al. 1994; Menz, Walker et al. 2001) and indicated by various shapes (Braig, Menz et al. 2000). The sequence of events for the ATP synthesis is shown by red arrows and for ATP hydrolysis by blue arrows. The schema made by Róża Kucharczyk.

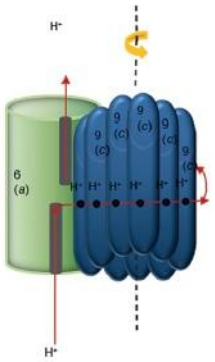

Figure 10 – A two-channel model of generation of rotation by movement of protons through the F_O domain of the ATP synthase proposed by Junge (Junge, Lill et al. 1997). Two half channels across the interface between the subunit *a* (Atp6p) and the *c* ring (the Atp9p-ring) are linked by the rotation of the *c* ring. The red arrow indicates the proton flux from the intermembrane space to the matrix. The schema made by Róża Kucharczyk.

I.3 BIOGENESIS OF THE F_1F_O-ATP SYNTHASE

The F_1F_O-ATP synthase from yeast *S. cerevisiae* is composed of subunits encoded both in nuclear and mitochondrial genomes. Atp6p, Atp9p and Atp8p are encoded in mtDNA while the rest is encoded in nuclear DNA (nDNA). Biogenesis of the complex requires coordination of expression of genes from two genomes and preserving the non-equal stoichiometry of subunits (10 subunits 9, 3 α and β, and one of each other subunit) (Fig. 11).

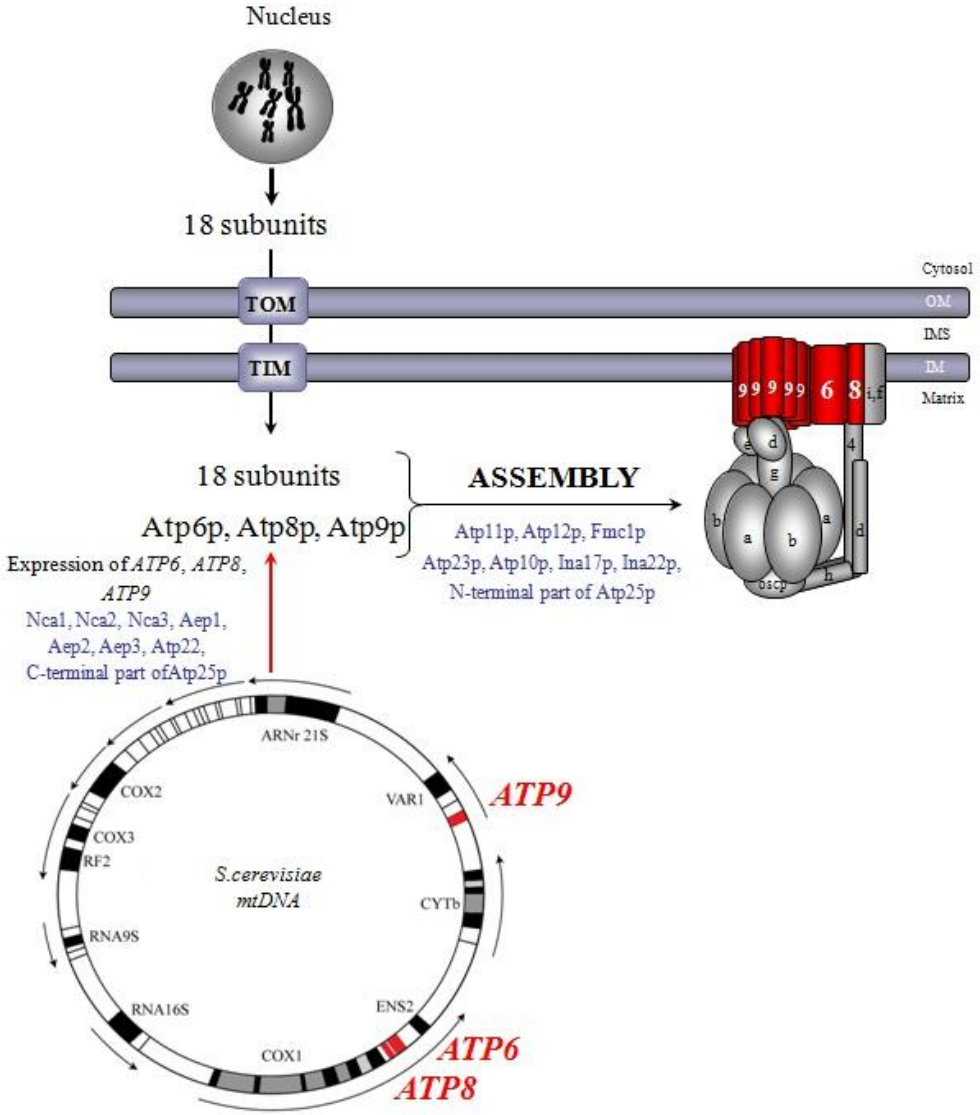

Figure 11 – A schema illustrating the origin of ATP synthase subunits and proteins essential for expression of mitochondrially encoded subunits and assembly of the enzyme (the schema made by Jean-Paul di Rago).

I.3.1 Assembly of the F_1 domain

Five subunits of the F_1 domain in stoichiometry $\alpha_3\beta_3\gamma\delta\varepsilon$ are encoded in nDNA, synthesized on cytoplasmic ribosomes and transported to the mitochondrial matrix where they are assembled. We know three proteins needed for the assembly of the catalytic head: Atp11p, Atp12p and Fmc1p (Ackerman and Tzagoloff 1990a; Wang and Ackerman 2000a; Wang, Sheluho et al. 2000b; Lefebvre-Legendre, Vaillier et al. 2001). Atp12p is a chaperon for subunit α (Wang, Sheluho et al. 2000b) while Atp11p is a chaperon for subunit β (Wang and Ackerman 2000a). Atp12p and Atp11p bind to the nucleotide binding sites of α and β, respectively, to prevent them from aggregation (Wang, Sheluho et al. 2000b). It was shown that in the strains lacking *ATP1* subunits β form large insoluble aggregates, and the same happens for subunit α when *ATP2* is absent. A similar situation was observed in strains deleted from either *ATP11* or *ATP12* genes (Ackerman and Tzagoloff 1990a). During assembly of the α/β hexamer, Atp11p bound to subunit β is released in exchange for subunit α whereas Atp12p bound to subunit α is released in exchange for β (Fig. 12) (Wang, Sheluho et al. 2000b; Ackerman 2002). Assembly of catalytic head requires also the presence of subunit γ as Atp12p-α and Atp11p-β accumulate in the absence of γ (Paul, Ackerman et al. 1994; Ludlam, Brunzelle et al. 2009).

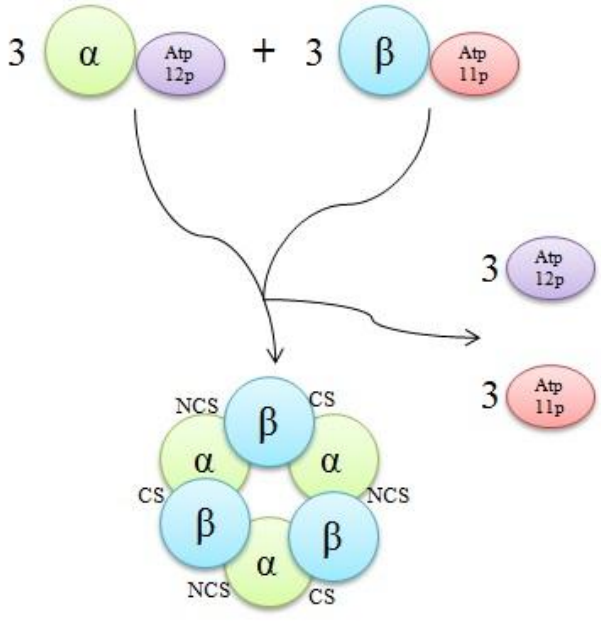

Figure 12 – Atp11p and Atp12p-mediated F1 assembly. CS – catalytic sites, NCS – non-catalytic sites. Based on (Ackerman 2002).

Fmc1p is needed for the F_1 assembly at elevated temperature (35 – 37°C). At the non-permissive temperature, α and β subunits aggregate in a *fmc1Δ* strain but not when it is grown at 30°C. The thermo-sensitive phenotype of *fmc1Δ* is reversed, if Atp12p is over-expressed. It was proposed that Fmc1p stabilizes Atp12p at elevated temperature (Lefebvre-Legendre, Vaillier et al. 2001).

I.3.2 Assembly of the F_O domain

The subunits of F_O domain in yeast *S. cerevisiae* are encoded in mtDNA and synthesized on mitochondrial ribosomes (see Fig. 5 and 11). Expression and assembly of these proteins require a number of factors, shown in Fig. 13.

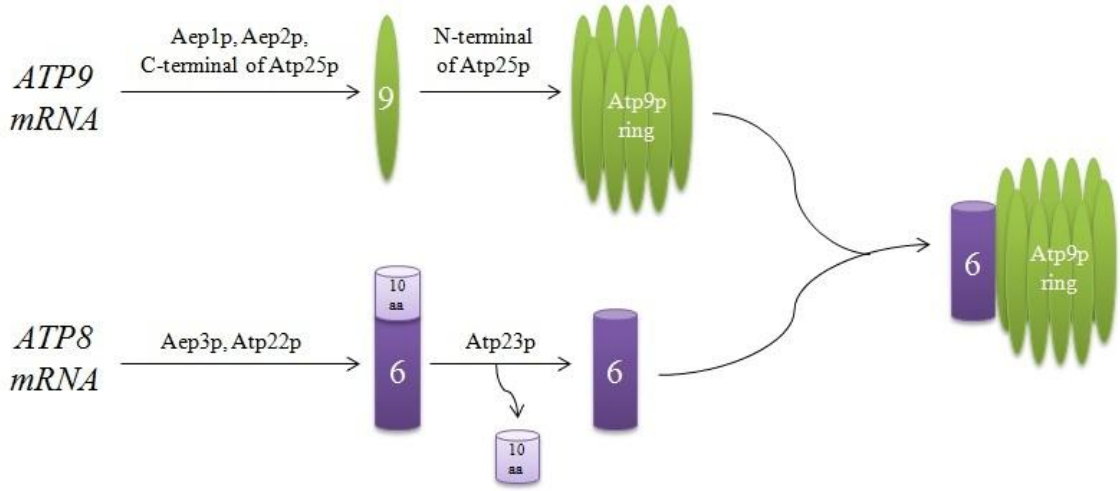

Figure 13 – Proteins needed for F_O domain biogenesis. 9 – subunit 9, 6 – subunit 6, 10aa – pres-sequence of subunit 6. Based on (Rak, Zeng et al. 2009b).

I.3.2.1 Expression of ATP9 and the Atp9p-ring assembly

ATP9 (*OLI1*) gene is transcribed with *VAR1* and *tRNA^{Ser}* (Fig. 14). This polycistron is transcribed from two initiation sites localized approximately 550bp and 630bp upstream of *ATP9* ORF. The first transcript is cleaved by endonucleases to obtain mature forms of *ATP9* (0.9kb) and *VAR1* (1.9kb) mRNA, and tRNA^{Ser} (Christianson and Rabinowitz 1983; Zassenhaus, Martin et al. 1984; Finnegan, Payne et al. 1991).

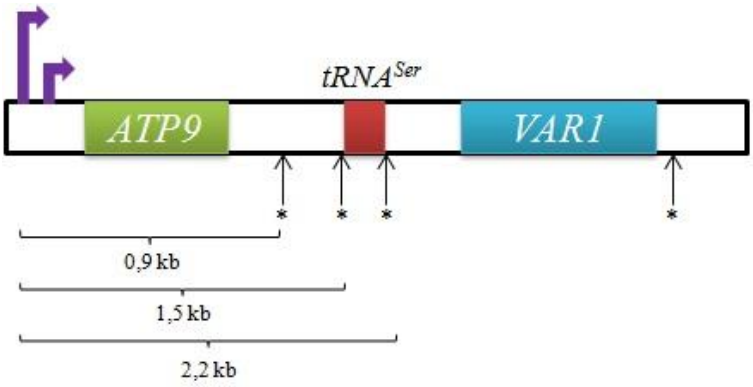

Figure 14 – Polycistronic transcript of *ATP9*, *tRNA*^{Ser} and *VAR1*. Transcription initiation sites are marked with horizontal arrows. Cleavage sites of the polycistronic transcripts that produce mature messengers are shown by asterisks. Based on (Rak, Zeng et al. 2009b).

So far there are three known proteins involved in regulation of expression of *ATP9*: Aep1p/Nca1p, Aep2/Atp13p and Atp25 (Ackerman, Gatti et al. 1991; Payne, Schweizer et al. 1991; Ziaja, Michaelis et al. 1993; Zeng, Barros et al. 2008). All of them are encoded in nuclear DNA.

Aep1p and Aep2p (ATP Expression protein 1 and 2, respectively) were first identified in 1991 (Payne, Schweizer et al. 1991) by the study of two mutants that could not grow on glycerol at 36°C (ts379 and ts1860). At the non-permissive temperature, these strains showed no synthesis of Atp9p and Atp8p, and a diminished synthesis of Atp6p. Further experiments revealed that a ts379 mutant did not produce mature *ATP9* mRNA about 1h after the temperature shift while in ts1860 it was present until 5h after the temperature shift. As no changes in *ATP8* and *ATP6* mRNA were detected, the authors proposed that lack of Atp8p and decrease in Atp6p synthesis are secondary effects of the absence of Atp9p. The authors postulated that the mutated protein in the ts379 strain, named Aep2p, is involved in stability or maturation of *ATP9* mRNA, whereas mutated protein in ts1860, named Aep1p, acts on the level of translation. Further analysis (Payne, Finnegan et al. 1993) showed that Aep1p has the size of *ca.* 59kDa. It is a hydrophilic protein with no membrane spanning domains. There are more basic than acidic residues in Aep1p indicating that it might interact with nucleic acids. Mature Aep2p is a protein of about 58kDa arising from the 64kDa precursor (Finnegan, Ellis et al. 1995). It is globally hydrophilic but contains two non-polar regions that can be membrane-spanning domains (Ackerman, Gatti et al. 1991). Another study suggested that Aep2p interacts with 5'UTR of *ATP9* mRNA and plays a direct role in translation as a RNA-

binding protein (Ellis, Lukins et al. 1999). Both Aep1p and Aep2p have N-terminal mitochondrial targeting sequences, are expressed at very low levels and have no homology to known proteins (Ackerman, Gatti et al. 1991; Finnegan, Payne et al. 1991; Payne, Finnegan et al. 1993; Finnegan, Ellis et al. 1995).

Atp25p was also studied with the use of a thermo-sensitive mutant that failed to grow on glycerol at elevated temperature. There was no Atp9p synthesis in this mutant due to lack of mature *ATP9* mRNA about 4h after the temperature shift (Zeng, Barros et al. 2008). The predicted size of the protein was about 70kDa but detailed analysis showed that Atp25p is cleaved into fragments – about 30kDa N-terminal and about 35kDa C-terminal. The cleavage site was determined as serine 293. The authors claim that C-terminus of Atp25 is an inner membrane protein facing the matrix side, while the N-terminus is associated to the inner membrane facing the inner membrane space. Both parts are necessary to restore the respiratory growth of the *atp25Δ* strain, however they have different functions. The C-terminus is necessary to stabilize *ATP9* mRNA whereas the N-terminus is a chaperon protein that promotes oligomerization of Atp9-ring (Zeng, Barros et al. 2008).

I.3.2.2 Expression of ATP6 and ATP8

ATP6 and *ATP8* genes are transcribed together with *COX1* (de Zamaroczy and Bernardi 1986; Foury, Roganti et al. 1998). The polycistron may also contain *ENS2* gene, downstream of *ATP6* and *ATP8*, encoding DNA endonuclease, but its presence depends on the strain (Fig. 15) (Nakagawa, Morishima et al. 1991). The primary transcript is cleaved twice and gives *COX1* mRNA and two *ATP8/ATP6* mRNAs. The first 5.2kb *ATP8/ATP6* mRNA originates after cleavage at 3'end of *COX1* mRNA, the second one originates from the cleavage site located 600bp downstream the 3'end of *COX1* mRNA and has 4.6kb (Beilharz, Cobon et al. 1982; Christianson and Rabinowitz 1983; Simon and Faye 1984). Both *ATP8/ATP6* transcripts are produced in equal quantity and are used for translation.

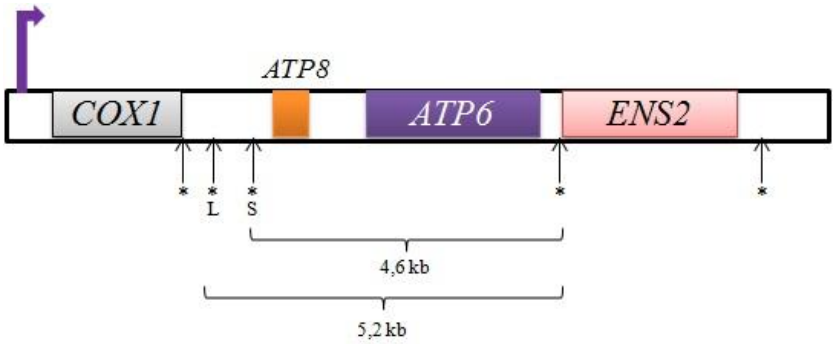

Figure 15 – Polycistronic transcript of *COX1, ATP8, ATP6* and *ENS2*. Transcription initiation site is marked with horizontal arrow. Cleavage sites of the polycistronic transcripts that produce mature messengers are shown by asterisks. Based on (Rak, Zeng et al. 2009b).

So far there are four known specific proteins implicated in expression of *ATP6* and *ATP8* genes: Nca2p, Nca3p, Aep3p and Atp22p (Pelissier, Camougrand et al. 1992; Camougrand, Pelissier et al. 1995; Pelissier, Camougrand et al. 1995; Helfenbein, Ellis et al. 2003; Ellis, Helfenbein et al. 2004). Nca2p and Nca3p were identified during the study of mutants that did not grow on glycerol at 14°C (Pelissier, Camougrand et al. 1992). These mutant strains had increased level of the primary transcript containing *COX1/ATP8/ATP6*, diminished levels of 5.2kb *ATP8/ATP6* transcript in comparison with its short version and lower Atp6p and Atp8p synthesis. The mature *COX1* transcript was not affected. Though the Nca2p and Nca3p proteins probably influence the maturation/stability of *ATP8/ATP6* mRNA (Pelissier, Camougrand et al. 1992; Camougrand, Pelissier et al. 1995; Pelissier, Camougrand et al. 1995).

Aep3p was shown to stabilize *ATP8/ATP6* transcripts. In the *aep3Δ* strain the level of longer transcript was severely diminished while the shorter one was not detected, although the levels of the primary transcript and mature *COXI* mRNA were not changed. The authors postulated also the role of Aep3p in Atp6p and Atp8p synthesis because neither of the two proteins were synthesized in the *aep3Δ* strain (Ellis, Helfenbein et al. 2004). Aep3p was also described as a component of the mitochondrial translation initiation complex, although its second function is stimulation of the yeast mitochondrial initiation factor 2 (ymIF2), a crucial factor for translation initiation, to bind unformylated Met-$tRNA_f^{Met}$ as the first amino acid (Lee, Tibbetts et al. 2009). Moreover the Aep3 protein was shown to be a PPR protein (Ellis, Helfenbein et al. 2004; Lee, Tibbetts et al. 2009). PPR proteins are characterized by one or

more degenerated pentatricopetptide repeat motifs that bind RNA. They are believed to be involved in stabilization and processing of mitochondrial mRNA.

Atp22 was first described as a factor necessary for assembly of F_O domain located in the inner membrane facing the matrix side (Helfenbein, Ellis et al. 2003). In *atp22Δ* strains both *ATP8/ATP6* transcripts are present, but only Atp8p is synthesized. Lack of Atp22p could be circumvented by the presence of heteroplasmy with *ATP6* gene under control of *COX1* 5'UTR, whereas other mitochondrial genes where expressed from *WT* mtDNA. Hence Atp22p is concerned as a translational activator specific for Atp6p (Zeng, Hourset et al. 2007a).

There is one more factor that influence stabilization/processing of *ATP8/ATP6* transcript, Nam1p. This protein is located in the mitochondrial matrix and is weakly associated to the inner membrane (Wallis, Groudinsky et al. 1994). It was shown to interact with mitochondrial RNA polymerase (Rpo41p) (Wallis, Groudinsky et al. 1994; Rodeheffer, Boone et al. 2001). In the *nam1* mutant, the levels of *COB*, *COX1* and *ATP8/ATP6* transcripts were diminished. In the intron-less mtDNA however, only *ATP8/ATP6* are affected (Groudinsky, Bousquet et al. 1993). Therefore Nam1p plays a role not only in maturation/stabilization of the intron containing transcripts but also in maturation/stabilization of *ATP8/ATP6* transcript (Groudinsky, Bousquet et al. 1993).

The synthesis of Atp6 and Atp8 proteins depends also on the presence of the assembled F_1 catalytic head (Rak and Tzagoloff 2009a). The authors suggest that this control is Atp22p-dependent as over-expression of the *ATP22* gene in a strain lacking F_1 restored synthesis of Atp6p and Atp8p (Rak and Tzagoloff 2009a).

I.3.3 Assembly of the F_1F_O-ATP synthase

The ATP synthase assembly is a gradual process (Fig. 16 and 17). As described in section I.3.1, the F_1 domain assembles independently from the F_O domain, as evidenced by the presence of F_1 in ρ^-/ρ^0 cells. The Atp9p-ring is believed to assemble independently from other ATP synthase subunits (Tzagoloff, Barrientos et al. 2004; Rak, Zeng et al. 2009b; Rak, Gokova et al. 2011). Newly synthesized Atp9p interacts with Oxa1p (mitochondrial inner membrane insertase), which helps Atp9p insertion into the membrane. This interaction is not essential, because in the *oxa1Δ* mutant the ATP synthase can still assemble, however with a lower efficiency (Jia, Dienhart et al. 2007). The oligomerization of the Atp9p-ring is

dependent on the presence of the N-terminal part of Atp25p (Zeng, Barros et al. 2008). After assembly, the Atp9p-ring associates with the F_1 domain (Kucharczyk, Zick et al. 2009c; Rak, Gokova et al. 2011).

The assembly of the peripheral stalk was long believed to occur spontaneously (self-assembly). However, recently a complex of inner membrane proteins (INAC), composed of Ina22 and Ina17 proteins, was shown to facilitate assembly of the peripheral stalk and its assembly with F_1 (Lytovchenko, Naumenko et al. 2014). It is however not clear at what moment of the ATP synthase assembly the peripheral stalk interacts with the F_1 and F_O domains (Fig. 16 and 17).

How subunit 8 assembles in not well understood. There is a study showing that assembly of Atp8p with the Atp9p ring occurs before assembly of Atp6p (Hadikusumo, Meltzer et al. 1988). A more recent analysis demonstrates however, that Atp8p and Atp6p associate before being incorporated into the ATP synthase (see Fig. 17) (Rak, Gokova et al. 2011). In other models, Atp6p is believed to be the last subunit to be incorporated into ATP synthase, with the help of two proteins: Atp10 (Ackerman and Tzagoloff 1990b; Tzagoloff, Barrientos et al. 2004) and Atp23p (Fig. 18) (Osman, Wilmes et al. 2007; Zeng, Neupert et al. 2007c). Atp10p is a mitochondrial matrix protein that interacts co- or post-translationally with newly synthesized Atp6p (Ackerman and Tzagoloff 1990b; Paul, Barrientos et al. 2000). Atp10p may protect Atp6p against proteases until its incorporation and/or directly intervene in the assembly with Atp9p. In the *atp10Δ* mutant strain, the Atp6p is rapidly degraded, but the formation of the Atp9p ring is not affected (Tzagoloff, Barrientos et al. 2004). Analysis of *atp10Δ* suppressors revealed that interaction between the two proteins probably involves the C-terminal part of Atp6p (Paul, Barrientos et al. 2000).

Subunit 6 in yeast *S. cerevisiae* is synthesized with a 10aa pre-sequence on the N-terminal that is cleaved during the assembly (Michon, Galante et al. 1988). Atp23p is an intermembrane metalloprotease that is responsible for Atp6p maturation (Osman, Wilmes et al. 2007; Zeng, Neupert et al. 2007c). Furthermore, presence of Atp23p is necessary for Atp6p assembly with the Atp9p-ring (Osman, Wilmes et al. 2007; Zeng, Neupert et al. 2007c). Interestingly, the cleavage of 10aa pre-sequence is not essential for Atp6p assembly. The presence of the *atp23-E168Q* mutation that blocks the proteolytic activity of Atp23p did not influence the assembly of the ATP synthase complex (Osman, Wilmes et al. 2007; Zeng, Neupert et al. 2007c). The pre-sequence is supposed to favor the interaction between Atp6p

and the Atp9p-ring. In a strain encoding Atp6p lacking the pre-sequence, ATP synthase complexes were assembled but two times less efficiently than in *WT* (Zeng, Kucharczyk et al. 2007b).

The ATP synthase was also shown to form dimers and oligomers in the IM (Fig. 16). The process is dependent on subunits e, g and k but is not essential for proper functioning of the enzyme (Kucharczyk, Zick et al. 2009c).

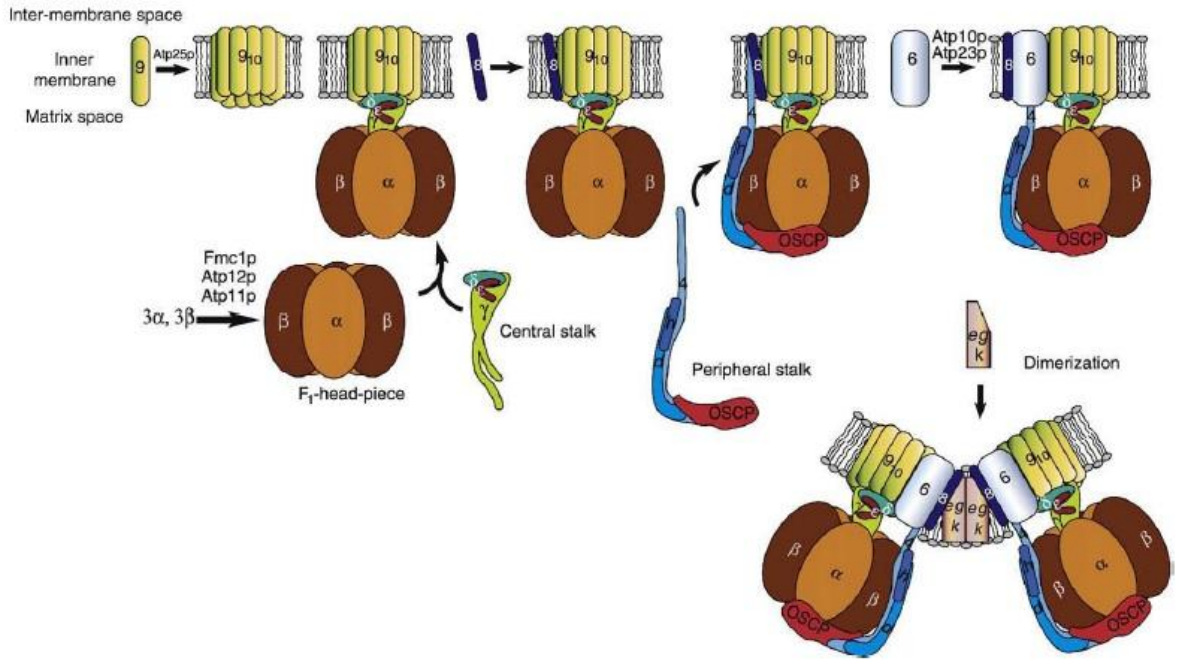

Figure 16 – Assembly of ATP synthase from *S. cerevisiae* according to Kucharczyk (Kucharczyk, Zick et al. 2009c).

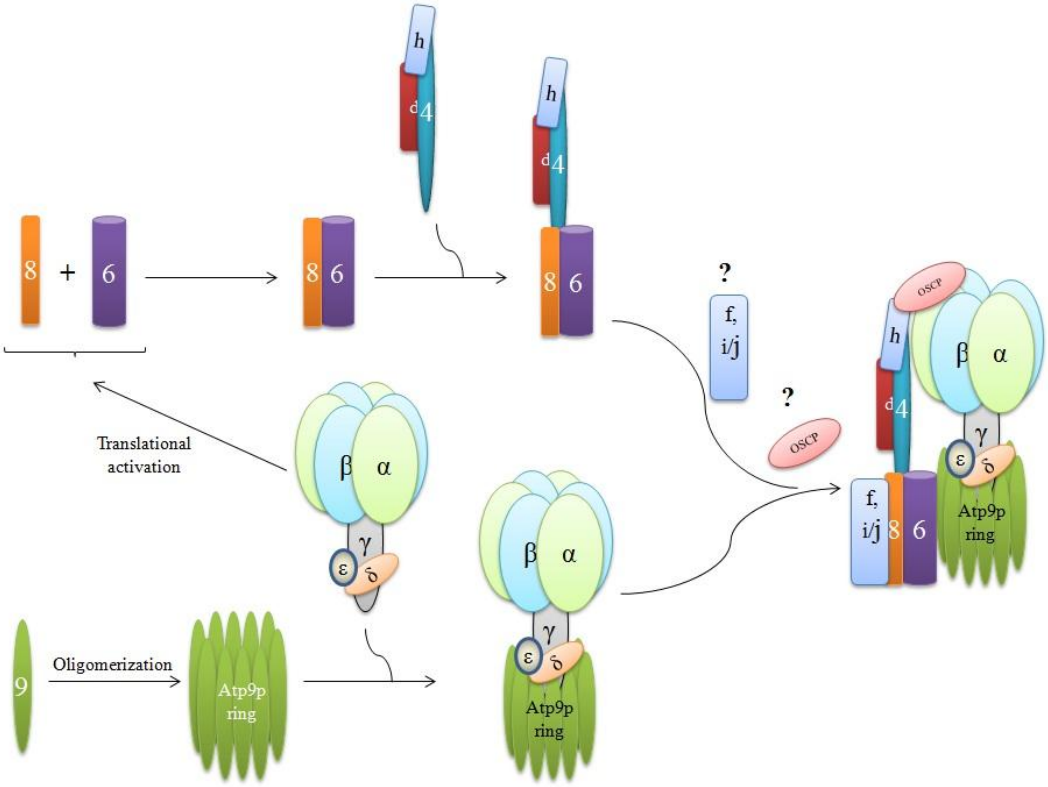

Figure 17 – Modular assembly of ATP synthase. A schema based on Rak and Tzagoloff (Rak, Gokova et al. 2011).

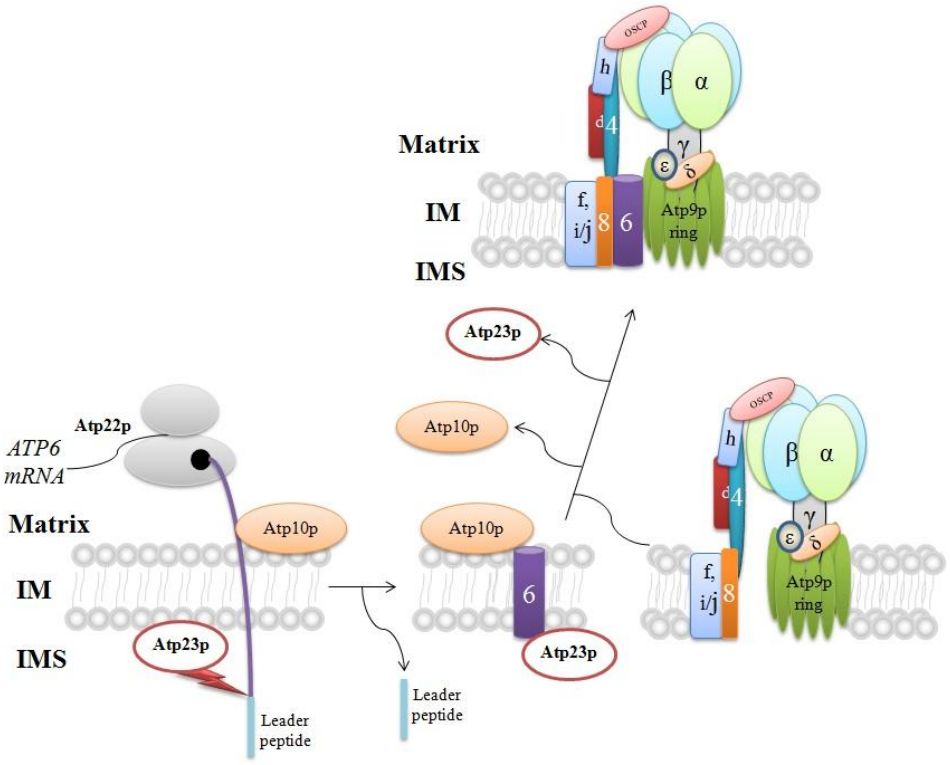

Figure 18 – Maturation and assembly of Atp6p. Atp6p is marked in violet, the 10aa pre-sequence in blue (leader peptide).

I.4. ATP SYNTHASE AND DISEASES

A number of human diseases have been associated with defects in the ATP synthase. Some of these diseases were shown to result from mutations affecting the assembly of ATP synthase. One was found in the nuclear gene encoding Atp12, a protein involved in the assembly of the F_1 sector. A patient carrying this mutation presented with dysmorphic features and atrophies in the nervous system, enlarged liver, hypotonia and increased urinary lactate, fumarate, methylglutaconic acid and amino acids. A biochemical analysis revealed decreased activity and content of the ATP synthase in the liver and skeletal muscles, and fibroblasts. The patient died at the age of 14 months (De Meirleir, Seneca et al. 2004). In 2008, a mutation in the *TMEM70* gene (c.317-2A>G) was identified in a patient with neonatal mitochondrial encephalocardiomyopathy and ATP synthase assembly deficiency (Cizkova, Stranecky et al. 2008). Since then a lot of other mutations were described in this gene (Shchelochkov, Li et al. 2010; Cameron, Levandovskiy et al. 2011; Jonckheere, Huigsloot et al. 2011; Spiegel, Khayat et al. 2011; Tort, Del Toro et al. 2011; Torraco, Verrigni et al. 2012; Atay, Bereket et al. 2013). The most common symptoms in *TMEM70* patients are lactic acidosis, cardiomyopathy, dysfunctions of central nervous system and 3-methylglutaconic aciduria (Houstek, Kmoch et al. 2009). The TMEM70 protein has no homologous in yeast *S. cerevisiae*. The exact role of this protein in the assembly of the ATP synthase remains unknown (Kratochvilova, Hejzlarova et al. 2014).

Diseases were also associated to mutations in genes encoding subunits of the ATP synthase. Two of these mutations were located in the nucleus. One was in the *ATP5E* gene encoding subunit ε (a tyrosine to cysteine change at position 12). This patient showed respiratory problems, hyperlactacidemia, 3-methylglutaconic aciduria, ataxia, exercise intolerance and muscle weakness, and severe peripheral neuropathy. The biochemical analysis revealed severely reduced amount of the ATP synthase in fibroblasts (Mayr, Havlickova et al. 2010). Another mutation was found in the *ATP5A1* gene encoding subunit *α* (arginine to cysteine change at position 329). The patient showed severe neonatal encephalopathy and died after one week. Considerable reduction of the ATP synthase amount and activity in the patient's fibroblasts, probably arose from the impaired assembly of *α/β* hexamers (Jonckheere, Renkema et al. 2013).

Diseases were also associated to the mitochondrial *ATP6* gene encoding subunit *a* (*MTATP6*) (Jonckheere, Smeitink et al. 2012). Mutations 8893T>G, 8893T>C, 9176T>G/C,

9035T>C, 9185T>C and 9191T>C in the *MTATP6* gene resulted in the NARP (Neurogenic Ataxia and Retinitis Pigmentosa) syndrome or maternally inherited Leigh syntdrome (MILS), the 8851T>C mutation resulted in FBSN (Familial Bilateral Stratial Sclerosis) (Kucharczyk, Zick et al. 2009c; Jonckheere, Smeitink et al. 2012). The main clinical phenotypes include progressive loss of vision, ataxia, dementia, muscle weakness, mental retardation, stroke-like episodes, neurological problems and myopathies (Zeviani and Di Donato 2004; Kucharczyk, Zick et al. 2009c). Pathogenic mutations were found also in the *A6L* gene (*MTATP8*) encoding subunit 8, 8529G>A and 8928T>C. These mutations affect tryptophan at position 55 and result in defective assembly and decreased activity of the ATP synthase (Jonckheere, Hogeveen et al. 2008; Ware, El-Hassan et al. 2009). In one patient the 8411A>G mutation was described, but the effect on the ATP synthase remains unknown (Mkaouar-Rebai, Kammoun et al. 2010). A very rare mutation, the deletion ΔTA9205, was identified in two patients and resulted in improper maturation of *ATP8-ATP6-COX3* transcript due to removal of the termination codon between the *ATP8* and *ATP6* genes (Seneca, Abramowicz et al. 1996; Jesina, Tesarova et al. 2004).

I.5. YEAST MODELS OF PATHOGENIC atp6 MUTATIONS

Point mutations of the human mtDNA are often heteroplasmic, *i.e.* co-existing with various amounts of wild type mtDNA within cells and tissues. The severity of diseases depends on the proportion of mutated *vs.* wild type mtDNA. For example, a milder NARP syndrome develops, if the level of heteroplasmy of 8993T>G mutation is between 70 and 90%. Higher mutation loads result in the more severe MILS disease. Mutations of mtDNA are usually considered to be highly recessive, which may render them difficult to evaluate the degree at which they affect the mitochondrial function. Furthermore, given the high mutational rate of the mitochondrial genome and the presence of numerous family- or population-specific polymorphisms, it may be difficult to distinguish between a neutral mtDNA variant and a disease-causing mutation. Also, it has been frequently recognized that the effects of deleterious mtDNA mutations may be exacerbated by mtDNA nucleotide changes that are not pathogenic *per se* or by some unknown nuclear genetic background specificities (Cai, Fu et al. 2008; Swalwell, Blakely et al. 2008).

In the absence of methods for manipulating mammalian mitochondrial genomes, yeast *S. cerevisiae* has been considered as an alternative model system to study specific mtDNA mutations found in patients. It is currently the only organism in which a mitochondrial genetic transformation is possible by the ballistic delivery into mitochondria of *in vitro* constructed mtDNA bearing mutations, followed by their integration into the *WT* mtDNA by homologous DNA recombination (Bonnefoy and Fox 2001b). Yeast is unable to maintain heteroplasmic DNA stably (Okamoto, Perlman et al. 1998), so it is very easy to obtain homoplasmic mtDNA and investigate the exact biochemical consequences of the mutation of interest.

R. Kucharczyk and J.-P. di Rago have used this approach to define the impact of five mutations in the mitochondrial *ATP6* gene found in patients with NARP and Leigh syndromes on ATP synthase (Rak, Tetaud et al. 2007a; Kucharczyk, Rak et al. 2009a; Kucharczyk, Salin et al. 2009b; Kucharczyk, Ezkurdia et al. 2010; Kucharczyk, Giraud et al. 2013). Three of these mutations (9176T>G, 8851T>C and 8993T>G) severely compromised the ability of yeast to grow on the respiratory carbon source, whereas it was much less, if at all, affected by the remaining two (9176T>C and 8993T>C). *In vitro*, the five mutations decreased the rate of mitochondrial ATP synthesis, by 30 to >95%. The three *atp6* mutants that grew well on the respiratory carbon source were much more sensitive *in vivo* to oligomycin, a specific inhibitor of ATP synthase, because less drug is required to reach the threshold of the ATP synthesis activity (20%) below which the yeast respiratory growth is compromised (Mukhopadhyay, Uh et al. 1994). The possibility to prepare large amounts of yeast mitochondria allowed to investigate the impact of the 8851T>C mutation with purified ATP synthase. It revealed a block in the rotation of the enzyme motor. It is to be noted that the pathogenic character of this mutation was uncertain due to the existence of only a very limited number of known cases. Its study in yeast provided strong evidence that it was truly responsible for the severe neurological disorders and premature death, a few weeks only after birth of the patients in whom the 8851T>C mutation was found. The 9176T>G mutation was shown to affect very severely the assembly of yeast ATP synthase by preventing incorporation of Atp6p, and we presented evidence that a similar effect occurs in human 9176T>G cells (Kucharczyk, Salin et al. 2009b). Interestingly, these studies in yeast were in line with what was known about the respective severities of these five mutations in humans they affect (De Meirleir, Seneca et al. 1995; Dionisi-Vici, Seneca et al. 1998; Baracca, Barogi et al. 2000; Carrozzo, Murray et al. 2000; Carrozzo, Rizza et al. 2004; Mattiazzi, Vijayvergiya et al. 2004; Houstek, Pickova et al.

2006; Morava, Rodenburg et al. 2006; Baracca, Sgarbi et al. 2007; Cortes-Hernandez, Vazquez-Memije et al. 2007).

I.6 MITOCHONDRIAL DNA MUTATIONS AND CANCER

One of the features of cancer cells is an enhanced level of lactic acid even in the presence of oxygen. The phenomenon is known as "aerobic glycolysis" or "Warburg effect" as it was first observed by Otto Warburg, who studied cancer cells. He proposed that this is a consequence of dysfunction of mitochondria (Warburg 1956a; Warburg 1956b). The intense studies of cancer cells showed that mitochondria in those cells have abnormal structures and impaired metabolism (John 2001; Ramanathan, Wang et al. 2005; Chen, Cairns et al. 2009; Galluzzi, Morselli et al. 2010). They produce more ROS, have altered calcium homeostasis and redox state of the cell, which change the activities of transcription factors, such as hypoxia-inducible factor 1α (HIF1α), and impair the intrinsic way of apoptosis (Galluzzi, Morselli et al. 2010; Wallace 2012). Mutations in the genes encoding isocytrate dehydrogenase, succinate dehydrogenase and fumarate hydratase were found in various cancers. They lead to accumulation of metabolic by-products (R-enantiomer of 2-hydroxyglutarate, succinate and fumarate, respectively) that were shown to have oncogenic activity (Wallace 2012; Gaude and Frezza 2014).

Mitochondrial DNA mutations were found in various tumors (1736 according to Lu at al., 2009), but it is not confirmed whether they are involved in tumorigenesis (Copeland, Wachsman et al. 2002; Brandon, Baldi et al. 2006; Lu, Sharma et al. 2009). Their direct impact was studied in cybrid cells, where mtDNA carrying mutations had been introduced to ρ^0 cells (King and Attardi 1989). Introduction of cybrid cells that carried mutations in the mtDNA at positions 8993T>G or 9176T>G of the *MTATP6* gene into nude mice, gave an advantage at the early stage of tumor growth probably by preventing apoptosis (Shidara, Yamagata et al. 2005). Moreover the PC3 prostate cancer cell line bearing the 8993T>G mutation in mtDNA generated tumors seven times larger than the same line without this mutation (Petros, Baumann et al. 2005). The 13997G>A and 13885insC mutations in the ND6 gene caused higher metastatic potential due to enhanced ROS production (Ishikawa, Takenaga et al. 2008). Human colorectal cancer cell line with the homoplasmic mtDNA mutation in ND5 gene was shown to have decreased oxygen consumption and ATP synthesis, increased lactate and ROS production, enhanced apoptotic potency and they were all

dependent on glucose. Interestingly, the same cell line with heteroplasmic mtDNA with the same mutation produced less ROS, probably due to activation of antioxidant enzymes, but showed enhanced growth of the tumor while the tumor growth in homoplasmic cell line was inhibited (Park, Sharma et al. 2009). The mitochondrial functions are, however, indispensable for cancer cells viability, as complete elimination of mtDNA reduces the growth of cancer cells on soft agar and tumor formation in nude mice (Morais, Zinkewich-Peotti et al. 1994; Cavalli, Varella-Garcia et al. 1997). Still, the role of mtDNA mutations in tumor development is not well known.

GOALS OF THE WORK

The first part of my work aimed at defining the consequences on yeast ATP synthase of two mutations of the mitochondrial *MTATP6* gene found in patients suffering from the NARP syndrome. Although the pathogenicity of these mutations has been established, nothing was known about their impact on the ATP synthase.

I then describe the construction of yeast models of mutations in *ATP6* that have been found in tumors. It has been hypothesized that these mutations may be at the origin or favor development of tumors by altering mitochondrial oxidative phosphorylation but the consequences of these mutations have never been characterized.

Yeast models of human ATP synthase can be used for the screening of drugs active against these disorders. I have investigated the suppressor mechanism of one of the hits that have been selected, chlorhexidine. My experiments aimed to determine how this drug influence the assembly of the ATP synthase in a mutant lacking a protein (Fmc1p) involved in this process.

Unexpectedly, some of the *atp6* mutations causing the NARP syndrome were found to up-regulate the Atp6p synthesis. My study of these mutations reveals a mechanism by which the synthesis of Atp6p is coupled to its assembly. Finally, I present experiments aiming to better understand how the Atp9p-ring is regulated in relation to its assembly. I present evidence for a mechanism in which Atp9p regulates its own synthesis.

MATERIALS AND METHODS

II. 1 STRAINS AND CULTURE CONDITIONS

II.1.1 Bacterial strains

Bacterial strains DH5α or XL1-Blue were used to amplify plasmids. Bacterial strain XL1-Gold was used to restore plasmids after ligation.

II.1.2 Yeast strains

All yeast strains used in this work are listed in Table 2:

Name	Alias	Nuclear genotype	Plasmid name	Insert	Ori.	Mitochondrial genotype	References
MR6	Ø	*Mata ade2-1 his3-11,15 trp1-1 leu2-3,112 ura3-1 CAN1 arg8::HIS3*	Ø	Ø	Ø	*WT*	(Rak, Tetaud et al. 2007b)
MR6 ρ^0	Ø	*Mata ade2-1 his3-11,15 trp1-1 leu2-3,112 ura3-1 CAN1 arg8::HIS3*	Ø	Ø	Ø	ρ^0	(Rak, Tetaud et al. 2007b)
RKY20	Ø	*Mata ade2-1 his3-11,15 trp1-1 leu2-3,112 ura3-1 CAN1 arg8::HIS3*	Ø	Ø	Ø	ρ^+ *atp6p L183P*	(Kucharczyk, Rak et al. 2009a)
RKY26	Ø	*Mata ade2-1 his3-11,15 trp1-1 leu2-3,112 ura3-1 CAN1 arg8::HIS3*	Ø	Ø	Ø	ρ^+ *atp9::ARG8*^{m}	(Bietenhader, Martos et al. 2012)
AMY10	Ø	*Mata ade2-1 his3-11,15 trp1-1 leu2-3,112 ura3-1 CAN1 arg8::HIS3*	pAM19	*ATP9-5*	2µ	ρ^+ *atp9::ARG8*^{m}	(Bietenhader, Martos et al. 2012)
MR10	Ø	*Mata ade2-1 his3-11,15 trp1-1 leu2-3,112 ura3-1 CAN1 arg8::HIS3*	Ø	Ø	Ø	ρ^+ *atp6::ARG8*^{m}	(Rak, Tetaud et al. 2007b)
DFS160/60 α	Ø	*Matα kar1-1 ade2-101 ura3-52 leu2 arg8::URA3*	Ø	Ø	Ø	ρ^0	(Steele, Butler et al. 1996)
DFS160/60 a	Ø	*Mata kar1-1 ade2-101 ura3-52 leu2 arg8::URA3*	Ø	Ø	Ø	ρ^0	(Steele, Butler et al. 1996)
NB40-3C	Ø	*Mata lys2 leu2-3,112 ura3-52 his3ΔHindIII arg8::hisG*	Ø	Ø	Ø	ρ^+ *cox2-62*	(Steele, Butler et al. 1996)
D273-10b	Ø	*Matα ade2-101 met6*	Ø	Ø	Ø	ρ^0	(Foury and Tzagoloff 1976)
AKY1	Ø	*Mata ade2-1 his3-11,15 trp1-1 leu2-3,112 ura3-1 CAN1 arg8::HIS3*	Ø	Ø	Ø	ρ^+ *atp6p I170V*	this study
AKY2	Ø	*Mata ade2-1 his3-11,15 trp1-1 leu2-3,112 ura3-1 CAN1 arg8::HIS3*	Ø	Ø	Ø	ρ^+ *atp6p L232P*	this study
AKY5	Ø	*Mata ade2-1 his3-11,15 trp1-1 leu2-3,112 ura3-1 CAN1 arg8::HIS3*	Ø	Ø	Ø	ρ^+ *atp6p S250P*	(Kabala, Lasserre et al. 2014)

Name	Alias	Nuclear genotype	Plasmid name	Insert	Ori.	Mitochondrial genotype	References
AKY6	MR6 *aep1*	*Mata ade2-1 his3-11,15 trp1-1 leu2-3,112 ura3-1 CAN1 arg8::HIS3 aep1::KanMX*	Ø	Ø	Ø	*WT*	this study
AKY7	MR6 *aep2*	*Mata ade2-1 his3-11,15 trp1-1 leu2-3,112 ura3-1 CAN1 arg8::HIS3 aep2::KanMX*	Ø	Ø	Ø	*WT*	this study
AKY8	Ø	*Matα kar1-1 ade2-101 ura3-52 leu2 arg8::URA3*	Ø	Ø	Ø	ρ^- *atp6p I170V*	this study
AKY9	Ø	*Matα kar1-1 ade2-101 ura3-52 leu2 arg8::URA3*	Ø	Ø	Ø	ρ^- *atp6p L232P*	this study
AKY13	Ø	*Matα kar1-1 ade2-101 ura3-52 leu2 arg8::URA3*	Ø	Ø	Ø	ρ^- *atp6p L250P*	(Kabala, Lasserre et al. 2014)
AKY14	Ø	*Matα kar1-1 ade2-101 ura3-52 leu2 arg8::URA3*	Ø	Ø	Ø	ρ^- *atp6p L252P*	(Kabala, Lasserre et al. 2014)
AKY27	RKY20 *atp23*	*Mata ade2-1 his3-11,15 trp1-1 leu2-3,112 ura3-1 CAN1 arg8::HIS3 atp23::KanMX*	Ø	Ø	Ø	ρ^+ *atp6p L183P*	this study
AKY28	MR6 *atp23*	*Mata ade2-1 his3-11,15 trp1-1 leu2-3,112 ura3-1 CAN1 arg8::HIS3 atp23::KanMX*	Ø	Ø	Ø	*WT*	this study
AKY27	Ø	*Mata ade2-1 his3-11,15 trp1-1 leu2-3,112 ura3-1 CAN1 arg8::HIS3 atp23::KanMX*	*pFL36*	*atp23-E168Q*		ρ^+ *atp6p L183P*	this study
AKY28	Ø	*Mata ade2-1 his3-11,15 trp1-1 leu2-3,112 ura3-1 CAN1 arg8::HIS3 atp23::KanMX*	*pFL36*	*atp23-E168Q*		*WT*	this study
AKY32	MR6 *atp15*	*Mata ade2-1 his3-11,15 trp1-1 leu2-3,112 ura3-1 CAN1 arg8::HIS3 atp15::KanMX*	Ø	Ø	Ø	*WT*	this study
AKY33	RKY20 *atp15*	*Mata ade2-1 his3-11,15 trp1-1 leu2-3,112 ura3-1 CAN1 arg8::HIS3 atp15::KanMX*	Ø	Ø	Ø	ρ^+ *atp6p L183P*	this study
AKY34	MR6 *atp7*	*Mata ade2-1 his3-11,15 trp1-1 leu2-3,112 ura3-1 CAN1 arg8::HIS3 atp7::KanMX*	Ø	Ø	Ø	*WT*	this study
AKY35	RKY20 *atp7*	*Mata ade2-1 his3-11,15 trp1-1 leu2-3,112 ura3-1 CAN1 arg8::HIS3 atp7::KanMX*	Ø	Ø	Ø	ρ^+ *atp6p L183P*	this study

Name	Alias	Nuclear genotype	Plasmid name	Insert	Ori.	Mitochondrial genotype	References
AKY36	MR6 *atp1*	*Mata ade2-1 his3-11,15 trp1-1 leu2-3,112 ura3-1 CAN1 arg8::HIS3 atp1::KanMX*	Ø	Ø	Ø	*WT*	this study
AKY37	RKY20 *atp1*	*Mata ade2-1 his3-11,15 trp1-1 leu2-3,112 ura3-1 CAN1 arg8::HIS3 atp1::KanMX*	Ø	Ø	Ø	ρ^+ *atp6p L183P*	this study
AKY38	MR6 *atp10*	*Mata ade2-1 his3-11,15 trp1-1 leu2-3,112 ura3-1 CAN1 arg8::HIS3 atp10::KanMX*	Ø	Ø	Ø	*WT*	this study
AKY39	RKY20 *atp10*	*Mata ade2-1 his3-11,15 trp1-1 leu2-3,112 ura3-1 CAN1 arg8::HIS3 atp10::KanMX*	Ø	Ø	Ø	ρ^+ *atp6p L183P*	this study
AKY40	MR6 *atp11*	*Mata ade2-1 his3-11,15 trp1-1 leu2-3,112 ura3-1 CAN1 arg8::HIS3 atp11::KanMX*	Ø	Ø	Ø	*WT*	this study
AKY41	RKY20 *atp11*	*Mata ade2-1 his3-11,15 trp1-1 leu2-3,112 ura3-1 CAN1 arg8::HIS3 atp11::KanMX*	Ø	Ø	Ø	ρ^+ *atp6p L183P*	this study
AKY42	MR6 *atp12*	*Mata ade2-1 his3-11,15 trp1-1 leu2-3,112 ura3-1 CAN1 arg8::HIS3 atp12::KanMX*	Ø	Ø	Ø	*WT*	this study
AKY43	RKY20 *atp12*	*Mata ade2-1 his3-11,15 trp1-1 leu2-3,112 ura3-1 CAN1 arg8::HIS3 atp12::KanMX*	Ø	Ø	Ø	ρ^+ *atp6p L183P*	this study
AKY52	AMY10/pRK57 *aep2*	*Mata ade2-1 his3-11,15 trp1-1 leu2-3,112 ura3-1 CAN1 arg8::HIS3 PaATP9-5 URA3 AEP1 LEU2 aep1::KanMX*	pAM19	*ATP9-5*	2µ	ρ^+ *atp9::ARG8*^{m}	this study
AKY60	AKY6/pAM19	*Mata ade2-1 his3-11,15 trp1-1 leu2-3,112 ura3-1 CAN1 arg8::HIS3 aep1::KanMX*	pAM19	*ATP9-5*	2µ	*WT*	this study
AKY60/pRK54	Ø	*Mata ade2-1 his3-11,15 trp1-1 leu2-3,112 ura3-1 CAN1 arg8::HIS3 aep1::KanMX*	pAM19	*ATP9-5*	2µ	*WT*	this study
			pRK54	*AEP1*	2µ		
AKY61	AKY7/pAM19	*Mata ade2-1 his3-11,15 trp1-1 leu2-3,112 ura3-1 CAN1 arg8::HIS3 aep2::KanMX*	pAM19	*ATP9-5*	2µ	*WT*	this study
AKY61/pRK57	Ø	*Mata ade2-1 his3-11,15 trp1-1 leu2-3,112 ura3-1 CAN1*	pAM19	*ATP9-5*	2µ	*WT*	this study

Name	Alias	Nuclear genotype	Plasmid name	Insert	Ori.	Mitochondrial genotype	References
		arg8::HIS3 aep2::KanMX	pRK57	*AEP2*	2µ		
AKY63	RKY20/pAM19 *aep1*	*Mata ade2-1 his3-11,15 trp1-1 leu2-3,112 ura3-1 CAN1 arg8::HIS3 aep1::KanMX*	pAM19	*ATP9-5*	2µ	ρ^+ *atp6p L183P*	this study
AKY64	RKY20/pAM19 *aep2*	*Mata ade2-1 his3-11,15 trp1-1 leu2-3,112 ura3-1 CAN1 arg8::HIS3 aep2::KanMX*	pAM19	*ATP9-5*	2µ	ρ^+ *atp6p L183P*	this study
AKY65	MR6/pAM19	*Mata ade2-1 his3-11,15 trp1-1 leu2-3,112 ura3-1 CAN1 arg8::HIS3*	pAM19	*ATP9-5*	2µ	*WT*	this study
AKY74	AKY65 *atp25*	*Mata ade2-1 his3-11,15 trp1-1 leu2-3,112 ura3-1 CAN1 arg8::HIS3 atp25::KanMX*	pAM19	*ATP9-5*	2µ	*WT*	this study
AKY74/pRK56	Ø	*Mata ade2-1 his3-11,15 trp1-1 leu2-3,112 ura3-1 CAN1 arg8::HIS3 atp25::KanMX*	pAM19	*ATP9-5*	2µ	*WT*	this study
			pRK56	*ATP25-HA*	2µ		
AKY74/pG29ST32	Ø	*Mata ade2-1 his3-11,15 trp1-1 leu2-3,112 ura3-1 CAN1 arg8::HIS3 atp25::KanMX*	pAM19	Pa*ATP9-5*	2µ	*WT*	this study
			pG29ST32	N-terminal *ATP25-HA*	2µ		
AKY75	RKY20/pAM19	*Mata ade2-1 his3-11,15 trp1-1 leu2-3,112 ura3-1 CAN1 arg8::HIS3*	pAM19	*ATP9-5*	2µ	ρ^+ *atp6p L183P*	this study
AKY76	MR6 *fmc1*	*Mata ade2-1 his3-11,15 trp1-1 leu2-3,112 ura3-1 CAN1 arg8::HIS3 fmc1::KanMX*	Ø	Ø	Ø	*WT*	this study
AKY77	RKY20 *fmc1*	*Mata ade2-1 his3-11,15 trp1-1 leu2-3,112 ura3-1 CAN1 arg8::HIS3 fmc1::KanMX*	Ø	Ø	Ø	ρ^+ *atp6p L183P*	this study
AKY121	AKY42/pAM19	*Mata ade2-1 his3-11,15 trp1-1 leu2-3,112 ura3-1 CAN1 arg8::HIS3 atp12::KanMX*	pAM19	*ATP9-5*	2µ	*WT*	this study
AKY138	Ø	*Mata ade2-1 his3-11,15 trp1-1 leu2-3,112 ura3-1 CAN1 arg8::HIS3 atp25::KanMX*	pAM19	*ATP9-5*	2µ	*WT*	this study
			pAK19	C-terminal *ATP25-HA*	2µ		

Name	Alias	Nuclear genotype	Plasmid name	Insert	Ori.	Mitochondrial genotype	References
AKY139	Ø	*Mata ade2-1 his3-11,15 trp1-1 leu2-3,112 ura3-1 CAN1 arg8::HIS3 atp25::KanMX*	pAM19	*ATP9-5*	2µ	*WT*	this study
			pAK19	C-terminal *ATP25-HA*	2µ		
			pG29ST32	N-terminal *ATP25-HA*	2µ		
AKY140	Ø	*Mata ade2-1 his3-11,15 trp1-1 leu2-3,112 ura3-1 CAN1 arg8::HIS3 atp25::KanMX*	pAM19	*ATP9-5*	2µ	ρ^+ *atp9::ARG8*^{m}	this study
			pAK19	C-terminal *ATP25-HA*	2µ		
AKY141	Ø	*Mata ade2-1 his3-11,15 trp1-1 leu2-3,112 ura3-1 CAN1 arg8::HIS3 atp25::KanMX*	pAM19	*ATP9-5*	2µ	ρ^+ *atp9::ARG8*^{m}	this study
			pAK19	C-terminal *ATP25-HA*	2µ		
			pG29ST32	N-terminal *ATP25-HA*	2µ		
RKY39	Ø	*Mata ade2-1 his3-11,15 trp1-1 leu2-3,112 ura3-1 CAN1 arg8::HIS3*	Ø	Ø	Ø	ρ^+ *atp6p-W136R*	this study
RKY39 1G	Ø	*Mata ade2-1 his3-11,15 trp1-1 leu2-3,112 ura3-1 CAN1 arg8::HIS3*	Ø	Ø	Ø	ρ^+ *atp6p-R136I*	this study
RKY39 5G	Ø	*Mata ade2-1 his3-11,15 trp1-1 leu2-3,112 ura3-1 CAN1 arg8::HIS3*	Ø	Ø	Ø	ρ^+ *atp6p-R136G*	this study
RKY39 6G	Ø	*Mata ade2-1 his3-11,15 trp1-1 leu2-3,112 ura3-1 CAN1 arg8::HIS3*	Ø	Ø	Ø	ρ^+ *atp6p-W136R,R179I*	this study
RKY39 16G	Ø	*Mata ade2-1 his3-11,15 trp1-1 leu2-3,112 ura3-1 CAN1 arg8::HIS3*	Ø	Ø	Ø	ρ^+ *atp6p-R136K*	this study
RKY60	Ø	*Mata ade2-1 his3-11,15 trp1-1 leu2-3,112 ura3-1 CAN1 arg8::HIS3*	Ø	Ø	Ø	ρ^+ *atp6p-P157T*	this study

Name	Alias	Nuclear genotype	Plasmid name	Insert	Ori.	Mitochondrial genotype	References
RKY61	Ø	*Mata ade2-1 his3-11,15 trp1-1 leu2-3,112 ura3-1 CAN1 arg8::HIS3*	Ø	Ø	Ø	ρ^+ *atp6p-P163S*	this study
RKY62	Ø	*Mata ade2-1 his3-11,15 trp1-1 leu2-3,112 ura3-1 CAN1 arg8::HIS3*	Ø	Ø	Ø	ρ^+ *atp6p-K90E*	this study
RKY66	Ø	*Mata ade2-1 his3-11,15 trp1-1 leu2-3,112 ura3-1 CAN1 arg8::HIS3*	Ø	Ø	Ø	ρ^+ *atp6p-L252P*	(Kabala, Lasserre et al. 2014)
RKY89	Ø	*Mata ade2-1 his3-11,15 trp1-1 leu2-3,112 ura3-1 CAN1 arg8::HIS3 atp25::KanMX4*	pAM19	*ATP9-5*	2µ	ρ^+ *atp9::ARG8*^{m}	this study
			pRK56	*ATP25-HA*	2µ		
RKY92	Ø	*Mata ade2-1 his3-11,15 trp1-1 leu2-3,112 ura3-1 CAN1 arg8::HIS3 aep1::KanMX4*	pAM19	*ATP9-5*	2µ	ρ^+ *atp9::ARG8*^{m}	this study
			pRK54	*AEP1*	2µ		
RKY93	Ø	*Mata ade2-1 his3-11,15 trp1-1 leu2-3,112 ura3-1 CAN1 arg8::HIS3 aep1::KanMX4*	pAM19	*ATP9-5*	2µ	ρ^+ *atp9::ARG8*^{m}	this study
RKY94	Ø	*Mata ade2-1 his3-11,15 trp1-1 leu2-3,112 ura3-1 CAN1 arg8::HIS3 aep2::KanMX4*	pAM19	*ATP9-5*	2µ	ρ^+ *atp9::ARG8*^{m}	this study
RKY95	Ø	*Mata ade2-1 his3-11,15 trp1-1 leu2-3,112 ura3-1 CAN1 arg8::HIS3 atp25::KanMX4*	pAM19	*ATP9-5*	2µ	ρ^+ *atp9::ARG8*^{m}	this study
RKY95/pG29ST32	Ø	*Mata ade2-1 his3-11,15 trp1-1 leu2-3,112 ura3-1 CAN1 arg8::HIS3 atp25::KanMX4*	pAM19	*ATP9-5*	2µ	ρ^+ *atp9::ARG8*^{m}	this study
			pG29ST32	N-terminal *ATP25-HA*	2µ		
RKY96	Ø	*Mata ade2-1 his3-11,15 trp1-1 leu2-3,112 ura3-1 CAN1 arg8::HIS3*	pAM19	*ATP9-5*	2µ	ρ^+ *atp9::ARG8*^{m}	this study
			pRK54	*AEP1*	2µ		
RKY97	Ø	*Mata ade2-1 his3-11,15 trp1-1 leu2-3,112 ura3-1 CAN1 arg8::HIS3*	pAM19	*ATP9-5*	2µ	ρ^+ *atp9::ARG8*^{m}	this study
			pRK57	*AEP2*	2µ		
FG146	MR10/pAM19	*Mata ade2-1 his3-11,15 trp1-1 leu2-3,112 ura3-1 CAN1 arg8::HIS3*	pAM19	*ATP9-5*	2µ	ρ^+ *atp6::ARG8*^{m}	this study

Name	Alias	Nuclear genotype	Plasmid name	Insert	Ori.	Mitochondrial genotype	References
FG151	*atp12Δatp6Δ*	*Mata ade2-1 his3-11,15 trp1-1 leu2-3,112 ura3-1 CAN1 arg8::HIS3 atp12::KanMX4*	Ø	Ø	Ø	ρ^+ *atp6::ARG8*^{m}	this study
FG152	FG151/pAM19	*Mata ade2-1 his3-11,15 trp1-1 leu2-3,112 ura3-1 CAN1 arg8::HIS3 atp12::KanMX4*	pAM19	*ATP9-5*	2μ	ρ^+ *atp6::ARG8*^{m}	this study
FG153	*atp12Δatp9Δ*	*Mata ade2-1 his3-11,15 trp1-1 leu2-3,112 ura3-1 CAN1 arg8::HIS3 atp12::KanMX4*	Ø	Ø	Ø	ρ^+ *atp9::ARG8*^{m}	this study
FG154	FG154/pAM19	*Mata ade2-1 his3-11,15 trp1-1 leu2-3,112 ura3-1 CAN1 arg8::HIS3 atp12::KanMX4*	pAM19	*ATP9-5*	2μ	ρ^+ *atp9::ARG8*^{m}	this study

Table 2 – Table of yeast strains used in the study.

II.1.3 Bacterial media

Lysogeny Broth (LB): bacto-tryptone 10 g/l, bacto-yeast extract 5 g/l, NaCl 10 g/l. Solid medium was prepared with 15 g/l of bactoagar. Optionally antibiotic ampiciline was added to obtain final concentration of 100 g/l (LBA).

SOC: bacto-peptone 20 g/l, bacto-yeast extract 5 g/l, 10 mM NaCl, 2.5 mM KCl, $1/100^{th}$ volume of 2 M glucose. Before use $1/100^{th}$ volume of sterile filtered 1 M $MgCl_2$/1 M $MgSO_4$ was added.

II.1.4 Yeast media

YPDA: bacto-yeast extract 10 g/l, bacto-peptone 10 g/l, glucose 20 g/l, adenine 50 mg/l, for solid medium agar 20 g/l.

YPDA for -80°C: bacto-yeast extract 10 g/l, bacto-peptone 10 g/l, glucose 20 g/l, adenine 50 mg/l, glycerol 250 ml/l.

YPGalA: bacto-yeast extract 10 g/l, bacto-peptone 10 g/l, galactose 20 g/l, adenine 50 mg/l, for solid medium agar 20 g/l.

YPGA: bacto-yeast extract 10 g/l, bacto-peptone 10 g/l, glycerol 20 ml/l, adenine 50 mg/l, for solid medium agar 20 g/l.

DOX: bacto-yeast extract 10 g/l, bacto-peptone 10 g/l, glycerol 20 ml/l, adenine 50 mg/l, for solid medium agar 20 g/l, doxycycline 40 μg/ml.

YPGEA: bacto-yeast extract 10 g/l, bacto-peptone 10 g/l, glycerol 20 ml/l, ethanol 30 ml/l, adenine 50 mg/l, for solid medium agar 20 g/l.

BET: bacto-yeast extract 10 g/l, bacto-peptone 10 g/l, glucose 20 g/l, adenine 50 mg/l, for solid medium agar 20 g/l, ethidium bromide 40 μg/l.

G418: bacto-yeast extract 10 g/l, bacto-peptone 10 g/l, glucose 20 g/l, adenine 50 mg/l, agar 20 g/l, G418 sulphate 200 or 250 mg/l.

Complete synthetic medium (CSM): glucose or galactose 20 g/l or glycerol 20 ml/l, yeast nitrogen base 1.7 g/l, ammonium sulfate 5 g/l, CSM-AA (a mix of amino acids and nucleotides without selected amino acids) as recommended, supplementary amino acids of need: adenine 50 mg/l, tryptophan 50 mg/l, leucine 100 mg/l, arginine 50 mg/l, uracil 20 mg/l.

W0 without amino acids and ammonium sulfate: galactose 20 g/l, yeast nitrogen base 1.7 g/l, supplementary amino acids of need: adenine 50 mg/l, tryptophan 50 mg/l, leucine 100 mg/l, arginine 50 mg/l, uracil 20 mg/l.

BIOL3: glucose 50 g/l, yeast nitrogen base 1.67 g/l, ammonium sulfate 5 g/l, CSM – leucine 0.8 g/l, sorbitol 182.7 g, adenine 40 mg/l, agar 30 g/l.

II.1.5 Culture conditions for bacteria

Bacteria cells were incubated at 37°C on plates or in liquid with shaking at 180 rpm. Optic density (OD) at 600 nm was measured to estimate the number of bacteria cells in the cultures.

II.1.6 Culture conditions for yeast

Yeast cells were incubated at 28°C, 35°C – 37°C on plates or in liquid with shaking at 150-180 rpm. Optic density (OD) at 650 nm was measured to estimate quantity of yeast cells in the cultures. 1 OD corresponds to 1.2 10^7 of cells per milliliter.

II.1.7 Preserving bacteria and yeast

Bacteria as well as yeast strains were preserved in -80°C. Bacteria in LB medium containing 50% v/v glycerol, yeast cells in YPDA medium contains 25 – 50% v/v glycerol.

II.2. GENETIC TECHNIQUES

II.2.1 Preparation of competent bacterial cells for transformation

Pre-culture of bacteria was prepared in LB liquid medium at 18°C for 2 days. Fresh 250 ml of SOC medium was inoculated and incubated with shaking (225-250 rpm) at 18°C till OD_{600} reached 0.6. Cultures were kept on ice for 10 minutes and centrifuged for 5 minutes at 4°C, 2,500 g. The pellet was re-suspended in TB buffer (10 mM PIPES, 15 mM $CaCl_2$, 250 mM KCl, 55 mM $MnCl_2$ $4H_2O$, pH 6.7), put in ice for 10 minutes and re-centrifuged in the same conditions as before. The pellet was re-suspended in 20 ml freshly prepared TB-DMSO (7% DMSO in ice-cold TB), incubated on ice for 10 minutes. After that time small portions of bacterial suspensions were frozen in liquid nitrogen. Competent cells were preserved at -80°C.

II.2.2 Transformation of bacteria by heat-shock

Plasmid DNA was introduced into cells by heat shock transformation. Previously prepared competent bacterial cells were thawed in ice. About 1 µg of plasmid or ligation mixture was added to 50 µl of bacteria and incubated for 30 minutes on ice. Heat shock was obtained by moving bacteria to 42°C for 2 minutes, and again into ice for 10 minutes. After the heat shock cells were regenerated at 37°C in liquid LB medium for 1 hour and spread on LBA plate to select cells with the plasmid of interest. Colonies were visible after one night incubation at 37°C.

II.2.3 Crossbreeding of two yeasts strains

Crossbreeding of yeast occurred between strains with opposite sexual mating types (*MATa* and *MATα*). It was realized by two methods. The first one, the so-called "drop on drop", took place on a YPDA plate where 10 µl drops of each strain pre-cultured in liquid medium, were laid one on another. In the second one, about 250 µl of one strain from fresh liquid culture were spread on a YPDA plate. Another strain was transferred on the plate by replica from the plate that contained single colonies. The crossed cells were replicated on selective medias to select the clones of interest.

II.2.4 Estimation of percentage of ρ^-/ρ^0 cells in a culture

Some mutations in both nuclear and mitochondrial DNA cause instability of mtDNA. In order to verify the stability of the mitochondrial genome, percentage of ρ^-/ρ^0 in cell cultures

was estimated. About 100 colonies from liquid cultures were spread on YPDA plates. A fermentable source of carbon permits growth of ρ^{-}/ρ^{0} as well as ρ^{+} cells. After appearance of single colonies they were replicated on medium permitting the growth of ρ^{+} cells only. Strains containing *WT* mtDNA were replicated on YPGA plates, whereas for strains containing *ARG8m* auxotrophic marker introduced into mtDNA, selection medium was CSM-R. Only cells containing intact mtDNA could grow.

Identification of ρ^{+} cells for strains with deletion of nuclear genes resulting in lack of growth on non-fermentable carbon source despite the presence of mtDNA, was achieved by crossing single colonies grown on YPDA plates with a D273.10B ρ^{0} strain and by replication of diploids on the YPGA medium. Crossbreeding with the D273.10B ρ^{0} strain complemented deletion in nuclear DNA but did not deliver any additional mtDNA. As a result, only cells that contained mtDNA from the analyzed strain could grow on the YPGA medium.

In each case the percentage of ρ^{-}/ρ^{0} cells was calculated between the number of colonies that grew on selective medium and the number of colonies that grew on YPDA plate.

II.2.5 Transformation of plasmid or linear DNA into yeast cells

10^{7} yeast cells from the fresh liquid culture were centrifuged and washed once with sterile water. The cells were re-suspended in 360 µl of the sterile solution containing: 34% (m/v) of polyethylene glycol 3350, lithium acetate 0.1 mol/L, denaturated DNA of salmon sperm 0.28 mg/ml, 1 – 2 µg of plasmid or linear DNA. Cells were incubated at 28°C with shacking for 30 minutes in order to loosen the cell wall. Heat shock for strains presenting *WT* respiratory growth was done at 42°C for 20 minutes (respiratory efficient cells) or at 37°C for 10 minutes (respiratory deficient cells). After the heat shock cells were centrifuged and re-suspended in 1ml of liquid YPDA and incubated at 28°C with shaking for maximal 1 hour to regenerate them after transformation. Then the cells were centrifuged again and spread on a solid selection medium (Gietz and Schiestl 2007)

II.2.6 Deletion of yeast nuclear genes

Deletions of yeast nuclear genes were made by homologous recombination of the *KanMX4* cassette into a *locus* of the gene of interest. Yeast bearing this gene acquired resistance to geneticin (G418). Deletion cassettes were amplified by PCR using as a matrix a total DNA isolated from strains from the *Euroscarf* collection of gene deletions. The *KanMX4* gene was amplified with 200 – 300bp flanks containing up-stream and down-stream

sequences of the gene of interest by "upper" and "lower" primers (Table 4, Fig. 19). Transformation with the cassette was performed as described above. Cells in which the *KanMX4* gene was integrated into nuclear DNA were selected on glucose medium supplemented with G418 (200 µg/ml). The correct integration was verified by PCR. Total DNA from the selected clones was isolated and PCR was performed using primers: complement to internal sequence of the *KanMX4* gene and to the up-stream sequence of the gene of interest before the sequence of "upper" primer used to amplify the cassette ("verif") (Fig. 19). Sequences of the primers used in the study are presented in Table 4.

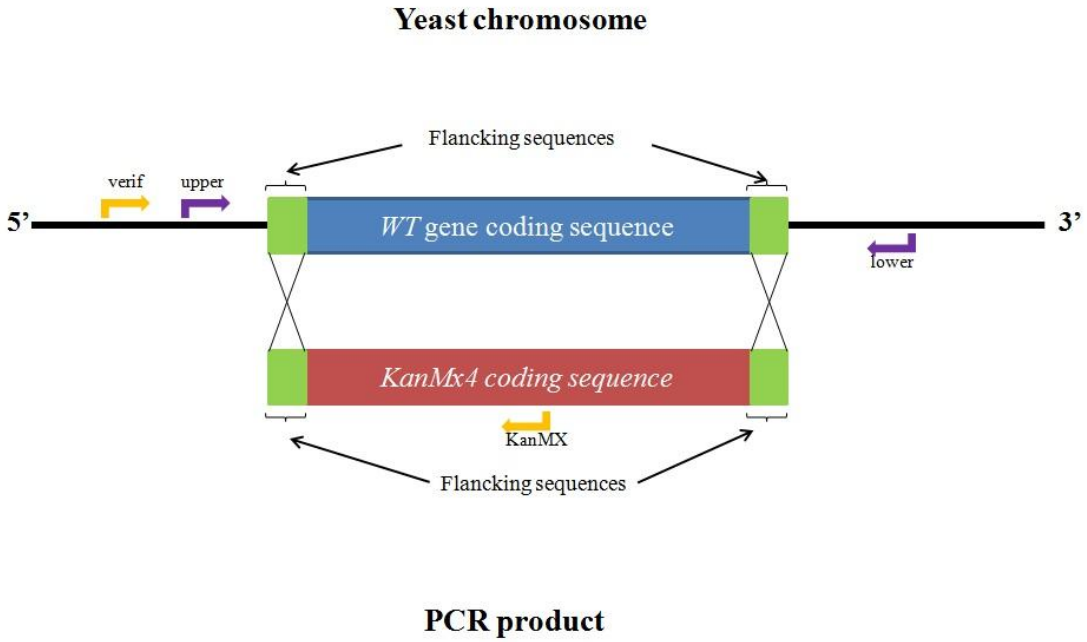

Figure 19 – Schema illustrating deletion of genes in yeast nuclear DNA with the*KanMX4* deletion cassette. Positions of primers designed for every gene are indicated with arrows.

II.2.7 Transformation of plasmid DNA into yeast mitochondria by the biolistic method

Plasmid encoding the mutated versions of the *ATP6* gene and wild type sequence of the *COX2* gene was co-transformed with the *LEU2*-bearing plasmid Yep351 into DFS160 ρ^0 strain by microprojectile bombardement with the use of the biolistic PDS-100/He particle delivery system (Bio-Rad) as described previously (Bonnefoy and Fox 2001b). Mitochondrial transformants were identified among leucine prototrophes by their ability to produce respiring clones when crossed to the non-respiring strain NB40-3c that contains a deletion of the mitochondrial *COX2* gene.

II.2.8 Cytoduction of mitochondrial genome between two yeasts strains

Cytoduction of mitochondrial DNA into ρ^0 cells is possible thanks to the mutation of the *kar1-1* in *KAR1* gene. Cells with this mutation can form zygotes but cannot form a diploid nucleus. Efficiency of diploid cells in crossing with wild type *KAR1* strains is 5% (Conde and Fink 1976). Cytoplasm of two parental cells mix in the zygote, enabling the transfer of mtDNA into ρ^0 strain. After crossing of the donor strain of mtDNA bearing the *kar1-1* (DFS160/60) mutation and the acceptor ρ^0 strain of desired nuclear background by the "drop on drop" method, the cells were cultured in 50 ml of YPDA liquid medium containing 5 – 10% glucose for a night. Cells were transferred into fresh YPDA (5% glucose) medium twice, to separate the nucleus and mitochondria of ρ^+ and ρ^0 types. 1,000 cells were spread on YPDA plates at the density of 100 cells per plate and their genotypes were analyzed by replication on selection media, to identify the type of nucleus and the presence/type of mtDNA.

II.2.9 Construction of atp6-mutant strains

The QuikChange XL Site-directed Mutagenesis Kit of Stratagene, was used for the mutagenesis reaction performed on the *Bam*HI-*Eco*RI fragment of the *ATP6* locus cloned into pUC19 (plasmid pSDC8, see (Zeng, Kucharczyk et al. 2007b)). The mutated *ATP6* fragments were liberated and ligated with pJM2 (Steele, Butler et al. 1996) cut with *Bam*HI and *Eco*RI, yielding plasmids that contained the yeast mitochondrial *COX2* gene as a marker for mitochondrial transformation and *Bam*HI-*Eco*RI fragments of mutated *ATP6* genes. The 3' part of the wild type *ATP6* locus was excised with SapI and EcoRI from pSDC9 (Rak, Tetaud et al. 2007a) and ligated between the same sites of previously obtained plasmids (pRK28, pRK29, pRK27, pRK30, pRK36, pSDC14-*atp6-S250P*, pSDC14-*atp6-L252P*, Table 3), which resulted in final plasmids used for yeast transformation (pRK32, pRK33, pRK31, pAK4-6, pAK5-1, pRK37, pRK38 Table 3). The plasmids were introduced by co-transformation with the nuclear selectable *LEU2* gene containing plasmid Yep351 into the ρ^0 strain DFS160 by microprojectile bombardment with the use of the biolistic PDS-1000/He particle delivery system (Bio-Rad) as described previously (Bonnefoy and Fox 2001b). Mitochondrial transformants (ρ^- synthetic) were identified among the Leu+ nuclear transformants by their ability to produce respiring clones when mated to the non-respiring NB40-3c strain bearing a deletion in the mitochondrial *COX2* gene. The ρ^- synthetic clones were crossed to the *atp6::ARG8m* deletion strain MR10 (Rak, Tetaud et al. 2007b) for the

production of clones harboring the MR10 nucleus and where the *ARG8m* ORF (Steele, Butler et al. 1996) had been replaced by recombination with the mutated *atp6* genes. The ρ+ clones were identified by its arginine auxotrophy and the ability to grow on respiratory medium. The presence of the desired mutation in *atp6* locus was verified by sequencing.

II.3. TECHNIQUES IN MOLECULAR BIOLOGY

II.3.1 List of plasmids used in the study

Plasmid name	**Marker gene**	**Origin of replication**	**Restriction sites used for construction**		**Original vector**	**Insert**	**Source**
			5'	**3'**			
pSDC8	AMP^r	pUC (E.coli origin of replication)	BamHI	EcoRI	pUC19	*ATP6* – N-terminal (1010 bp)	(Rak, Tetaud et al. 2007a)
pSDC9	AMP^r	pUC (E.coli origin of replication)	EcoRI	BamHI	pUC19	*ATP6* – C-terminal (360 bp)	(Rak, Tetaud et al. 2007a)
pJM2	AMP^r	pUC (E.coli origin of replication)	Ø	Ø	pTZ18u	*COX2*	(Bonnefoy, Bsat et al. 2001a)
pSDC14	AMP^r	pUC (E.coli origin of replication)	BamHI	EcoRI	pJM2	*ATP6* – N-terminal (1010 bp)	(Rak, Tetaud et al. 2007a)
pSDC14-*atp6-S250P*	AMP^r	pUC (E.coli origin of replication)	BamHI	EcoRI	pJM2	*atp6-S250P* short	(Kabala, Lasserre et al. 2014)
pSDC14-*atp6-L252P*	AMP^r	pUC (E.coli origin of replication)	BamHI	EcoRI	pJM2	*atp6-L252P* short	(Kabala, Lasserre et al. 2014)
pRK37	AMP^r	pUC (E.coli origin of replication)	EcoRI	SapI	pJM2	*atp6-S250P* whole gene	(Kabala, Lasserre et al. 2014)
pRK38	AMP^r	pUC (E.coli origin of replication)	EcoRI	SapI	pJM2	*atp6-L252P* whole gene	(Kabala, Lasserre et al. 2014)
pAK1	AMP^r	pUC (E.coli origin of replication)	BamHI	EcoRI	pJM2	*atp6p-I170V* short	this study
pAK2	AMP^r	pUC (E.coli origin of replication)	BamHI	EcoRI	pJM2	*atp6p-L232P* short	this study
pRK27	AMP^r	pUC (E.coli origin of replication)	BamHI	EcoRI	pJM2	*atp6-P163S* short	this study
pRK28	AMP^r	pUC (E.coli origin of replication)	BamHI	EcoRI	pJM2	*atp6-K90E* short	this study

Plasmid name	**Marker gene**	**Origin of replication**	**Restriction sites used for construction**		**Original vector**	**Insert**	**Source**
			5'	**3'**			
pRK29	AMP^r	pUC (E.coli origin of replication)	BamHI	EcoRI	pJM2	*atp6-P157T* short	this study
pAK4	AMP^r	pUC (E.coli origin of replication)	EcoRI	SapI	pJM2	*atp6p-I170V* whole gene	this study
pAK5	AMP^r	pUC (E.coli origin of replication)	EcoRI	SapI	pJM2	*atp6p-L232P* whole gene	this study
pRK31	AMP^r	pUC (E.coli origin of replication)	EcoRI	SapI	pJM2	*atp6-P163S* whole gene	this study
pRK32	AMP^r	pUC (E.coli origin of replication)	EcoRI	SapI	pJM2	*atp6-K90E* whole gene	this study
pRK33	AMP^r	pUC (E.coli origin of replication)	EcoRI	SapI	pJM2	*atp6-P157T* whole gene	this study
pAM19	URA3	2µ	BamHI	PstI	pCM190	*ATP9-5*	(Bietenhader, Martos et al. 2012)
pFL38	URA3	CEN	BamHI	BamHI	pFL38	*atp23-E168Q*	(Osman, Wilmes et al. 2007)
pRK56	LEU2	2µ	SacI	HindIII	Yep351	*ATP25-HA*	this study
pG29ST32	LEU2	2µ	BamHI	PstI	Yep351	N-terminal of *ATP25-HA*	(Zeng, Barros et al. 2008)
pG29ST23	URA3	2µ	BamHI	HindIII	Yep352	C-terminal of *ATP25-*HA	(Zeng, Barros et al. 2008)
pAK19	TRP1	2µ	blunt (NotI)	BamHI	pRS424	MTS-C-terminal of *ATP25-HA*	this study
pRK54	LEU2	2µ	BamHI	PstI	Yep351	*AEP1*	this study
pRK57	LEU2	2µ	XbaI	SalI	Yep351	*AEP2*	this study
pYX232	AMP^r	TPI	EcoRI	HindIII	pYX	*mtGFP*	(Westermann and Neupert 2000)

Table 3 – Table of plasmids used in the study

II.3.2 List of primers used in the study

Gene	Sequence of primers for construction of the strains
ATP1 (YBL099W)	Upper: 5' GTAGAGATATTATACTGTCATAGCTC 3'
	Lower: 5' GAATAAACTAGAGGCTATTGTGG 3'
	Verif: 5' GGTCATATCAAATTCACATCAGAC 3'
ATP7 (YKL016C)	Upper: 5' CACTTGCTGCTTAGCGTAGGTG 3'
	Lower: 5' TTCACGTTCATGCTTGATGCTTG 3'
	Verif: 5' GATTGGATATTTGTCTTGATGCC 3'
ATP10 (YLR393W)	Upper: 5' CTCGCCACATCACTATGCAGC 3'
	Lower: 5' GCTGCGAACAGAGGATATGAGC 3'
	Verif: 5' CCACCTGACTAATTGCATTACAG 3'
ATP11 (YNL315C)	Upper: 5' GTGCCGTATCAGTAGTCGTAGAAGC 3'
	Lower: 5'GCTGCTGGGAGGTACTCAACATCAG 3'
	Verif: 5'GTACTCATCGAGCACCCTTTGC 3'
ATP12 (YJL180C)	Upper: 5' GTGTCCTGGCGTTTCTTAAGCTCAC 3'
	Lower: 5' CACACGGAAGCTGTATCGCACTC 3'
	Verif: 5' GCTAGCTGCTGATTGACCATATCC 3'
ATP15 (YPL271W)	Upper: 5' CACACTAAGTCTGGCAACGCGC 3'
	Lower: 5' GCGATTGGCGATGATGGGAC 3'
	Verif: 5' GCCATGAACTTGAGGAATTGG 3'
ATP23 (YNR020C)	Upper: 5' GTTCGTCATATGATAATGCTTGG 3'
	Lower: 5'GACCAAGTGTCATGTGTACGTTG 3'
	Verif: 5' GAACAACACACCTAGAGCACAC 3'
FMC1 (YIL098C)	Upper: 5' GCTTGATACGTTTGGACAGTAGTTC 3'
	Lower: 5' TACTTCATTCTGGGATGCCTATC 3'
	Verif: 5'GCTAGTGCCAACTCGTCGTG 3'
AEP1 (YMR064W)	Upper: 5' CGTAGCACTTTGTTGTTCCATGC 3'
	Lower: 5' CATTTGTCGCAACGGAATTATCTG 3'
	Verif: 5' GGTTCACCCGATTTCACTGG 3'
AEP2 (YMR282C)	Upper: 5' CCTTTGTACCAAATATACTGAAG 3'
	Lower: 5' CATCGTTTTAAAGTACAACTCC 3'
	Verif: 5' GCTTTACGATCCACATTCCC3'
ATP25 (YMR098C)	Upper: 5' CTAACCTCTCTTCTAATATACTTGC 3'
	Lower: 5' GCATTCAGGTCTGAGTAATGAGC 3'
	Verif: 5' GAAATGGGGTCACAATCATCC 3'
KanMX	5' GGATGTATGGGCTAAATGTACG 3'
atp6-K90E	forward: 5`GCTTAAAGGACAAATTGGAGGT**GAA**AATTGAGGTTTATATTTCCCTATG 3'
	reverse: 5'CATAGGGAAATATAAACCTCAATT**TTC**ACCTCCAATTTGTCCTTTAAGC 3'
atp6-P157T	forward: 5`GGTTGAGTATTCTTCTCATTATTCGTA**ACT**GCTGGTACACCATTACC 3'
	reverse: 5' GGTAATGGTGTACCAGC**AGT**TACGAATAATGAGAAGAATACTCAACC 3'
atp6-P163S	forward: 5`TCATTATTCGTACCTGCTGGTACACCATTA**TCA**TTAGTACCTTTATTAGTTATTA TTGAAACTTTATCTTATTTCGCTAGA 3'
	reverse: 5' TCTAGCGAAATAAGATAAAGTTTCAATAATAACTAATAAAGGTACTAA**TGA**TAA TGGTGTACCAGCAGGTACGAATAATGA 3'
atp6-I170V	forward: 5`CCATTAGTACCTTTATTAGTT**GTT**ATTGAAACTTTATCTTATTTCGCTAGAGC 3'
	reverse: 5' GCTCTAGCGAAATAAGATAAAGTTTCAAT**AAC**AACTAATAAAGGTACTAATGG 3'

Gene	Sequence of primers for construction of the strains
atp6-L232P	forward: 5`GCTATGATCTTAGCCATTATGATG**CCA**GAATTCACTGGCCGTCGTTTTACAACG TCG 3’
	reverse: 5’ CGACGTTGTAAAACGACGGCCAGTGAATTC**TGG**CATCATAATGGCTAAGATCAT AGC 3’
atp6-S250P	forward: 5’ GTCTGGGCTATTTTAACAGCA**CCA**TATTTAAAAGATGCAGTATACTTACAT 3’
	reverse: 5’ATGTAAGTATACTGCATCTTTTAAATA**TGG**TGCTGTTAAAATAGCCCAGAC
atp6-L252P	forward: 5’ GTCTGGGCTATTTTAACAGCATCATAT**CCA**AAAGATGCAGTATACTTACAT 3’
	reverse: 5’ ATGTAAGTATACTGCATCTTT**TGG**ATATGATGCTGTTAAAATAGCCCAGAC 3’

Table 4 – The list of primers used for amplification of deletion cassettes and introduction of mutations into *ATP6* gene

II.3.3 Isolation of plasmids from bacterial cells

Plasmids were extracted from bacteria with the alcalic lysis method. Bacteria cells cultured in liquid LBA medium were centrifuged and treated with GTE solution (50 mM glucose, 25 mM Tris-HCl pH 8, 10 mM EDTA pH 8) containing RNAse (0.5 µg/µl final concentration). After 5 minutes lysis buffer (0.2 M NaOH, 1% SDS) was added and cells were kept for 5 minutes on ice. To stop the lysis and precipitate proteins 7.5 M NH_3Ac were added and suspension was shaken strongly 3 – 4 times and incubated for 5 minutes more on ice and then centrifuged for 6 minutes at 14,000 rpm. The supernatant containing plasmid DNA was recuperated and followed by precipitation of plasmid DNA with 96% ethanol.

II.3.4 Extraction of yeast DNA

Extraction of yeast DNA was used to obtain templates for PCR. 1.2 10^9 of the cells were centrifuged. The pellet was re-suspended in solution I (1 M sorbitol, 0.1 M EDTA pH 7.5) containing 200 µg of Zymolyase 20T. Cells were incubated for 1 hour at 37°C to have the cell wall digested. Spheroplasts were centrifuged at 6,000 g for 5 minutes and the pellet was re-suspended in solution II (50 mM Tris-HCl, 20 mM EDTA pH 7.4, SDS for the final concentration of 1% m/v). After 30 minutes of incubation at 65°C, potassium acetate was added to final concentration of 1.4 M. The suspension was incubated at 4°C for 30 minutes and centrifuged at 13,000 g for 5 minutes. The supernatant was collected, mixed with 3 ml of isopropanol and incubated for 5 minutes at RT. DNA was centrifuged at 1,000 g for

5 minutes, washed with 1 ml of 70% ethanol, re-centrifuged for 3 minutes and dried at 37°C for 10 minutes. The obtained DNA was re-suspended in 30 µl of sterile water.

II.3.5 Precipitation of DNA with ethanol

DNA was precipitated by ethanol in the presence of sodium cations. A tenth part of 3 M sodium acetate (v/v) and two and a half of 100% ethanol (v/v) were added to the solution containing DNA, mixed and kept at -20°C for at least 30 minutes. The pellet obtained after centrifugation at 16,000 g, 4°C for 30 minutes, washed with 1 ml of 70% ethanol and re-centrifuged at 16,000 g for 3 minutes. Finally the precipitated DNA was dried at 37°C for 10 minutes and re-suspended in sterile water.

II.3.6 Electrophoresis of DNA in agarose gel

Agarose gels, 0.8 – 1% (m/v), were used to separate DNA. Agarose was dissolved in a 1X TAE buffer (40 mM Tris, 20 mM acetic acid, 1 mM EDTA, pH 8). The same buffer was used during migration. Ethidium bromide or GelRed from Biotium were used to visualize DNA in UV. Force (50 – 100 V) and time (20 – 40 minutes) of the migration were dependent on size of the gel.

II.3.7 Purification of DNA from agarose gel

DNA after enzymatic digestion was separated in agarose gel as described before. Fragments of interest were cut out from the gel and purified with the use of the freeze-squeeze method or by the QIAEX II Gel Extraction Kit from Qiagen. The extraction with the kit was proceeded as recommended with a manufacture protocol. The freeze-squeeze purification method is based on the Tautz and Renz article (Tautz and Renz 1983). A DNA fragment cut from the gel was immediately frozen in liquid nitrogen and placed in a 0.5 ml eppendorf tube filled with polypropylene wool. The tube had been previously pounced and placed in 1.5 ml eppendorf tube. Then the frozen agarose slice was thawed at 37°C for at least 10 minutes and centrifuged for 5 minutes at 16,000 g. The DNA was precipitated with ethanol.

II.3.8 Nucleic acids measurement

The quantity of nucleic acid was measured in spectrophotometer at λ 260 nm.

II.3.9 Enzymatic digestion

DNA was incubated with 1 – 5 units of the enzyme per µg of DNA and with an appropriate digestion buffer at 37°C for at least 2 hours. The enzyme was inactivated by the DNA precipitation procedure. The Klenow enzyme or T4-DNA polymerase were used as recommended with manufactures protocols to produce the blunt ends in linear DNA after digestion.

II.3.10 Ligation of DNA fragments

T4 DNA-ligase was used to clone the linear DNA into the vector. Before ligation, the vector and the insert were digested with appropriate restriction enzymes, separated in the agarose gel and purified from the gel. The insert and the vector were mixed at the 3:1 ratio, respectively. The mass added to the reaction mix was calculated in accordance with the following formula:

$$\text{ng of insert} = (\text{ratio insert: vector}) \times \frac{\text{size of the insert (bp)}}{\text{size of the vector (bp)}} \times \text{ng of the vector.}$$

The reaction was proceeded at RT for 1h or at 16°C o/n.

II.3.11 Polymerase chain reaction (PCR) of DNA fragments

To amplify DNA the Taq recombinant polymerase (Life Technology) or Pfu-Ultra polymerase (Stratagene) were used. The PCRs were prepared as recommended with manufactures protocols.

Freshly grown colonies were also used as templates for verification of the deletion strains. A little portion of a colony was suspended in 20 µl of 0.2 M NaOH and warmed for 30 minutes at 95°C. 0.5 µl of the solution containing DNA released from cells was added to the reaction mixture as a template.

II.4. TECHNIQUES IN BIOCHEMISTRY

II.4.1 Isolation of mitochondria from yeast cells

Isolation of mitochondria from yeast cells (Guerin, Labbe et al. 1979) includes enzymatic digestion of the cell wall, mechanic disruption of the cells and differential centrifugations to obtain a fraction rich in mitochondria. Mitochondria were extracted with the use of iso-osmotic buffers which makes it possible to use them for functional studies.

Yeast cells were cultured in 2 liters of liquid YPGalA (for respiratory deficient strains) or YPEGA (for respiratory efficient strains) to exponential phase of growth (OD_{650} between 2 and 4). The whole procedure was carried out at 4°C. Cells were centrifuged for 5 minutes at 5,740 g and washed with sterile water (4°C). The pellet was re-suspended in solution containing 0.1 M Tris, 0.5 M β-mercaptoethanol, pH 9.3. 20 ml of solution was used per 1 g of dry mass of yeast. Dry mass of yeast was calculated in accordance with the following formula:

$$\text{dry mass (g)} = \text{OD}_{650} \text{ / ml } \times \text{volume of the culture (l)} \times 0.28 \text{ .}$$

Yeasts were incubated for 10 minutes at 32°C in order to reduce the disulfide bonds in proteins of the cell wall with β-mercaptoethanol. The solution was completed with a buffer containing: 0.5 M KCl, 10 mM Tris pH 7, and centrifuged for 5 minutes at 3,840 g. This step was repeated twice. The obtained pellet was re-suspended in 10 ml par 1g of dry mass of the digestion buffer (1.35 M sorbitol, 1 mM EGTA, 10 mM citric acid, 30 mM disodium phosphate, pH 5.8) mixed with zymolyase (15 mg/g of dry mass). Digestion was done at 32°C for 20 minutes. To verify if the process had been completed, 4 µl of digested yeast cells were mixed with 15 µl of sterile water. In the absence of the cell wall protoplasts break due to osmotic shock, which can be seen with the use of an optic microscope. If digestion was not completed, the time was prolonged. When the process was finished, the cell suspension was completed with a protoplasts washing buffer (0.75 M sorbitol, 0.4 M mannitol, 10 mM Tris – maleate, 0.1% (m/v) BSA, pH 6.8) and centrifuged for 5 minutes at 12,000 g. Protoplasts were washed twice by delicate re-suspending in the same protoplasts washing buffer with use of 15 cm^3 potter and centrifuged for 5 minutes at 12,000g. In the same manner protoplasts were re-suspended in a homogenization buffer (0.6 M mannitol, 2 mM EGTA, 10 mM Tris – maleate, 0,2% (m/v) BSA, pH 6.8). Lysis of the protoplasts was achieved by mixing 3 times for 5 seconds in a Mixer blender (Waring). The next steps of the procedure make it possible to

separate mitochondria from other cellular parts by differential centrifugation. After lysis, the extract was centrifuged for 8 minutes at 750 g. The collected supernatant was centrifuged for 10 minutes at 12,000 g. The pellet containing the isolated mitochondria was washed once in a recuperation buffer (0.6 M mannitol, 2 mM EGTA, 10 mM Tris – maleate, pH 6.8) with the use of a potter. Washed, pure mitochondria were transferred into glass tube and kept on ice during respiration, ATP synthesis and mitochondrial membrane potential measurements. Remaining mitochondria were frozen in liquid nitrogen in form of drops and conserved at -80°C.

II.4.2 Measurement of respiration in isolated mitochondria

The Oxygraph system with the Clark's electrode from Heito (France) was used to measure the respiration in freshly isolated mitochondria. This electrode was separated from the reaction chamber with a membrane that is permeable only to oxygen, which is reduced when it reaches the cathode. The reduction creates a potential difference that represents the oxygen present in the reaction chamber and, therefore, may be visualized. The electrode, surrounded by the membrane, was placed in a reaction glass chamber of 1 ml and maintained at 28°C. 150 µg/ml of the mitochondrial proteins were deposed into the chamber filled with a respiration buffer (0.65 M mannitol, 0.36 mM EGTA, 5 mM Tris – phosphate, 10 mM Tris – maleate, pH 6.8) and constantly agitated.

Activities of the respiratory chain complexes and ATP synthase were determined as the rate of oxygen consumption in the presence of different substrates and inhibitors. The following substrates and inhibitors were used: 4 mM NADH, 150 µM ADP, 4 µM CCCP, oligomycin 3 µg/ml, 12.5 mM ascorbate, 1.4 mM TMPD. The oxygen consumption rate was presented in nmol of oxygen consumed per minute per milligram of proteins.

NADH was added to the chamber as first. It is the substrate of complex I that permits generation of the proton gradient and stimulates the oxygen consumption by the respiratory chain. At this stage ATP synthase can use the substrates that have been already present in mitochondria, hence we measured the basal level of the respiratory chain activity known as state 4.

In the presence of NADH and ADP, ATP synthase uses the proton gradient to synthesize ATP from ADP and Pi. As a consequence, the respiratory chain increases its

activity and consumes oxygen faster. At this stage we measured the respiratory chain activity in phosphorylating conditions (state 3).

The maximal activity of respiratory chain was measured in the presence of NADH and CCCP, a compound that dissipates the proton gradient on the inner mitochondrial membrane.

The maximal activity of complex IV was determined by adding ascorbate and TMPD which deliver electrons directly to cytochrome *c*, which transfers them to cytochrome *c* oxidase. Therefore complex IV functions independently from other respiratory chain complexes. Introduction of CCCP dissipates the proton gradient, so the oxygen consumption dependents only on the maximal activity of complex IV.

Use of NADH and oligomycin was the internal control for preparation of mitochondria. The experiment shows whether the basal respiratory chain activity is not a consequence of proton leak through F_O domain of ATP synthase. Oligomycin blocks the proton transfer through the channel of ATP synthase. If the rate of oxygen consumption in the presence of NADH is higher than the consumption in the presence of NADH and oligomycin, it means that there is a proton leak through F_O.

II.4.3 Measurement of mitochondrial membrane potential

Mitochondrial membrane potential ($\Delta\Psi$) was measured in isolated mitochondria using fluorescent dye rhodamine 123 (Emaus, Grunwald et al. 1986). Fluorescence emitted by rhodamine 123 was quenched because of its entering into mitochondria in response to $\Delta\Psi$ – the higher the membrane potential was, the more of rhodamine entered the mitochondria. Therefore changes in the membrane potential could be visualized by the changing fluorescence of the dye in the reaction buffer. The capacity of the respiratory chain and ATP synthase to maintain the membrane potential was measured in the presence of different substrates and inhibitors, as it was done for the purpose of measurement of oxygen consumption. The measurements were done in a spectrofluorometer (Flax de Safas). Wave lengths were 485 nm for excitation and 525 nm for emission of fluorescence. The obtained values are arbitrary and semi-quantitative.

A volume of mitochondria corresponding to 150 µg/ml of mitochondrial proteins suspended in 1 ml of the respiratory buffer (0.65 M mannitol, 0.36 mM EGTA, 5 mM Tris – phosphate, 10 mM Tris – maleate, pH 6.8) in the presence of 0.5 µg/ml of rhodamine 123, was added to the spectrofluorometer cuvette. 10 mM ethanol was used as a substrate to

generate the mitochondrial membrane potential. Ethanol was preferred because auto-fluorescence of rhodamine can be excited by NADH. Presence of a respiratory chain substrate leads to generation of the membrane potential, rhodamine 123 entering the mitochondria and quenching of fluorescence. Maintaining of the mitochondrial membrane was measured in the presence of different compounds: 75 µM ADP, 4 µM oligomycin, 4 µM CCCP, 2 mM KCN, 0.2 mM ATP. KCN was used as an inhibitor of cytochrome *c* oxidase.

II.4.4 Quantification of ATP produced by isolated mitochondria

A volume of freshly isolated mitochondria corresponding to 150 µg/ml of mitochondrial proteins was added to the oxygraph chamber containing 1 ml of the respiratory buffer (0.65 M mannitol, 0.36 mM EGTA, 5 mM Tris – phosphate, 10 mM Tris – maleate, pH 6.8) at 28°C. The substrate of respiratory chain was NADH (4 µM). The ATP synthesis was done in an excess of ADP (1 mM). After addition of ADP, 100 µl of the reaction mixture was taken from the chamber every 15 seconds within 1 minute (for well respiring strains) or every 30 seconds within 2 minutes (for respiratory deficient strains) and rapidly precipitated with 25 µl of: 7% (v/v) perchloric acid and 25 mM EDTA. To measure the ATP synthesis independent of the ATP synthase, the enzyme was blocked with oligomycin (3 µg/ml) for 3 minutes before addition of ADP and samples were collected as described. All samples were centrifuged for 5 min at 15,000 g at 4°C, 110 µl of supernatants were preserved and pH was adjusted to 7 with addition of 2 M KOH and 0.3 M MOPS. The samples were stocked at -20°C before quantification of the produced ATP. Quantification of the produced ATP was based on bioluminescent reaction of luciferin oxidation to oxyluciferin by the luciferase enzyme. One ATP molecule was used per one molecule of oxidized luciferine. Light emitted during this reaction was measured in a bioluminometer. Bioluminescence Assay Kit CLS II from Roche Applied Science was used. The previously collected samples were thawed on ice and centrifuged for 5 minutes at 4°C, 16,000 g. 1 µl was mixed with 200 µl solution containing: 0.1 M Tris, 0.2 mM EDTA at pH 7.75 and luciferine/luciferase. Emission of the light measured in the bioluminometer was proportional to amount of ATP in the mix. First the calibration curve was determined using 10 µM ATP from 0 to 100 µL. Calculation of ATP in the samples was based on this curve and was expressed in nmol of ATP per milligram of mitochondrial proteins per minute. Values obtained from the samples collected in the presence of oligomycin represent ATP that was not produced by ATP synthase (basal ATP in mitochondria).

II.4.5 Estimating ATPase activity of ATP synthase

ATPase activity of ATP synthase was determined in thawed mitochondria. Mitochondria were thawed on ice and the protein concentration was measured *de novo* with the use of Lowry's method. A volume of mitochondria corresponding to 150 µg of mitochondrial proteins was mixed with 900 µl of the ATPase buffer (0.2 M KCl, 3 mM $MgCl_2$, 10m M Tris-HCl, pH 8.4) and incubated at 30°C. A series of five tubes was provided for each sample: two without oligomycin, two with 10 µg/ml oligomycin and one with 1% TCA. All tubes were incubated for 3 minutes at 30°C (time necessary to inhibit F_O domain with oligomycin). Then ATP that corresponds to 5 µM final concentration was added to the reaction mix and the tubes were incubated for 2 more minutes at 30°C. The reaction was stopped by addition of 5% TCA. The quantity of phosphate produced during the reaction of ATP hydrolysis to ADP and Pi was measured as described by Somlo (Somlo 1968). Tubes were centrifuged for 10 minutes at 4°C, 9,300 g. Half of the supernatant of each tube was added to 5 volumes of the MARIKA reaction solution (5.4 mM Ammonium HeptaMolybdate $(NH_4)Mo_7O_{24}$ $4H_2O$, 28.8 mM $FeSO_4$ $7H_2O$), mixed on vortex and incubated in the dark for 10 minutes. Pi released in the reaction associates with molybdate and forms phosphomolybdate that when reduced by iron (II) sulfate in acidic environment becomes violet. The intensity of the violet color was measured in a spectrophotometer at wave length 610 nm. At the same time the calibration curve was made with growing concentration of 1 mM KH_2PO_4 (from 0 to 300 nmol of Pi). ATP hydrolyzed by complex V was presented as µmol of Pi produced per minute per milligram of mitochondrial proteins. Measurements made in the presence of oligomycin represent the ATPase activity of free F_1 or other enzymes with ATPase activity. Percentage of oligomycin inhibition corresponds to the complete complex of ATP synthase.

II.4.6 Extraction of total proteins from yeasts cells

Total protein extract was prepared from 10 OD of yeast cells in exponential phase of growth (OD_{650} 2 – 4). The cells were centrifuged for 3 minutes, 2,000 g. The pellet was re-suspended in 500 µl of lysis buffer (1.85 M NaOH, 7.4% (v/v) β-mercaptoethanol and incubated at 4°C for 10 minutes. The same volume of 5 % TCA was added and the samples were incubated at 4°C for 10 minutes. After centrifugation for 5 minutes at 4°C, 16,000 g, the pellet was washed first with 3 M Tris at pH 8.9 and then with sterile water. The final pellet was re-suspended in 50 µl of 5% SDS and neutralized with 3 M Tris at pH 8.9, if needed

(final pH of the samples should be about 7 – 8). In the next step the sample was warmed for 15 minutes at 42°C and centrifuged for 5 minutes at 1,000 g at RT. The supernatant was collected and stocked at -20°C.

To verify if Atp9p synthesized in excess has formed the inclusion bodies in mitochondria, the pellet from the final centrifugation was re-suspended in highly denaturing buffer (7 M urea, 2 M Triton, 4 % Chaps, 65 mM DTT) and centrifuged for 5 minutes at 16,000 g. The supernatant was collected and stocked at -20°C. The pellet was treated in the same manner one more time and the final supernatant was kept and stocked at -20°C. Protein concentration in each sample was determined with Lowry's method.

II.4.7 Measuring of protein content with the use of colorimetric method of Lowry

Protein concentration in total extracts from yeast cells or mitochondria was based on the method described by Lowry (Lowry, Rosebrough et al. 1951). The samples were diluted 1/10 (for measurements of proteins from the yeast cells) or 1/20 (for measurements of mitochondrial proteins) in 5% SDS. 5 µl of dilution was mixed with 70 µl of 5% SDS and 750 µl of the reaction solution (0.01% (m/v) $CuSO_4$, 0.02% (m/v) NaK, 3.92% (m/v) Na_2CO_3 dissolved in 0.1 M NaOH). After a three-minute incubation at 37°C, 75 µl of Folin solution (diluted 1/3) was added to each sample and incubated for 6 more minutes at 37°C. At the same time the calibration curve was made with known concentration of the bovine albumin (from 0 to 10 µg of proteins) treated in the same way as the samples. The absorbance at wave length of 750 nm was measured and concentration of the proteins in samples was determined in milligrams per milliliter.

II.4.8 Separation of mitochondrial membrane complexes by BN-PAGE

The already isolated mitochondria were quickly thawed and the protein concentration was measured *de novo* by Lowry's method. A volume corresponding to 250 – 500 µg of mitochondrial proteins were centrifuged for 5 minutes at 4°C, 16,000 g. The pellets of mitochondria were re-suspended in 50 µl of extraction buffer (30 mM HEPES, 150 mM potassium acetate, 12% (m/v) glycerol, 2 mM aminocaproic acid, 1 mM EDTA, cocktail of inhibitors of proteases from Roche) containing 2 g of digitonin per 1 g of proteins. Digitonin is a mild detergent that extracts mitochondrial membrane complexes in their native forms (Kun, Kirsten et al. 1979). The mix was incubated for 30 minutes on ice and centrifuged for 30 minutes at 4°C, 25,000 g. The supernatants with mitochondrial membrane complexes were

collected and mixed with a charging buffer (final concentrations: 0.1% (m/v) of Coomassie blue G250 and 32 mM 6-aminocaproic acid).

Mitochondrial membrane complexes were separated by migration in BN-PAGE gel. This technique makes it possible to separate different supramolecular forms of ATP synthase preserving at the same time its enzymatic activities. After extraction from the inner mitochondrial membrane, complexes were separated in non-denaturing gradient polyacrylamide gel in a migration buffer containing Coomassie Blue. The protocol was based on the publication of Schägger and von Jagow (Schagger and von Jagow 1991). Commassie blue G250 interacts with proteins and gives them negative charge. Electrophoretic mobility of proteins depends on the size of complexes and the amount of Coomassie blue interacting with them. Two solutions of different concentrations of acrylamide (3 and 13%) were used to create a polyacrylamide gradient gel. They were placed in two compartments connected in an interior. One of the compartments was connected to a peristaltic pomp. The pomp creates an effect of aspiration and a 3% solution overfilled gradually to a 13% solution. Homogenization of the two solutions was guaranteed by agitation in the compartment of the 13% solution. Thanks to the pomp system, the lower part of the gel contained only the 13% solution, then there was a mix of the solutions gradually changing the percentage of acrylamide to 3% solution at the top of the gel. The 3% solution contained: 2.96% of acrylamide/bis-acrylamide mix (29.1:0.9), 1X gel buffer (25 mM imidazol, 0.5 M 6-aminocaproic acid, pH 7), 0.04% APS, TEMED. The 13% solution contained: 200 g/l of glycerol, 13% of acrylamide/bis-acrylamide mix (29.1:0.9), 1X gel buffer (25 mM imidazol, 0.5 M 6-aminocaproic acid, pH 7), 0,03% APS, TEMED. The gradient gel mixer was filled with 12 ml of 3% solution and 11.5 ml of 13% solution. The stacking gel was composed of: 2.96% of acrylamide/bis-acrylamide mix (29.1:0.9), 1X gel buffer (25 mM imidazol, 0.5 M 6-aminocaproic acid, pH 7), 0.08% APS, TEMED. Cathode buffer was composed of: 7.5 mM imidazol, 50 mM tricine, 40 mg/l of Coomassie blue G250, adjusted to pH 7 at 4°C. Anode buffer was composed of: 25 mM imidazol adjusted to pH 7 at 4°C. Migration was proceeded at 10 mA constant for about 8h.

II.4.9 Visualization of ATPase activity on gel

ATP synthase can be detected after separation of inner mitochondrial membrane complexes in non-denaturing conditions (BN-PAGE) by its ATPase activity. In mitochondria the main enzyme with ATPase activity is the F_1 domain of ATP synthase. The method of

revealing this activity on gel was described by Grandier-Vazeille and Guérin (Grandier-Vazeille and Guerin 1996). The gel was incubated for 3 hours with shaking in a revelation buffer (270 nM glycine, 35 mM Tris at pH 8.4). After this time the gel was incubated with the same buffer completed with 14 mM $MgSO_4$, 0.2% $Pb(NO_3)$ and 8 mM ATP until the moment of apparition of white bands. These bands corresponded to the precipitated plumb and phosphate due to hydrolysis of ATP by ATP synthase.

After revealing of ATPase activity, the revelation buffer was removed and the gel was de-colored with a solution containing 30% ethanol and concentrated HCl. Next the gel was colored with Coomassie blue to visualize all proteins presented in the gel.

II.4.10 Separation of the proteins in denaturing conditions (SDS-PAGE)

The method was based on the publication of Schägger and von Jagow (Schagger and von Jagow 1987). Proteins were deposed in an acrylamide/bis-acrylamide gel containing SDS. SDS is an anionic detergent keeping the proteins in denatured, non-native and negatively charged forms. Electrophoretic mobility of proteins in the gel depends on their size. Separation of proteins in denaturing conditions was performed in commercially available pre-casted gels and migration buffers from kit NuPAGE Novex 4-12% Bis-Tris Gel from Invitrogen. Migration was done at constant 200 V for 35 – 55 minutes. Immediately thereafter the migration proteins were transferred onto a nitrocellulose membrane.

II.4.11 Transfer of the proteins onto a nitrocellulose membrane

Proteins separated on the gel were transferred onto a nitrocellulose membrane with the use of the iBlot Transfer Stack kit and iBlot Dry Blotting System from Invitrogen. The proteins were fixed on the membrane due to its non-specific affinity to amino acids.

II.4.12 Immunodetection of proteins

The nitrocellulose membrane with fixed proteins was incubated with shaking for at least 30 minutes in a 1X PBS-T buffer (2.7 mM KCl, 10 mM Na_2HPO_4 $2H_2O$, 1.76 mM KH_2PO_4, 0.14 M NaCl, 0.05% (v/v) Tween-20, adjusted to pH 7.4) mixed with 5% (m/v) dehydrated skim milk. A primary antibody in the same buffer was added immediately thereafter and incubation was continued for at least two hours in RT. The overnight incubation was done at 4°C. Concentration of the antibody dependents on its type and is presented in Table 5. After hybridization with a primary antibody the membrane was washed

in 1X PBS-T buffer for 5 minutes. This step was repeated five times. Next, the membrane was incubated with a secondary antibody for at least 1.5 h. The secondary antibody, conjugated with horseradish peroxidase, was either anti-rabbit or anti-mouse following the type of the primary antibody. It was diluted in the same 1X PBS-T buffer with 5% (m/v) dehydrated skim milk. Next the membrane was washed as after the incubation with the primary antibody. The presence of bound antibodies was detected thanks to the reaction catalyzed by horseradish peroxidase in the presence of its substrate ECL from GE Healthcare. Exposition time was from 30 seconds to 30 minutes.

Antibody	**Provenance**	**Dilution**	**Epitope**	**Origin**
Anti-α	Rabbit polyclonal	1/50 000	The whole protein	J. Velours
Anti-Atp4p	Rabbit polyclonal	1/10 000	The whole protein	J. Velours
Anti-Atp6p	Rabbit polyclonal	1/5 000	The whole protein	J. Velours
Anti-Atp9p	Rabbit polyclonal	1/7 500	LINGVSRNPSIKDT	J. Velours
Anti-cyt *b*	Rabbit polyclonal	1/5 000	The whole protein	J. Velours
Anti-Cox2	Mouse monoclonal	1/5 000	The whole protein	Molecular Probes
Anti-Arg8	Rabbit polyclonal	1/ 5 000	The whole protein	T. Fox
Anti-porine	Mouse monoclonal	1/10 000	The whole protein	Molecular Probes
Anti-Ade13	Rabbit	1/50 000	The whole protein	B. Pinson
Anti-rabbit HRP	Goat polyclonal	1/10 000	The whole protein	Promega
Anti-mouse HRP	Goat polyclonal	1/10 000	The whole protein	Promega

Table 5 – Table of the antibodies used in the study.

II.4.13 In vivo labelling of the products of mitochondrial translation

In vivo labeling of the products of mitochondrial translation was based on the publication of Barrientos (Barrientos, Korr et al. 2002). Yeast cells were cultured in a liquid medium for 5 – 7 generations. The media used were YPGalA for strains without plasmids and CSM galactose supplemented with appropriate amino acids for strains bearing plasmids. 10 OD of the cells at the exponential phase of growth (OD_{650} 2 – 4) were centrifuged for 3 minutes at 2,000 g and washed twice with minimal galactose medium without ammonium sulfate and amino acids. Cells were finally re-suspended in the same minimal galactose medium without ammonium sulfate supplemented with auxotrophic amino acids (without methionine and cysteine) and incubated for 2 hours at 28°C with shacking. After starvation, 6 OD of the cells were taken for further analysis and centrifuged for 3 minutes at 2,000 g. The cell pellets were re-suspended in 500 µl of the same medium. Freshly prepared 1 mM cycloheximide was added and the mix was incubated for 5 minutes at 28°C. 50 microcuries of the methionine/cysteine, where methionine is labeled with ^{35}S (1000 Ci/mmol, Promix Amersham Bioscience), was added. The samples were then incubated for 20 minutes at 28°C. Next, the cells were centrifuged for 1 minute 10,000 g and 75 µl of the lysis buffer (1.85 M NaOH, 14% (v/v) β-mercaptoethanol, 10 mM phenylmethylsulfonyl fluoride) was added. The lysis was stopped with 1 ml of 25% TCA and centrifuged for 5 minutes at 14,000 g. The pellet was washed once with 3 M Tris pH 8.9 and once with sterile water. The final pellet was re-suspended in 50 µl of Laemmli buffer (2% SDS, 10% glycerol, 2.5% β-mercaptoethanol, 0.06 M Tris-HCl, pH 6.8, 0.002% (m/v) of bromophenol blue). Emitted radioactivity was measured in the presence of scintillation reagent with a scinitillator.

The following two gel systems were used to visualize the products of mitochondrial translation: 17.5% SDS-PAGE (Laemmli 1970) to separate Atp8p and Atp9p, 12% urea/glycerol gel to separate Atp6p and Cox3p and Cox2p and cytochrome *b*. The same amount of radioactivity for each sample was deposed in the gel. 17.5% SDS-PAGE resolving gel was composed of: 17.5% acrylamide/bis-acrylamide (37.5:1), 0.375 M Tris-HCl pH 8.9, 0.1% SDS, 0.05% APS and TEMED. The stacking gel was composed of: 5% acrylamide/bis-acrylamide (37.5:1), 0.06 M Tris-HCl pH 6.8, 0.1% SDS, 0.05% APS and TEMED. The migration was made in the buffer composed of: 0.4 M Tris, 0.2 M glycine and 0.1% SDS at 35 mA constant for 4 hours. 12% urea/glycerol resolving gel was composed of: 12% acrylamide/bis-acrylamide (37.5:1), 4 M urea, 25% (m/v) glycerol, 0.75 M Tris-HCl pH 8.9, 0,26% APS and TEMED. The stacking gel was composed of: 6% acrylamide/bis-

acrylamide (37.5:1), 0.125 M Tris-HCl pH 6.8, 0.1% SDS, 0.025% APS and TEMED. The migration was made in the buffer composed of: 0.4 M Tris, 0.2 M glycine and 0.1% SDS at 150 V constant for 16 hours. This method of protein separation has been adapted from the publication of Kunkele *et al.* (Kunkele, Heins et al. 1998). After migration both gels were dried and radioactively marked proteins were visualized by autoradiography in PhosphorImager after a one-week exposition.

RESULTS

III.1. MUTATIONS IN *ATP6* GENE AND HUMAN DISEASES

In the first part of my work I was interested in analyzing the effects of mutations in mitochondrial *ATP6* gene found in cells from patients. Two of them are newly identified mutations causing the NARP (neurogenic myopathy, ataxia, retinitis pigmentosa) syndrome. Five were found in various human tumors in conserved positions between yeast and human subunit 6. Mitochondrial *ATP6* gene encodes subunit 6 of F_1F_O-ATP synthase that forms a proton channel together with the ring of subunit 9. Mutations in subunit 6 may impair the proton transport through inner mitochondrial membrane leading to malfunctioning of F_1F_O-ATP synthase and decreased ATP production.

III.1.1 Analysis of the two newly identified NARP mutations

NARP syndrome is one of mitochondrial diseases caused by mutations in mtDNA in *MTATP6* gene. Previously in our laboratory, we modeled in yeast five other NARP *ATP6* mutations: 8993T>G (Rak, Tetaud et al. 2007a), 8993T>C (Kucharczyk, Rak et al. 2009a), 9176T>G (Kucharczyk, Salin et al. 2009b), 9176T>C (Kucharczyk, Ezkurdia et al. 2010) and 8851T>C (Kucharczyk, Giraud et al. 2013). As two novel mutations (9185T>C and 9191T>C) were described (Moslemi, Darin et al. 2005) we decided to introduce them into yeast mtDNA and investigated their effects on F_1F_O-ATP synthase. The obtained results are described in (Kabala, Lasserre et al. 2014) which I have attached and summarized below.

9185T>C and 9191T>C mutations in human *MTATP6* change leucine 220 into proline and leucine 222 into proline, respectively, in human subunit 6. These amino acids correspond to serine 250 and leucine 252 residues in yeast protein, respectively. Yeast clones with *atp6-S250P* mutation grow well on non-fermentable carbon source (glycerol) but are sensitive on oligomycin which indicates diminished production of ATP by ATP synthase. *atp6-L252P* mutation disabled yeast growth on respiratory carbon source (Fig. 1 in the article below).

In the next step I measured: oxygen consumption, ATP synthesis and hydrolysis, and inner membrane potential in isolated mitochondria. For strain bearing *atp6-S250P* mutation, about a 10-15% drop in oxygen consumption at state 3 was observed, while for *atp6-L252P* this drop was about 67-85%. The ATP synthesis rates were also diminished: about 30% and 90% in *atp6-S250P* and *atp6-L252P*, respectively. The hydrolysis rates were similar in both mutants as compared to *WT* (Table 2 in the article below). Interestingly, in the *atp6-L252P*

strain the hydrolysis rate did not change after addition of oligomycin, which suggests the presence of free F_1 domain. Analysis of ATP synthase assembly/stability in native gels confirmed it, both by coomasie-blue staining and hydrolysis activity in gel. No change in ATP synthase stability could be seen in the *atp6-S250P* strain (Fig. 2A in the article below). Like in *WT* we could observe fully assembled monomeric and dimeric ATP synthase complexes. Inner mitochondrial membrane potential was evaluated by measuring of the proton pumping activity coupled to F_1-mediated ATP hydrolysis. In the *atp6-S250P* strain the level of proton pumping was comparable to that of *WT* in contrast to the *atp6-L252P* strain, from which this activity was almost absent (Fig. 3 in the article below).

In the two examined mutant strains I analyzed also synthesis of mitochondrially encoded proteins by *in vivo* labeling. No change in this activity could be observed (Fig. 4 in the article below). Shift of Atp6p migration may be caused by mutations that change protein mobility in the gel. Although the level of synthesis is normal in both strains, in the *atp6-L252P* strain steady state level of subunit 6 is strongly diminished (Fig. 2B in the article below) while no change is observed in the *atp6-S250P* strain as compared to *WT*. This result also suggests a dysfunction of F_1F_O-ATP synthase assembly in the *atp6-L252P* strain as Atp6p is rapidly degraded when not assembled into the complex.

Both mutations are located in the last helix of the Atp6 protein in the vicinity of amino acids that are well-conserved between different species and make contact sites with subunits 9 ring (Fillingame, Angevine et al. 2002; Kucharczyk, Zick et al. 2009c). Results obtained for the *atp6-S250P* mutation indicate relatively mild effects on F_1F_O-ATP synthase. There is about 30% less ATP produced in this strain but neither defects in assembly of the enzyme nor proton leakage could have been observed. We suggested that this mutation could create some local structural modifications that influence proton transport through the channel as it was proposed before for the 9176T>C mutant (Kucharczyk, Ezkurdia et al. 2010). The 30% drop in ATP production may be sufficient to mildly compromise human health. In contrast, the *atp6-L252P* mutation affects the ATP synthase very severely. Probably due to the mutation Atp6p cannot be efficiently assembled into the enzyme or interact with the ring of subunits 9. This can explain severe clinical phenotype in the patient similar to those presented in the patient bearing the 9176T>G mutation (Kucharczyk, Salin et al. 2009b).

ARTICLE IN PRESS

Biochimie xxx (2013) 1–7

Contents lists available at ScienceDirect

Biochimie

journal homepage: www.elsevier.com/locate/biochi

Research paper

Defining the impact on yeast ATP synthase of two pathogenic human mitochondrial DNA mutations, T9185C and T9191C

Anna Magdalena Kabala [a,b], Jean-Paul Lasserre [b], Sharon H. Ackerman [c], Jean-Paul di Rago [b], Roza Kucharczyk [a,*]

[a] Institute of Biochemistry and Biophysics, Polish Academy of Sciences, Warsaw, Poland
[b] Institut de Biochimie et Génétique Cellulaires, CNRS UMR5095, Université Bordeaux Segalen, 1 Rue Camille Saint-Saëns, Bordeaux 33077 cedex, France
[c] Department of Biochemistry and Molecular Biology, Wayne State University School of Medicine, Detroit, MI, USA

ARTICLE INFO

Article history:
Received 15 July 2013
Accepted 25 November 2013
Available online xxx

Keywords:
ATP synthase
ATP6
Mitochondria
Energetics
Disease
mtDNA mutation

ABSTRACT

Mutations in the human mitochondrial ATP6 gene encoding ATP synthase subunit *a*/6 (referred to as Atp6p in yeast) are at the base of neurodegenerative disorders like Neurogenic Ataxia and Retinitis Pigmentosa (NARP), Leigh syndrome (LS), Charcot–Marie–Tooth (CMT), and ataxia telangiectasia. In previous studies, using the yeast *Saccharomyces cerevisiae* as a model we were able to better define how several of these mutations impact the ATP synthase. Here we report the construction of yeast models of two other ATP6 pathogenic mutations, T9185C and T9191C. The first one was reported as conferring a mild, sometimes reversible, CMT clinical phenotype; the second one has been described in a patient presenting with severe LS. We found that an equivalent of the T9185C mutation partially impaired the functioning of yeast ATP synthase, with only a 30% deficit in mitochondrial ATP production. An equivalent of the mutation T9191C had much more severe effects, with a nearly complete block in yeast Atp6p assembly and an >95% drop in the rate of ATP synthesis. These findings provide a molecular basis for the relative severities of the diseases induced by T9185C and T9191C.

1. Introduction

A quite large number of point mutations (sixteen) has been found in the mitochondrial *ATP6* gene in patients presenting with various neurodegenerative disorders, Neurogenic Ataxia and Retinitis Pigmentosa (NARP), Leigh syndrome (LS), Leber's Hereditary Optic Neuropathy (LHON), Charcot–Marie–Tooth (CMT) or ataxia telangiectasia [1–8]. The *ATP6* gene encodes ATP synthase subunit *a*, which is referred to as Atp6p in yeast. The ATP synthase (also called complex V) synthesizes ATP from ADP and inorganic phosphate using the energy of the electrochemical proton gradient established by the mitochondrial electron transport chain (complexes I–IV) [9]. Atp6p is a key subunit of the F_O proton-translocating domain of the ATP synthase. Proton movements mediated by Atp6p lead to the rotation of a transmembrane ring of Atp9p subunits (referred to as subunit *c* in humans) which ends up in conformational changes at the level of the catalytic sites in the F_1 extra-membrane domain of the enzyme that favor the synthesis ATP and its release into the mitochondrial matrix [10,11].

We previously constructed yeast models of the pathogenic ATP6 mutations T8993G [12], T8993C [13], T9176G [14], T9176C [15] and T8851C [16]. The effects of these mutations on yeast ATP synthase correlated well with those observed in humans, which reflects the high level of evolutionary conservation within the regions of Atp6p affected by these mutations.

Two other pathogenic mutations at the focus of the present study were described at positions 9185 (T9185C) and 9191 (T9191C) of ATP6 [17]. The first one changes a leucine into proline at position 220 near the carboxyl terminus of the protein. It was found in thirty-four patients from eight independent families suffering from LS, NARP, CMT or spinocerebellar ataxia syndromes [3,17–21]. In all cases the disease was maternally inherited, with a relatively mild, sometimes reversible, clinical phenotype and occurred at a minimum of 85% heteroplasmy. Mitochondria from patients's cells (muscle or skin fibroblasts) showed normal complexes I–IV activities [3,21] and only a slightly reduced ATPase activity [18,20]. The second mutation, T9191C, was found in a patient presenting with very severe LS [17]. It changes a leucine to proline at position 222 of the human homolog of yeast Atp6p. This mutation causes a substantial (50%) reduction in mitochondrial ATPase activity and a lower respiration rate (60% *vs.* control) [17]. We report here yeast models of

* Corresponding author. Tel.: +48 225921217; fax: +48 226584636.
E-mail address: roza@ibb.waw.pl (R. Kucharczyk).

0300-9084/$ – see front matter © 2013 Published by Elsevier Masson SAS.
http://dx.doi.org/10.1016/j.biochi.2013.11.024

Please cite this article in press as: A.M. Kabala, et al., Defining the impact on yeast ATP synthase of two pathogenic human mitochondrial DNA mutations, T9185C and T9191C, Biochimie (2013), http://dx.doi.org/10.1016/j.biochi.2013.11.024

the mutations T9185C and T9191C that help to better define how they impact the ATP synthase.

2. Materials and methods

2.1. Construction of yeast atp6-S250P and atp6-L252P mutants

The strains used in the study are listed in Table 1. Using the QuikChange XL Site-directed Mutagenesis Kit of Stratagene, we changed the serine TCA codon at position 250 in the yeast *ATP6* gene into proline CCA codon, with primers 5′ GTCTGGGCTATTTTAACAGCA**CCA**TATTTAAAAGATGCAGTATACTTACAT and 5′ ATGTAAGTATACTGCATCTTTTAAATA**TGG**TGCTGTTAAAATAGCCCAGAC and the leucine TTA codon at position 252 into proline CCA codon, with primers 5′ GTCTGGGCTATTTTAACAGCATCATAT**CCA**AAAGATGCAGTATACTTACAT and 5′ ATGTAAGTATACTGCATCTTTT**TGG**ATATGATGCTGTTAAAATAGCCCAGAC (in bold the mutator codon). The mutagenesis was performed on an EcoRI–BamHI fragment containing the last 38 codons of *ATP6* cloned in pUC19 (plasmid pSDC9) [12]. The mutated fragment was liberated by restriction with EcoRI and SapI and ligated with pSDC14 [12] cut with the same enzymes to reconstruct a whole *ATP6* gene with the S250P or L252P mutations. The resulting plasmids (pRK37 and pRK38, respectively) also contain the yeast mitochondrial *COX2* gene as a marker for mitochondrial transformation. The plasmids were introduced by co-transformation with the nuclear selectable *LEU2* plasmid Yep351 into the rho^0 strain DFS160 by microprojectile bombardment using a biolistic PDS-1000/He particle delivery system (Bio-Rad) as described [22]. Mitochondrial transformants (synthetic AKY13 and AKY14 respectively) were identified among the Leu + nuclear transformants by their ability to produce respiring clones when mated to the nonrespiring NB40-3C strain bearing a deletion in the mitochondrial *COX2* gene. One AKY13 and AKY14 clone was crossed to the *atp6::ARG8m* deletion strain MR10 [23] for the production of clones (called AKY5 and RKY66) harboring the MR10 nucleus and where the *ARG8m* ORF [24] had been replaced by recombination with the mutated *atp6-S250P* or *atp6-L252P* genes. The AKY5 clone was identified by its inability to grow in the absence of an external source of arginine and the ability to grow on respiratory medium. The RKY66 clone was identified by its inability to grow in the absence of an external source of arginine and the ability to grow on respiratory medium when crossed with the SDC30 strain bearing in the mitochondrial DNA the wild type copy of *ATP6* gene. Sequencing of the mutated *atp6* locus in AKY5 and RKY66 revealed no other changes than S250P or L252P, respectively.

2.2. Measurement of respiration and ATP synthesis/hydrolysis activities in whole mitochondria

For these assays, mitochondria were prepared by the enzymatic method of Ref. [25]. The rates of ATP synthesis were determined as described in Ref. [23]. For respiration ATP synthesis and transmembrane potential ($\Delta\Psi$) measurements, freshly prepared mitochondria were diluted to 0.15 mg/ml in the reaction medium thermostated at 28 °C and containing 10 mM Tris-maleate (pH 6.8), 0.65 M sorbitol, 0.3 mM EGTA, and 3 mM potassium phosphate. Oxygen consumption rates were measured using a Clarke electrode and an OXM204 oxymeter from Heito (France) as described [26]. The different respiration states were measured after consecutive additions of 4 mM NADH for State 2, 150 μM ADP for State 3 and State 4, 4 μM carbonyl cyanide m-chlorophenylhydrazone (CCCP) for uncoupled respiration and finally 12.5 mM ascorbate (Asc), 1.4 mM N,N,N,N,-tetramethyl-p-phenylenediamine (*TMPD*) for Complex IV respiration activity. The rates of ATP synthesis were determined in the same condition using 750 μM ADP. Aliquots were withdrawn from the oxygraph cuvette every 15 s and reaction was stopped by 3.5% (w/v) perchloric acid, 12.5 mM EDTA. Samples were then neutralized to pH 6.5 by addition of KOH, 0.3 M MOPS. ATP was quantified by luciferin/luciferase assay (ATPLite kit from Perkin Elmer) on an LKB bioluminometer. Participation of the F_1F_O-ATP synthase to ATP production was assessed by oligomycin addition (3 μg/ml). Variations in transmembrane potential ($\Delta\Psi$) were evaluated as in Ref. [27] by monitoring the quenching of rhodamine 123 fluorescence (0.5 μM) using a λ_{exc} of 485 nm and a λ_{em} of 533 nm using an FLX Spectrofluorimeter (SAFAS, Monaco) under constant stirring. Transmembrane potential was generated by addition of ethanol [1% (v/v) final concentration]. ATP synthesis (state 3 of respiration) was initiated by addition of 50 μM ADP. When State 4 was reached, respiratory was inhibited by adding 0.3 mM KCN in order to measure the $\Delta\Psi$ produced by the hydrolysis of the synthetized ATP. $\Delta\Psi$ was collapsed by adding 4 μM CCCP. The specific ATPase activity at pH 8.4 of non-osmotically protected mitochondria was measured as described in Ref. [28].

2.3. Miscellaneous procedures

Determination of ρ^+/ρ^0 cells in yeast cultures, SDS-PAGE and BN-PAGE, western blotting, Coomassie brilliant blue staining, pulse labeling of mtDNA encoded proteins were performed as described in Ref. [23].

3. Results

3.1. Respiratory growth and genetic stability of yeast mutants atp6-S250P and atp6-L252P

The leucine residues 220 and 222 of the human homolog of yeast Atp6p that are modified by the T9185C and T9191C mutations correspond respectively to serine 250 and leucine 252 of Atp6p [29]. The TCA and TTA codons specifying these residues were converted into proline CCA codon (see Materials and methods). Yeast *atp6*-S250P clones grew well on non-fermentable carbon

Table 1
Genotypes and sources of yeast strains.

Strain	Nuclear genotype	mtDNA	Source
DFS160	*MATa leu2Δ ura3-52 ade2-101 arg8::URA3 kar1-1*	ρo	[24]
NB40-3C	*MATa lys2 leu2-3,112 ura3-52 his3ΔHinDIII arg8::hisG*	ρ^+ *cox2-62*	[24]
MR6	*MATa ade2-1 his3-11,15 trp1-1 leu2-3,112 ura3-1 CAN1 arg8::hisG*	ρ^+	[23]
MR10	*MATa ade2-1 his3-11,15 trp1-1 leu2-3,112 ura3-1 CAN1 arg8::hisG*	ρ^+ *atp6::ARG8*^{m}	[23]
SDC30	*MATa leu2Δ ura3-52 ade2-101 arg8: URA3 kar1-1*	ρ *ATP6*	[23]
AKY13	*MATα leu2Δ ura3-52 ade2-101 arg8::URA3 kar1-1*	ρ *atp6-S250P*	This study
AKY14	*MATα leu2Δ ura3-52 ade2-101 arg8::URA3 kar1-1*	ρ *atp6-L252P*	This study
AKY5	*MATa ade2-1 his3-11,15 trp1-1 leu2-3,112 ura3-1 CAN1 arg8::hisG*	ρ^+ *atp6 S250P*	This study This study
RKY66	*MATa ade2-1 his3-11,15 trp1-1 leu2-3,112 ura3-1 CAN1 arg8::hisG*	ρ *atp6-L252P*	This study This study

Please cite this article in press as: A.M. Kabala, et al., Defining the impact on yeast ATP synthase of two pathogenic human mitochondrial DNA mutations, T9185C and T9191C, Biochimie (2013), http://dx.doi.org/10.1016/j.biochi.2013.11.024

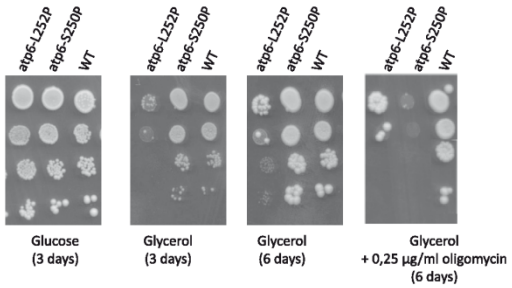

Fig. 1. Respiratory growth of *atp6-S250P* and *atp6-L252P* mutants. Freshly grown cells of wild type yeast (MR6) and the *atp6* mutants were serially diluted and 5 µl of each dilution were spotted onto rich glucose, rich glycerol and rich glycerol + oligomycin. The plates were incubated at 28 °C and photographed after the indicated number of days.

sources (like glycerol) whereas *atp6*-L252P ones failed to grow in these conditions, as shown by the drop tests in Fig. 1. The few growing colonies in the *atp6*-L252P drops presumably arose from genetic suppressors restoring mitochondrial function.

Even though the mutant *atp6*-S250P had a normal respiratory growth this does not necessarily mean that mitochondrial ATP synthesis was not compromised. Indeed as previously shown through the analysis of numerous yeast ATP synthase mutants, the activity of this enzyme needs to be decreased by at least 80% to see an obvious respiratory growth defect, which indicates that ATP synthase is far from limiting for the proliferation of yeast cells producing ATP by oxidative phosphorylation [15,30]. However, when the rate of mitochondrial ATP production is diminished cells become more sensitive to chemical inhibition of ATP synthase with oligomycin [15], a compound that is presumed to target the F_O because mutations in Atp9p and Atp6p can confer an increased resistance to it [31,32]. Thus, the higher *in vivo* sensitivity to oligomycin of mutants in which ATP synthase is partially compromised is due to the fact that less of the drug is required to reach the 20% oxidative phosphorylation threshold under which the production of ATP becomes limiting for growth [15]. We therefore tested the *in vivo* sensitivity to oligomycin of the mutant *atp6*-S250P. As shown in Fig. 1, in the presence of 0.25 µg/ml oligomycin the *atp6*-S250P mutant stopped growing on glycerol whereas wild type yeast (*WT*, strain MR6) was unaffected. This finding indicated that the S250P change in Atp6p was not without any deleterious consequence on the ATP synthase, which was confirmed by *in vitro* experiments on isolated mitochondria as described below. It is to be noted that the few revertants of the *atp6*-L252P mutant displayed a normal sensitivity to oligomycin, indicating that ATP synthase function was largely, if not totally, restored in these clones.

In yeast, defects in ATP synthase often increase the production of ρ^-/ρ^0 *petites* issued from large deletions in the mtDNA [33,34]. The *atp6*-S250P mutant never produced more than 5% ρ^-/ρ^0 cells like the *WT*. The *atp6*-L252P mutant had a higher but still moderate propensity (36%) to produce *petites* showing that its severe respiratory growth deficiency was not due, at least solely, to a failure in mtDNA maintenance. Full respiratory competence was restored in *atp6*-L252P cells that contained a complete ($\rho+$) mitochondrial genome by crossing with SDC30, a synthetic ρ^- strain whose mitochondria contain only the wild type *ATP6* gene. This result proved that the L252P change in Atp6p was responsible for the observed respiratory growth phenotype of the *atp6*-L252 mutant.

3.2. Consequences of the atp6-S250P and atp6-L252P mutations on various activities related to respiration and oxidative phosphorylation

3.2.1. Mitochondrial oxygen consumption

We first measured oxygen consumption in isolated mitochondria using NADH as an electron donor, at state 3 (i.e. in the presence of ADP, phosphorylating conditions), state 4 (i.e. without addition of ADP, basal respiration) and in the presence of the membrane potential uncoupler CCCP (i.e. conditions at which respiration is maximal). We also used ascorbate/TMPD to deliver electrons directly at the level of complex IV, the last complex of the electron transport chain. The *atp6*-S250P mutation had a minor impact in all tested conditions, with only a 10–15% decrease at state 3 with respect to *WT* (Table 2). Much more important oxygen consumption deficits (67–85%) were observed in *atp6*-L252P mitochondria. A respiratory defect, especially at the level of complex IV, is a common property of yeast ATP synthase mutants [23,35]. Not surprisingly, a pronounced decrease in the content of complex IV was observed also in the mutant *atp6*-L252P whereas the abundance of this complex was almost normal in the *atp6*-S250P mutant, as revealed by BN-PAGE analysis of mitochondrial protein digitonin-extracts (Fig. 2A).

3.2.2. Mitochondrial ATP synthesis/hydrolysis

We analyzed further the influence of the *atp6*-S250P and *atp6*-L252P mutations by measuring the rate of ATP synthesis in isolated mitochondria, which was done in the presence of a large excess of external ADP to keep constant a minimal intra-mitochondrial concentration of ATP. An ~30% decrease in ATP synthesis rate was observed in *atp6*-S250P mitochondria while this activity was less than 10% that of *WT* (Table 2) in the *atp6*-L252P mutant. As the rates of oxygen consumption were reduced in similar proportions (see above), it can be inferred that the efficiency of oxidative

Table 2
Influence of the *atp6-S250P* and *atp6-L252P* mutations on yeast mitochondrial respiration, and ATP synthesis and hydrolysis activities.

Strain	Respiration rates nmol O min^{-1} mg^{-1}				ATP synthesis rate nmol Pi min^{-1} mg^{-1}		ATPase activity µmol Pi min^{-1} mg^{-1}	
	NADH	NADH + ADP	NADH + CCCP	Asc/TMPD + CCCP	−oligo	+oligo	−oligo	+oligo
MR6	470 ± 59	898 ± 124	1437 ± 316	2540 ± 434	1112 ± 185	52 ± 25	4.1 ± 1.6	0.48 ± 0.27
AKY5	420 ± 41	774 ± 61	1374 ± 129	2606 ± 185	779 ± 37	10 ± 5	4.5 ± 2.0	0.71 ± 0.37
RKY66	154 ± 1	180 ± 7	356 ± 57	559 ± 33	71 ± 1	29 ± 3	5.1 ± 0.3	4.1 ± 1.9

Mitochondria were isolated from wild type strain MR6 (*wt*) and mutants *atp6*-S250P and *atp6*-L252P grown for 5–6 generations in YPGALA medium (rich galactose) at 28 °C. Reaction mixes for assays contained 0.15 mg/ml protein, 4 mM NADH, 150 (for respiration assays) or 750 (for ATP synthesis) µM ADP, 12.5 mM ascorbate (*Asc*), 1.4 mM N,N,N,N,-tetramethyl-p-phenylenediamine (*TMPD*), 4 µM CCCP, 3 µg/ml oligomycin (*oligo*). The two MR6 cultures contained 2–5% of ρ^-/ρ° cells, while those of *atp6*-S250P and *atp6*-L252P contained 5% and 36% ρ^-/ρ° cells. The values reported are averages of triplicate assays ± standard deviation. Respiratory and ATP synthesis activities were measured using freshly isolated, osmotically protected mitochondria buffered at pH 6.8. For the ATPase assays, mitochondria kept at −80 °C were thawed and the reaction performed in absence of osmotic protection and at pH 8.4.

Please cite this article in press as: A.M. Kabala, et al., Defining the impact on yeast ATP synthase of two pathogenic human mitochondrial DNA mutations, T9185C and T9191C, Biochimie (2013), http://dx.doi.org/10.1016/j.biochi.2013.11.024

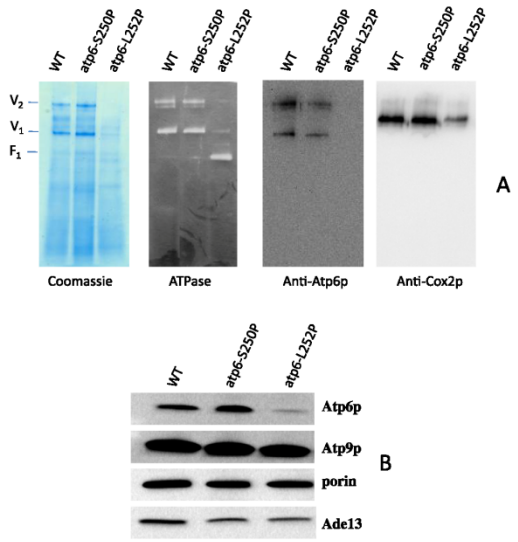

Fig. 2. ATP synthase and complex IV in the mutants *atp6-S250P* and *atp6-L252P*. A: BN-PAGE analysis of mitochondrial protein digitonin-extracts (50 μg of protein). The proteins were, as indicated, stained in-gel by Coomassie brilliant blue and their ATPase activity, and by Western blot with antibodies against Atp6p and Cox2p. Fully assembled, dimeric (V_2) and monomeric (V_1), F_1F_O-ATP synthase complexes accumulate normally in the atp6-S250P mutant while only trace amounts are detected in the atp6-L252P mutant. This mutant accumulates large amounts of free F_1 particles. The anti-cox2 Western reveals that the atp6-L252P mutant has low contents in cytochrome oxidase (complex IV) while the levels of this enzyme in the atp6-S250P mutant are similar to those seen in the WT. B: SDS-PAGE of total mitochondrial proteins (20 μg). After migration the proteins were transferred to a nitrocellulose membrane and probed with antibodies against porin and Atp6p.

phosphorylation (*i.e.* the number of ATP molecules formed per electron transferred to oxygen) was largely unaffected by both mutations.

We next measured the rate of ATP hydrolysis by non-osmotically protected mitochondria buffered at pH 8.4 and in the presence of saturating amounts of ATP, conditions under which this activity is maximal. Both mutants had an ATPase activity similar to that of the *WT* (Table 2). Of particular interest, oligomycin inhibited the ATPase activity by 85% in the *WT* and *atp6*-S250P samples, but only by 20% in the *atp6*-L252P mutant.

3.2.2.1. ATP-driven translocation of protons across the mitochondrial inner membrane. We next measured the proton-pumping activity coupled to F_1-mediated ATP hydrolysis in samples of whole mitochondria, using a fluorescent dye, Rhodamine 123, to monitor changes in the membrane potential ($\Delta\Psi$) (Fig. 3). This dye accumulates inside the mitochondrial matrix, where its fluorescence is quenched, in response to an established $\Delta\Psi$ [27]. Before testing for ATP-driven proton translocation, the mitochondria were energized with ethanol in order to elicit release of the natural inhibitory peptide (IF1) that binds F_1F_O in the resting state and prevents ATP hydrolysis [36]. The imposed $\Delta\Psi$ was then collapsed with KCN and less than 2 min later ATP was added, i.e. well before rebinding of IF1 to F_1 could occur. The added ATP is counter-exchanged for ADP in the matrix compartment and is then hydrolyzed by the ATP synthase coupled to the pumping of protons out of the mitochondrial matrix through the F_O. Comparable levels of proton pumping coupled to ATP hydrolysis was manifested in the *WT* and *atp6*-S250P mitochondria by a large and sustained fluorescence quenching that was fully reversed upon addition of oligomycin. It is to be noted that the concentration of oligomycin used in these assays is in far excess of the one that is minimally required to inhibit all ATP synthase complexes in wild type mitochondria, which explains that the ATP-induced $\Delta\Psi$ in mutant and wild type mitochondria showed the same sensitivity to oligomycin. In the growth tests of Fig. 1 showing that the *atp6*-S250P mutant has an increased *in vivo* sensitivity to oligomycin, the drug was used at a suboptimal concentration not sufficient to inhibit the respiratory growth of wild type yeast. Mitochondria from the *atp6*-L252P mutant produced only a small change in fluorescence upon addition of ATP and this change was almost insensitive to oligomycin.

3.2.3. Assembly/stability of the ATP synthase in the atp6-S250P and atp6-L252P mutants

We finally investigated the influence of the *atp6*-S250P and *atp6*-L252P mutations on ATP synthase assembly/stability, by BN-PAGE analysis of mitochondrial proteins extracted with digitonin (Fig. 2A). The BN gels were first stained with Coomassie brilliant blue. *WT* and *atp6*-S250P samples showed similar amounts of fully assembled ATP synthase dimers and monomers, whereas these

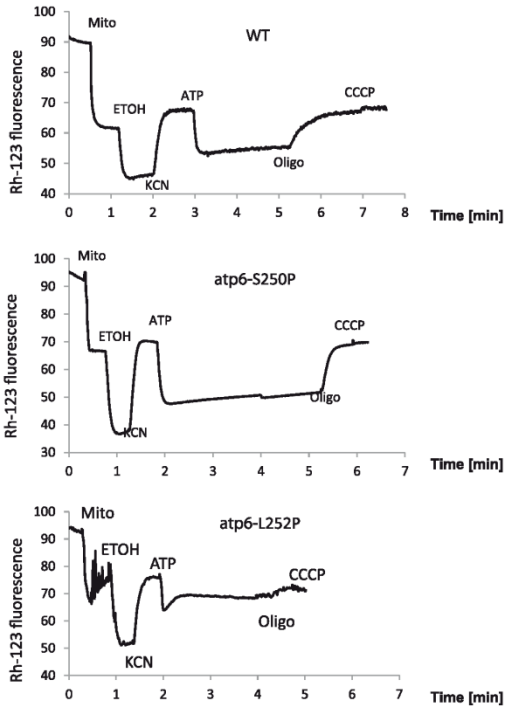

Fig. 3. ATP-driven energization of mitochondria. Energization of the mitochondrial inner membrane in intact mitochondria from wild type, *atp6-S250P* and *atp6-L252P* mutants grown in rich galactose at 28 °C was monitored by Rhodamine 123 (Rh-123) fluorescence quenching. The additions were 0.5 μg/ml Rhodamine 123, 0.15 mg/ml mitochondrial proteins (Mito), 10 μl of ethanol (EtOH), 0.2 mM potassium cyanide (KCN), 1 mM ATP, 6 μg/ml oligomycin (oligo) and 3 μM CCCP.

Please cite this article in press as: A.M. Kabala, et al., Defining the impact on yeast ATP synthase of two pathogenic human mitochondrial DNA mutations, T9185C and T9191C, Biochimie (2013), http://dx.doi.org/10.1016/j.biochi.2013.11.024

complexes were barely detectable in *atp6*-L252P samples. The protein complexes were further analyzed in-gel via their ATPase activity. Two major ATPase signals corresponding to ATP synthase dimers and monomers were detected for both the WT and *atp6*-S250P mutant. Similar signals were seen also but with a much weaker intensity for the *atp6*-L252P mutant. Of particular interest this mutant displayed a strong lower-size ATPase signal corresponding to free F_1. Finally, the protein complexes were transferred to a nitrocellulose membrane and decorated with antibodies against Atp6p, which further illustrated the failure of the *atp6*-L252P mutant to assemble correctly the ATP synthase.

In SDS gels of total mitochondrial protein extracts, Atp6p was barely detected in the *atp6*-L252P mutant whereas the steady state levels of this protein were normal in the *atp6*-S250P mutant (Fig. 2B). Pulse labeling of the proteins encoded by the mitochondrial genome revealed that Atp6p was synthesized efficiently in both mutants (Fig. 4). It can be inferred that the nearly absence of Atp6p in the mutant *atp6*-L252P is caused by a high susceptibility of this protein to degradation. There is a visible difference in the migration of Atp6p in both mutants where this protein appears to be larger than in the *WT*. It seems unlikely that this effect is due to a block in the processing of the leader peptide of Atp6p, a stretch of 10 amino acids that is removed during assembly of the protein [37–40]. Indeed, if this were the case, both mutant proteins would have the same migration rate, which is not observed. Atp6p like other very hydrophobic proteins has aberrant electrophoretic properties; while it migrates as a 21 KDa protein it has a predicted molecular weight of about 30 KDa. The differences in the migration of Atp6p in the *atp6*-S250P and *atp6*-L252P mutants most likely result from the structural changes induced by the mutations themselves. That a single amino acid replacement may change the electrophoretic properties of a protein has been observed on many occasions (see Fig. 3 in Ref. [41] for an example).

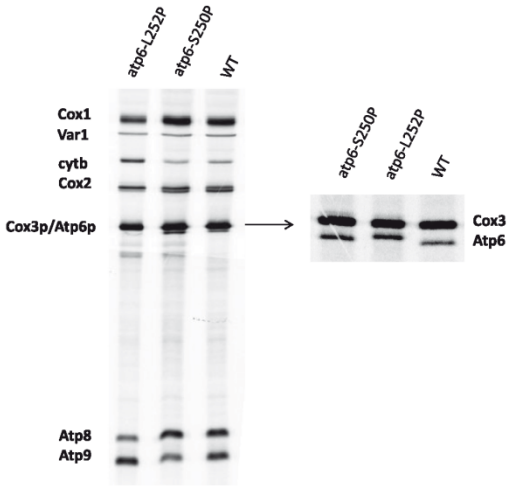

Fig. 4. *In vivo* labeling of mitochondrial translation products. Proteins encoded by mtDNA were labeled in whole cells from wild type (MR6) and strains bearing *atp6-S250P* and *atp6-L252P* mutations with [35S]-(methionine + cysteine) for 20 min in the presence of cycloheximide to inhibit cytosolic protein synthesis. After the labeling reactions, total protein extracts were prepared from the cells (0.2 OD at 650 nm) and separated by SDS-PAGE on a 16.5% polyacrylamide gel (left). For a better resolution of Cox3p and Atp6p, a 12% polyacrylamide gel containing 6 M urea was used (right). The gels were dried and analyzed with a PhosphorImager.

4. Discussion

We have investigated the consequences on yeast ATP synthase of two mutations of the human mitochondrial ATP6 gene, T9185C and T9191C, that were identified in patients suffering from neurological disorders [17]. Both mutations change a leucine residue into proline near the C-terminal end of the human homolog of yeast Atp6p, at positions 220 and 222 respectively. These leucine residues show moderate evolutionary conservation as manifested by the presence of different amino acids at corresponding positions in other species (like Ser, Val, Ile, and Gly at position 220; Ala, Met, Ser and Ile at position 222) (see Ref. [29] for amino acids alignments). In current folding models [29], these residues belong to the last α-helical transmembrane segment (helix V) of Atp6p. This segment would contact the Atp9p-ring and is presumed to play a key role in proton transport through the F_O [42]. Nearby the leucine 220 and 222 of the human homolog of yeast Atp6p are two residues within helix V, leucine 217 and tyrosine 221, that have possible crucial importance as indicated by their strict evolutionary conservation [29]. It is therefore not very surprising that replacing leucine 220 or 222 by an α-helix breaker residue like proline is detrimental to human health. Consistent with this, some of the most severe ATP6 pathogenic mutations were located at position 217 [43].

Mutations in yeast Atp6p equivalent to T9185C (*atp6*-S250P) and T9191C (*atp6*-L252P) lead to 30% and 90% drops in the rate of mitochondrial ATP synthesis respectively (Table 2). The *atp6*-S250P mutation had no visible influence on yeast ATP synthase assembly/stability (Fig. 2A), indicating a partial functional impairment of the enzyme. There was no evidence of proton leakage across the mitochondrial inner membrane, and the efficiency of oxidative phosphorylation in *atp6*-S250P mitochondria in terms of ATP molecules synthesized per electron transferred to oxygen was almost normal. The main effect of this mutation is thus a partial functional impairment of F_O. Since the leucine 220 (serine 250 in yeast) is predicted to be very close to the matrix side of the membrane, a proline in this position could possibly create some local structural modification resulting in a less efficient exit of protons from the F_O. Alternatively, the mutation might induce long-range effects impacting the entry of protons from the intermembrane space or their exchange with the *c*-ring near the middle of the membrane. Nearly identical defects, i.e. a 30% deficit in ATP production with no visible impact on assembly/stability of ATP synthase, were found in a yeast model of the T9176C mutation (amino acid position 217 in humans, 247 in yeast) that gives also relatively mild clinical phenotypes [15]. These findings reveal that a deficit in mitochondrial ATP production so modest as 30% is sufficient to impact human health.

The >95% drop in ATP synthesis in the *atp6*-L252P mutant is caused by defects in ATP synthase assembly. Only trace amounts of fully assembled F_1F_O complexes were detected by BN-PAGE analysis in this mutant (Fig. 2A). The mutated Atp6p was synthesized efficiently (Fig. 3) but failed to accumulate at the steady state (Fig. 2B) indicating that it is rapidly eliminated from cells after synthesis [9,44]. Yeast Atp6p is typically degraded when it cannot assemble. It is presumed to insert in a late step after assembly of the other ATP synthase subunits [23,44]. When subjected to BN-PAGE analysis the Atp6p-less intermediate easily dissociates into several subcomplexes, among which free F_1 particles [23] (this study, Fig. 2A). The rapid degradation of neo-synthesized Atp6p and the presence of substantial amounts of free F_1 in the *atp6*-L252P mutant are strong indications that the mutated protein is unable to be stably incorporated into ATP synthase. As the region of Atp6p affected by the L252P change is presumed to contact the *c*-ring, it is possible that the mutated protein cannot interact properly with the *c*-ring.

Please cite this article in press as: A.M. Kabala, et al., Defining the impact on yeast ATP synthase of two pathogenic human mitochondrial DNA mutations, T9185C and T9191C, Biochimie (2013), http://dx.doi.org/10.1016/j.biochi.2013.11.024

Alternatively, the mutation may prevent insertion of Atp6p within the membrane or acquisition of a folded structure required to interact with the *c*-ring. In this respect, it is to be noted that the C-terminal region of Atp6p seems to be critical for interaction with Atp10p [45], an accessory protein that helps insertion of Atp6p into ATP synthase either directly or by protecting it against proteolytic degradation until it is assembled [46]. Nearly identical defects were found in a yeast model of the pathogenic mutation T9176G mutation, which changes the highly conserved leucine 217 (247 in yeast) into arginine [14]. This mutation results in very severe clinical phenotypes too similar to those of the patient with the T9191C mutation [43]. Since this mutation was found in only one patient, its pathogenesis remained uncertain. Our study provides strong evidence that this mutation was actually responsible for the clinical phenotypes displayed by this patient.

Acknowledgments

This work was supported by the National Science Center of Poland grant nr 1932/B/P01/2010/39 to R.K, and by the Fondation de la Recherche Médicale (FRM) and the Association Française contre les Myopathies (AFM) to J.P.dR.

References

[1] M. Duno, F. Wibrand, K. Baggesen, T. Rosenberg, N. Kjaer, A.L. Frederiksen, A novel mitochondrial mutation m.8989G > C associated with neuropathy, ataxia, retinitis pigmentosa – the NARP syndrome, Gene 515 (2013) 372–375.
[2] M. Houshmand, S. Kasraie, S. Etemad Ahari, M. Moin, M. Bahar, A. Zamani, Investigation of tRNA and ATPase 6/8 gene mutations in Iranian ataxia telangiectasia patients, Arch. Med. Sci. 7 (2011) 523–527.
[3] G. Pfeffer, E.L. Blakely, C.L. Alston, A. Hassani, M. Boggild, R. Horvath, D.C. Samuels, R.W. Taylor, P.F. Chinnery, Adult-onset spinocerebellar ataxia syndromes due to MTATP6 mutations, J. Neurol. Neurosurg. Psychiatry 83 (2012) 883–886.
[4] J.D. Tsai, C.S. Liu, T.F. Tsao, J.N. Sheu, A novel mitochondrial DNA 8597T > C mutation of Leigh syndrome: report of one case, Pediatr. Neonatol. 53 (2012) 60–62.
[5] S. Rahman, R.B. Blok, H.H. Dahl, D.M. Danks, D.M. Kirby, C.W. Chow, J. Christodoulou, D.R. Thorburn, Leigh syndrome: clinical features and biochemical and DNA abnormalities, Ann. Neurol. 39 (1996) 343–351.
[6] T. Lamminen, A. Majander, V. Juvonen, M. Wikstrom, P. Aula, E. Nikoskelainen, M.L. Savontous, A mitochondrial mutation at nt 9101 in the ATP synthase 6 gene associated with deficient oxidative phosphorylation in a family with Leber hereditary optic neuroretinopathy, Am. J. Hum. Genet. 56 (1995) 1238–1240.
[7] T. Pulkes, Adult-onset spinocerebellar ataxia due to MTATP6 mutations: are they more common than previously thought? J. Neurol. Neurosurg. Psychiatry 83 (2012) 857–858.
[8] J. Finsterer, Inherited mitochondrial neuropathies, J. Neurol. Sci. 304 (2011) 9–16.
[9] S.H. Ackerman, A. Tzagoloff, Function, structure, and biogenesis of mitochondrial ATP synthase, Prog. Nucleic Acid Res. Mol. Biol. 80 (2005) 95–133.
[10] R.H. Fillingame, C.M. Angevine, O.Y. Dmitriev, Mechanics of coupling proton movements to c-ring rotation in ATP synthase, FEBS Lett. 555 (2003) 29–34.
[11] D. Stock, C. Gibbons, I. Arechaga, A.G. Leslie, J.E. Walker, The rotary mechanism of ATP synthase, Curr. Opin. Struct. Biol. 10 (2000) 672–679.
[12] M. Rak, E. Tetaud, S. Duvezin-Caubet, N. Ezkurdia, M. Bietenhader, J. Rytka, J.P. di Rago, A yeast model of the neurogenic ataxia retinitis pigmentosa (NARP) T8993G mutation in the mitochondrial ATP synthase-6 gene, J. Biol. Chem. 282 (2007) 34039–34047.
[13] R. Kucharczyk, M. Rak, J.P. di Rago, Biochemical consequences in yeast of the human mitochondrial DNA 8993T > C mutation in the ATPase6 gene found in NARP/MILS patients, Biochim. Biophys. Acta 1793 (2009) 817–824.
[14] R. Kucharczyk, B. Salin, J.P. di Rago, Introducing the human Leigh syndrome mutation T9176G into *Saccharomyces cerevisiae* mitochondrial DNA leads to severe defects in the incorporation of Atp6p into the ATP synthase and in the mitochondrial morphology, Hum. Mol. Genet. 18 (2009) 2889–2898.
[15] R. Kucharczyk, N. Ezkurdia, E. Couplan, V. Procaccio, S.H. Ackerman, M. Blondel, J.P. di Rago, Consequences of the pathogenic T9176C mutation of human mitochondrial DNA on yeast mitochondrial ATP synthase, Biochim. Biophys. Acta 1797 (2010) 1105–1112.
[16] R. Kucharczyk, M.F. Giraud, D. Brethes, M. Wysocka-Kapcinska, N. Ezkurdia, B. Salin, J. Velours, N. Camougrand, F. Haraux, J.P. di Rago, Defining the pathogenesis of human mtDNA mutations using a yeast model: the case of T8851C, Int. J. Biochem. Cell Biol. 45 (2013) 130–140.
[17] A.R. Moslemi, N. Darin, M. Tulinius, A. Oldfors, E. Holme, Two new mutations in the MTATP6 gene associated with Leigh syndrome, Neuropediatrics 36 (2005) 314–318.
[18] A.E. Castagna, J. Addis, R.R. McInnes, J.T. Clarke, P. Ashby, S. Blaser, B.H. Robinson, Late onset Leigh syndrome and ataxia due to a T to C mutation at bp 9,185 of mitochondrial DNA, Am. J. Med. Genet. A 143A (2007) 808–816.
[19] A.M. Childs, T. Hutchin, K. Pysden, L. Highet, J. Bamford, J. Livingston, Y.J. Crow, Variable phenotype including Leigh syndrome with a 9185T > C mutation in the MTATP6 gene, Neuropediatrics 38 (2007) 313–316.
[20] R.D. Pitceathly, S.M. Murphy, E. Cottenie, A. Chalasani, M.G. Sweeney, C. Woodward, E.E. Mudanohwo, I. Hargreaves, S. Heales, J. Land, J.L. Holton, H. Houlden, J. Blake, M. Champion, F. Flinter, S.A. Robb, R. Page, M. Rose, J. Palace, C. Crowe, C. Longman, M.P. Lunn, S. Rahman, M.M. Reilly, M.G. Hanna, Genetic dysfunction of MT-ATP6 causes axonal Charcot–Marie–Tooth disease, Neurology 79 (2012) 1145–1154.
[21] R.P. Saneto, K.K. Singh, Illness-induced exacerbation of Leigh syndrome in a patient with the MTATP6 mutation, m. 9185 T > C, Mitochondrion 10 (2010) 567–572.
[22] N. Bonnefoy, T.D. Fox, Genetic transformation of *Saccharomyces cerevisiae* mitochondria, Method Cell Biol. 65 (2001) 381–396.
[23] M. Rak, E. Tetaud, F. Godard, I. Sagot, B. Salin, S. Duvezin-Caubet, P.P. Slonimski, J. Rytka, J.P. di Rago, Yeast cells lacking the mitochondrial gene encoding the ATP synthase subunit 6 exhibit a selective loss of complex IV and unusual mitochondrial morphology, J. Biol. Chem. 282 (2007) 10853–10864.
[24] D.F. Steele, C.A. Butler, T.D. Fox, Expression of a recoded nuclear gene inserted into yeast mitochondrial DNA is limited by mRNA-specific translational activation, Proc. Natl. Acad. Sci. U. S. A. 93 (1996) 5253–5257.
[25] B. Guerin, P. Labbe, M. Somlo, Preparation of yeast mitochondria (*Saccharomyces cerevisiae*) with good P/O and respiratory control ratios, Method Enzymol. 55 (1979) 149–159.
[26] M. Rigoulet, B. Guerin, Phosphate transport and ATP synthesis in yeast mitochondria: effect of a new inhibitor: the tribenzylphosphate, FEBS Lett. 102 (1979) 18–22.
[27] R.K. Emaus, R. Grunwald, J.J. Lemasters, Rhodamine 123 as a probe of transmembrane potential in isolated rat-liver mitochondria: spectral and metabolic properties, Biochim. Biophys. Acta 850 (1986) 436–448.
[28] M. Somlo, Induction and repression of mitochondrial ATPase in yeast, Eur. J. Biochem. 5 (1968) 276–284.
[29] R. Kucharczyk, M. Zick, M. Bietenhader, M. Rak, E. Couplan, M. Blondel, S.D. Caubet, J.P. di Rago, Mitochondrial ATP synthase disorders: molecular mechanisms and the quest for curative therapeutic approaches, Biochim. Biophys. Acta 1793 (2009) 186–199.
[30] A. Mukhopadhyay, M. Uh, D.M. Mueller, Level of ATP synthase activity required for yeast *Saccharomyces cerevisiae* to grow on glycerol media, FEBS Lett. 343 (1994) 160–164.
[31] U.P. John, P. Nagley, Amino acid substitutions in mitochondrial ATPase subunit 6 of *Saccharomyces cerevisiae* leading to oligomycin resistance, FEBS Lett. 207 (1986) 79–83.
[32] M.K. Ray, I.F. Connerton, D.E. Griffiths, DNA sequence analysis of the Olir2-76 and Ossr1-92 alleles of the Oli-2 region of the yeast *Saccharomyces cerevisiae*. Analysis of related amino-acid substitutions and protein-antibiotic interaction, Biochim. Biophys. Acta 951 (1988) 213–219.
[33] V. Contamine, M. Picard, Maintenance and integrity of the mitochondrial genome: a plethora of nuclear genes in the budding yeast, Microbiol. Mol. Biol. Rev. 64 (2000) 281–315.
[34] M. Bietenhader, A. Martos, E. Tetaud, R.S. Aiyar, C.H. Sellem, R. Kucharczyk, S. Clauder-Munster, M.F. Giraud, F. Godard, B. Salin, I. Sagot, J. Gagneur, M. Dequard-Chablat, V. Contamine, S. Hermann-Le Denmat, A. Sainsard-Chanet, L.M. Steinmetz, J.P. di Rago, Experimental relocation of the mitochondrial ATP9 gene to the nucleus reveals forces underlying mitochondrial genome evolution, PLoS Genet. 8 (2012) e1002876.
[35] I.C. Soto, F. Fontanesi, M. Valledor, D. Horn, R. Singh, A. Barrientos, Synthesis of cytochrome c oxidase subunit 1 is translationally downregulated in the absence of functional F1F0-ATP synthase, Biochim. Biophys. Acta 1793 (2009) 1776–1786.
[36] R. Venard, D. Brethes, M.F. Giraud, J. Vaillier, J. Velours, F. Haraux, Investigation of the role and mechanism of IF1 and STF1 proteins, twin inhibitory peptides which interact with the yeast mitochondrial ATP synthase, Biochemistry 42 (2003) 7626–7636.
[37] T. Michon, M. Galante, J. Velours, NH2-terminal sequence of the isolated yeast ATP synthase subunit 6 reveals post-translational cleavage, Eur. J. Biochem. 172 (1988) 621–625.
[38] X. Zeng, W. Neupert, A. Tzagoloff, The metalloprotease encoded by ATP23 has a dual function in processing and assembly of subunit 6 of mitochondrial ATPase, Mol. Biol. Cell 18 (2007) 617–626.
[39] C. Osman, C. Wilmes, T. Tatsuta, T. Langer, Prohibitins interact genetically with Atp23, a novel processing peptidase and chaperone for the F1Fo-ATP synthase, Mol. Biol. Cell 18 (2007) 627–635.
[40] X. Zeng, R. Kucharczyk, J.P. di Rago, A. Tzagoloff, The leader peptide of yeast Atp6p is required for efficient interaction with the Atp9p ring of the mitochondrial ATPase, J. Biol. Chem. 282 (2007) 36167–36176.
[41] G. Arselin, M.F. Giraud, A. Dautant, J. Vaillier, D. Brethes, B. Coulary-Salin, J. Schaeffer, J. Velours, The GxxxG motif of the transmembrane domain of subunit e is involved in the dimerization/oligomerization of the yeast ATP

Please cite this article in press as: A.M. Kabala, et al., Defining the impact on yeast ATP synthase of two pathogenic human mitochondrial DNA mutations, T9185C and T9191C, Biochimie (2013), http://dx.doi.org/10.1016/j.biochi.2013.11.024

synthase complex in the mitochondrial membrane, Eur. J. Biochem. 270 (2003) 1875–1884.
[42] R.H. Fillingame, O.Y. Dmitriev, Structural model of the transmembrane Fo rotary sector of H+-transporting ATP synthase derived by solution NMR and intersubunit cross-linking in situ, Biochim. Biophys. Acta 1565 (2002) 232–245.
[43] R. Carrozzo, A. Tessa, M.E. Vazquez-Memije, F. Piemonte, C. Patrono, A. Malandrini, C. Dionisi-Vici, L. Vilarinho, M. Villanova, H. Schagger, A. Federico, E. Bertini, F.M. Santorelli, The T9176G mtDNA mutation severely affects ATP production and results in Leigh syndrome, Neurology 56 (2001) 687–690.
[44] M. Rak, X. Zeng, J.J. Briere, A. Tzagoloff, Assembly of F0 in *Saccharomyces cerevisiae*, Biochim. Biophys. Acta 1793 (2009) 108–116.
[45] M.F. Paul, A. Barrientos, A. Tzagoloff, A single amino acid change in subunit 6 of the yeast mitochondrial ATPase suppresses a null mutation in ATP10, J. Biol. Chem. 275 (2000) 29238–29243.
[46] A. Tzagoloff, A. Barrientos, W. Neupert, J.M. Herrmann, Atp10p assists assembly of Atp6p into the F0 unit of the yeast mitochondrial ATPase, J. Biol. Chem. 279 (2004) 19775–19780.

Please cite this article in press as: A.M. Kabala, et al., Defining the impact on yeast ATP synthase of two pathogenic human mitochondrial DNA mutations, T9185C and T9191C, Biochimie (2013), http://dx.doi.org/10.1016/j.biochi.2013.11.024

III.1.2 Use of yeast Saccharomyces cerevisiae as a model organism for drug screening

In the following article (Couplan, Aiyar et al. 2011), which is summarized below, we use the *fmc1* deletion mutant as a model of diseases caused by mutations in human *ATP12* (De Meirleir, Seneca et al. 2004) and *TMEM70* (Cizkova, Stranecky et al. 2008) genes that are characterized by a low content of ATP synthase. The *fmc1* mutant grows poorly on glycerol at 35°C. We used this mutant for screening of drugs that can improve its ability to grow on glycerol at this temperature. Two active drugs were selected: chlorhexidine (CH) and oleate (OA), which were then tested on five yeast *atp6*-NARP models and in a human cybrid-based model of NARP.

We demonstrated that DHLA, a compound already used as a treatment in patients with mitochondrial encephalopathy (Mattiazzi, Vijayvergiya et al. 2004; DiMauro, Hirano et al. 2006), recovered respiratory growth of the *fmc1* mutant at 35°C. It was also true for OA, a compound that induces *ODC1* gene in yeast. *ODC1* gene was previously shown as a suppressor of respiratory growth defect in the *fmc1Δ* strain (Tibbetts, Sun et al. 2002). The next step was to test about 12,000 compounds from chemical libraries and identify those that rescue the *fmc1* mutant. Chlorhexidine from Prestwick Chemical Library, a collection of drugs already tested in humans, was identified. It was also active in the *atp6*-NARP 8993T>G and 8851T>C strains.

Deletion of the *FMC1* gene from yeast strain results in multiple defects when cells are grown at 35°C. We observed lower oxygen consumption by respiratory chain complexes due to low amounts of these complexes in mitochondria, weak energization of inner mitochondrial membrane, decreased level of ATP synthesis, strongly reduced content in ATP synthase, presence of inclusion bodies in mitochondrial matrix and almost no *cristae* in the mitochondria. Figure 2 in the article below shows that CH attenuates all these phenotypes whereas had no influence on *WT* strain.

To answer the question whether CH has a global effect in *fmc1Δ* mutant we analyzed the transcriptional response in the *WT*, *fmc1Δ* mutant treated and not treated with the drug. The obtained results revealed that the most affected genes with a reduced expression due to the *fmc1* deletion are connected with the mitochondrial respiration and the retrograde signaling pathway. Presence of CH in the medium partially reversed this effect. With respect to *WT*, we found that CH dramatically increase the expression of *QRC9* (Fig. 3B in the article below), a gene that encodes a subunit of cytochrome bc_1 complex. Interestingly,

over-expression of the *QRC9* gene from a plasmid was alone able to improve the respiratory growth of *fmc1Δ*, indicating that this gene plays a key role in the CH rescue (Fig. 3C in the article below).

Further analysis pertained to the effect of DHLA, OA and CH in human NARP cybrid cells. We could observe a significant increase in growth rates of these cells in glucose-deprived medium (Fig. 4A in the article below). No such effect could be observed for *WT* cells As mitochondrial disorders often result in lactic acidosis due to enhanced glycolysis, we measured the levels of glycolytic byproducts (pyruvate and lactate) secreted by the human NARP cells upon treatment with CH. The levels of these metabolic intermediates were diminished in comparison to non-treated cybrid cells (Fig. 4B and C in the article below).

Results presented in the publication below show that yeast can be successfully used as a model for screening of drugs active against ATP synthase disorders.

A yeast-based assay identifies drugs active against human mitochondrial disorders

Elodie Couplan[a,1], Raeka S. Aiyar[b,1], Roza Kucharczyk[c,d], Anna Kabala[c,d], Nahia Ezkurdia[c], Julien Gagneur[b], Robert P. St. Onge[e], Bénédicte Salin[c], Flavie Soubigou[a], Marie Le Cann[a], Lars M. Steinmetz[b], Jean-Paul di Rago[c,2,3], and Marc Blondel[a,2,3]

[a]INSERM U613; Université de Brest, Faculté de Médecine et des Sciences de la Santé; Etablissement Français du Sang (EFS) Bretagne; Centre Hospitalier Régional Universitaire Brest, Hop Morvan, Laboratoire de Génétique Moléculaire, F-29200 Brest, France; [b]Genome Biology Unit, European Molecular Biology Laboratory, 69117 Heidelberg, Germany; [c]Institut de Biochimie et de Génétique Cellulaire, Centre National de la Recherche Scientifique, Université Victor Segalen Bordeaux 2, Bordeaux, F-33077 Cedex, France; [d]Institute of Biochemistry and Biophysics, Polish Academy of Sciences, 02-901, Warsaw, Poland; and [e]Department of Biochemistry, Stanford Genome Technology Center, Stanford University, Palo Alto, CA 94304

Edited by Gottfried Schatz, University of Basel, Reinach, Switzerland, and approved June 6, 2011 (received for review February 9, 2011)

Due to the lack of relevant animal models, development of effective treatments for human mitochondrial diseases has been limited. Here we establish a rapid, yeast-based assay to screen for drugs active against human inherited mitochondrial diseases affecting ATP synthase, in particular NARP (neuropathy, ataxia, and retinitis pigmentosa) syndrome. This method is based on the conservation of mitochondrial function from yeast to human, on the unique ability of yeast to survive without production of ATP by oxidative phosphorylation, and on the amenability of the yeast mitochondrial genome to site-directed mutagenesis. Our method identifies chlorhexidine by screening a chemical library and oleate through a candidate approach. We show that these molecules rescue a number of phenotypes resulting from mutations affecting ATP synthase in yeast. These compounds are also active on human cybrid cells derived from NARP patients. These results validate our method as an effective high-throughput screening approach to identify drugs active in the treatment of human ATP synthase disorders and suggest that this type of method could be applied to other mitochondrial diseases.

budding yeast | drug screening | transcription profiling | NARP cybrid

Although our understanding of the molecular mechanisms underlying mitochondrial diseases has considerably improved, the development of effective treatments has still been extremely limited (1). The insufficiency of relevant disease models in conjunction with the absence of high-throughput drug screening assays may, at least in part, explain this failure.

Among these disorders, some are associated with primary deficiencies in the mitochondrial ATP synthase (2), an enzyme that catalyzes the final steps of mitochondrial ATP production. To date, seven point mutations in the mitochondrial *ATP6* gene encoding subunit *a* of ATP synthase have been associated with a group of maternally inherited neurodegenerative syndromes with onset in early infancy (1, 3), including NARP (neuropathy, ataxia, and retinitis pigmentosa). In diseases resulting from mutations in mitochondrial DNA (mtDNA), wild-type and mutated mtDNA coexist in patient mitochondria, a characteristic called heteroplasmy. The severity of the disease depends on the proportion of mutant alleles, with a minimal critical proportion of ~70% for penetrance of a clinical phenotype; this property is known as the threshold effect (4, 5).

The budding yeast *Saccharomyces cerevisiae* serves as a good model for mitochondrial disease because (*i*) mitochondrial genes and function are particularly well conserved from yeast to human (1); (*ii*) yeast are genetically tractable; and (*iii*) yeast have the ability to survive either by fermentation or by respiration, where only the latter requires oxidative phosphorylation (OXPHOS). This last point is particularly beneficial because mutant strains in which ATP synthase activity is impaired can be easily maintained on fermentable media (e.g., glucose); therapeutic strategies can then be tested on media where respiration is required (e.g., glycerol, ethanol, or lactate). In addition, along with *Chlamydomonas reinhardtii* (6), yeast is the only eukaryote in which site-directed mutagenesis of the mitochondrial genome has been established (7). Because of the natural instability of heteroplasmy in yeast, homoplasmic populations in which 100% of mitochondria contain mutated mtDNA can be easily generated. Thus, yeast models of the five most common *ATP6* mutations found in NARP patients (T8993G, T8993C, T9176G, T9176C, and T8851C) have been generated and characterized (8–11). Other patients exhibiting ATP synthase deficiency have been found to carry mutations in two nuclear genes, *ATP12* (12) and *TMEM70* (13), which encode proteins that are required for ATP synthase assembly. An appropriate yeast model of such disorders is the deletion mutant for the nuclear gene *FMC1* that encodes a protein required at high temperatures (35–37 °C) for assembly of the F_1 sector of ATP synthase (14). When the *fmc1Δ* mutant is grown at high temperatures, its mitochondria contain far fewer assembled ATP synthase complexes than a wild-type (*WT*) strain, whereas the ones that assemble are fully functional. This heterogeneity is also found in patients with decreased levels of ATP synthase due to *ATP12*, *TMEM70*, or heteroplasmic *ATP6* mutations. Therefore, the *fmc1Δ* mutant constitutes an appropriate model of these disorders.

In this study, we establish a two-step screening assay designed to identify drugs active against inherited ATP synthase disorders modeled in yeast. In the primary screen, ~12,000 compounds from various chemical libraries were tested for their ability to suppress the respiratory growth defect of the *fmc1Δ* mutant. In the secondary screen, active compounds were tested on the five yeast *atp6*-NARP mutants. Our screen identified chlorhexidine (CH) and oleate (OA); further experiments confirmed that they improve various respiratory phenotypes of both the *fmc1Δ* and NARP mutants. Dihydrolipoic acid (DHLA), which has previously been reported as active against mitochondrial encephalopathies and is currently being tested in patients (15, 16), was also active in our yeast-based method. Moreover, we show that CH, OA, and DHLA are effective in a human cybrid-based model of NARP. These results validate our yeast-based approach as a method for identifying compounds with potential to treat inherited mitochondrial diseases affecting ATP synthase.

Author contributions: R.S.A., L.M.S., J.-P.d.R., and M.B. designed research; E.C., R.S.A., R.K., A.K., N.E., R.P.S.O., B.S., F.S., M.L.C., J.-P.d.R., and M.B. performed research; R.K. contributed new reagents/analytic tools; E.C., R.S.A., J.G., R.P.S.O., L.M.S., J.-P.d.R., and M.B. analyzed data; and E.C., R.S.A., L.M.S., J.-P.d.R., and M.B. wrote the paper.

The authors declare no conflict of interest.

This article is a PNAS Direct Submission.

[1]E.C. and R.S.A. contributed equally to this work.

[2]J.-P.d.R. and M.B. contributed equally to this work.

[3]To whom correspondence may be addressed. E-mail: marc.blondel@univ-brest.fr or jp.dirago@ibgc.u-bordeaux2.fr.

This article contains supporting information online at www.pnas.org/lookup/suppl/doi:10.1073/pnas.1101478108/-/DCSupplemental.

GENETICS

Results

Development of a Yeast-Based Screen for Drugs That Suppress NARP Phenotypes. The *fmc1Δ* mutant and the five yeast *atp6*-NARP mutants exhibit growth defects on glycerol-based medium at 35 and 37 °C (Fig. 1*A*). At 35 °C, the temperature used for the screening assay, the different mutants present growth defects of varying severity, with the *atp6*-NARP T9176G, T8851C, and T8993G mutants (the latter being the most frequent mutation in human) exhibiting the most severe phenotypes. Our measurements of mitochondrial ATP synthesis in these mutants (Fig. 1*A Right*) correlate well with their fitness on glycerol. They also confirm previous observations that defects in ATP synthesis must be severe (estimated at ~80% or more; refs. 8 and 17) before a clear growth defect on respiratory medium can be observed in yeast. Even more significant is the fact that these observations also correlate with what is known about the relative severity of the corresponding *atp6*-NARP mutations in human (2, 18, 19), which likely reflects a high level of evolutionary conservation within the region of subunit *a* affected by these mutations. These observations constitute a preliminary validation of the use of yeast to model human inherited mitochondrial diseases affecting ATP synthase. Because the *fmc1Δ* strain displays an intermediate respiratory growth phenotype and is a good model of heteroplasmy, we selected it for our primary screen.

We next tested candidate compounds that could hold therapeutic potential for mitochondrial disease in our yeast-based assay. We selected DHLA because it has already been used as a treatment for patients presenting mitochondrial encephalopathies (15, 16). We also selected OA, a fatty acid known to induce expression of the mitochondrial Odc1p protein (20), a carrier for various Krebs cycle intermediates encoded by the *ODC1* gene in yeast (21). We have previously isolated *ODC1* as a multicopy suppressor of the respiratory growth defect of the *fmc1Δ* strain (22). By using our simple assay described below, we found that both DHLA and OA partially suppress, in a dose-dependent manner, the growth defect of the *fmc1Δ* strain (Fig. 1*B*). The fact that DHLA, a compound displaying therapeutic benefits for patients affected by mitochondrial encephalopathies, also suppresses the respiratory growth phenotype of the *fmc1Δ* strain further validates our yeast-based method.

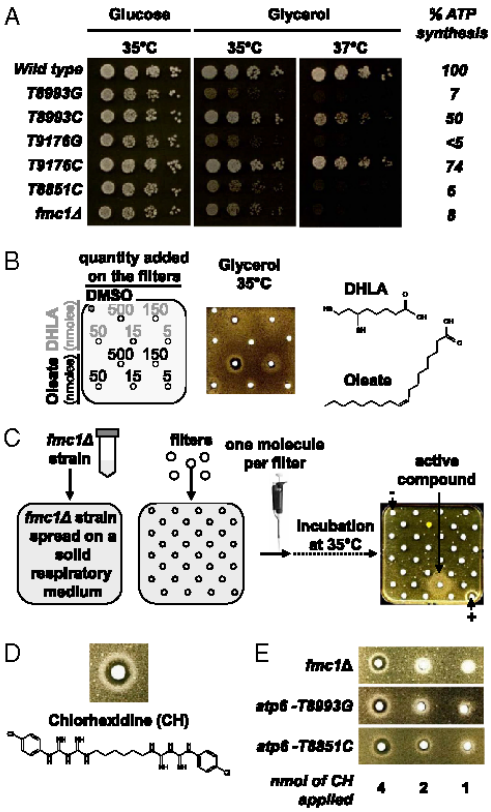

Fig. 1. Development of a yeast-based screening assay for NARP-related diseases and identification of CH. (*A*) Serial dilutions of the *WT* strain, five *NARP* mutants, and the *fmc1Δ* strain were spotted onto glucose and glycerol plates. The plates were incubated at the indicated temperature for 3 d (glucose) or 7 d (glycerol). Rates of ATP synthesis relative to *WT* are indicated in the right-hand column. (*B*) Candidate screen. The *fmc1Δ* strain was spread onto rich glycerol plates. Small sterile filters were then placed on the agar surface and DHLA or OA (chemical structures depicted at *Right*) were added to the filters at the indicated quantities. The plates were then incubated at 35 °C for 7 d. (*C*) Screening assay carried out as described in *B* except that DMSO was added to the upper left filter (negative control, –) and DHLA to the bottom right filter (positive control, +). At the remaining positions, compounds from the chemical libraries were added, and plates were incubated for 7 d at 35 °C. (*D*) The improvement of fmc1Δ growth obtained with CH is shown, and its molecular structure is depicted. (*E*) The dose-dependent effect of CH on three yeast mutants is shown.

Primary Screen of Chemical Libraries Using Yeast-Based Assay. We then performed our primary screen by testing 12,000 compounds from various chemical libraries for their ability to suppress the respiratory growth defect of the *fmc1Δ* mutant strain. Similarly to an assay we previously developed (23, 24), *fmc1Δ* cells are spread on solid glycerol medium and exposed to filters spotted with the compounds. Active compounds are then identified by a halo of enhanced growth around a filter (example in Fig. 1*C Right*). The advantage of this method is that, in one simple experiment, it allows numerous compounds to be tested across a large range of concentrations due to diffusion of the drugs in the growth medium. This design improves the sensitivity of the screen drastically because many compounds (including OA and CH, see below) are toxic at high concentrations (Fig. 1*B* and *C*). The positive hits obtained were then tested in a secondary screen by using the yeast *atp6*-NARP mutants in the same experimental procedure.

Our screen used, among others, the Prestwick Chemical Library, a collection of drugs for which bioavailability and toxicity studies have already been carried out in humans; therefore, active compounds from this library can directly enter drug optimization programs. The percentage of active compounds in our primary screen was quite low (only ~10 of 12,000 molecules tested, corresponding to <0.1%), indicating that the screening assay is specific and stringent.

Identification of CH. Among the hits from our primary screen was CH, an antiseptic compound from the Prestwick Chemical Library (Fig. 1*D*). The secondary screen (Fig. 1*E*) showed that, in addition to its activity in the *fmc1Δ* strain, CH elicits a dose-dependent partial suppression of the respiratory growth defects of the *atp6*-NARP T8993G and T8851C strains. In contrast, CH had no visible effect on the *atp6*-NARP T9176G strain, which is the most severe NARP mutation in both human and yeast (Fig. 2*A*). The severity of this phenotype is due to an almost complete lack of incorporation of subunit *a* into ATP synthase (10), whereas substantial residual mitochondrial ATP synthesis is observed in the mutants that are rescued by CH (11).

CH Rescues Multiple Mitochondrial Defects in *fmc1Δ* Cells. To characterize the effects of CH, we used the *fmc1Δ* strain because it responds best to the drug. The *fmc1Δ* strain exhibits a low rate of ATP synthase assembly and low levels of respiratory complexes

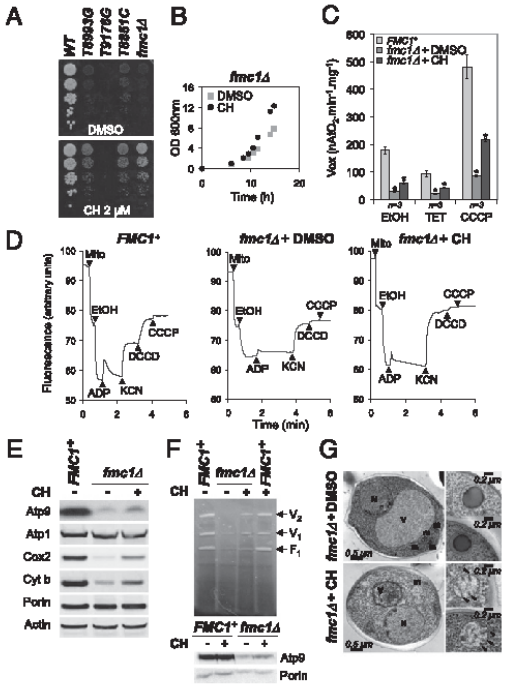

Fig. 2. CH suppresses multiple phenotypes of yeast models of ATP synthase disorders. (*A*) Serial dilutions of the *WT* strain, three *NARP* mutants, and the *fmc1Δ* strain were spotted onto glycerol plates supplemented with CH (2 μM final concentration) or the equivalent quantity of DMSO (– control). The plates were incubated at 35 °C for 7 d. (*B*) Growth curves of the *fmc1Δ* strain grown at 35 °C in liquid galactose medium supplemented with 1.25 μM CH (the optimal concentration) or DMSO. (*C*) Mean respiration rates of the *WT* and *fmc1Δ* strains treated in vivo with 1.25 μM CH or DMSO were determined using three different substrates as indicated. Error bars represent SD. * represents significant difference compared with untreated cells (P = 0.05, one-sided Wilcoxon rank test). (*D*) Energization of the mitochondrial membrane was determined by rhodamine 123 fluorescence quenching with intact mitochondria from the *fmc1Δ* strain treated in vivo with 1.25 μM CH (*Right*) or DMSO (*Center*), and the *WT* isogenic strain (*FMC1*$^+$; *Left*). The contents were added as follows: mitochondrial proteins (Mito), ethanol (EtOH), ADP, potassium cyanide (KCN), DCCD, and CCCP. (*E*) SDS-PAGE and Western blot analysis of mitochondrial proteins from the mitochondria used in *D*. Porin was used as a loading control. (*F*) BN-PAGE, ATPase activity, and Western blot analysis of extracts from isolated mitochondria. V_2 and V_1 indicate the dimeric and monomeric forms of the F_1F_0 ATP synthase complex, respectively; F_1 indicates the free F_1 particles. (*G*) Ultrastructure electron micrographs of *fmc1Δ* cells grown at 35 °C in presence of 1 μM CH (*Lower*) or DMSO as control (*Upper*). Arrowheads indicate mitochondrial cristae.

III and IV when grown at high temperatures (35-37 °C; ref. 25). In addition, its mitochondria are devoid of cristae and contain large inclusion bodies composed mostly of aggregated, unassembled α and β subunits of the F_1 moiety of ATP synthase. Finally, its inner mitochondrial membrane energization and respiration rate are impaired. We thus set out to determine whether CH treatment could rescue these phenotypes. For growth in liquid, we selected galactose as a carbon source to allow faster growth of the mutant strains while retaining their mitochondrial activity; although galactose is a fermentable substrate, unlike glucose it does not elicit repression of mitochondrial biogenesis. In addition, the growth defect of *fmc1Δ* yeast as well as its rescue by CH could be clearly observed in liquid galactose medium (Fig. 2*B*).

Oxygen consumption rates. Using ethanol as an electron donor, we measured the oxygen consumption levels of *WT* (*FMC1*$^+$) and *fmc1Δ* whole cells grown at 35 °C in rich galactose medium with or without CH. In the absence of CH, *fmc1Δ* cells exhibited respiration activity six times lower than *WT*; treatment with CH resulted in a significant (2.2-fold; P = 0.05, *SI Methods*) increase in respiration (Fig. 2*C*). We also measured respiration in the presence of triethyltin (TET), an inhibitor of ATP synthase (basal or state 4 respiration), and the mitochondrial membrane uncoupler carbonyl cyanide *m*-chlorophenylhydrazone (CCCP), i.e., in conditions where respiration is maximal (uncoupled state). In these conditions, treatment of *fmc1Δ* cells with CH also resulted in significantly improved respiration rates (2.1- and 2.5-fold, respectively; P = 0.05; Fig. 2*C*).

Respiratory enzyme abundance. The respiration data suggest that CH treatment increases the amount of respiratory enzymes in *fmc1Δ* cells, which we confirmed by Western blot analysis (Fig. 2*E*). We observed a partial restoration of steady-state levels of complex III–V subunits except for Atp1p, whose abundance is unaffected by the *FMC1* deletion as previously observed (14). In contrast, CH treatment did not affect the amount of respiratory enzymes in *WT* cells (Fig. S1).

Energization of mitochondrial membrane. We assessed the proton pumping activity of isolated mitochondria prepared from *WT* (*FMC1*$^+$) and *fmc1Δ* cells grown with or without CH using the fluorescent membrane potential (ΔΨ)-sensitive dye rhodamine 123 (26). Consistent with their low oxygen consumption and our previous results (14), mitochondria from untreated *fmc1Δ* cells were poorly energized with ethanol relative to *WT*, whereas those from *fmc1Δ* cells grown in the presence of CH were energized almost as efficiently as *WT* mitochondria (Fig. 2*D*). In *WT* mitochondria, a further addition of ADP, as expected, led to a transient decrease of fluorescence quenching, reflecting the use of ΔΨ by ATP synthase to phosphorylate the added ADP. Because of the low levels of ATP synthase in *fmc1Δ* mitochondria, the addition of ADP had little effect on membrane potential. In contrast, a significant ΔΨ decrease was induced by ADP addition in mitochondria isolated from CH-treated *fmc1Δ* cells. This observation reflects a higher level of ADP phosphorylation in mitochondria from *fmc1Δ* cells upon CH treatment.

ATP synthesis rates. We measured ATP synthesis rates of mitochondria isolated from both *WT* and *fmc1Δ* cells grown with or without CH, using NADH as a respiratory substrate and an excess of external ADP. In good agreement with the partial suppression of the respiratory growth phenotype, we observed a modest but reproducible effect of CH on ATP synthesis rates in *fmc1Δ* cells, whereas CH had almost no effect on *WT* mitochondria (Table S1).

Blue native (BN)-PAGE and ATPase activity. We evaluated the effect of CH on both assembly and activity of ATPase in isolated mitochondria from both *fmc1Δ* and *WT* cells grown with or without CH. The BN-PAGE and ATPase activity stain demonstrate that CH treatment led to a significant increase in fully assembled ATP synthase in the *fmc1Δ* strain (Fig. 2*F*).

Mitochondrial morphology. We evaluated the effect of CH on the mitochondrial morphology of *fmc1Δ* cells using electron microscopy. Consistent with previous observations (25), 77% of cell sections of *fmc1Δ* cells grown at 35 °C display matrix-localized, electron-dense inclusion bodies consisting of ATP synthase subunits α and β. Strikingly, this proportion was reduced to 6% when *fmc1Δ* cells were grown in the presence of CH (Fig. 2*G* and Table S2). Moreover, mitochondrial cristae were clearly discernible in some of these cells, whereas they were completely absent in untreated *fmc1Δ* cells. The restoration of cristae is consistent with the CH-induced increase in oxygen consumption and respiratory chain subunits, because cristae allow higher amounts of respiratory enzymes to be assembled within mitochondria.

Transcription Profile of *fmc1Δ* Strain and Its Response to CH Treatment. To investigate the global effects of CH on cellular function in the *fmc1Δ* mutant, we carried out genome-wide

comparative analyses of the transcriptional responses to the *FMC1* gene deletion and the addition of the drug using high-resolution tiling microarrays (ref. 27; Fig. 3*A*). Overall, 336 of 5,446 expressed genes [defined in *SI Methods*; results in Dataset S1 and available from ArrayExpress (details in *SI Methods*)] showed at least 1.5-fold differential expression in response to the deletion of *FMC1* (Fig. 3*A*, triangles). We analyzed these genes according to Gene Ontology (28) and transcription factor targets (ref. 29; *SI Methods*; results in Dataset S2). As expected, these genes are mostly related to mitochondrial respiration; in particular, the down-regulated genes are enriched for subunits of the respiratory chain complexes (30/47; $P = 6 \times 10^{-17}$; *P* values corrected for multiple testing; *SI Methods*) and targets of the respiratory gene expression activator Hap4p (25/38; $P = 5 \times 10^{-24}$). Additionally, enrichment for targets of the transcription factors Rtg3p (5/31; $P = 8 \times 10^{-2}$) and Gcn4p (15/121; $P = 5 \times 10^{-3}$) indicate that the retrograde pathway, a transcriptional program that responds to mitochondrial dysfunction by modulating metabolism, was activated in the *fmc1Δ* mutant (30–32). Finally, iron homeostasis was also perturbed in the *fmc1Δ* strain (11/38; $P = 6 \times 10^{-7}$).

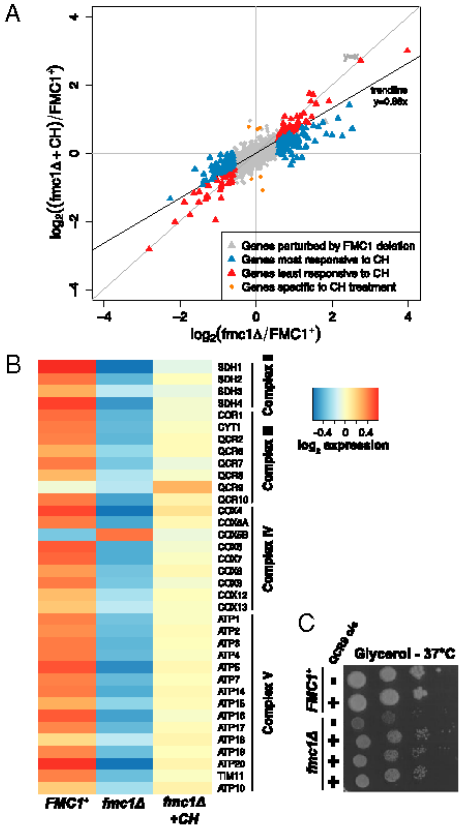

Fig. 3. Transcription profiles of *fmc1Δ*, *fmc1Δ* + CH, and *WT* (FMC1$^+$). (*A*) Scatterplot of $\log_2$-fold changes in gene expression of CH-treated (*y* axis) and untreated (*x* axis) *fmc1Δ* yeast relative to *WT* in rich galactose medium at 35 °C. CH treatment induces a genome-wide shift toward *WT* expression levels of ~1/3 as evidenced by the trendline $y = 0.66x$. (*B*) Expression of genes encoding respiratory chain complex subunits. Log_2-scale normalized expression values were centered for each gene by subtracting the mean expression level from all values per gene. Subunits show a general pattern of down-regulation in *fmc1Δ* yeast relative to *WT* and partial rescue by CH treatment. (*C*) Overexpression of the *QCR9* gene in the *fmc1Δ* strain (bottom three rows, compared with the *fmc1Δ* strain in third row and *WT* strain in first two rows) results in partial recovery of growth on rich glycerol medium at a nonpermissive temperature.

The drug CH induced a partial rescue of the *fmc1Δ* mutant at the transcriptional level, with gene expression fold changes compared with *WT* reduced genome-wide by ~1/3 (Fig. 3*A*; trendline $y = 0.66x$, where complete rescue would be ~0 and no drug effect would be ~1). Almost all genes perturbed in the *fmc1Δ* mutant responded positively to CH treatment, although to varying extents. The most responsive genes (perturbed genes whose fold change relative to *WT* was reduced by >1/3; Fig. 3*A*, blue), included all 30 respiratory chain complex subunits and 23/25 ($P = 3 \times 10^{-21}$) of the Hap4p targets down-regulated in the mutant; they were also enriched for genes involved in cristae formation (3/4; $P = 10^{-3}$). Accordingly, signals of the retrograde response largely disappeared after CH treatment. Among the genes least responsive to CH treatment (perturbed genes whose response to the drug was lower than the genome-wide trend; Fig. 3*A*, red) were those involved in iron homeostasis. The small number of genes (six) specific to CH treatment (those whose treatment-induced expression was significantly different from both other conditions) and their lack of functional enrichments suggests that the drug has no major side effects unrelated to the mutant phenotype.

The transcriptional behavior of the respiratory chain subunits provides important insight into the regulatory impact of CH on the *fmc1Δ* mutant (Fig. 3*B*). Among the subunits, there was a clear pattern of down-regulation in the *fmc1Δ* mutant relative to *WT*, with CH treatment recovering expression to intermediate levels (corroborating the measurements of protein levels; Fig. 2*E*). The only genes that did not follow this pattern were *COX5B* (encoding an "anaerobic" isoform of cytochrome *c* oxidase subunit 5) and, more interestingly, *QCR9*, encoding a component of cytochrome bc_1 complex, whose expression was up-regulated beyond *WT* levels by CH treatment. The unique response of *QCR9* prompted us to investigate whether overexpression of this gene alone was sufficient to suppress the respiratory growth defect of the *fmc1Δ* strain. Indeed, a partial rescue was observed in *fmc1Δ* cells overexpressing the *QCR9* gene (Fig. 3*C*). These findings suggest that *QCR9* could be a key regulatory target for determining the cellular levels of bc_1 complex (*Discussion*). Together, our transcription data correspond well to our biochemical data and strongly indicate that the main effect CH has on the *fmc1Δ* strain is improvement of its respiratory function, in which *QCR9* may play a role. Notably, *WT* cells displayed a very limited response to CH at the transcriptional level that included neither activation of respiratory pathways nor up-regulation of *QCR9* expression (Dataset S1). These results suggest that CH does not act via a general transcriptional induction of respiratory pathways; rather, it requires specific conditions to exert its beneficial effects (*Discussion*).

Drugs Active in the Yeast-Based Assay are also Active in Human NARP Cells. We next tested the compounds that were active in our yeast-based assay in a human cell-based model nearly homoplasmic for the NARP T8993G mutation (33). To encourage the cells to rely on OXPHOS rather than glycolysis, we used glucose-deprived medium (34), in which the NARP cybrids exhibit a significant growth defect (33). Strikingly, DHLA, CH, and OA all significantly increased the growth rate of NARP cybrids (Fig. 4*A*). In agreement with its effects in mitochondrial encephalopathy patients, treatment with 200 μM DHLA increased the survival of NARP cybrid cells by 2.2-fold, recovering their survival to nearly the rate measured in control cybrids (Fig. 4*A*). Remarkably, CH (Fig. 4*A Right*) and OA (Fig. 4*A Left*) treatments resulted in a clear dose-dependent improvement of NARP cybrid survival (the maximal increases were 1.5- and 1.6- fold, respectively). As in yeast, however, CH did not affect growth of WT cybrids (Fig. S2). The improved survival of

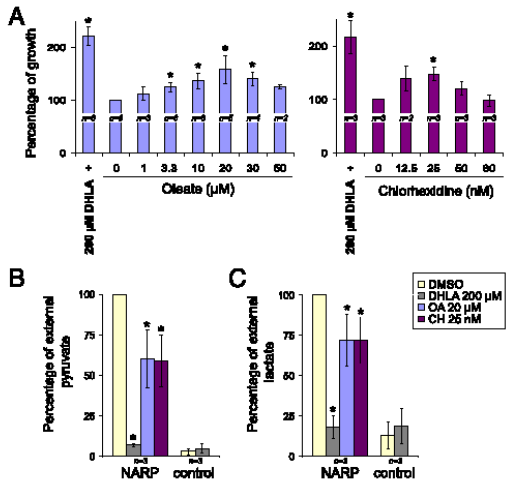

Fig. 4. DHLA, CH, and OA are active in a human cybrid-based model of NARP syndrome. NARP and control cybrids were grown in glucose-deprived medium with DHLA, CH, and OA at the indicated final concentrations or with the equivalent quantity of DMSO as a control (0). (*A*) Percentage of growth after 3 d in glucose-deprived medium containing OA or CH at the indicated concentrations, compared with treatment with DHLA at 200 μM final concentration (+), a compound being tested in clinical trials for the treatment of mitochondrial encephalopathies. * represents conditions with growth significantly different from in DMSO ($P < 0.05$; *Methods*). (*B*) Mean percentage of external pyruvate in NARP cybrids treated with DHLA, CH, OA (left-hand side of graph) compared with control cybrids (right-hand side of graph). Error bars represent SD. * represents significant difference compared with the DMSO condition ($P = 0.01$). (*C*) Mean percentage of external lactate as in *B*.

the NARP cybrids suggests that DHLA, OA, and CH improve OXPHOS production of ATP in these cells.

As one of the main symptoms of NARP-related mitochondrial disorders is lactic acidosis, which is most likely due to a shift toward glycolytic metabolism, it would be particularly valuable if these compounds could reduce glycolysis. Indeed, CH, OA, and DHLA effected a reduction in extracellular levels of the glycolytic byproducts pyruvate and lactate in NARP cybrids (Fig. 4*B* and *C*), comparable to their amelioration of growth: DHLA reduced external pyruvate and lactate to the levels observed in control cybrids, and OA and CH each reduced pyruvate by ~40% and lactate by ~30% ($P = 0.01$; *Methods*). These observations demonstrate that DHLA, OA, and CH reduce glycolysis in NARP cybrids, indicating that they induce a metabolic shift toward OXPHOS.

Discussion

Our results validate the use of a yeast-based assay to identify compounds potentially active in the treatment of inherited mitochondrial diseases caused by ATP synthase deficiency. Firstly, there is a strong correlation between the severity of mutations in patients and the respiratory defects caused by the homologous mutations in yeast. Secondly, DHLA, a compound previously found to be active against mitochondrial encephalopathies in humans, is also active in yeast. Thirdly, CH and OA, two compounds identified by our yeast-based assay, are also active in human cybrids derived from NARP patients.

>CH has remarkable suppressor activity in our yeast model (*fmc1Δ*) of ATP synthase assembly disorders, with a substantial (more than twofold) increase in respiration due to higher amounts of respiratory complexes III and IV. Consistent with this result, the *fmc1Δ* mutant recovered an effective capacity to energize the inner mitochondrial membrane upon CH treatment. Another striking effect of CH is the restoration of mitochondrial cristae and elimination of matrix-localized inclusion bodies formed by aggregation of α and β ATP synthase subunits. In agreement with these suppressive effects, CH partially restored the expression of most components of the OXPHOS pathway perturbed in the *fmc1Δ* mutant. The transcription data, which provide insight into the cellular response to CH treatment, tell us that the strongest beneficial effect of CH is at the level of the respiratory chain. The fact that CH did not exert this effect on *WT* cells indicates that (*i*) the transcriptional response of *fmc1Δ* cells to CH is more likely a downstream rather than a direct effect of treatment, and (*ii*) CH requires specific conditions to improve respiratory function, including but not limited to ATP synthase deficiency (otherwise it would have rescued all of the *atp6*-NARP mutants).

The expression pattern of *QCR9*, which encodes a subunit (Qcr9p) of complex III, suggests that this gene plays a role in the rescue mediated by CH. The possibility that increased Qcr9p synthesis alone could result in a higher abundance of complex III is in line with previous studies showing that such a regulatory mechanism is commonly used in the expression of mitochondrial and chloroplastic energy-transducing enzymes (35–37). Because complexes III and IV are mainly present together in the form of supercomplexes (38), increasing complex III abundance may allow more complex IV to be incorporated into mitochondria. *QCR9* overexpression does indeed improve respiratory growth of the *fmc1Δ* mutant, but to a lesser extent than CH treatment; CH treatment also effected a partial increase in ATP synthase assembly (Fig. 2 *E* and *F*). It is therefore possible that CH works by increasing both the number of ATP synthase complexes and the efficiency with which they are used (via the stronger protonmotive force produced by complexes III/IV, whose increase in quantity may be mediated by up-regulation of *QCR9*). The combination resulted in a modest but significant improvement of ATP production in *fmc1Δ* cells, leading to restoration of respiratory growth. The modest improvement of ATP production by CH has significant therapeutic potential when considering the threshold phenomenon: Small increases in ATP production can be sufficient to restore a healthy state (4, 5). Further investigations into how exactly CH improves the abundance of respiratory chain complexes and ATP synthase are needed to more thoroughly characterize the therapeutic potential of this drug. In addition, evidence of CH displaying detrimental effects at high concentrations (39) will be important to consider as CH continues to be developed as a therapeutic.

In addition to providing a simple and powerful screening assay for identifying drugs active against ATP synthase disorders, the system presented here constitutes a proof of principle that yeast can be used as a pharmacological model for the study of mitochondrial diseases. The drugs identified can be used in various reverse screening strategies (40) to identify their intracellular targets, potentially revealing novel cellular mechanisms involved in disease pathologies (41, 42). In addition, the use of multiple *atp6*-NARP mutants in our secondary screen, which resulted in candidate compounds with allele-specific efficacies, holds promise for the development of personalized therapeutics for mitochondrial diseases.

As yeast models of inherited mitochondrial disorders continue to be developed, we believe the screening approach presented here will continue to yield promising chemical therapeutics and insights into disease mechanisms (1, 43).

Methods

Yeast Strains and Culture Medium. The *S. cerevisiae* strains used and their genotypes are listed in Table S3. For details on growth procedures, see *SI Methods*.

Yeast-Based Drug Screening Assay. This assay was adapted from an existing test (23, 24). Two hundred forty microliters of exponentially growing cell cultures, adjusted to an OD_{600} of 0.2, was spread homogeneously with sterile glass beads (~3 mm diameter) on a square Petri dish (12 cm × 12cm) containing YPAGly solid medium. Sterile filters (similar to those used for anti-

GENETICS

biograms) were placed on the agar surface, and 2.5 μl of individual compounds from the various chemical libraries were applied to each filter in addition to DMSO, the vehicle, as a negative control, and a DHLA solution in DMSO as a positive control. Plates were then incubated at 35 °C for 7 d and scanned using a Snap Scan1212 (Agfa). For information on compounds screened, see *SI Methods*.

Isolation of Yeast Mitochondria and Subsequent Experiments. Mitochondria were prepared by the enzymatic method as described (44) from cells grown for 7–8 generations in YPAGal medium at 35 °C in the presence of CH or DMSO. For details on the experiments with isolated mitochondria, see *SI Methods*.

Ultrastructural Studies. Please see *SI Methods* for details.

Transcription Profiling. Two biological replicates of strains MC1 and MC6 were cultured in YPAGal + DMSO/CH at 35 °C and harvested; total RNA was isolated and reverse-transcribed into cDNA, which was hybridized to whole-genome tiling arrays. For more details, see *SI Methods*.

Statistical Analysis of Transcription Profiles. Raw tiling array data were processed to provide normalized intensity values for each probe in each hybridization. The expression level of each transcript was estimated by the median value of the probe intensities of the transcript across both arrays per strain and condition (27). For more details, see *SI Methods*.

Human Cell Lines and Culture Conditions. The cybrid cell lines JCP213 (control) and JCP239 (NARP T8993G) (33) were cultivated in high-glucose DMEM; growth measurements were performed in glucose-deprived DMEM supplemented with CH, DHLA, OA, or DMSO. For each treatment condition, four wells were used. After 3 d of incubation with the drugs, cell proliferation was estimated by using Neutral Red staining (45) and also by cell counting with an Adam cell counter. The cells were then assayed for lactate and pyruvate by using kits from DiaSys-Poles. For more details, see *SI Methods*.

ACKNOWLEDGMENTS. Part of this work was initiated in the Centre National de la Recherche Scientifique laboratory of L. Meijer, whom we thank for his continuous support and friendship. We also thank P. Lehn, Y. Bizais, and M.-F. Giraud for their warm welcome, encouragements, and helpful scientific discussions; and C. Voisset for critical reading of the manuscript. This work was supported by grants from the following organizations: Agence Nationale de la Recherche (ANR) "Maladies Rares" from the French government, Association Française Contre les Myopathies (AFM; to M.B. and J.-P.d.R.), the "Conseil Régional de la Région Aquitaine" (to J.-P.d.R.), and the National Institutes of Health/Deutsche Forschungsgemeinschaft (to L.M.S.). E.C., R.K., and N.E. were supported by postdoctoral fellowships from ANR and AFM. The study was supported technically by the European Molecular Biology Laboratory Genomics Core Facility.

1. Kucharczyk R, et al. (2009) Mitochondrial ATP synthase disorders: Molecular mechanisms and the quest for curative therapeutic approaches. *Biochim Biophys Acta* 1793:186–199.
2. Houstek J, et al. (2006) Mitochondrial diseases and genetic defects of ATP synthase. *Biochim Biophys Acta* 1757:1400–1405.
3. Tuppen HA, Blakely EL, Turnbull DM, Taylor RW (2010) Mitochondrial DNA mutations and human disease. *Biochim Biophys Acta* 1797:113–128.
4. Letellier T, Heinrich R, Malgat M, Mazat JP (1994) The kinetic basis of threshold effects observed in mitochondrial diseases: A systemic approach. *Biochem J* 302:171–174.
5. Rossignol R, et al. (2003) Mitochondrial threshold effects. *Biochem J* 370:751–762.
6. Remacle C, Cardol P, Coosemans N, Gaisne M, Bonnefoy N (2006) High-efficiency biolistic transformation of Chlamydomonas mitochondria can be used to insert mutations in complex I genes. *Proc Natl Acad Sci USA* 103:4771–4776.
7. Bonnefoy N, Fox TD (2001) Genetic transformation of Saccharomyces cerevisiae mitochondria. *Methods Cell Biol* 65:381–396.
8. Kucharczyk R, et al. (2010) Consequences of the pathogenic T9176C mutation of human mitochondrial DNA on yeast mitochondrial ATP synthase. *BBA Bioenergetics* 1797:1105–1112.
9. Kucharczyk R, Rak M, di Rago JP (2009) Biochemical consequences in yeast of the human mitochondrial DNA 8993T>C mutation in the ATPase6 gene found in NARP/MILS patients. *Biochim Biophys Acta* 1793:817–824.
10. Kucharczyk R, Salin B, di Rago JP (2009) Introducing the human Leigh syndrome mutation T9176G into Saccharomyces cerevisiae mitochondrial DNA leads to severe defects in the incorporation of Atp6p into the ATP synthase and in the mitochondrial morphology. *Hum Mol Genet* 18:2889–2898.
11. Rak M, et al. (2007) A yeast model of the neurogenic ataxia retinitis pigmentosa (NARP) T8993G mutation in the mitochondrial ATP synthase-6 gene. *J Biol Chem* 282:34039–34047.
12. De Meirleir L, et al. (2004) Respiratory chain complex V deficiency due to a mutation in the assembly gene ATP12. *J Med Genet* 41:120–124.
13. Cízková A, et al. (2008) TMEM70 mutations cause isolated ATP synthase deficiency and neonatal mitochondrial encephalocardiomyopathy. *Nat Genet* 40:1288–1290.
14. Lefebvre-Legendre L, et al. (2001) Identification of a nuclear gene (FMC1) required for the assembly/stability of yeast mitochondrial F(1)-ATPase in heat stress conditions. *J Biol Chem* 276:6789–6796.
15. DiMauro S, Hirano M, Schon EA (2006) Approaches to the treatment of mitochondrial diseases. *Muscle Nerve* 34:265–283.
16. Mattiazzi M, et al. (2004) The mtDNA T8993G (NARP) mutation results in an impairment of oxidative phosphorylation that can be improved by antioxidants. *Hum Mol Genet* 13:869–879.
17. Mukhopadhyay A, Uh M, Mueller DM (1994) Level of ATP synthase activity required for yeast Saccharomyces cerevisiae to grow on glycerol media. *FEBS Lett* 343:160–164.
18. Baracca A, et al. (2007) Biochemical phenotypes associated with the mitochondrial ATP6 gene mutations at nt8993. *Biochim Biophys Acta* 1767:913–919.
19. Vazquez-Memije ME, et al. (2009) Cellular and functional analysis of four mutations located in the mitochondrial ATPase6 gene. *J Cell Biochem* 106:878–886.
20. Tibbetts AS, Sun Y, Lyon NA, Ghrist AC, Trotter PJ (2002) Yeast mitochondrial oxodicarboxylate transporters are important for growth on oleic acid. *Arch Biochem Biophys* 406:96–104.
21. Fiermonte G, et al. (2001) Identification of the human mitochondrial oxodicarboxylate carrier. Bacterial expression, reconstitution, functional characterization, tissue distribution, and chromosomal location. *J Biol Chem* 276:8225–8230.
22. Schwimmer C, et al. (2005) Increasing mitochondrial substrate-level phosphorylation can rescue respiratory growth of an ATP synthase-deficient yeast. *J Biol Chem* 280:30751–30759.
23. Bach S, et al. (2003) Isolation of drugs active against mammalian prions using a yeast-based screening assay. *Nat Biotechnol* 21:1075–1081.
24. Bach S, et al. (2006) A yeast-based assay to isolate drugs active against mammalian prions. *Methods* 39:72–77.
25. Lefebvre-Legendre L, et al. (2005) Failure to assemble the alpha 3 beta 3 subcomplex of the ATP synthase leads to accumulation of the alpha and beta subunits within inclusion bodies and the loss of mitochondrial cristae in Saccharomyces cerevisiae. *J Biol Chem* 280:18386–18392.
26. Emaus RK, Grunwald R, Lemasters JJ (1986) Rhodamine 123 as a probe of transmembrane potential in isolated rat-liver mitochondria: Spectral and metabolic properties. *Biochim Biophys Acta* 850:436–448.
27. David L, et al. (2006) A high-resolution map of transcription in the yeast genome. *Proc Natl Acad Sci USA* 103:5320–5325.
28. Ashburner M, et al.; The Gene Ontology Consortium (2000) Gene ontology: Tool for the unification of biology. *Nat Genet* 25:25–29.
29. MacIsaac KD, et al. (2006) An improved map of conserved regulatory sites for Saccharomyces cerevisiae. *BMC Bioinformatics* 7:113.
30. Crespo JL, Powers T, Fowler B, Hall MN (2002) The TOR-controlled transcription activators GLN3, RTG1, and RTG3 are regulated in response to intracellular levels of glutamine. *Proc Natl Acad Sci USA* 99:6784–6789.
31. Epstein CB, et al. (2001) Genome-wide responses to mitochondrial dysfunction. *Mol Biol Cell* 12:297–308.
32. Guaragnella N, Butow RA (2003) ATO3 encoding a putative outward ammonium transporter is an RTG-independent retrograde responsive gene regulated by GCN4 and the Ssy1-Ptr3-Ssy5 amino acid sensor system. *J Biol Chem* 278:45882–45887.
33. Manfredi G, et al. (1999) Oligomycin induces a decrease in the cellular content of a pathogenic mutation in the human mitochondrial ATPase 6 gene. *J Biol Chem* 274:9386–9391.
34. Weber TP, Widger WR, Kohn H (2002) The Mg2+ requirements for rho transcription termination factor: Catalysis and bicyclomycin inhibition. *Biochemistry* 41:12377–12383.
35. Barrientos A, Zambrano A, Tzagoloff A (2004) Mss51p and Cox14p jointly regulate mitochondrial Cox1p expression in Saccharomyces cerevisiae. *EMBO J* 23:3472–3482.
36. Kramarova TV, et al. (2008) Mitochondrial ATP synthase levels in brown adipose tissue are governed by the c-Fo subunit P1 isoform. *FASEB J* 22:55–63.
37. Wollman FA, Minai L, Nechushtai R (1999) The biogenesis and assembly of photosynthetic proteins in thylakoid membranes1. *Biochim Biophys Acta* 1411:21–85.
38. Schägger H, Pfeiffer K (2000) Supercomplexes in the respiratory chains of yeast and mammalian mitochondria. *EMBO J* 19:1777–1783.
39. Christensen F, Bleeg HS, Jensen JE (1975) The effect of chlorhexidine on some biochemical parameters of rat liver mitochondria. *Acta Pharmacol Toxicol (Copenh)* 36:1–12.
40. Tribouillard D, et al. (2007) Antiprion drugs as chemical tools to uncover mechanisms of prion propagation. *Prion* 1:48–52.
41. Tribouillard-Tanvier D, et al. (2008) Protein folding activity of ribosomal RNA is a selective target of two unrelated antiprion drugs. *PLoS ONE* 3:e2174.
42. Voisset C, Thuret JY, Tribouillard-Tanvier D, Saupe SJ, Blondel M (2008) Tools for the study of ribosome-borne protein folding activity. *Biotechnol J* 3:1033–1040.
43. Schwimmer C, et al. (2006) Yeast models of human mitochondrial diseases: from molecular mechanisms to drug screening. *Biotechnol J* 1:270–281.
44. Guérin B, Labbe P, Somlo M (1979) Preparation of yeast mitochondria (Saccharomyces cerevisiae) with good P/O and respiratory control ratios. *Methods Enzymol* 55:149–159.
45. Auré K, et al. (2007) Impact on oxidative phosphorylation of immortalization with the telomerase gene. *Neuromuscul Disord* 17:368–375.

Supporting Information

Couplan et al. 10.1073/pnas.1101478108

SI Methods

Yeast Cell Culture, Serial Dilutions, and Growth Curves. The media used for yeast growth were: YPAD [1% (wt/vol) yeast extract, 2% (wt/vol) peptone, 2% (wt/vol) glucose, and 40 mg·L ^{1} adenine], YPAGal [1% (wt/vol) yeast extract, 2% (wt/vol) peptone, 2% (wt/vol) galactose, and 40 mg·liter ^{1} adenine] and YPAGly [1% (wt/vol) yeast extract, 2% (wt/vol) peptone, 2% (wt/vol) glycerol, and 60 mg·liter ^{1} adenine]. Solid media contained 2% (wt/vol) agar.

For liquid culture of yeast cells, YPAD overnight cultures at 29 °C of the appropriate strains were diluted in YPAGal and grown for 4 h at 29 °C and then adapted to 35 °C for an additional 4 h. Cultures were then diluted in fresh YPAGal medium supplemented either with the compounds of interest dissolved in DMSO at a 2,000× concentration or with the equivalent quantity of DMSO as a negative control and grown at 35 °C. For growth curves, aliquots were removed at the appropriate times, and their OD_{600} was determined. For all of the other experiments, cells were collected after 7–8 generations and used directly. To measure respiration and mitochondrial membrane potential, mitochondria were first isolated (see below) from collected cells.

For serial dilutions, YPAD overnight cultures of the appropriate strains grown at 29 °C were diluted in YPAGly medium to an OD_{600} of 0.05. This culture was then fivefold serially diluted in YPAGly to obtain cultures diluted 5, 25, and 125 times. Five microliters of each culture was serially spotted at the top of agar surface onto YPAD and YPAGly solid medium containing, when applicable, the compound of interest or DMSO as a control. Plates were then incubated for 3 d (YPAD) or 7 d (YPAGly) and scanned by using a Snap Scan 1212 (Agfa).

Isolation of Yeast Mitochondria and Subsequent Experiments. Mitochondria were prepared by the enzymatic method as described (1) from cells grown for 7–8 generations in YPAGal medium at 35 °C in the presence of 1.25 μM CH or equivalent quantity of DMSO, the compound vehicle. Protein amounts were determined by using the Lowry procedure in the presence of 5% SDS (2). Oxygen consumption rates were measured at 30 °C with a Clark electrode in respiration buffer (0.65 M mannitol, 0.36 mM EGTA, 5 mM Tris phosphate, 10 mM Tris maleate, pH 6.8) with isolated mitochondria (150 μg/mL) as described (3) or directly in fresh YPAGal medium containing whole cells (OD_{600}/mL for the *WT* strain and 3 OD_{600}/mL for the *fmc1Δ* strain). Variations in transmembrane potential (ΔΨ) were evaluated in the respiration buffer by measurement of rhodamine 123 fluorescence quenching with a SAFAS Monaco fluorescence spectrophotometer and were performed as described in ref. 4 and references therein. The contents were added as follows: 0.5 μg/mL rhodamine 123, 0.15 mg/mL mitochondrial proteins (*Mito*), 10 μl of ethanol (*EtOH*), ADP, 0.2 mM potassium cyanide (*KCN*), DCCD, and 3 μM CCCP. Measurements were repeated at least three times.

Chemical Libraries Used for Screening. Approximately 12,000 compounds were screened from various chemical libraries, including the Prestwick Chemical Library, a collection of compounds at least in phase II of clinical trials. This library is composed of 880 molecules, among which 90% are marketed drugs and 10% are bioactive alkaloids or related substances, thus representing a high degree of drug-likeness. Screening of this drug library followed the "SOSA approach" consisting of submitting to the screening target only a limited number of highly diverse drugs for which bioavailability and toxicity studies have already been performed and whose effectiveness in human has been proven (5). The other compounds came from various academic chemical libraries that collect highly diverse compounds, mostly from synthetic origin.

Mitochondrial Protein Extraction and Detection by Western Blots. For protein extracts, a total of 10 OD_{600} of yeast cells were harvested by centrifugation. The pellets were cooled at 4 °C on ice, resuspended in 500 μL of cold lysis solution (1.85 M NaOH, 13% β-mercaptoethanol) and 500 μL of a cold TCA solution (50%) was added in each tube. The samples were then centrifuged at 15,000 x *g* for 2 min at 4 °C. The pellets were then washed with 1 mL of ice-cold acetone and centrifuged again. The acetone was discarded, and 200 μL of Laemmli buffer was added to each tube. Following soft heat denaturation (20 min at 37 °C) and addition of 1 μL of chloroform per sample, the protein extracts were analyzed by 4–12% SDS/PAGE (precast NuPAGE, Invitrogen, 1-mm thick gel) and transferred to a nitrocellulose membrane (Schleicher & Schuell). The membranes were incubated in TBST buffer (50 mM Tris·HCl, pH 7.4, 150 mM NaCl, 0.1% Tween 20) containing 5% nonfat dry milk for 1 h at which time primary antibodies (see list and dilutions below) were added and incubated overnight at 4 °C. The membranes were then washed with fresh TBST buffer and incubated with secondary antibody (goat anti-rabbit or goat anti-mouse; Bio-Rad) conjugated to horseradish peroxidase at a 1:3,000 dilution except for anti-actin antibody, in which the secondary antibody is a goat anti-mouse IgM (Calbiochem) at a 1:2,000 dilution. Polyclonal antibodies against Atp1 and Atp9 (two subunits of the yeast ATP synthase) were a kind gift from J. Velours and were used, respectively, at 1:10,000 and 1:7,500 dilutions. The polyclonal antibody against yeast complex III cytochrome *b* subunit (a kind gift from T. Langer) was used at a 1:10,000 dilution. Monoclonal antibodies raised against Cox2, porin (Molecular Probes, Invitrogen), and actin (Calbiochem) were used respectively at 1:5,000, 1:1,000, and 1:10,000 dilutions. Each experiment was repeated at least three times independently.

BN-PAGE. Mitochondria were prepared from cells grown in rich galactose medium at 35 °C for 7 generations. The mitochondria (150 μg) were solubilized with 2 g of digitonin per gram of protein. The digitonin-extracted proteins (50 μg) were resolved by BN-PAGE, and the F_1F_0 complexes, dimeric (V_2) and monomeric (V_1) forms, as well as free F_1 particles, were detected in-gel by incubating the gel in a solution of 5 mM ATP, 5 mM $MgCl_2$, 0.05% lead acetate, and 50 mM glycine-NaOH (pH 8.6), which reveals ATPase activity as a white lead precipitate.

Mitochondrial Respiration and ATP Synthesis/Hydrolysis Activities. Mitochondria were prepared from cells grown in rich galactose medium for seven generations at 35 °C. Additions were 0.15 mg/mL proteins, 4 mM NADH, 150 μM ADP (for respiration assays) or 750 μM (for ATP synthesis), 12.5 mM ascorbate (*Asc*), 1.4 mM *N,N,N,N*,-tetramethyl-*p*-phenylenediamine (TMPD), 4 μM CCCP, 3 μg/mL oligomycin (*oligo*). The values reported are averages of duplicate assays ± SD. Respiratory and ATP synthesis activities were measured on freshly isolated osmotically protected mitochondria buffered at pH 6.8. For the ATPase assays, mitochondria kept at −80 °C were thawed, and the reaction performed in absence of osmotic protection at pH 8.4.

Ultrastructural Studies. The *WT* (MC1) and the *fmc1Δ* (MC6) yeast strains (see Table S3) were grown to early exponential phase (~10^7 cells/mL) in YPAGal medium at 35 °C. The yeast

pellets were placed on the surface of a copper electron microscopy grid (400 mesh) coated with Formvar. Each loop was very quickly submersed in precooled liquid propane and held at −180 °C with liquid nitrogen. The loops were then transferred to a precooled solution of 4% osmium tetroxide in dry acetone in a 1.8 mL of polypropylene vial and kept at −82 °C for 48 h (substitution fixation), warmed gradually to room temperature, and washed three times in dry acetone. Specimens were stained for 1 h at 4 °C in a dark room with 1% uranyl acetate in acetone. Following another rinse in dry acetone, the loops were progressively infiltrated with araldite (epoxy resin, Fluka). Ultrathin sections were contrasted with lead citrate.

Transcription Profiling. The strains MC1 and MC6 were cultured as follows (two biological replicates per strain): (*i*) 5 mL overnight culture from single colonies at 30 °C; (*ii*) transferred to 20 mL culture at OD 0.2 with either 1.25 μM CH or corresponding amount of DMSO (0.05%), grown for 9 h at 35 °C; (*iii*) transferred to 50 mL culture of same composition s.t. OD~1 following 7–8 generations, 35 °C. Two biological replicates of each strain were used (note: the same biological replicates were used in CH and DMSO cultures). Upon reaching OD_{600} = 1, each sample was collected by centrifugation and snap-frozen in liquid nitrogen. Total RNA was isolated by the hot phenol method (6), and treated with DNaseI (Turbo DNA-free Kit, Ambion) for 25 min at 37 °C according to the manufacturer's instructions. The RNA was then reverse-transcribed to single-stranded cDNA as follows: each 105-μL reaction (carried out in duplicate per sample) contained 20 μg of total RNA, 1.72 μg of random hexamers (RH6), 34 ng of oligo(dT), 20 μg/mL Actinomycin D (ActD), 0.4 mM dNTPs containing dUTP (dTTP:dUTP = 4:1), 20 μL of 5× first strand synthesis buffer (Invitrogen), 10 μL of 0.1 M DTT (Invitrogen), and 2,000 units of SuperScript II (Invitrogen). The synthesis lasted 1 h 10 min (10 min at 25 °C, 30 min at 37 °C, 30 min at 42 °C), followed by reverse transcriptase inactivation at 70 °C for 10 min. Total RNA and RNA in heteroduplex with cDNA were digested by a mixture of 3 μL of RNAseA/T mixture (Ambion) and 3 μL of RNAseH (Invitrogen) for 15 min at 37 °C followed by inactivation of the enzymes for 15 min at 70 °C. Replicate cDNA samples were combined, applied to MinElute cleanup columns (QIAGEN), and eluted in 30 μL of DEPC-H_2O. Then 4.6 μg of purified cDNA was fragmented and labeled with the WT terminal labeling kit (Affymetrix) and hybridized to Affymetrix (PN 520055) (6) whole-genome tiling arrays, all according to the manufacturer's instructions.

Statistical Analysis of Transcription Profiles. Raw tiling array data were processed to provide normalized intensity values for each probe in each hybridization (all values available in Dataset S1). The expression level of each transcript was estimated by the median value of the probe intensities of the transcript across both arrays per strain and condition. The expression level cutoff for calling a transcript expressed was obtained by using the same procedure as described (6). Briefly, the distribution of background microarray signal intensities was estimated from the intensities of the probes outside transcript boundaries. The cutoff for an intensity to be significantly above background was then set at an estimated false discovery rate (FDR) of 0.01 (6). By this definition, 5,446 of 6,609 yeast transcripts were expressed in at least one strain. Next, significance for differential expression between conditions of interest was determined by using Limma's moderated *t* test and corrected for multiple testing by using the Benjamini–Hochberg method (7). All categories of genes were selected according to an FDR ≤ 10%. For Fig. 3*A*, the trendline $y = 0.66x$ was calculated by using Principal Component Analysis. Gene categories were defined as follows: (*i*) genes perturbed in MC6 were defined by a fold change ≥ 1.5 and a statistically significant difference (FDR < 0.1) between MC1 and (untreated) MC6; (*ii*) genes most responsive to CH treatment are those in category (*i*) where $\log_2(MC6+CH/MC1) < 0.66*\log_2(MC6/MC1)$ (i.e., genes whose response was greater than the trend) and where the difference between MC6+CH and MC6 expression values was statistically significant (FDR ≤ 0.1); (*iii*) genes least responsive to CH treatment are those in category (*i*) where $\log_2(MC6+CH/MC1) \geq 0.66*\log_2(MC6/MC1)$ (i.e., genes whose response was lower than the trend); (*iv*) genes specific to CH treatment are those not in category (*i*) where $\log_2(MC6+CH/MC1) > \log_2(1.5)$, $\log_2(MC6+CH/MC6) > \log_2(1.5)$ and the differences between MC6+CH and both other conditions was statistically significant (FDR ≤ 0.1). Functional enrichments were calculated using the Ontologizer tool (8) on Gene Ontology (9) and transcription factor targets (10) with the "Term-for-term" analysis corrected for multiple testing by using the Benjamini–Hochberg method (Dataset S2). Raw data are available from the ArrayExpress repository (http://www.ebi.ac.uk/arrayexpress) under accession no. E-TABM-1176.

Human Cell Lines and Culture Conditions. The cybrid cell lines JCP213 (control) and JCP239 (NARP T8993G) were generated by fusion of human osteosarcoma cell line 143BK-ρ^0 with platelets (thus devoid of nuclei) from healthy donors to generate JCP213 or from NARP patients bearing the T8993G mutation to generate JCP239 (11). JCP213 and JCP239 containing 0 and 84 ± 4% mtDNA molecules bearing the T8993G mutation, respectively, were cultivated at 37 °C and 5% CO_2 in DMEM containing high glucose (4.5 g/L) and supplemented with 5% FBS (FBS Gold, PAA), 1 mM sodium pyruvate, 4 mM glutamine, 200 M uridine, and 20 units/mL penicillin/streptomycin. For growth measurement experiments, 10^4 cells were plated in 24-wells plate containing DMEM with glucose as described above but without antibiotic. After 24 h of growth, the medium was removed< and the cells were washed with PBS (1×) and then DMEM without glucose. The cells were then grown in the same glucose-deprived DMEM supplemented with CH, DHLA, OA, or DMSO (negative control). For each treatment condition, four wells were used. CH and OA solutions in DMSO were diluted 1:1,000 in the medium and used at final concentrations from 12.5 to 80 nM for CH and from 1 to 50 μM for OA. DHLA at 200 μM or the same quantity of DMSO were used as positive and negative controls, respectively. After 3 d of incubation with the drugs, cell proliferation was estimated by using Neutral Red staining (12) and also by cell counting with an Adam cell counter. For Neutral Red staining, cells were incubated for 4 h at 37 °C in the presence of 33 g/mL Neutral Red staining in DMEM without glucose, washed twice in PBS (1×) and air-dried for 15 min. Neutral Red-stained cells were then solubilized in 1 mL of a solution containing 50% ethanol and 1% acetic acid and quantified by determining their absorbance at 540 nm. Experiments were done at least three times per condition. Cell counts in each condition were expressed in proportion of cell counts in DMSO control experiments ("percentage of growth"). Each condition was measured three to five times, at the exception of OA 50 μM with only two measurements. For the OA and the CH series separately, an ANOVA model was fitted with intercept at 100% growth and significance of the effect for each concentration was assessed by the *t* test using the R-package lmtest.

External Lactate and Pyruvate Measurements. The cybrid cell lines JCP213 (control) and JCP239 (NARP T8993G) were grown and treated as described above. At 24 h after plating in DMEM supplemented with glucose, cells were grown for 3 d in DMEM without glucose and containing either one of the drugs or, as a control, the equivalent quantity of DMSO. Stock solutions for each drug were prepared in DMSO so that these solutions were diluted 1:1,000 in DMEM to reach the following final concentrations: 200 μM for DHLA, 25 nM for CH, and 200 μM for

OA. As control DMSO was diluted 1:1,000 in DMEM. For these experiments, cells were seeded at 7.5 × 10^5 cells in T75 flasks (two dishes per condition). After 3 d of growth, the media were collected from each flask, and two volumes of 12% trichloroacetic acid (TCA) were added to precipitate the proteins. After vortexing, the mixtures were kept on ice for 5 min and then centrifuged for 10 min at 1,500 × g. Aliquots of the supernatants were kept on ice and assayed for lactate and pyruvate by using kits commercialized by DiaSys-Poles following the manufacturer's instructions. The amount of pyruvate was monitored by following the oxidation of NADH to NAD+ at 340 nm, the decrease in NADH being directly proportional to pyruvate concentration. The lactate assay is based on lactate deshydrogenase, and NADH formation was used as a readout of lactate concentration. For each dish, cells were harvested by using trypsin-EDTA and counted to express lactate and pyruvate levels as μmol per 10^6 cells. Experiments were done three times per condition.

1. Guérin B, Labbe P, Somlo M (1979) Preparation of yeast mitochondria (Saccharomyces cerevisiae) with good P/O and respiratory control ratios. *Methods Enzymol* 55:149–159.
2. Lowry OH, Rosebrough NJ, Farr AL, Randall RJ (1951) Protein measurement with the Folin phenol reagent. *J Biol Chem* 193:265–275.
3. Rigoulet M, Guerin B (1979) Phosphate transport and ATP synthesis in yeast mitochondria: Effect of a new inhibitor: the tribenzylphosphate. *FEBS Lett* 102:18–22.
4. Rak M, et al. (2007) Yeast cells lacking the mitochondrial gene encoding the ATP synthase subunit 6 exhibit a selective loss of complex IV and unusual mitochondrial morphology. *J Biol Chem* 282:10853–10864.
5. Wermuth CG (2004) Selective optimization of side activities: Another way for drug discovery. *J Med Chem* 47:1303–1314.
6. David L, et al. (2006) A high-resolution map of transcription in the yeast genome. *Proc Natl Acad Sci USA* 103:5320–5325.
7. Benjamini Y, Drai D, Elmer G, Kafkafi N, Golani I (2001) Controlling the false discovery rate in behavior genetics research. *Behav Brain Res* 125:279–284.
8. Bauer S, Gagneur J, Robinson PN (2010) GOing Bayesian: Model-based gene set analysis of genome-scale data. *Nucleic Acids Res* 38:3523–3532.
9. Ashburner M, et al.; The Gene Ontology Consortium (2000) Gene ontology: Tool for the unification of biology. *Nat Genet* 25:25–29.
10. Macisaac KD, et al. (2006) An improved map of conserved regulatory sites for Saccharomyces cerevisiae. *BMC Bioinformatics* 7:113.
11. Manfredi G, et al. (1999) Oligomycin induces a decrease in the cellular content of a pathogenic mutation in the human mitochondrial ATPase 6 gene. *J Biol Chem* 274:9386–9391.
12. Auré K, et al. (2007) Impact on oxidative phosphorylation of immortalization with the telomerase gene. *Neuromuscul Disord* 17:368–375.

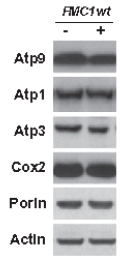

Fig. S1. Western blot analysis of total protein extract of *FMC1wt* strain grown in galactose at 35 °C with or without 1.25 μM CH.

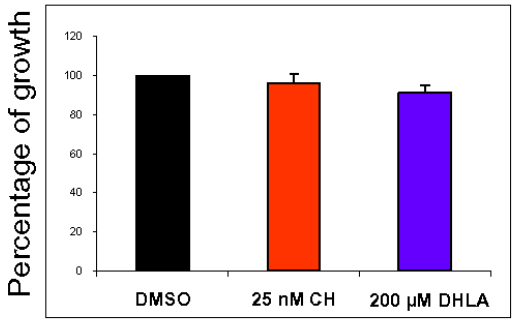

Fig. S2. CH and DHLA have no effect on control (JCP213) cybrid growth.

Table S1. Mitochondrial respiration and ATP synthesis/hydrolysis activities

Strain	Respiration rates, nmol of O per min/mg				ATP hydrolysis, μmol of Pi per min/mg	ATP synthesis rate, nmol of Pi per min/mg
	NADH	NADH +ADP	NADH +CCCP	Asc/TMPD + CCCP		
MC1	257 ± 10	461 ± 34	1004 ± 32	2003 ± 033	4.364 ± 0.035	820 ± 20
MC1 + 1 μM CH	373 ± 31	568 ± 10	1066 ± 34	1943 ± 106	4.107 ± 0.043	771 ± 15
MC6	67 ± 5	73 ± 8	132 ± 10	366 ± 22	0.786 ± 0.019	110 ± 5
MC6 + 1 μM CH	88 ± 10	119 ± 4	203 ± 15	500 ± 15	0.898 ± 0.005	145 ± 11

Mitochondria were prepared from cells grown in rich galactose medium from seven generations at 35 °C. Additions were 0.15 mg/mL proteins, 4 mM NADH, 150 μM ADP (for respiration assays) or 750 μM (for ATP synthesis), 12.5 mM ascorbate (Asc), 1.4 mM TMPD, 4 μM CCCP, 3 μg/mL oligomycin (*oligo*). The values reported are averages of duplicate assays ± SD. Respiratory and ATP synthesis activities were measured on freshly isolated osmotically protected mitochondria buffered at pH 6.8. For the ATPase assays, mitochondria kept at −80 °C were thawed, and the reaction was performed in absence of osmotic protection and at pH 8.4. MC1, control WT strain + DMSO; MC6, *fmc1Δ* strain + DMSO.

Table S2. Frequency of mitochondria with inclusion bodies in *fmc1Δ* cells with or without CH

Strain	Growth temp., °C	Percentage of cell section with IB	Percentage mitochondrial profiles with IB
MC6 (*fmc1Δ*)*	28	0.0 (*n* = 20)	0.0 (*n* = 101)
MC6 (*fmc1Δ*)*	37	70.0 (*n* = 40)	33.0 (*n* = 109)
MC6 (*fmc1Δ*) + DMSO	35	76.6 (*n* = 47)	28.3 (*n* = 173)
MC6 (*fmc1Δ*) + 1 μM CH	35	6.0 (*n* = 50)	2.8 (*n* = 106)

IB, inclusion bodies.
*Results described in ref. 1.

1. Lefebvre-Legendre L, et al. (2005) Failure to assemble the alpha 3 beta 3 subcomplex of the ATP synthase leads to accumulation of the alpha and beta subunits within inclusion bodies and the loss of mitochondrial cristae in Saccharomyces cerevisiae. *J Biol Chem* 280:18386–18392.

Table S3. Strain list

Strain name	Relevant nuclear genotype	mtDNA	Source
MC1	*MATa ade2–1 his3–11,15 trp1–1 leu2–3,112 ura3–1 [Δi E^R O^R]*	ρ+ WT	Ref. 1
MC6	*MATa ade2–1 his3–11,15 trp1–1 leu2–3,112 ura3–1 fmc1::HIS3 [Δi E^R O^R]*	ρ+ WT	Ref. 1
MR6	*MATa ade2-1 his3-11,15 trp1-1 leu2-3,112 ura3-1 CAN1 arg8::HIS3*	ρ+ WT	Ref. 2
MR14	*MATa ade2-1 his3-11,15 trp1-1 leu2-3,112 ura3-1 CAN1 arg8::HIS3*	ρ+ atp6-L183R	Ref. 3
RKY20	*MATa ade2-1 his3-11,15 trp1-1 leu2-3,112 ura3-1 CAN1 arg8::HIS3*	ρ+ atp6-L183P	Ref. 4
RKY25	*MATa ade2-1 his3-11,15 trp1-1 leu2-3,112 ura3-1 CAN1 arg8::HIS3*	ρ+ atp6-L247R	Ref. 5
RKY38	*MATa ade2-1 his3-11,15 trp1-1 leu2-3,112 ura3-1 CAN1 arg8::HIS3*	ρ+ atp6-L247P	Ref. 6
RKY39	*MATa ade2-1 his3-11,15 trp1-1 leu2-3,112 ura3-1 CAN1 arg8::HIS4*	ρ+ atp6-W136R	

1. Lefebvre-Legendre L, et al. (2001) Identification of a nuclear gene (FMC1) required for the assembly/stability of yeast mitochondrial F(1)-ATPase in heat stress conditions. *J Biol Chem* 276:6789–6796.
2. Rak M, et al. (2007) Yeast cells lacking the mitochondrial gene encoding the ATP synthase subunit 6 exhibit a selective loss of complex IV and unusual mitochondrial morphology. *J Biol Chem* 282:10853–10864.
3. Rak M, et al. (2007) A yeast model of the neurogenic ataxia retinitis pigmentosa (NARP) T8993G mutation in the mitochondrial ATP synthase-6 gene. *J Biol Chem* 282:34039–34047.
4. Kucharczyk R, et al. (2009) Biochemical consequences in yeast of the human mitochondrial DNA 8993T>C mutation in the ATPase6 gene found in NARP/MILS patients. *Biochim Biophys Acta* 1793:817–824.
5. Kucharczyk R, et al. (2009) Introducing the human Leigh syndrome mutation T9176G into Saccharomyces cerevisiae mitochondrial DNA leads to severe defects in the incorporation of Atp6p into the ATP synthase and in the mitochondrial morphology. *Hum Mol Genet* 18:2889–2898.
6. Kucharczyk R, et al. (2010) Consequences of the pathogenic T9176C mutation of human mitochondrial DNA on yeast mitochondrial ATP synthase. *BBA Bioenergetics* 1797:1105–1112.

Other Supporting Information Files

Dataset S1 (XLS)
Dataset S2 (XLS)

III.1.3 Analysis of the five mutations in ATP6 gene identified in human tumors

In humans two subunits, *MTATP6* and *A6L*, are encoded in the mitochondrial genome. Numerous mutations in these genes – 55 in *MTATP6* and 9 in *A6L* – have been found in cancer cells (Lu, Sharma et al. 2009). We have analyzed conservation of residues in Atp6p, between yeast and humans. We have investigated in yeast *S. cerevisiae* five mutations that affect highly conserved residues: 8716A>G, 8914C>A, 8932C>T, 8953A>G and 9131T>C (Maximo, Soares et al. 2002; Tan, Bai et al. 2002; Petros, Baumann et al. 2005; Abu-Amero, Alzahrani et al. 2006; Costa-Guda, Tokura et al. 2007). All mutations and the corresponding amino acid changes in human and yeast proteins have been presented in Table 6. To characterize their impact on ATP synthase, we have created and biochemically characterized yeast strains bearing equivalents of these mutations.

Type of tumor	**Nucleotide position and change in human mtDNA**	**Amino acid change in human Atp6 protein**	**Amino acid and codons changes in yeast Atp6p**
Thyroid	8716A>G	Lys^{64}>Glu	Lys^{90}>Glu AAA>GAA
Thyroid	8914C>A	Pro^{130}>Thr	Pro^{157}>Thr CCT>ACT
Prostate	8932C>T	Pro^{136}>Thr	Pro^{163}>Ser CCA>TCA
Thyroid	8953A>G	$Ileu^{143}$>Val	$Ileu^{170}$>Val ATT>GTT
Breast	9131T>C	Leu^{202}>Pro	Leu^{232}>Pro TTA>CCA

Table 6 – Mutations in *ATP6* gene found in tumors and chosen for modeling in yeast.

III.1.3.1 Respiratory growth and genetic stability of the yeast atp6 "cancer" mutants

Growth analysis of the *atp6* mutants revealed that they all grew well on rich glucose and glycerol media, at both 28 and 36°C (Fig. 20). Growth was also analyzed on glycerol medium supplemented with 0.25 µg/ml and 0.5 µg/ml oligomycin. Oligomycin is an inhibitor of the F_O domain. In these conditions the *atp6-P157T* mutant grew slower whereas *atp6-L232P* stopped growing with respect to wild type yeast. This higher *in vivo* sensitivity is possibly due to the fact that a smaller dose of the drug is required to reach the 20% oxidative phosphorylation threshold under which the production of ATP becomes limiting for respiratory growth (Mukhopadhyay, Uh et al. 1994; Kucharczyk, Ezkurdia et al. 2010). In contrast, the *atp6-P163S*, *atp6-K90E* and *atp6-I170V* mutants were more resistant to oligomycin than the wild type. This result is in accordance with the previous studies showing that mutations at the level of residues I171 and S175 within the loop connecting helix 3 and helix 4 of subunit 6 can compromise the binding of oligomycin to ATP synthase (Macino and Tzagoloff 1980; John and Nagley 1986).

The logarithmic growth of all *atp6* mutant strains on liquid glucose and glycerol media was comparable to the wild type strain growth in both temperatures. However, they needed more time than *WT* (2 days *vs*. a couple of hours) to adapt in glycerol at 36°C before starting to grow.

In yeast, ATP synthase mutations often increase the production of ρ^-/ρ^0 *petites* cells with large deletions in the mtDNA or a total loss of mtDNA (Contamine and Picard 2000; Bietenhader, Martos et al. 2012). The parental strain MR6 (*WT*) never produced more than 5% of ρ^-/ρ^0 cells when cultured in complete glucose or galactose media at 28 and 35°C. All but one mutant produced the same percentage of *petites* as the *WT* strain. The *atp6-P163S* mutant had two times higher propensity to produce ρ^-/ρ^0 cells at the elevated temperature.

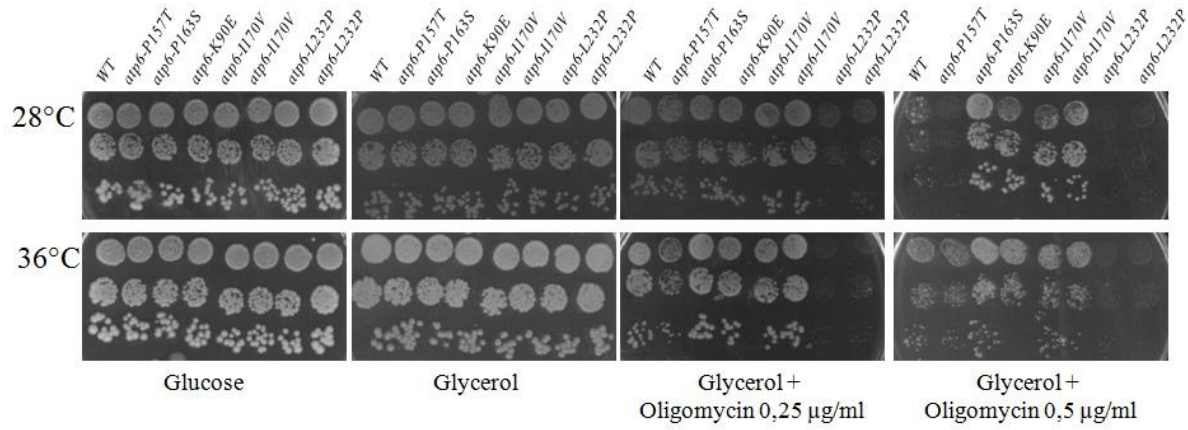

Figure 20 – Growth phenotypes of yeast strains bearing the *MTATP6* mutations identified in cancer cells from patients. Freshly grown cells of wild type yeast (*WT*) and *atp6* mutants were serially diluted and 5µl of each were spotted onto plates containing glucose, glycerol and glycerol supplemented with oligomycin (0.25 µg/ml and 0.5 µg/ml) media. The plates were incubated at 28°C and 36°C. Photos were made after 3 days of incubation.

III.1.3.2 Mitochondrial oxygen consumption

First, I measured oxygen consumption in isolated mitochondria using NADH as an electron donor for respiratory chain, at state 4 (*i.e.* without addition of ADP – basal respiration), at state 3 (*i.e.* in the presence of ADP – phosphorylating conditions), and in the presence of the membrane potential uncoupler CCCP (*i.e.* maximal respiration). I also used ascorbate/TMPD to deliver electrons directly to complex IV, the last complex of the electron transport chain. Mitochondria were isolated from yeast cultured on rich liquid glycerol/ethanol at 28°C or, to avoid the selection of spontaneous revertants during the two days of adaptation to the glycerol medium, in rich liquid galactose at 36°C. Galactose is a fermentable carbon source, which unlike glucose does not elicit repression of mitochondrial function.

The respiratory activities have been presented in Table 7A and B. The oxygen consumption by mitochondria isolated from strains cultured at 28°C were similar between the *WT* and *atp6* mutant strains at state 3 and 4, before and after dissipation of mitochondrial membrane potential by CCCP, and at the level of complex IV (Table 7A). In contrast, these activities at state 3 and 4 differed from the wild type strain for the *atp6-L232P*, *atp6-P163S* and *atp6-K90E* mutants, when mitochondria were isolated from the cultures at 36°C, by 30%,

60% and 20%, respectively. (Table 7B). A decrease in oxygen consumption at the level of complex IV from 19 to 44% was observed in the *atp6-P163S* mutant. Accordingly complex IV was significantly less abundant in mutant *atp6-P163S*, whereas it was unaffected in the other *atp6* mutants. These observations are in line with the previous studies showing that less complex IV accumulates in yeast ATP defective synthase mutants (Rak, Tetaud et al. 2007b; Soto, Fontanesi et al. 2009).

III.1.3.3 Mitochondrial ATP synthesis

I determined the influence of the *atp6* mutations on the rate of ATP synthesis in isolated mitochondria in the presence of a large excess of external ADP to avoid accumulation of intra-mitochondrial ATP, which would otherwise prevent ATP synthase from functioning. Mitochondria isolated from the *atp6-P157T*, *atp6-P163S*, *atp6-I170V* and *atp6-L232P* mutant strains cultivated at 28°C produced about 15 to 28% less ATP than those isolated from the *WT* strain (Table 7A). Mitochondria isolated from the *atp6-P157T*, *atp6-I170V* and *atp6-L232P* mutant strains cultivated at 36°C also produced about 15 to 28% less ATP than the *WT* mitochondria (Table 7B). Mitochondria isolated from the *atp6-P163S* mutant at 36°C produced about 42% less ATP than the *WT* mitochondria. Mitochondria isolated from the *atp6-K90E* mutant strain produced about 15 to 50% more ATP in comparison to the *WT* mitochondria, at both temperatures (Table 7A and B).

III.1.3.4 Mitochondrial ATP hydrolysis

I measured the hydrolytic activity of ATP synthase in isolated mitochondria in non-osmotic conditions buffered at pH 8.4 and in the presence of saturating amounts of ATP to obtain the maximal activity of the enzyme. With the exception of *atp6-K90E* all *atp6* mutants had similar ATPase activity as compared to *WT*. The *atp6-K90E* mutant presented elevated activity – about 50% at both temperatures (Table 7A and B). In mitochondria isolated from cells grown at 28°C ATPase activity was inhibited by oligomycin at the level of *ca.* 66% in *WT* and 73 – 89% in the *atp6* mutants. When mitochondria were isolated from cells grown at 36°C, inhibition by oligomycin was at the level of *ca.* 60% for *WT* and 48 – 65% for four *atp6* mutants. The *atp6-L232P* mutant was inhibited only at the level of *ca.* 24% (Table 7A and B).

A.

Strain	Respiration rates nmol O.min.$^{-1}$.mg^{-1}				ATP synthesis rate nmol Pi.min.$^{-1}$.mg^{-1}		ATPase activity µmol Pi.min.$^{-1}$.mg^{-1}	
	NADH	**NADH +ADP**	**NADH +CCCP**	**Asc/TMPD + CCCP**	**- oligo**	**+ oligo**	**- oligo**	**+oligo**
ATP6	249+/-55	653+/-147	1261+/-167	1848+/-458	680+/-20	77+/-7	4.16 +/- 0.32	1.43+/-0.53
atp6 P157T	259+/-45	709+/-126	1278+/-290	2335+/-704	604+/-170	26+/-12	4.5 +/- 0.26	0.49+/-0
atp6 P163S	291+/-57	740+/-113	1328+/-22	2460+/-368	653+/-42	33+/-14	4.39 +/- 0.54	0.71+/-0.29
atp6 K90E	304+/-2	717+/-43	1311+/-82	2363+/-231	758+/-148	44+/-16	6.0 +/- 0.08	0.68+/-0.08
atp6 I170V	260+/-7.8	609+/-52	1247+/-13	1837+/-71	566+/-45	64+/-18	3.87 +/- 1.1	1.03+/-0.05
atp6L232P	292+/-26	683+/-78	1464+/-78	2448+/-235	563+/-39	24+/-10	4.21 +/- 1.30	0.98+/-0.05

B.

Strain	% *petites*	Respiration rates nmol O.min.$^{-1}$.mg^{-1}				ATP synthesis rate nmol Pi.min.$^{-1}$.mg^{-1}		ATPase activity µmol Pi.min.$^{-1}$.mg^{-1}	
		NADH	**NADH +ADP**	**NADH +CCCP**	**Asc/TMPD + CCCP**	**- oligo**	**+ oligo**	**- oligo**	**+oligo**
ATP6	*34*+/-15	249+/-17	590+/-32	1088+/-74	1602+/-78	1672+/-157	103+/-35	4.09 +/- 0.77	1.69+/-0.49
atp6 P157T	*29*+/-8	212±41	580±55	908±67	1311±70	1213+/-165	95+/-9	4.92 +/- 1.67	1.97+/-0.66
atp6 P163S	*64*+/-13	116±13	240±11	352±24	712±112	703+/-18	142+/-20	4.27 +/- 1.63	2.16+/-2.09
atp6 K90E	*30*+/-9	259+/-43	711+/-86	1268+/-91	1719+/-177	1870+/-228	319+/-61	6.08 +/- 1.95	2.15+/-0.67
atp6 I170V	*33*+/-15	242+/-23	542+/-25	1102+/-111	1176+/-77	1215+/-45	246+/-91	4.04 +/- 0.26	2.10+/-0.63
atp6L232P	*38*+/-23	170±13	412±24	659±20	926±124	1446+/-142	64+/-15	4.43 +/- 0.65	3.30 ± 0.26

Table 7 – Influence of the *atp6*- mutations on yeast mitochondrial respiration, ATP synthesis and hydrolysis activities. Mitochondria were isolated from wild type and mutants strains grown for 5 – 6 generations in YPGEA at 28°C (A) or YPGalA at 36°C (B). Reaction mix for assays contained 0.15 mg/ml protein, 4 mM NADH, 150 µM ADP (for respiration assays) or 750 µM ADP (for ATP synthesis), 12.5 mM ascorbate (*Asc*), 1.4 mM TMPD, 4 µM CCCP, 3 µg/ml oligomycin (*oligo*). All strains contained 2 –5% of ρ^{-}/ρ^{0} cells at 28°C, the percent of ρ^{-}/ρ^{0} cells at 36°C is indicated in the table. The values reported are averages of triplicate assays ± standard deviation. Respiratory and ATP synthesis activities were measured using freshly isolated, osmotically protected mitochondria buffered at pH 6.8. For the ATPase assays, mitochondria kept at –80°C were thawed and the reaction performed in absence of osmotic protection and at pH 8.4.

III.1.3.5 Measurements of inner mitochondrial membrane potential

Mitochondrial membrane potential ($\Delta\Psi$) was measured in isolated mitochondria using fluorescent dye rhodamine 123 (see Materials and methods). Mitochondria were energized similarly in the *WT* and *atp6* mutants at 28°C and 36°C. Addition of ADP caused a rapid increase in fluorescence due to ATP synthesis by F_1F_O-ATP synthase in all analyzed strains at both temperatures, but the time lag of restoration of the potential to the level established before the addition of ADP was longer for *atp6-P163S* at both temperatures and for *atp6-L232P* at 36°C (Fig. 21). The proton pumping activity coupled to F_1-mediated ATP hydrolysis was comparable between the *WT* and all *atp6* mutants at both temperatures.

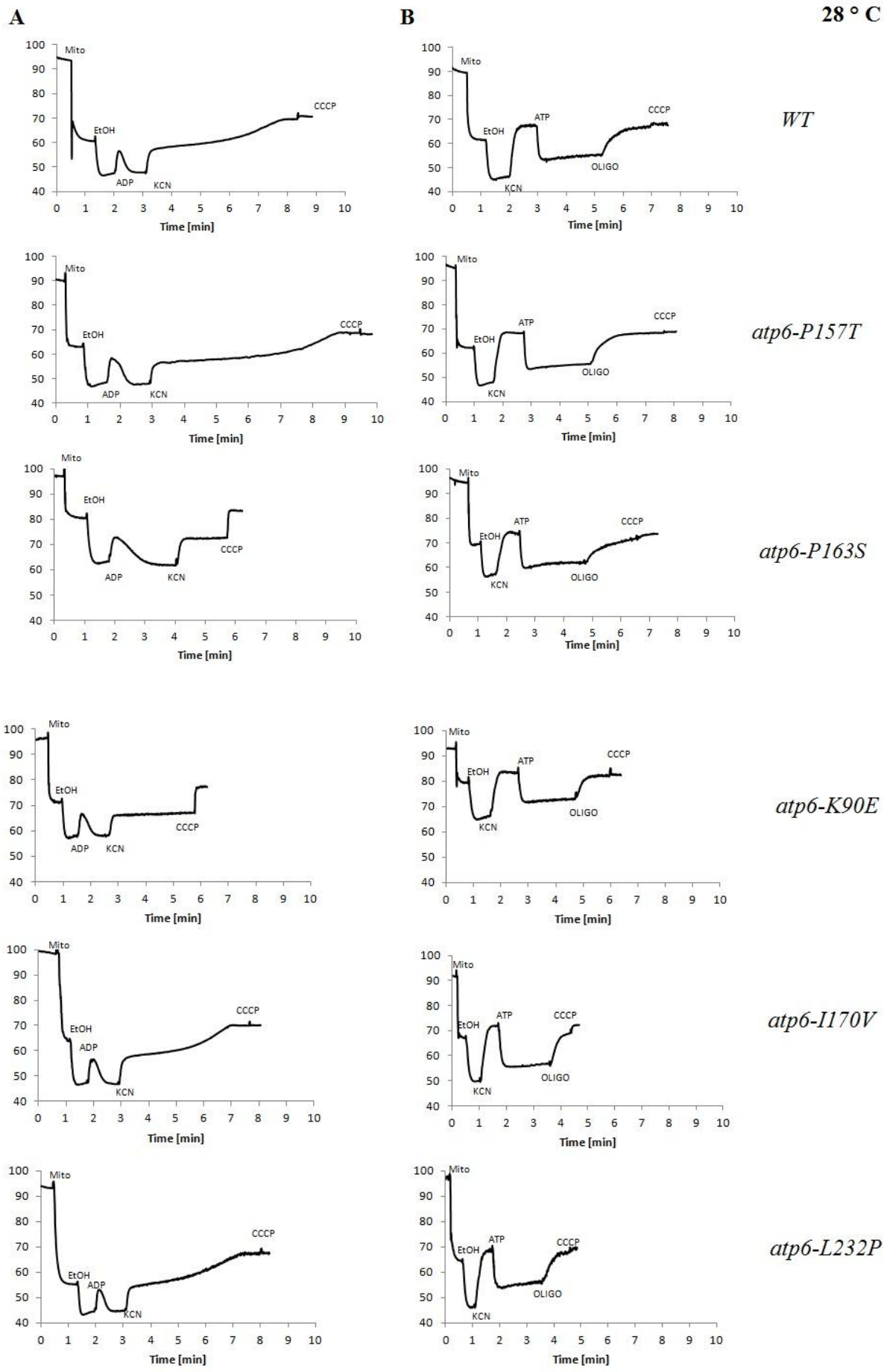
A
B
28 ° C
WT
atp6-P157T
atp6-P163S
atp6-K90E
atp6-I170V
atp6-L232P
Mito
EtOH
ADP
KCN
ATP
OLIGO
CCCP
Time [min]

C **D** **36 ° C**

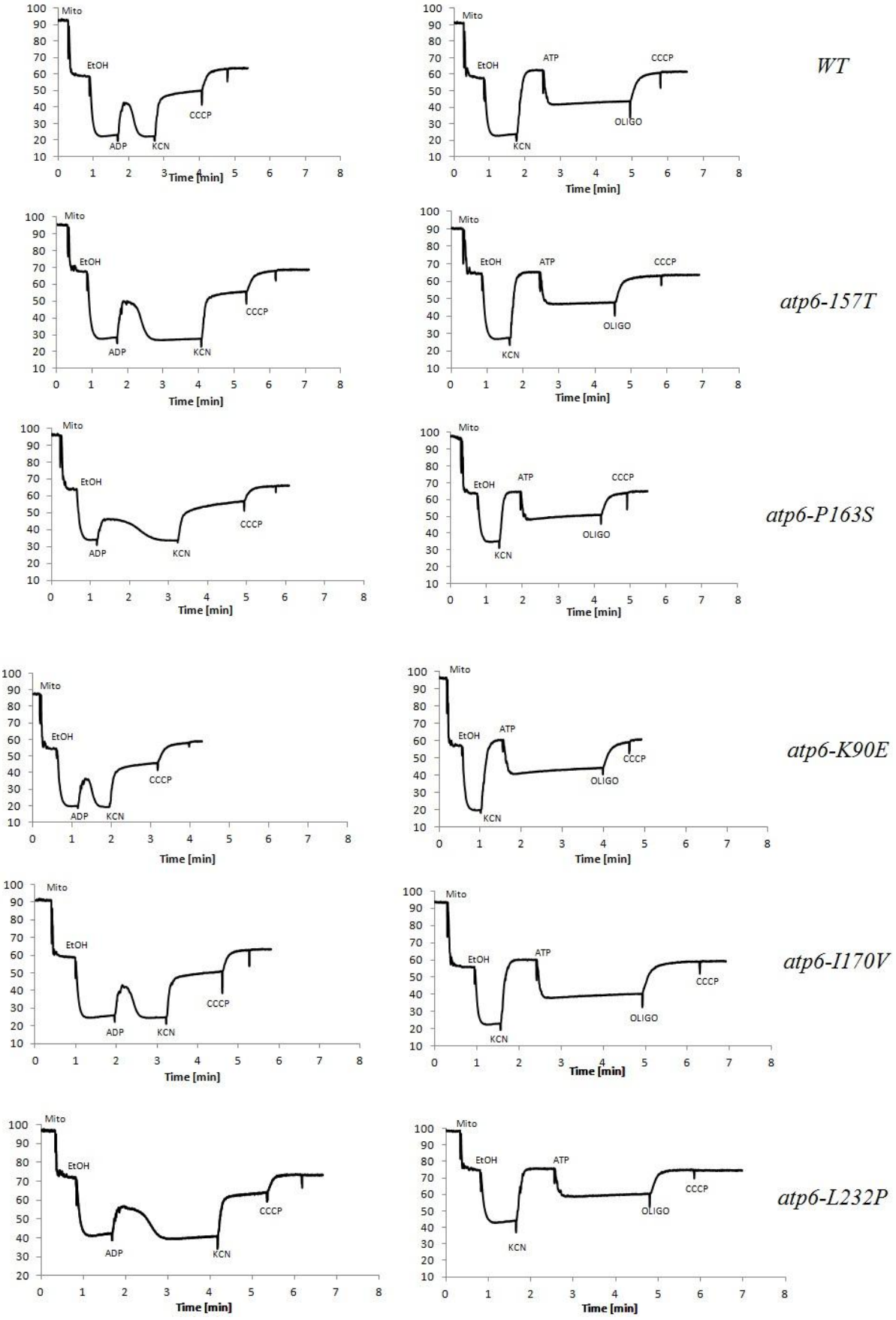

WT

atp6-157T

atp6-P163S

atp6-K90E

atp6-I170V

atp6-L232P

Figure 21 – Energization of inner mitochondria membrane of *WT* (MR6), *atp6-P157T* (RKY60), *atp6-P163S* (RKY61), *atp6-K90E* (RKY62), *atp6-I170V* (AKY1) and *atp6-L232P* (AKY2) strains. Energization of the mitochondrial inner membrane by ADP (panels A and C) or ATP (panels B and D) in intact mitochondria isolated from strains grown in YPGEA at 28°C or YPGalA at 36°C, was monitored by Rhodamine 123 fluorescence quenching. The additions were 0.5 µg/ml Rhodamine 123, 0.15 mg/ml mitochondrial proteins (Mito), 10 mM ethanol (EtOH), 75 µM ADP, 1 mM ATP, 0.2 mM potassium cyanide (KCN), 6 µg/ml oligomycin (OLIGO) and 3 µM CCCP.

III.1.3.6 Assembly/stability of the ATP synthase

Finally, I investigated the influence of the *atp6* mutations on ATP synthase assembly/stability. To visualize the complex, I extracted mitochondrial membrane proteins with 2% digitonin from thawed mitochondria isolated from 28°C and 36°C cultures. I separated them in native polyacrylamide gel which I stained with coomasie brilliant blue (BN-PAGE) or analyzed the hydrolyzing activity of the complex in the gel (Fig. 22A and B). I also transferred proteins on nitrocellulose membrane and revealed them with antibodies (Fig. 22C and D).

Complexes extracted from mitochondria derived from cultures at 28°C demonstrate similar amounts of fully assembled ATP synthase dimers and monomers in the *WT* and all *atp6* mutants (Fig. 22A). They are also well visualized in gel via their ATPase activity, which revealed also free F_1 (Fig. 22A). This reflects partial damaging of the complex during extraction as the same amount of free F_1 is present in the *WT* and *atp6* mutants. No difference could be observed in the enzyme amount after transferring native complexes to membrane and staining them with anti-Atp1p antibody (Fig. 22C). Analysis of steady state levels of three ATP synthase subunits, Atp1p, Atp4p and Atp6p, in denaturing conditions (separation in SDS polyacrylamide gels) revealed that they were also in a normal amount in all mutant strains as compared to *WT* (Fig. 22E).

Complexes extracted from mitochondria derived from cultures at 36°C demonstrate a diminished amount of ATP synthase monomers in the *atp6-P163S* mutant, when the complexes were transferred to a nitrocellulose membrane and stained with antibodies against Atp9p and Atp1p (Fig. 22D). The ATPase signal corresponding to the monomeric form of the enzyme in this mutant had a much lower intensity than *WT* (Fig. 22B). We can also observe an increased signal of free F_1 in *atp6-L163S* mutant in the ATPase activity (Fig. 22B) and on the membrane stained with antibody against Atp1p (Fig. 22D). This may indicate a smaller stability of ATP synthase in this mutant. All other mutants showed no changes in ATP synthase stability in comparison to *WT*.

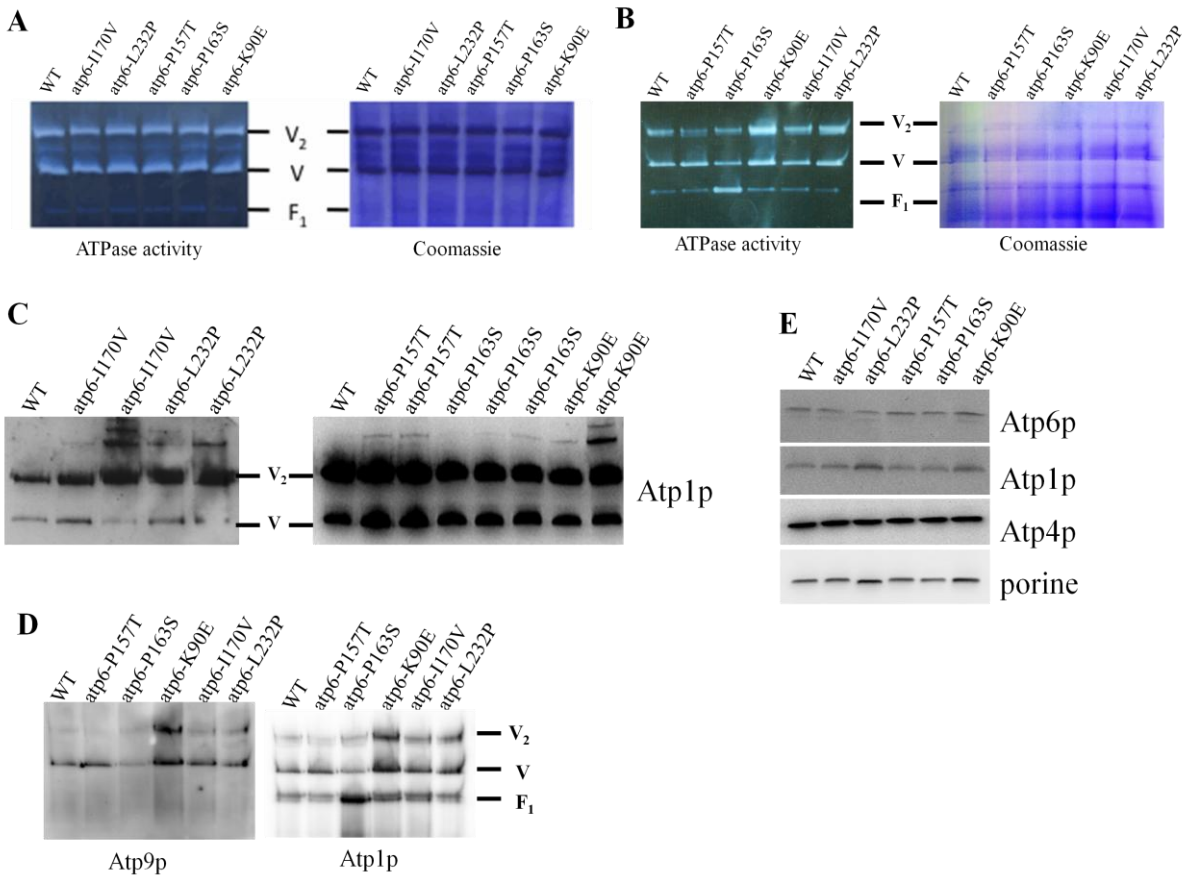

Figure 22 – Analysis of assembly/stability of the ATP synthase complex in the *WT* (MR6), *atp6-P157T* (RKY60), *atp6-P163S* (RKY61), *atp6-K90E* (RKY62), *atp6-I170V* (AKY1) and *atp6-L232P* (AKY2) strains. A and B: BN-PAGE analysis of mitochondrial protein extracted with 2% digitonin from strains cultivated at 28°C (A) and 36°C (B). Fully assembled ATP synthase complexes (V_2 – dimeric. V-monomeric, F_1 – free F_1) are stained in-gel by Coomassie brilliant blue and their ATPase activity. **C and D**: BN-PAGE analysis of mitochondrial proteins transferred to a nitrocellulose membrane and stained with antibodies against different subunits of ATP-synthase. Proteins were obtained from mitochondria derived from cultures at 28°C (C) and 36°C (D). **E:** SDS-PAGE analysis of total protein extracts from cultures at 28°C. Proteins (20 µg) were separated by SDS-PAGE, transferred to a nitrocellulose membrane and probed with antibodies against Atp6p, Atp1p, Atp4p and porine.

I analyzed also synthesis of mitochondrially encoded proteins by *in vivo* labeling with a mix of [^{35}S] methionine/cysteine, in the presence of cycloheximide to inhibit cytosolic protein synthesis. This revealed that proteins encoded by the mitochondrial genome were synthesized efficiently in all *atp6* mutant strains (Fig. 23).

The analysis of five *atp6-"cancer"* yeast mutant strains showed no significant effect on ATP synthase and respiratory chain at 28°C and only a mild effect in the *atp6-P163S*, *atp6-L232P* and *atp6-K90E* mutant strains at 36°C, although the mutations were identified in the conserved positions between yeasts and humans.

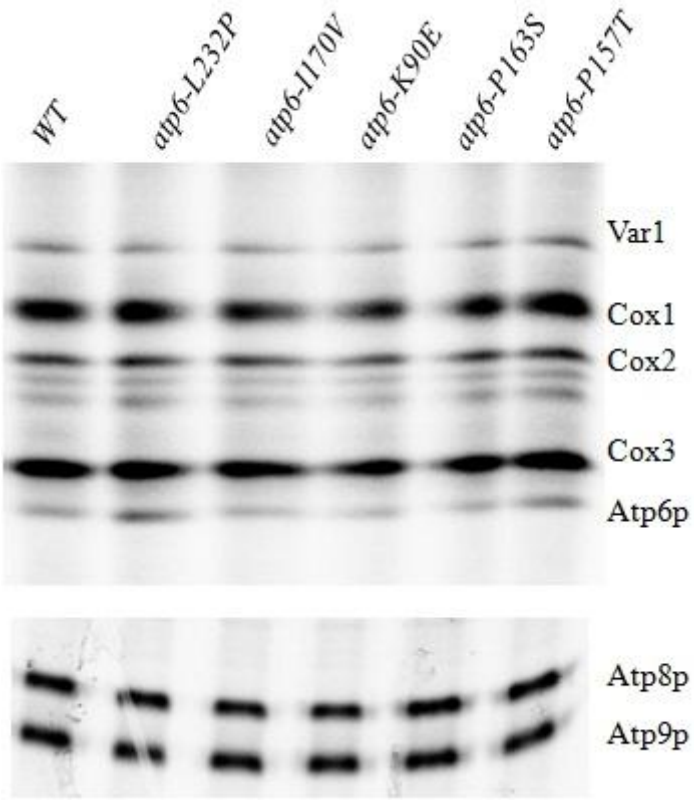

Figure 23 – Mitochondrial protein synthesis. Proteins encoded by mtDNA of the *WT* (MR6), *atp6-P157T* (RKY60), *atp6-P163S* (RKY61), *atp6-K90E* (RKY62), *atp6-I170V* (AKY1) and *atp6-L232P* (AKY2) strains were labeled with [^{35}S]-(methionine + cysteine) for 20 min. at 30°C in the presence of cycloheximide (7.5 mg/ml) to inhibit cytosolic protein synthesis. Total proteins extracts were prepared from cells and separated on 12% urea/glycerol polyacrylamide gel and 17.5% polyacrylamide gel (the same amount of radioactivity per line). After electrophoresis the gels were dried and visualized with a Phosphoimager.

III.2. REGULATION OF EXPRESSION OF *ATP6* IN RELATION TO ITS ASSEMBLY INTO THE F_1F_O-ATP SYNTHASE COMPLEX

As I have demonstrated in section III.1, yeast *S. cerevisiae* can be successfully used to analyze the effects of mutations in the *ATP6* gene responsible for human diseases. Interestingly, in one mutant *atp6-L183P* (Kucharczyk, Rak et al. 2009a), Atp6p was synthesized much (3 – 4 times) more rapidly than in the *WT* due to increased translation, and not because of a higher accumulation of *ATP6* transcripts (Fig. 24A, B and C). Despite its up-regulation, the mutated protein was less abundant in the steady state than the wild type Atp6p, whereas other subunits of ATP synthase were not affected in the mutant (Fig. 24D). This indicates that incorporation of Atp6p into ATP synthase is partially compromised by the L183P change and that unassembled Atp6p is proteolytically degraded, as usually observed in mutants where Atp6p cannot assemble. As a result, partial ATP synthase assemblies lacking Atp6p form in the *atp6-L183P* mutant. These assemblies are quite fragile and partially dissociate in BN-PAGE gel into free F_1 and Atp9p-rings (Fig. 24E). Such an up-regulation of Atp6p was not observed in other yeast NARP mutants (W136R (Kucharczyk, Giraud et al. 2013), L183R (Rak, Tetaud et al. 2007a) and L247P (Kucharczyk, Ezkurdia et al. 2010); see Fig. 26A). In these mutants the assembly of ATP synthase was not affected. Thus, it was possible that the up-regulation of Atp6p in *atp6-L183P* mutant was provoked by the defective incorporation of Atp6p into ATP synthase. To test this hypothesis I have generated other *atp6* mutants, as revertants from the *atp6-W136R* mutant, and analyzed their properties, as described hereafter.

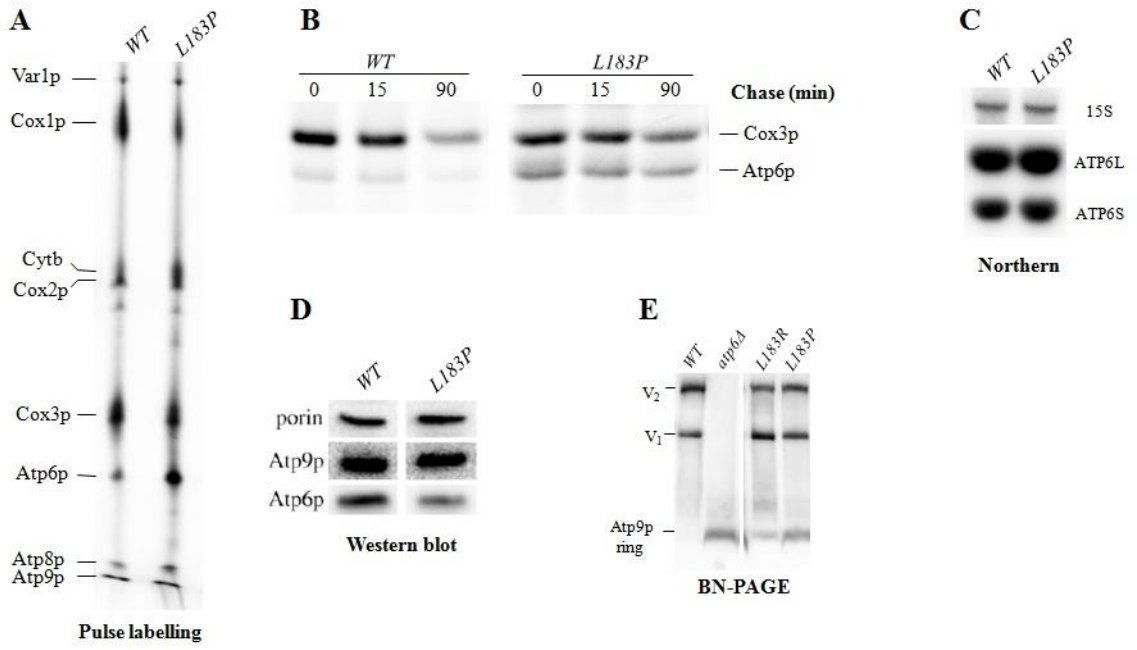

Kucharczyk BBA 1793 (2009), 817-824

Figure 24 – Analysis of *WT* and *atp6-L183P* strains. A: Mitochondrial protein synthesis. Proteins encoded by mtDNA were labeled in whole cells with [35S]-(methionine+cysteine) for 20 min. in the presence of cycloheximide to inhibit cytosolic protein synthesis. The mitochondrial membranes were extracted and loaded on the SDS-PAGE gel (100 000 cpm per lane). After electrophoresis the gel was dried and the proteins were visualized with a Phosphoimager. **B:** Pulse chase analysis. Proteins encoded by mtDNA were labeled in whole cells with [^{35}S]-(methionine+cysteine) for 5, 20 and 90 min. in the presence of cycloheximide to inhibit cytosolic protein synthesis. The mitochondrial membranes were extracted and loaded on the SDS-PAGE gel (100 000 cpm per lane). After electrophoresis the gel was dried and the proteins were visualized with a Phosphoimager. **C:** Northern blot analysis of mitochondrial transcripts. Total mitochondrial RNAs were isolated from strains grown for 6 – 8 generations in liquid YPGalA at 28°C. The RNAs were separated in formaldehyde agarose gel and transferred to a nitrocellulose membrane. The same membrane was hybridized successively with ^{32}P-radiolabeled DNA probes specific for 15S rRNA, ATP6L and ATP6S transcripts. **D:** SDS-PAGE analysis of total mitochondrial proteins. Mitochondrial proteins (10 µg) were separated by SDS-PAGE, transferred to a nitrocellulose membrane and probed with antibodies against Atp6p, Atp9p and porine. **E:** BN-PAGE analysis of ATP synthase. Mitochondria were solubilized with 2% digitonin. The digitonin-extracted proteins (50 µg) were separated by BN-PAGE, transferred to a nitrocellulose membrane, and hybridized with antibody against Atp9p.

III.2.1 Isolation of revertants from the atp6-W136R mutant

To generate novel *atp6* mutants, I have isolated revertants from *atp6-W136R* on glycerol plates. To this end ten independent cultures of the *atp6-W136R* mutant in liquid rich glucose medium were prepared and 10^8 cells from each culture were spread on the glycerol medium. After a few days of incubation at 28°C, clones with improved respiratory growth (Fig. 26) were taken from each plate and their *ATP6* gene was sequenced, which led to identification of 4 different intragenic reversions: *atp6-R136I*, *atp6-R136G*, *atp6-R136K*, *atp6-W136R, R179I*.

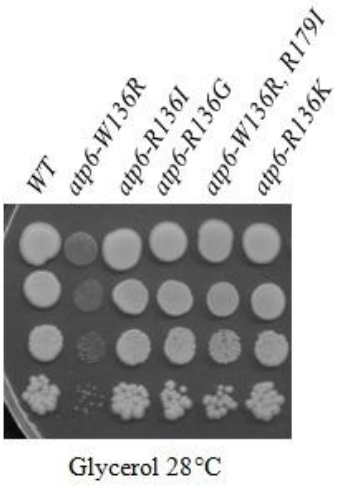

Figure 25 – Growth phenotypes of the *atp6-W136R* revertant strains. Freshly grown strains of *WT* (MR6) and *atp6* mutants: *atp6-W136R* (RKY39), *atp6-R136I* (RKY39-1G), *atp6-R136G* (RKY39-5G), *atp6-W136R,R179I* (RKY39-6G), *atp6-R136K* (RKY39-16G) were spotted on rich glycerol medium (YPGA). The plate was incubated at 28°C and photographed after 7 days of incubation.

III.2.2 Influence of the novel atp6 mutations on ATP synthase assembly/stability and Atp6p synthesis

Among the four revertants, we have found only one (*atp6-W136R, R179I*) where a free Atp9p-ring was present in BN-PAGE gels (Fig. 26B). In this revertant, the steady state accumulation of Atp6p was decreased in comparison to the *WT* and to the three other revertants (Fig. 26E). I next analyzed the *in vivo* labeling of mitochondrial translation products. Interestingly, in the *atp6-W136R, R179I* strain Atp6p synthesis was up-regulated as in the *atp6-L183P* strain, whereas the synthesis of this protein was normal in the three other revertants (Fig. 26C and D).

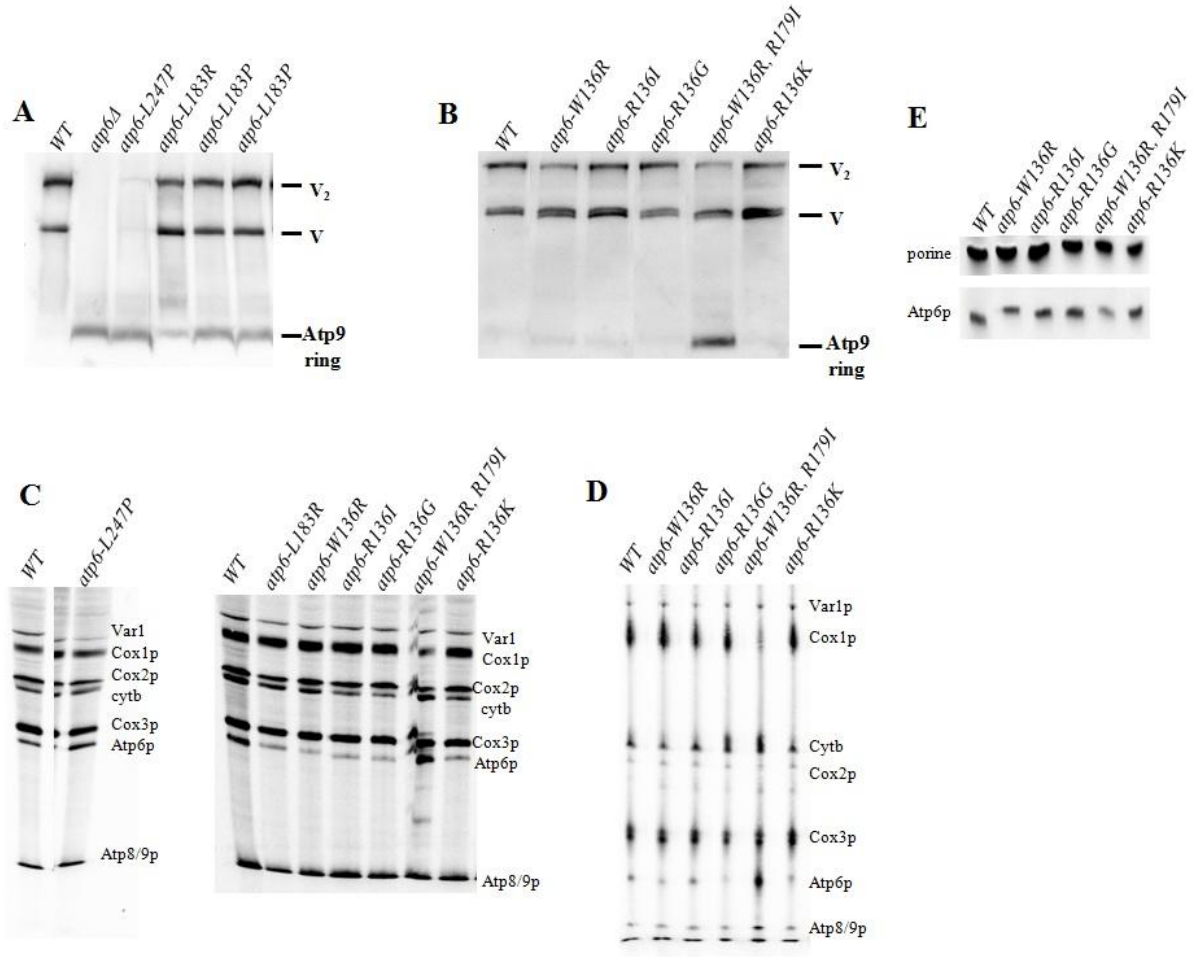

Figure 26 – BN-PAGE, mitochondrial protein synthesis and SDS-PAGE analysis of the *WT* (MR6) and *atp6* mutants: *atp6Δ* (MR10), *atp6-L247P* (RKY38), *atp6-L183R* (MR14) and *atp6-L183P* (RKY20) from panel A, *WT* (MR6), *atp6-W136R* (RKY39), *atp6-R136I* (RKY39-1G), *atp6-R136G* (RKY39-5G), *atp6-W136R,R179I* (RKY39-6G), *atp6-R136K* (RKY39-16G). A and B: BN-PAGE analysis of ATP synthase. Mitochondria from the indicated strains were solubilized with 2% digitonin. The digitonin-extracted proteins (50 µg) were separated by BN-PAGE, transferred to a nitrocellulose membrane, and hybridized with an antibody against Atp9p. **C and D:** Mitochondrial protein synthesis. Proteins encoded by mtDNA were labeled in whole cells with [^{35}S]-(methionine+cysteine) for 20 min. in the presence of cycloheximide to inhibit cytosolic protein synthesis. The total protein extracts from cells (panel C) or the mitochondrial membranes (panel D) were extracted and loaded on the SDS-PAGE gel (100 000 cpm per lane). After electrophoresis the gel was dried and the proteins were visualized with a Phosphoimager. **E:** SDS-PAGE analysis of total mitochondrial proteins. Mitochondrial proteins (20 µg) were separated by SDS-PAGE, transferred to a nitrocellulose membrane and probed with antibodies against Atp6p and porine.

III.2.3 Hypothesis

As described in the literature, Atp6p is the last subunit to be incorporated into the ATP synthase complex and unassembled Atp6p is known to be highly sensitive to proteolytic degradation, which indicates that this protein is post-translationally controlled to avoid accumulation of unassembled Atp6p. However, Atp6p seems to be also subject to translational controls: in yeast strains failing to express or assemble the α-F_1 and β-F_1 proteins, translation of Atp8p and Atp6p is strongly down regulated, presumably as a means to prevent the accumulation of free F_O particles that have the potential to uncouple the mitochondrial membrane (Rak and Tzagoloff 2009a; Rak, Gokova et al. 2011). The data presented above suggest that *atp6* mutations that compromise the assembly of Atp6p results in a higher rate of Atp6p synthesis. This led us to hypothesize that the Atp6p-less ATP synthase complex that forms before incorporation of Atp6p controls the synthesis of Atp6p as a means to couple the synthesis of Atp6p to its assembly (Fig. 27).

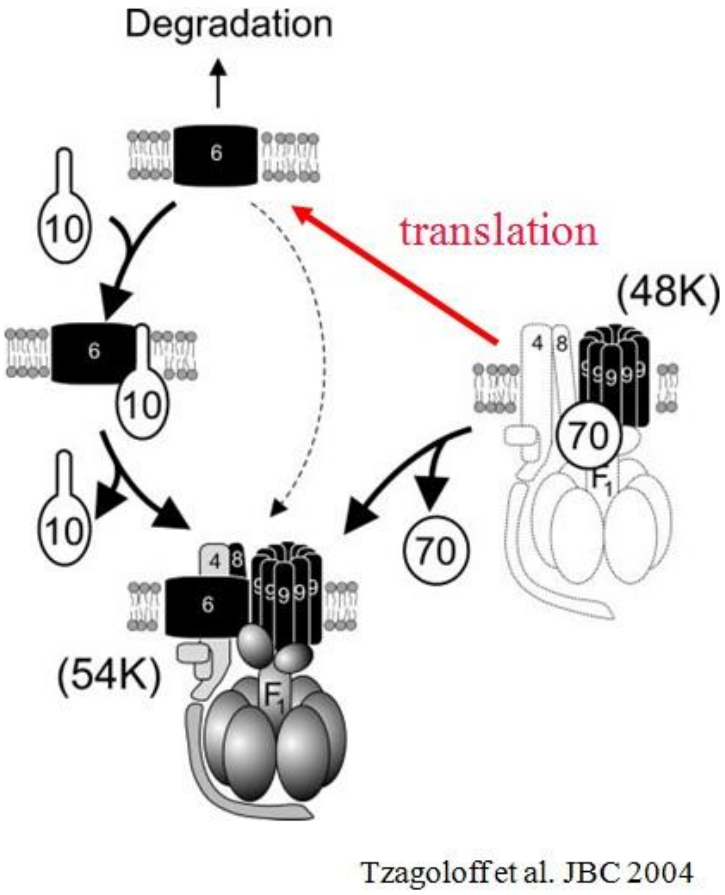

Figure 27 – The schema illustrating hypothesis of influence of ATP synthase sub-complex on Atp6p synthesis.

To test this hypothesis I have combined the *atp6-L183P* mutation with mutations that prevent synthesis or assembly of other components of the ATP synthase, and we have then determined whether the synthesis of the mutated Atp6p is still up-regulated. The goal was to know which part of ATP synthase is necessary for this up-regulation.

III.2.3.1 Construction of deletion mutant strains

Deletions of genes encoding subunits of ATP synthase or genes encoding proteins that take part in ATP synthase biogenesis were done in the *WT* and in the *atp6-L183P* mutant. As mentioned in the Introduction, ATP synthase is composed of two functional domains: F_1, formed of the so-called catalytic head and the central stalk, and of F_O, formed of the proton channel and the peripheral stalk. I deleted different genes representing each part of the enzyme. To deprive ATP synthase of the catalytic head I deleted *ATP1* gene that encodes subunit α, *ATP11*, *ATP12* and *FMC1* genes that encode chaperons needed for α/β hexamer assembly. Regarding the central stalk, I deleted the *ATP15* gene that encodes subunit ε. To test the influence of the peripheral stalk I deleted the *ATP7* gene encoding subunit d. To know if Atp9p is required for the up-regulation of Atp6p, I deleted two genes, *AEP1* and *AEP2*, encoding proteins that take part in *ATP9* expression. I also deleted genes *ATP10* and *ATP23* that encode proteins taking part in Atp6p maturation and assembly. To create these strains I used *KanMX4* disruption cassettes (see Materials and Methods). Below I present the schema showing constructed deletion mutants (Fig. 28).

A common feature of ATP synthase mutants is an enhanced production of ρ^-/ρ^0 cells. I therefore systematically scored the number of ρ^-/ρ^0 cells in the cultures of the different strains I constructed (see Table 8).

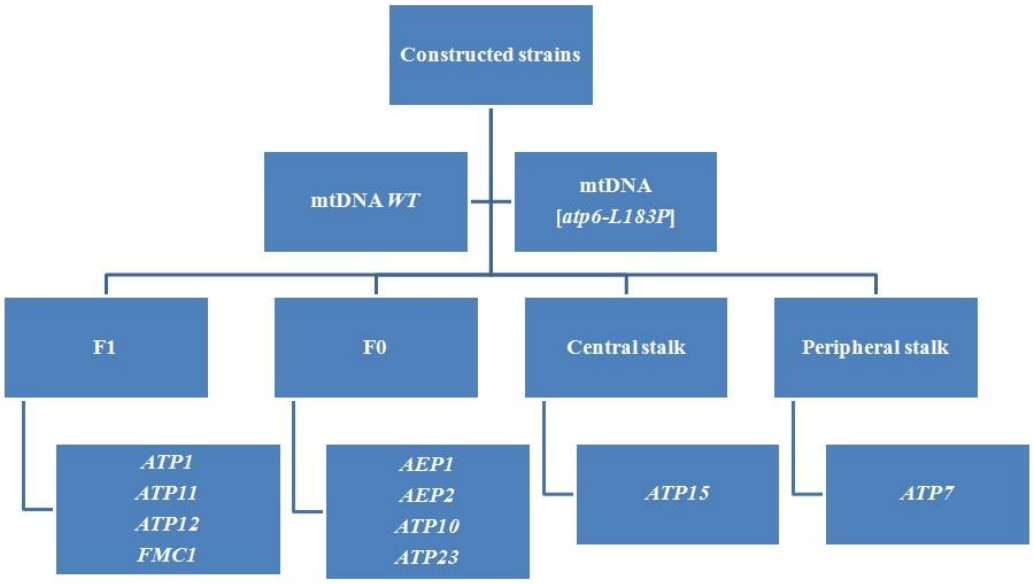

Figure 28 – The schema presenting constructed deletion mutant strains. Collection of strains with deletions in different nuclear *loci* of mitochondrial genes in *WT* and *atp6-L183P* mtDNA backgrounds to study regulation ofAtp6p synthesis in relation to its assembly into the ATP synthase.

Deleted gene	**mtDNA background**	
	WT	*atp6-L183P*
no deletion	10%	16%
atp1	39%	60%
atp11	58%	62%
atp12	64%	60%
fmc1	15%	16%
atp7	66%	65%
atp15	64%	48%
atp10	41%	44%
atp23	54%	42%
atp23-E168Q	83%	78%
aep1	33%	60%
aep2	31%	38%

Table 8 Percentage of ρ^-/ρ^0 cells in constructed deletion strain collection.

III.2.3.2 The catalytic head of F_1 domain is necessary for up-regulation of Atp6p synthesis

As expected, strains *atp1Δ*, *atp11Δ*, *atp12Δ, and fmc1Δ* I have constructed grew poorly on glucose supplemented with ethidium bromide (EtBr), a drug that prevents propagation of mtDNA (Fig. 29). This is because F_1 is required to energize the mitochondrial inner membrane when yeast is unable to respire (Giraud and Velours 1997; Lefebvre-Legendre, Balguerie et al. 2003). It is to be noted that phenotype of the *fmc1Δ* strain manifests only at elevated temperature (Lefebvre-Legendre, Vaillier et al. 2001), hence all analysis aimed to determination of the influence of the lack of Fmc1p were performed on the basis of cells grown at 35°C.

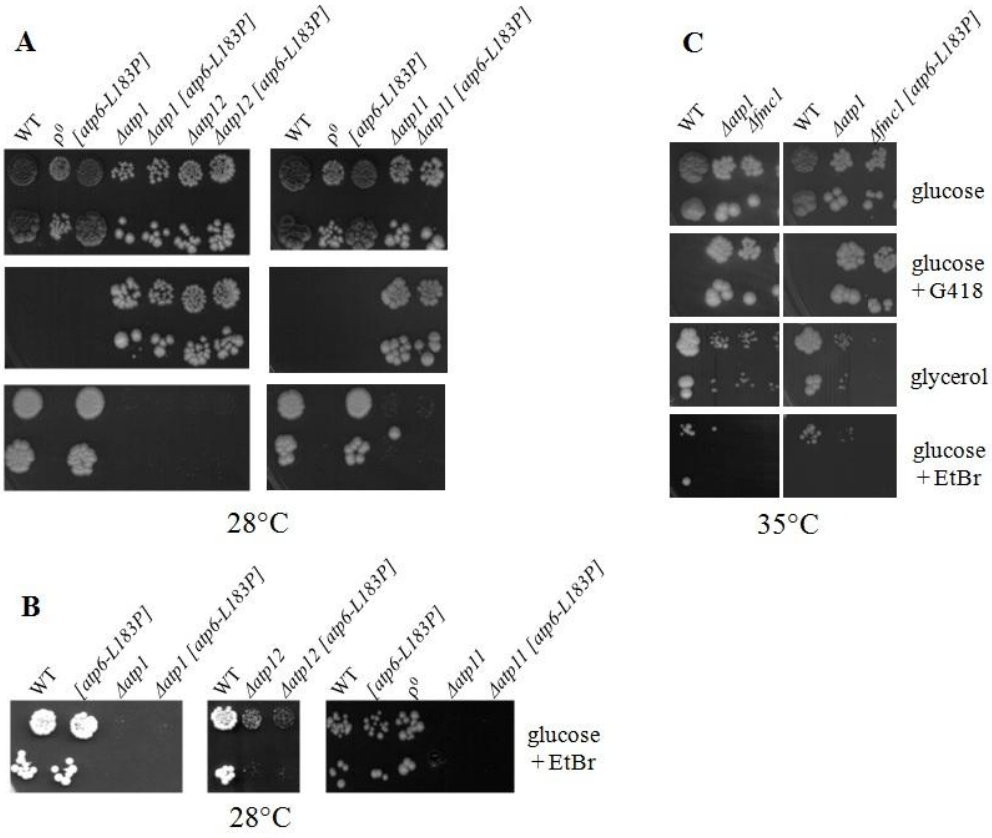

Figure 29 – Growth phenotypes of F_1 deletion strains. Freshly grown wild type (MR6), ρ^0 (MR6 ρ^0), *atp6-L183P* (RKY20), *atp1Δ* (AKY36), *atp1Δ [atp6-L183P]* (AKY37), *atp11Δ* (AKY40), *atp11Δ [atp6-L183P]* (AKY41), *atp12Δ* (AKY42), *atp12Δ [atp6-L183P]* (AKY43), *fmc1Δ* (AKY76), *fmc1Δ [atp6-L183P]* (AKY77), were spotted on plates with rich glucose (YPDA), rich glucose supplemented with G418 (200 µg/ml), rich glycerol (YPGA) and rich glucose supplemented with ethidium bromide (BET, 40 µg/l). The plates were incubated at 28°C or 35°C and photographed after 6 days of incubation.

Analysis of translation of mitochondrially encoded proteins clearly showed that there is neither Atp6p nor Atp8p synthesis in the examined deletion strains without distinction of the mtDNA background (Fig. 30A). It was demonstrated before that synthesis of Atp6 and Atp8 proteins is F_1-dependent (Rak and Tzagoloff 2009a). My result confirmed those data (Fig. 30A). In *fmc1Δ* strains grown at 35 – 37°C, where there is also a substantial but not complete lack of F_1, the synthesis of Atp6p and Atp8p was only moderately affected, if at all (Lefebvre-Legendre, Vaillier et al. 2001). Interestingly, up-regulation of Atp6p synthesis was not longer observed in *atp6-L183P* cells lacking Fmc1p (Fig. 30B). Hence we can say that sufficient amount of F_1-catalytic head is required for this up-regulation.

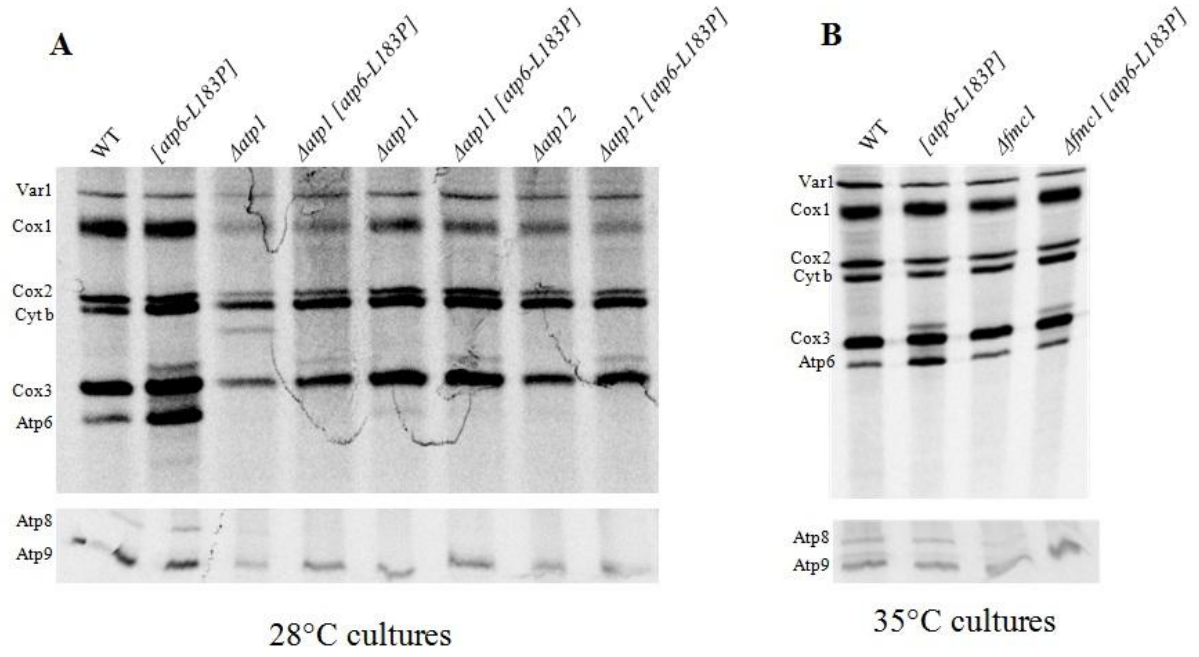

Figure 30 – Mitochondrial protein synthesis. Proteins encoded by mtDNA were labeled in whole cells from the wild type (MR6), *atp6-L183P* (RKY20), *atp1Δ* (AKY36), *atp1Δ [atp6-L183P]* (AKY37), *atp11Δ* (AKY40), *atp11Δ [atp6-L183P]* (AKY41), *atp12Δ* (AKY42), *atp12Δ [atp6-L183P]* (AKY43), *fmc1Δ* (AKY76), *fmc1Δ [atp6-L183P]* (AKY77) strains with [^{35}S]-(methionine+cysteine) for 20 min. in the presence of cycloheximide to inhibit cytosolic protein synthesis. The total protein extracts from cells were prepared and loaded on 12% urea/glycerol polyacrylamide gel and 17.5% polyacrylamide gel (the same amount of radioactivity per line). After electrophoresis the gel was dried and the proteins were visualized with a Phosphoimager.

III.2.3.3 The Atp9p-ring is also necessary for up-regulation of Atp6p synthesis

Combining the *atp6-L183P* mutation to *ATP9* deletion is not easy to achieve. Therefore, to test the influence of Atp9p on the synthesis of Atp6p in the *atp6-L183P* mutant, I deleted *AEP1* and *AEP2* genes, which are both required to express Atp9p. However, lack of any of their protein products very strongly affects the stability of mtDNA. In the laboratory, it was shown that the nuclear *ATP9-5* gene from *Podospora anserina* can partially complement the yeast *atp9Δ* strain and stabilizes mtDNA. I introduced a plasmid bearing *ATP9-5* gene into the *WT* and *atp6-L183P* strains and then transformed them with *aep1::KanMX4* and *aep2::KanMX4* deletion cassettes. The *ATP9-5* gene is under control of Tet-O promoter and its expression can be shut down in the presence of doxycycline. The phenotype analysis showed that growth on glycerol of the *aep1Δ* and *aep2Δ* strains is dependent on the presence of Atp9-5 protein, because they stopped growing on glycerol in the presence of doxycycline (Fig. 31A). As it will be shown below, these strains as expected failed to express the mitochondrial *ATP9* gene. The up-regulation of Atp6p conferred by the *atp6-L183P* mutation was largely lost upon deletion of *AEP1* and *AEP2* (Fig. 31B). Even though, they produce functional Atp9-rings from the nuclear *ATP9-5* gene, they do so very poorly. Thus, it can be inferred that a normal expression of Atp9p is needed for the up-regulation of Atp6p in the *atp6-L183P* mutant, similarly to what was observed with a null mutation in *FMC1* where expression of F_1 is dramatically but not totally compromised (see above).

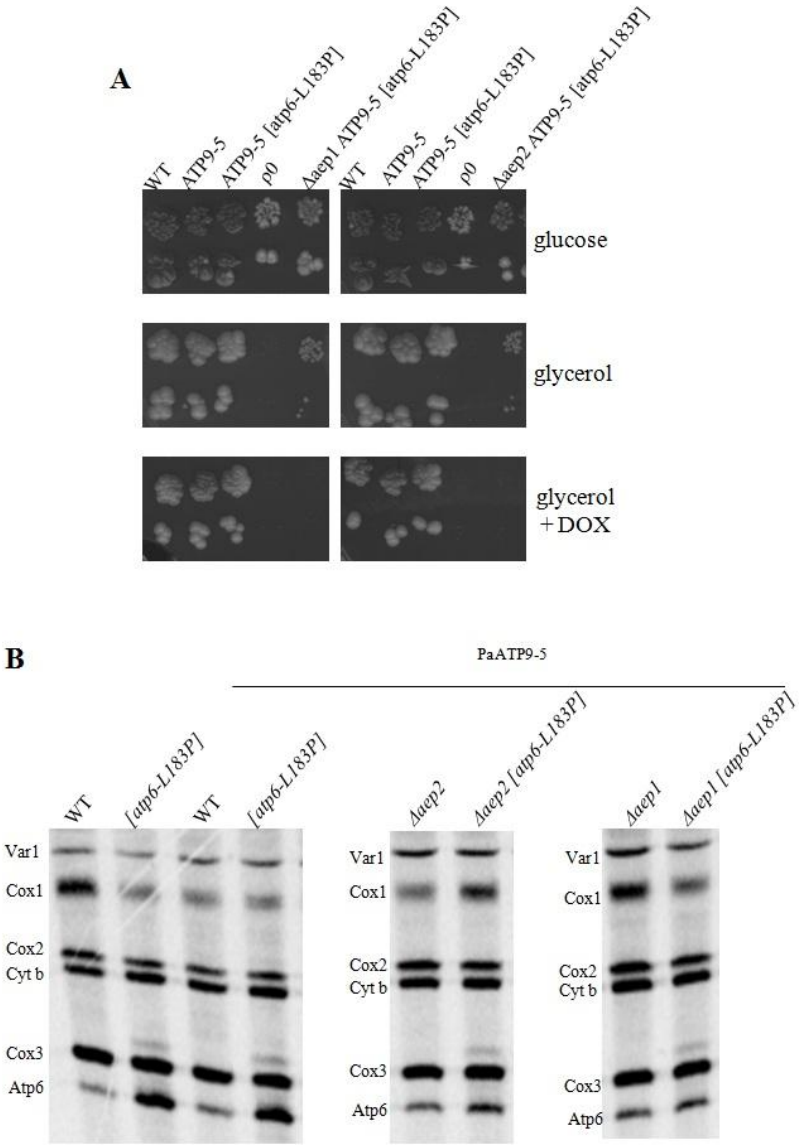

Figure 31 – Analysis of *WT* (MR6), ρ^0 (MR6 ρ^0), *atp6-L183P* (RKY20), *ATP9-5* (AKY65), *ATP9-5 [atp6-L183P]* (AKY75), *aep1Δ ATP9-5 [atp6-L183P]* (AKY63) and *aep2Δ ATP9-5 [atp6-L183P]* (AKY64). A: Growth phenotypes of the *aep1* and *aep2* deletion strains. Freshly grown strains were spotted on plates with rich glucose (YPDA), rich glycerol (YPGA) and rich glycerol supplemented with doxycycline (DOX, 40 µg/ml). The plates were incubated at 28°C and photographed after 6 days of incubation. **B: Mitochondrial protein synthesis.** Proteins encoded by mtDNA were labeled in whole cells with [^{35}S]-(methionine+cysteine) for 20 min. in the presence of cycloheximide to inhibit cytosolic protein synthesis. The total protein extracts from cells were prepared and loaded on 12% urea/glycerol gel (the same amount of radioactivity per each line). After electrophoresis the gel was dried and the proteins were visualized with a Phosphoimager.

III.2.3.4 Assembly factors Atp10p and Atp23p also play a role in the regulation of Atp6p synthesis

I next examined, whether proteins known to take part in the assembly/maturation of Atp6p (Atp10p and Atp23p) are required for the up-regulation of Atp6p synthesis in the *atp6-L183P* mutant. Atp10p protects newly synthesized Atp6 against mitochondrial proteases until its assembly and/or helps its incorporation into the ATP synthase (Ackerman and Tzagoloff 1990b; Tzagoloff, Barrientos et al. 2004). Atp23p has a double function (Zeng, Neupert et al. 2007c). As a metalloprotease, it cleaves off the first 10 aa of Atp6p, a peptide that facilitates the interaction of Atp6p with Atp9p. Its second function is required to fold Atp6p (Osman, Wilmes et al. 2007; Zeng, Neupert et al. 2007c). In the laboratory we have a plasmid encoding catalytically inactive Atp23p (*atp23-E168Q*). The presence of this plasmid in *atp23Δ* strains permits yeast cells to fold Atp6p despite their inability to mature Atp6p. It allowed me to determine which function, perhaps both or none, is required for Atp6p up-regulation in the *atp6-L183P* mutant.

As expected, the *atp10Δ* and *atp23Δ* strains I constructed were unable to grow on glycerol (Fig. 32A and B).

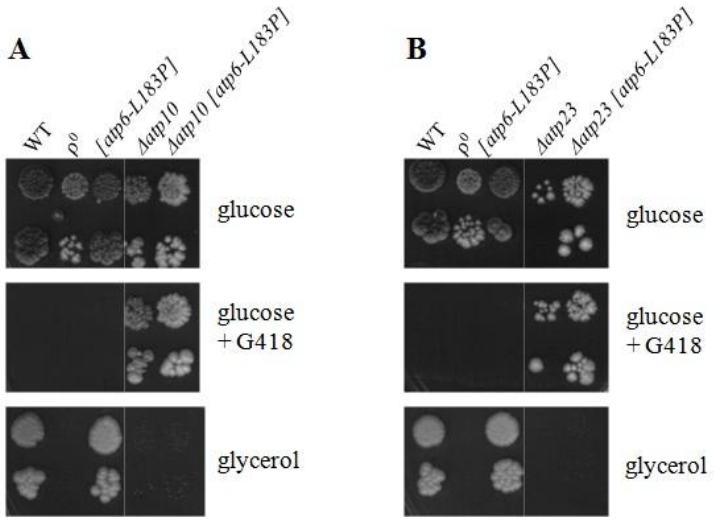

Figure 32 – Growth phenotypes of *atp10* (panel A) and *atp23* (panel B) deletion strains. Freshly grown wild type (MR6), ρ^0 (MR6 ρ^0), *atp6-L183P* (RKY20), *atp10Δ* (AKY38), *atp10Δ [atp6-L183P]* (AKY39), *atp23Δ* (AKY28) and *atp23Δ [atp6-L183P]* (AKY27) were spotted on plates with rich glucose (YPDA), rich glucose supplemented with G418 (200 µg/ml) and rich glycerol (YPGA). The plates were incubated at 28°C and photographed after 6 days of incubation.

In accordance with literature (Tzagoloff, Barrientos et al. 2004), Atp6p synthesis was almost normal in *atp10Δ* strains with a wild type mtDNA (Fig. 33A). The level of Atp6 synthesis in *atp10Δ* with the *atp6-L183P* mtDNA was normal too, indicating that the up-regulation of Atp6p, seen with mutations in Atp6p that compromise its assembly, depend upon Atp10p. The steady state levels of Atp6p in the *atp10Δ* strains were strongly diminished due to rapid degradation (Fig. 33B), as was shown before (Tzagoloff, Barrientos et al. 2004).

Fig. 33A shows that presence of Atp23p is not necessary for *WT* Atp6p synthesis. As expected Atp6p cannot be maturated and the protein migrates a bit slower than its maturated form, as shown in (Zeng, Neupert et al. 2007c). However *atp23Δ* in *atp6-L183* mtDNA background results in the loss of Atp6p synthesis up-regulation. In *atp23Δ* strain where I had introduced a plasmid encoding catalytically inactive form of Atp23p (*atp23-E168Q)* Atp6p up-regulation was still present. I can conclude that the assembly function of Atp23p but not its proteolytic activity is required for the up-regulation of Atp6p synthesis in the *atp6-L183P* mutant.

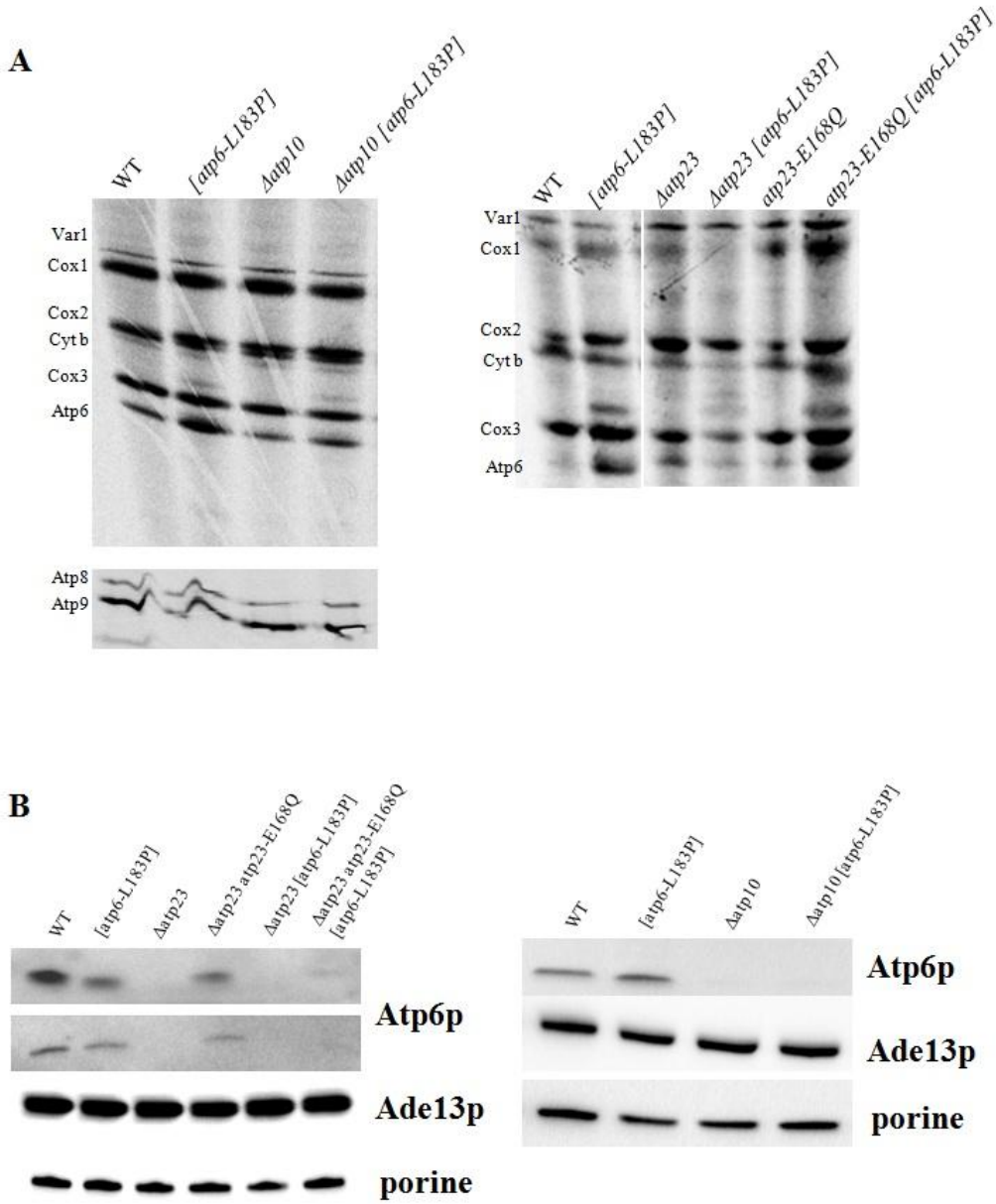

Figure 33 – Mitochondrial protein synthesis and SDS-PAGE of wild type (MR6), *atp6-L183P* (RKY20), *atp10Δ* (AKY38), *atp10Δ [atp6-L183P]* (AKY39), *atp23Δ* (AKY28), *atp23Δ [atp6-L183P]* (AKY27), *atp23-E168Q* (AKY28*) and *atp23-E168Q [atp6-L183P]* (AKY27*). A: Mitochondrial protein synthesis. Proteins encoded by mtDNA were labeled in whole cells from strains with [^{35}S]-(methionine+cysteine) for 20 min. in the presence of cycloheximide to inhibit cytosolic protein synthesis. The total protein extracts from cells were prepared and loaded on 12% urea/glycerol gel and 17.5% polyacrylamide gel (the same amount of radioactivity per each line). After electrophoresis the gel was dried and the proteins were visualized with a Phosphoimager. **B:** SDS-PAGE analysis of total mitochondrial proteins. Mitochondrial proteins (20 μg) were separated by SDS-PAGE, transferred to a nitrocellulose membrane and probed with antibodies against Atp6p, Ade13p and porine.

III.2.3.5 Influence of the central and the peripheral stalks on up-regulation of Atp6p synthesis

The central stalk is composed of three subunits: γ, δ and ε encoded by *ATP3*, *ATP16* and *ATP15* genes, respectively. Deletion of the first two results in 100% ρ^{-}/ρ^{0} cells, due to massive proton leaks through the F_O, whereas cultures of *atp15Δ* cells retain a significant proportion of ρ^{+} cells. Thus, to test the influence of the central stalk on the synthesis of Atp6p in the *atp6-L183P* mutant I deleted the *ATP15* gene. Peripheral stalk stabilizes the connection between catalytic the head and the proton channel in ATP synthase. To determine how it influences Atp6p synthesis in the *atp6-L183P* mutant, I deleted the *ATP7* gene, encoding subunit d. The loss of *ATP7* also increases the production of ρ^{-}/ρ^{0} cells, but usually not to 100%.

As expected, neither *atp15Δ* nor *atp7Δ* could grow on non-fermentable carbon source (Fig. 34A and B). In the absence of subunit ε Atp6p is still synthesized both in the *WT* as well as in the *atp6-L183P* backgrounds (Fig. 34C). Deletion of *ATP15* did not specifically influence Atp6p synthesis in the *WT* background. However in the *atp6-L183P* cells, the effect of Atp6p synthesis up-regulation disappeared and the synthesis was comparable to that of *WT*. Unfortunately the *atp7Δ* strain produced too many ρ^{-}/ρ^{0} cells rendering the results less clear even though they suggested that synthesis of Atp6p was no longer up-regulated in the *atp6-L183P* mutant (Fig. 34C). I conclude that the presence of central and peripheral stalks in ATP synthase sub-complex is necessary for appearance of Atp6p synthesis up-regulation in the *atp6-L183P* mutant.

Considered together the results strongly support our hypothesis that a partial ATP synthase assembly lacking only Atp6p (see Fig 27) drives the synthesis of Atp6p, which provides a means to couple the synthesis of this protein to its assembly, and that this control depends on the two proteins (Atp10p and Atp23p) known to be involved in the assembly of Atp6p.

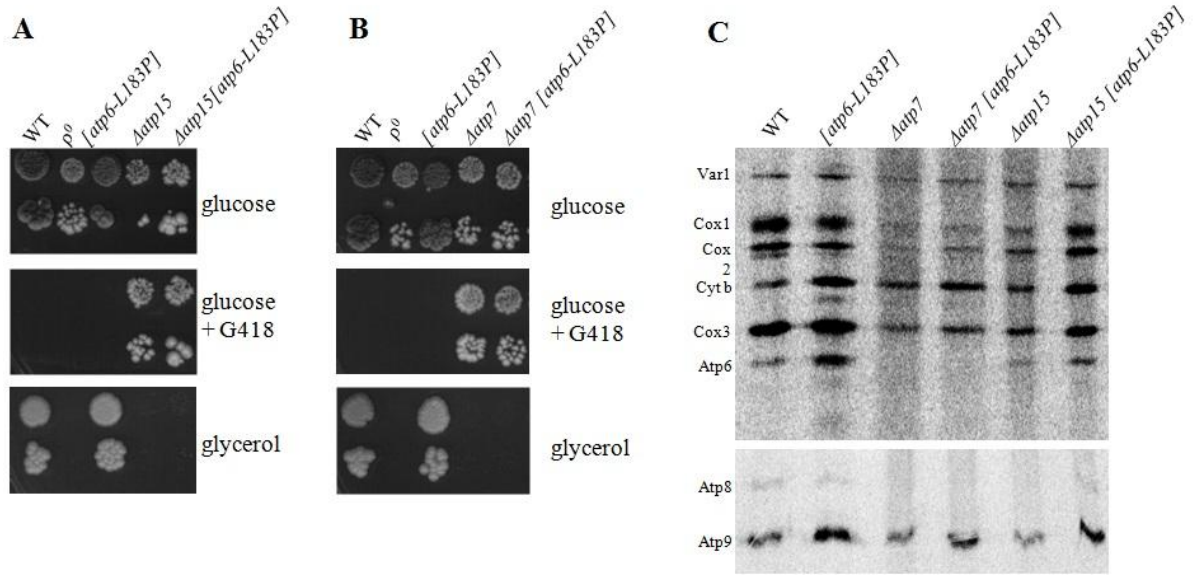

Figure 34 – Growth phenotypes and mitochondrial protein synthesis of wild type (MR6), ρ^0 (MR6 ρ^0), *atp6-L183P* (RKY20), *atp15Δ* (AKY32), *atp15Δ [atp6-L183P]* (AKY33), *atp7Δ* (AKY34) and *atp7Δ [atp6-L183P]* (AKY35). A: Growth test. Freshly grown cultures were spotted on plates with rich glucose (YPDA), rich glucose supplemented with G418 (200 µg/ml) and rich glycerol (YPGA). The plates were incubated at 28°C and photographed after 6 days of incubation. **B:** Mitochondrial protein synthesis. Proteins encoded by mtDNA were labeled in whole cells from strains with [^{35}S]-(methionine+cysteine) for 20 min. in the presence of cycloheximide to inhibit cytosolic protein synthesis. The total protein extract from cells were prepared and loaded on 12% urea/glycerol gel and 17.5% polyacrylamide gel (the same amount of radioactivity per each line). After electrophoresis the gel was dried and the proteins were visualized with a Phosphoimager.

III.3. REGULATION OF EXPRESSION OF *ATP9*

The results shown in the previous section indicate that Atp6p synthesis is coupled to its assembly. In this section, I present results indicating that the synthesis of Atp9p, the protein partner of Atp6p within the ATP synthase, is also regulated in relation with its assembly.

In yeast *S. cerevisiae* expression of mitochondrially encoded *ATP9* gene is controlled by at least three proteins: Aep1, Aep2 and Atp25. Aep1p and Aep2p interact with 5'UTR of *ATP9* mRNA and are essential for translation. Aep2p also takes part in mRNA maturation, its stability and/or initiation of translation (Finnegan, Payne et al. 1991; Payne, Schweizer et al. 1991; Payne, Finnegan et al. 1993). Atp25p is cleaved in two fragments of similar length: the C-terminal part is responsible for *ATP9* mRNA stability, N-terminal part would be a chaperon needed for formation of the Atp9-ring (Zeng, Barros et al. 2008). It is not known, whether this cleavage occurs before or after the import of Atp25p into mitochondria. It is believed that Atp9-ring assembles separately and then interacts with the F_1. The F_1-Atp9-ring sub-complex finally associates with a second sub-complex containing the peripheral stalk, Atp8p and Atp6p, to form fully assembled ATP synthase (Rak, Gokova et al. 2011).

It is to be mentioned that so far detailed analysis of the roles of these proteins in the *ATP9* gene expression was very difficult because of strong instability of mtDNA in strains from which *AEP1, AEP2* or *ATP25* genes had been deleted. What we know about their functions was largely obtained using thermo-sensitive mutants in these genes. In the laboratory we showed that the nuclear *ATP9-5* gene from *Podospora anserina* can partially complement a yeast strain in which the *ATP9* gene has been replaced in-frame by *ARG8m* (Bietenhader, Martos et al. 2012). It was expected that Atp9-5 protein expression does not require the presence of Aep1p, Aep2p and C-terminal part of Atp25p, as these proteins are only required to express the mitochondrial *ATP9* gene, whereas the N-terminal part of Atp25p could still be needed to assemble the Atp9-5 rings. To test this hypothesis, we have deleted *AEP1, AEP2* and *ATP25* genes in a wild type yeast strain (MR6) transformed with a plasmid expressing *ATP9-5* under the control of the Tet-O doxycycline repressible promoter (pAM19). We have also deleted these genes in the *atp9Δ* strain transformed with the same plasmid (pAM19), to see whether expression of the *ARG8m* marker requires Aep1p, Aep2p, and Atp25p or not.

III.3.1 Growth phenotypes of ATP9 relocation strains lacking AEP1, AEP2 and ATP25, and containing a wild type mtDNA

III.3.1.1 ATP25

On non-fermentable carbon source (Fig. 35), the *atp25Δ + ATP9-5* strain grew, although at a slower rate than the *WT*. This growth was inhibited by doxycycline, which indicated that it was totally dependent on the expression of *ATP9-5*. As expected, the *atp25Δ + ATP9-5* strain recovered the normal respiratory growth upon transformation with a plasmid containing a wild type *ATP25* gene, even in the presence of doxycycline, due to the restoration of expression of the mitochondrial *ATP9* gene. When transformed with a plasmid expressing only the C-terminal part of the *ATP25* gene, growth was not improved and remained entirely dependent on *ATP9-5*. Interestingly, growth of *atp25Δ + ATP9-5* was significantly improved by the N-terminal part of *ATP25*, but only in the absence of doxycycline, presumably because the assembly of Atp9-5p becomes more efficient. Finally, after transformation with both the N- and C-terminal fragments, *atp25Δ + ATP9-5* could grow in the presence of doxycycline but at a much slower rate than wild type yeast. This result indicates that expression of *ATP9* is much less efficient when the two regions of Atp25p are expressed separately (see below).

III.3.1.2 AEP1, AEP2

Strains lacking the *AEP1* or *AEP2* gene could grow on glycerol if transformed with the *ATP9-5* gene, and this growth was fully inhibited by doxycycline, which demonstrated that it was entirely dependent on *ATP9-5*. Upon transformation with *AEP1* or *AEP2* plasmid, growth was fully restored and was no longer inhibited by doxycycline, because of *ATP9* expression restoration (Fig. 36).

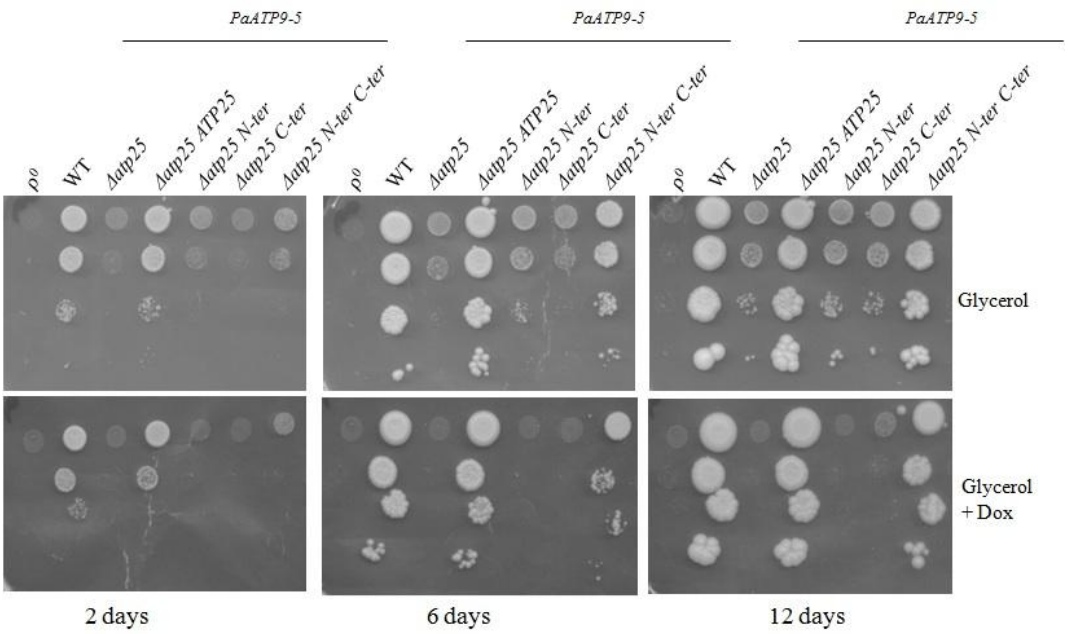

Figure 35 – Growth phenotypes of *atp25Δ* strains in *WT* mtDNA background. Freshly grown strains *WT* (MR6), ρ^0 (MR6 ρ^0), *atp25Δ PaATP9-5* (AKY74), *atp25Δ PaATP9-5 pATP25* (AKY74/pRK56), *atp25Δ PaATP9-5 pN-ter* (AKY74/pG29ST32), *atp25Δ PaATP9-5 pC-ter* (AKY138) and), *atp25Δ PaATP9-5 pN-ter pC-ter* (AKY139) were spotted on rich glycerol medium (YPGA) and rich glycerol supplemented with doxycycline (DOX, 40 µg/ml). The plates were incubated at 28°C and photographed after indicated number of days.

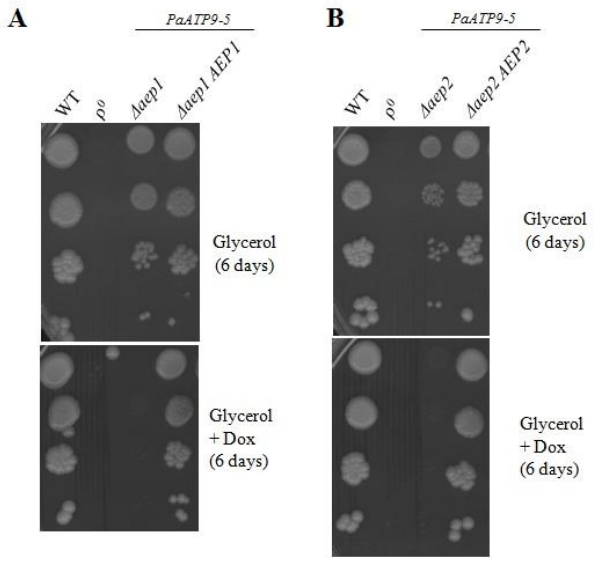

Figure 36 – Growth phenotypes of *aep1Δ* and *aep2Δ* strains in *WT* mtDNA background. Freshly grown strains *WT* (MR6), ρ^0 (MR6 ρ^0), *aep1Δ PaATP9-5* (AKY60), *aep1Δ PaATP9-5 pAEP1* (AKY60/pRK54), *aep2Δ PaATP9-5* (AKY61) and *aep2Δ PaATP9-5 pAEP2* (AKY61/pRK57) were spotted on rich glycerol medium (YPGA) and rich glycerol supplemented with doxycycline (DOX, 40 µg/ml). The plates were incubated at 28°C and photographed after 6 days.

III.3.2 Growth phenotypes of ATP9 relocation strains lacking AEP1, AEP2 and ATP25, and in which ATP9 is replaced by ARG8m

III.3.2.1 ATP25

WT strain (MR6) is respiratory competent but cannot grow on medium without arginine, because it lacks the *ARG8* gene in nuclear DNA and does not have its mitochondrial version (*ARG8m*) in mtDNA. The strain (RKY26) where *ATP9* has been replaced with *ARG8m* is respiratory deficient but can grow on glucose plates lacking arginine (-Arg). There is no difference in growth on –Arg medium between *atp9Δ* and *atp9Δ + ATP9-5*. Upon deletion of the *ATP25* gene, the strain *atp9Δ + ATP9-5* became arginine auxotroph, and this phenotype was suppressed by a transformation with a plasmid containing wild type *ATP25* (Fig. 37A). Presence of the N-terminal part of *ATP25* on plasmid did not restore growth on medium without arginine. This is not surprising because as a chaperon protein which facilitates oligomerization of the Atp9-ring the N-terminal fragment of Atp25p should not be needed for *ARG8m* expression. On the opposite the C-terminal part of Atp25p, which is known to stabilize *ATP9* mRNA was able to restore arginine prototrophy (Fig. 37A). It is to be noted that only a part of the coding sequences of *ATP9* have been replaced by *ARG8m*. It is possible that the 5' and 3' untranslated regions of the *ATP9* transcripts that are preserved in the *atp9* deletion strain are the sequences on which the C-terminal part of Atp25p is acting. However the growth on arginine of the modified yeast strain was slower as compared to *atp9Δ* and *atp9Δ + ATP9-5*, and was not significantly improved upon addition of the N-terminal fragment of Atp25p (Fig. 37A). Perhaps the interaction of the C-terminal fragment of Atp25p is less efficient with the *atp9::ARG8m* transcripts than with intact *ATP9* transcripts.

III.3.2.2 AEP1 and AEP2

Lack of Aep1p or Aep2p in the *atp9Δ* strain prevents growth on medium without arginine. Introduction of plasmids with the *AEP1* or *AEP2* genes restores arginine prototrophy. Thus, as the C-terminal fragment of Atp25p, the Aep1p and Aep2p proteins are required for expression of the *ARG8m* gene integrated at the mitochondrial *ATP9* locus (Fig. 37B and C).

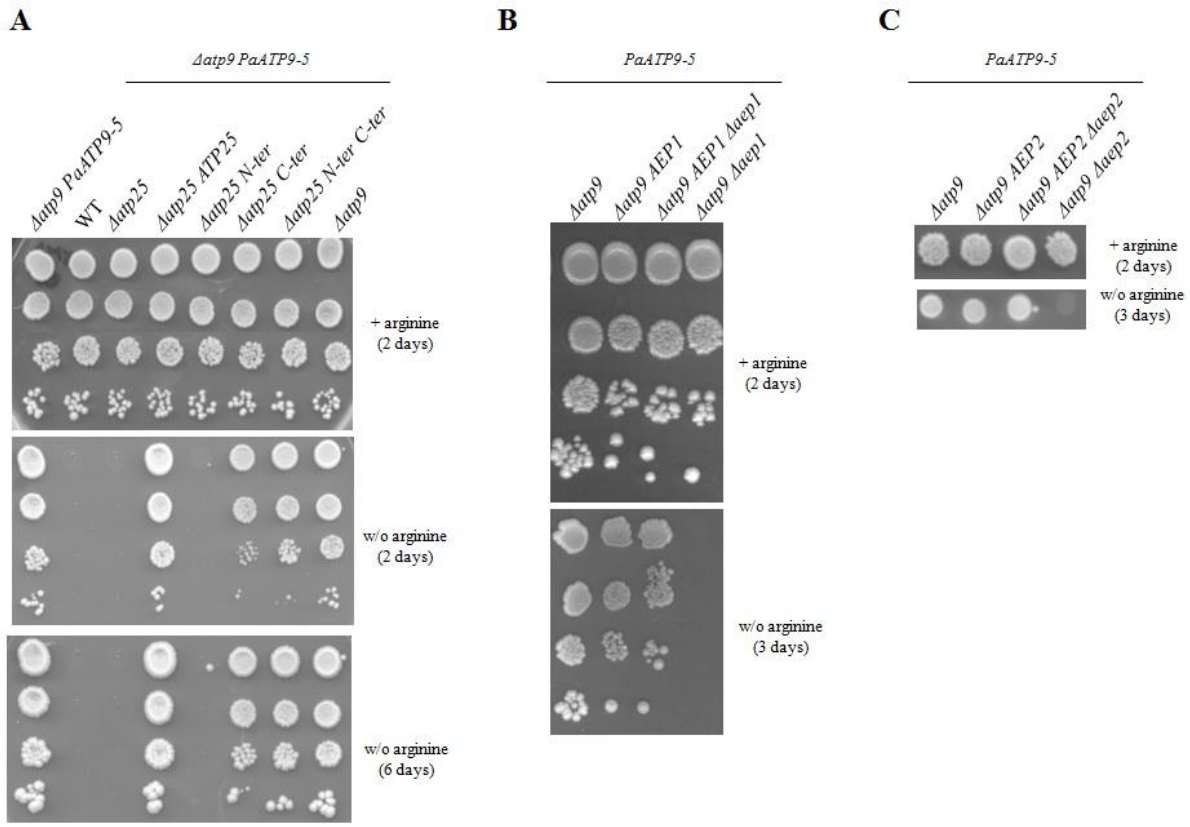

Figure 37 – Growth phenotypes of *atp25Δ*, *aep1Δ* and *aep2Δ* strains in *atp9::ARG8m* mtDNA background. Freshly grown strains *WT* (MR6), *atp9Δ* (RKY26), *atp9Δ PaATP9-5* (AMY10), *atp25Δ PaATP9-5 atp9Δ* (RKY95), *atp25Δ PaATP9-5 pATP25 atp9Δ* (RKY89), *atp25Δ PaATP9-5 pN-ter atp9Δ* (RKY95/pG29ST32), *atp25Δ PaATP9-5 pC-ter atp9Δ* (AKY140), *atp25Δ PaATP9-5 pN-ter pC-ter atp9Δ* (AKY141), *atp9Δ PaATP9-5 pAEP1* (RKY96), *atp9Δ PaATP9-5 pAEP1 aep1Δ* (RKY92), *atp9Δ PaATP9-5 aep1Δ* (RKY93), *atp9Δ PaATP9-5 pAEP2* (RKY97), *atp9Δ PaATP9-5 pAEP2 aep2Δ* (AKY52) and *atp9Δ PaATP9-5 aep2Δ* (RKY94) were spotted on rich glucose (+arginine) and synthetic glucose without arginine (w/o arginine) plates. The plates were incubated at 28°C and photographed after indicated number of days.

III.3.3 In vivo analysis of mitochondrially encoded proteins translation in ATP25, AEP1 and AEP2 deprived strains in WT and atp9::ARG8m mtDNA backgrounds

For these analyses, strains were cultivated in synthetic galactose media deprived of nutrients (uracil and leucine), making the presence of different plasmids indispensable for growth. Consistent with the growth tests described above, Atp9p (*WT* mtDNA) or Arg8m (*atp9::ARG8m* mtDNA) was not synthesized in the strains lacking *AEP1*, *AEP2* or *ATP25*, whereas all other proteins encoded by the mitochondrial genome were normally synthesized (Fig. 38A – D). In *atp25Δ* + *ATP9-5* strains with *WT* mtDNA and transformed with the C-terminal fragment of *ATP25*, the synthesis of Atp9p was almost undetectable, and remained poor when the N-terminal fragment was added. However trace amounts of Atp9p could be detected by Western blot in these strains (Fig. 39A). Similarly, the synthesis and steady state accumulation of Arg8m were very poor in strains containing only the C-terminal fragment of *ATP25*, and only a modest improvement was observed when both fragments of Atp25p were present (Fig. 39B), despite the ability of these strains to grow in media lacking arginine.

Western blots were performed to determine the amount of the C-terminal and N-terminal fragments of Atp25p in the cells, when these were expressed separately instead of an intact *ATP25* gene. This could be done due to the inclusion of an HA epitope in these fragments. Somewhat surprisingly, both fragments were in a very low amounts compared to cells that express a wild type *ATP25* gene (Fig. 39C). We do not know the reason of this. One possibility is that these fragments are more susceptible to degradation (outside and/or inside mitochondria) when they are not produced by the cleavage of a whole Atp25p protein. Anyway, these data provide an explanation for the poor expression of Atp9p or Arg8p in the strains expressing these two fragments separately, alone or in combination.

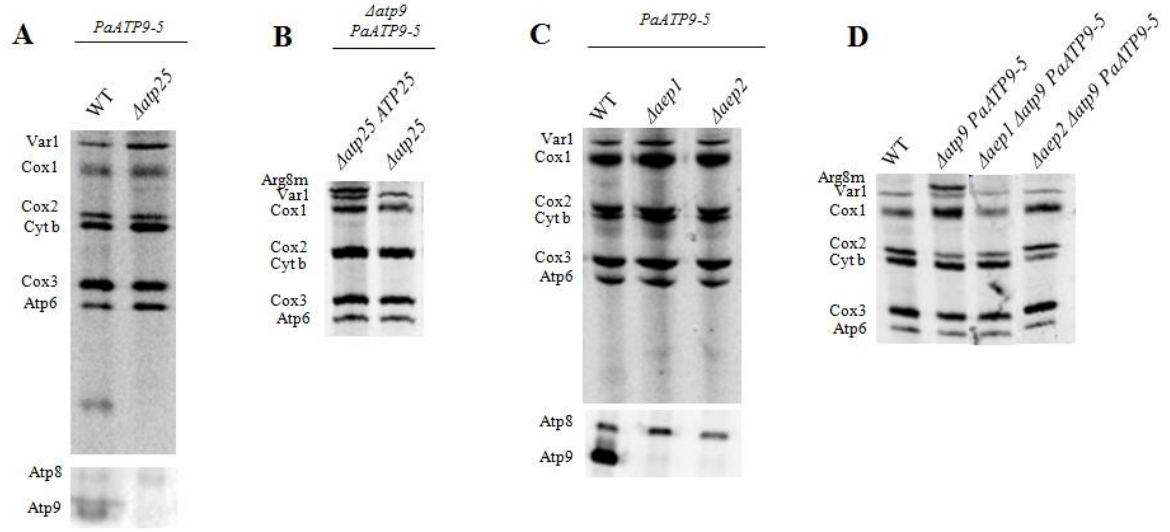

Figure 38 – Mitochondrial protein synthesis. Proteins encoded by mtDNA were labeled in whole cells from wild type with the *pATP9-5* (AKY65), *atp25Δ PaATP9-5* (AKY74), *atp25Δ PaATP9-5 pATP25 atp9Δ* (RKY89), *atp25Δ PaATP9-5 atp9Δ* (RKY95), *aep1Δ PaATP9-5* (AKY60), *aep2Δ PaATP9-5* (AKY61), wild type (MR6), *atp9Δ PaATP9-5* (AMY10), *atp9Δ PaATP9-5 aep1Δ* (RKY93) and *atp9Δ PaATP9-5 aep2Δ* (RKY94) strains with [^{35}S]-(methionine+cysteine) for 20 min. in the presence of cycloheximide to inhibit cytosolic protein synthesis. The total protein extracts from cells were prepared and loaded on 12% urea/glycerol gel (to separate Cox3p and Atp6p) and 17.5% SDS polyacrylamide gel (to separate Atp8p and Atp9p). The same amount of radioactivity per each line was loaded. After electrophoresis the gel was dried and the proteins were visualized with a Phosphoimager.

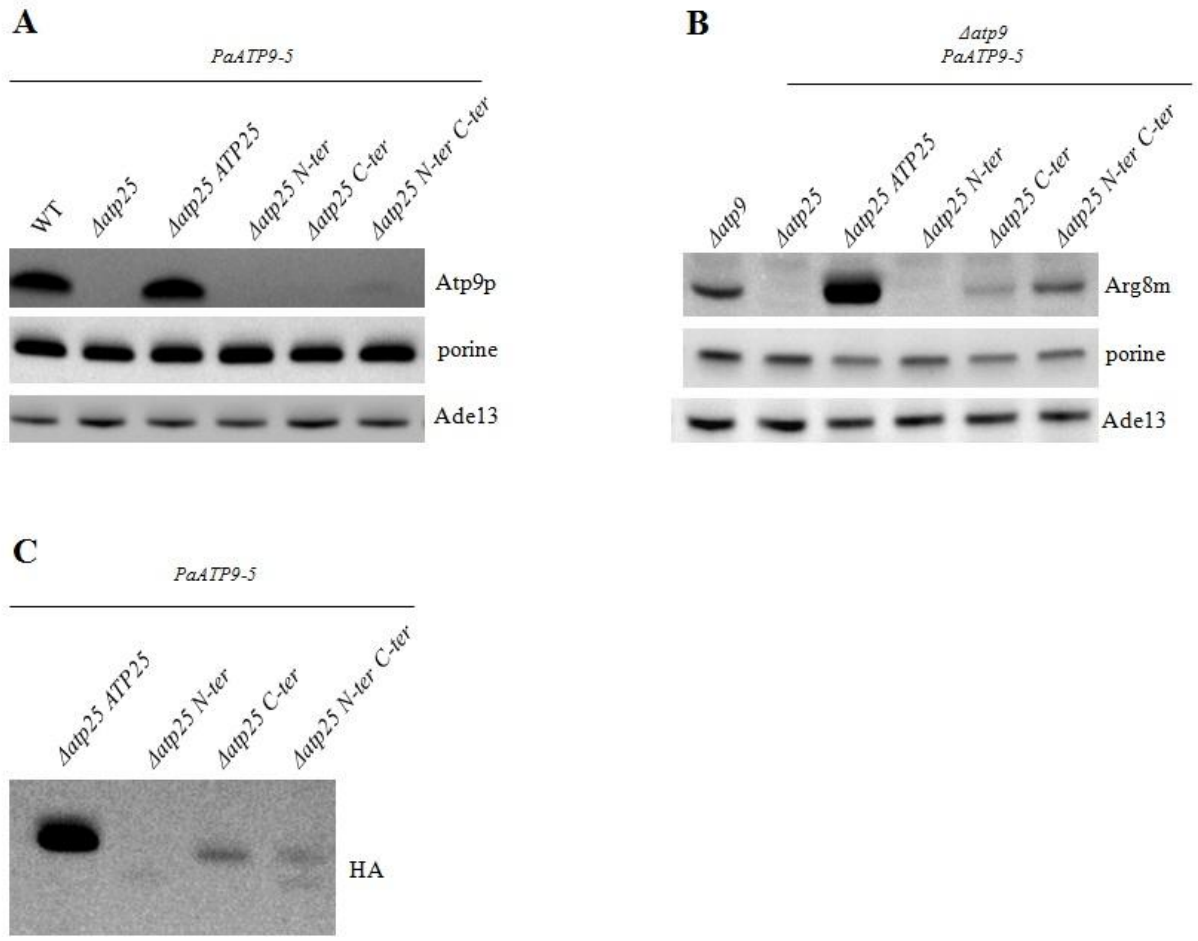

Figure 39 – SDS-PAGE analysis of total mitochondrial proteins. Total protein extracts were prepared from *WT PaATP9-5* (AKY65), *atp25Δ PaATP9-5* (AKY74), *atp25Δ PaATP9-5 pATP25* (AKY74/pRK56), *atp25Δ PaATP9-5 pN-ter* (AKY74/pG29ST32), *atp25Δ PaATP9-5 pC-ter* (AKY138), *atp25Δ PaATP9-5 pN-ter pC-ter* (AKY139), *atp9Δ* (RKY26), *atp25Δ PaATP9-5 atp9Δ* (RKY95), *atp25Δ PaATP9-5 pATP25 atp9Δ* (RKY89), *atp25Δ PaATP9-5 pN-ter atp9Δ* (RKY95/pG29ST32), *atp25Δ PaATP9-5 pC-ter atp9Δ* (AKY140) and *atp25Δ PaATP9-5 pN-ter pC-ter atp9Δ* (AKY141). Mitochondrial proteins (20 µg) were separated by SDS-PAGE, transferred to a nitrocellulose membrane and probed with antibodies against Atp9p (panel A), Arg8m (panel B) Ade13p, porine (panel A and B) and HA (panel C).

III.3.4 Atp9-5 protein stimulates expression of mitochondrial ATP9 locus

One of the control strains used in the experiments described above (but not presented yet) was the *WT* strain where I introduced the plasmid encoding *ATP9-5* gene. During the analysis of synthesis of mitochondrially encoded proteins I observed an unexpected phenomena. In the presence of the Atp9-5 protein, synthesis of mitochondrial Atp9p augmented about twice (Fig. 40A). This effect disappeared, if the strain was grown in a medium supplemented with doxycycline (Fig. 40B), indicating that the up-regulation of Atp9p is in some way provoked by the nuclearly encoded Atp9-5 protein. I next prepared total cellular protein extracts and separated them in denaturing gels, transferred them to nitrocellulose membranes and stained them with an antibody against yeast Atp9p. It is worth to mention that this antibody does not recognize Atp9-5p. The obtained result shows that the steady state level of Atp9p was exactly the same in the two analyzed strains, *WT* and *WT + ATP9-5* (Fig. 40C). I checked, whether an excess of synthesized Atp9p aggregates by treating the protein samples with denaturing agents (as described in Materials and Methods) before loading on gel. No increase in the state accumulation was observed in *WT + ATP9-5* (Fig. 40C), showing that the Atp9p proteins synthesized in excess compared to *WT* do not accumulate in cells but are eliminated instead, presumably by proteolytic degradation.

I then aimed to know, whether the mitochondrial expression of the *ARG8m* marker under control of the *ATP9* regulatory sequences would also be stimulated by *ATP9-5*. As shown in Fig. 40D, the synthesis of Arg8p was indeed significantly stimulated, at least 2-fold. In contrast to Atp9p, steady-state accumulation of Arg8p was increased in similar proportion (Fig. 40E), indicating that the excess of newly synthesized Arg8 proteins is not degraded.

Previous work has shown that in a *atp9Δ* strain, Atp6p is apparently poorly synthesized ((Bietenhader, Martos et al. 2012), see also Fig. 42). Interestingly, the synthesis of Atp6p was fully restored upon transformation of *atp9Δ* with *ATP9-5* (Fig. 42). This observation is consistent with the results presented in section III.2.3.3, showing that Atp9p positively influences the synthesis of Atp6p.

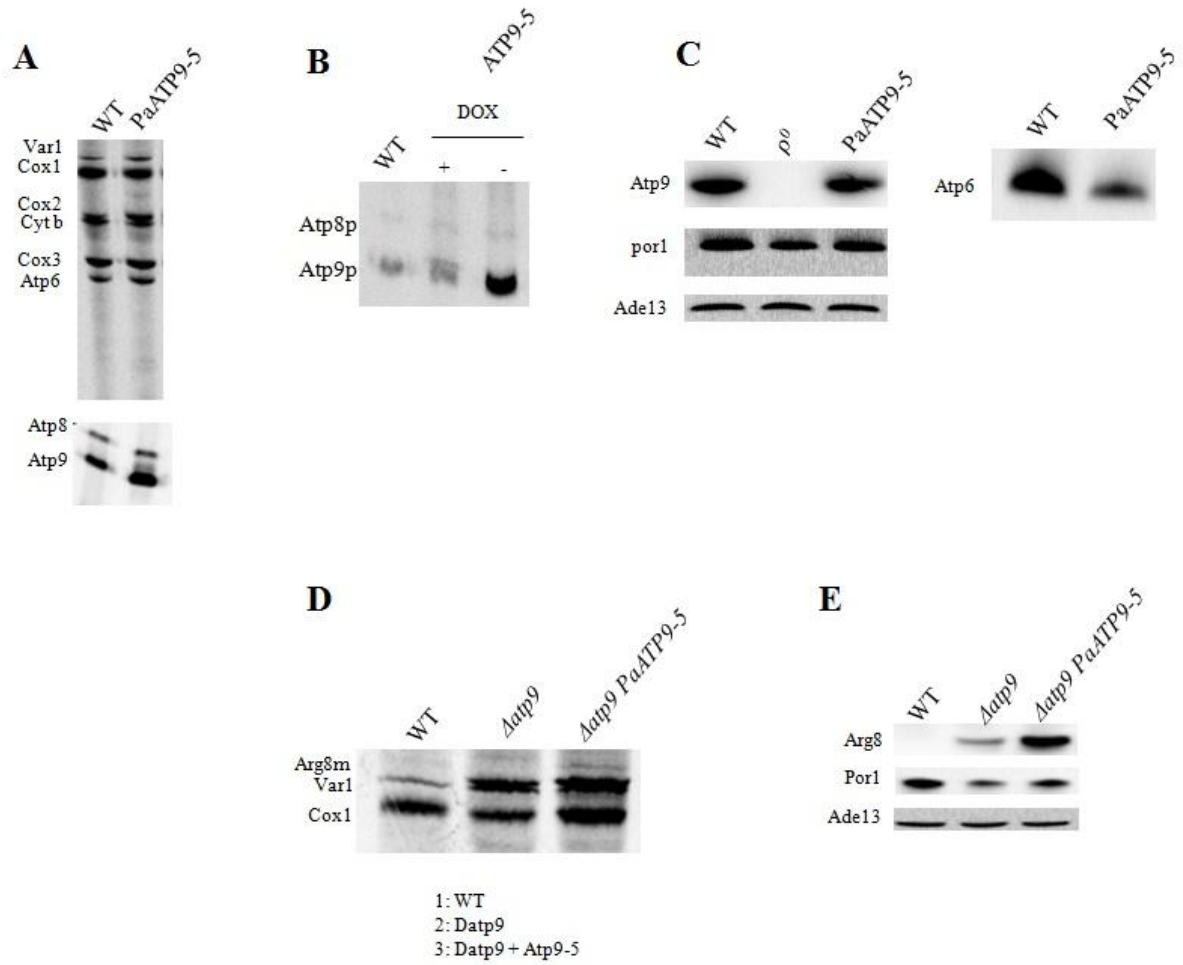

Figure 40 – Mitochondrial protein synthesis and SDS-PAGE analysis of wild type (MR6), wild type with *PaATP9-5* (AKAK65), *atp9Δ* (RKY26), *atp9Δ PaATP9-5* (AMY10) and ρ^0 (MR6 ρ^0). A, B and D: Proteins encoded by mtDNA were labeled in whole cells with [^{35}S]-(methionine+cysteine) for 20 min. in the presence of cycloheximide to inhibit cytosolic protein synthesis. The total protein extracts from cells were prepared and loaded on 12% urea/glycerol gel and 17.5% SDS polyacrylamide gel. The same amount of radioactivity per each line was loaded. After electrophoresis the gel was dried and the proteins were visualized with a Phosphoimager. **C, E:** SDS-PAGE analysis of total mitochondrial proteins. Mitochondrial proteins (20 µg) were separated by SDS-PAGE, transferred to a nitrocellulose membrane and probed with antibodies against Atp9p, Atp6p (panel C), Arg8m (panel E) Ade13p and porine (panel C and E).

III.3.5 Expression of ATP9-5 in wild type yeast dramatically affects the stability of Atp6p.

As described above, expression of *ATP9-5* in wild type yeast stimulates Atp9p synthesis in mitochondria. Although Atp6p synthesis remained normal, the steady-state accumulation of this protein was strongly diminished (see Fig. 40A and C). A possible explanation is the following. The Atp9-5 protein differs from yeast Atp9p by a number of amino acids, notably in the second transmembrane helix. This domain interacts with Atp6p, which allows protons to be transferred from Atp6p to the Atp9p-ring. Although the mitochondrial *ATP9* gene is efficiently expressed in *WT + ATP9-5*, even better than in untransformed *WT*, it is possible that the co-expression of *ATP9* and *ATP9-5* is detrimental. Indeed, although Atp9-5p and Atp9p are not structurally identical, they may associate with each other and form mixed oligomers that interact less efficiently with Atp6p than pure yeast Atp9p-rings. Because of this, the Atp6p protein may become more susceptible to degradation. As explained below, the decreased stability of Atp6p in *WT + ATP9-5* might be responsible for the up-regulation of *ATP9* by *ATP9-5*.

III.3.6 Is Atp9p stability F_1-dependent?

It has been proposed that ATP synthase F_1 domain activates Atp6p and Atp8p translation (Rak and Tzagoloff 2009a). Although expression of Atp9p is usually considered as F_1-independent, we observed that the steady-state accumulation of this protein is dramatically reduced in α-F_1 and/or β-F_1 deficient strains (Fig. 41). Since Atp9p synthesis is not obviously impacted, it can be inferred that this effect is caused by post-translational degradation. The steady-state accumulation of Atp9p was not affected in the *atp6Δ* strain, indicating that it is the interaction between the Atp9 and/or Atp9p ring with F_1 that is critical for protection of Atp9p from degradation.

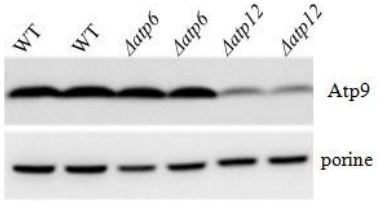

Figure 41 – SDS-PAGE analysis of total mitochondrial proteins. Total protein extracts were prepared from the wild type (MR6), *atp6Δ* (MR10) and *atp12Δ* (AKY42) strains. Mitochondrial proteins (20 μg) were separated by SDS-PAGE, transferred to a nitrocellulose membrane and probed with antibodies against Atp9p and porine.

III.3.7 The up-regulation of Atp9p by Atp9-5 is enhanced by lack of Atp6p and is F_1-dependent

I demonstrated above that in the presence of nuclear Atp9-5 protein synthesis of mitochondrial Atp9p is enhanced. Interestingly, this effect was dramatically exacerbated when the mitochondrial *ATP6* gene was absent (Fig. 42 lane *Δatp6 PaATP9-5*). In the absence of the Atp9-5 protein, deletion of *ATP6* also stimulated the Atp9p synthesis, yet somewhat less efficiently (Fig. 42 lane *Δatp6*). Although Atp9p can be synthesized in the absence of F_1, we aimed to know, whether this up-regulation of Atp9p was F_1-dependent. This was investigated with a null mutation of *ATP12*. Clearly, all the up-regulations of Atp9p synthesis stimulated by Atp9-5p and lack of Atp6p, disappeared upon deletion of *ATP12* (Fig. 42 lanes *Δatp12* to *Δatp12 Δatp6 PaATP9-5*).

As described below in the General Discussion, the data presented in this chapter indicate that Atp9p control its own synthesis, as a means to adjust the production of this protein in relation to its protein partners within ATP synthase.

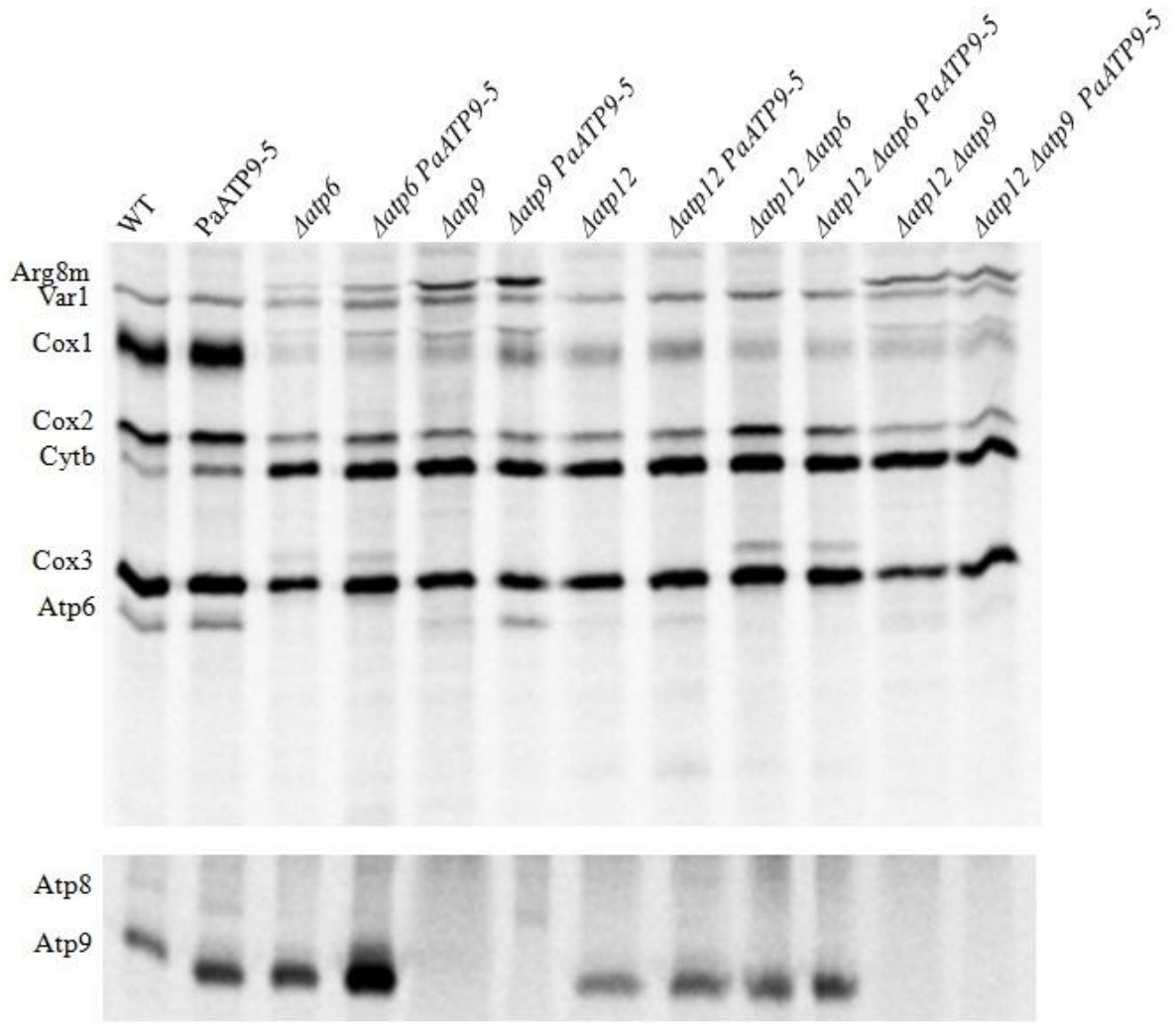

Figure 42 – Mitochondrial protein synthesis. Proteins encoded by mtDNA were labeled in whole cells from wild type (MR6), wild type with *pATP9-5* (AKAK65), *atp6Δ* (MR10), *atp6Δ PaTP9-5* (FG146), *atp9Δ* (RKY26), *atp9Δ PaATP9-5* (AMY10), *atp12Δ* (AKY42), *atp12Δ PaATP9-5* (AKY121), *atp12Δ atp6Δ* (FG151), *atp12Δ atp6Δ PaATP9-5* (FG152), *atp12Δ atp9Δ* (FG153) and *atp12Δ atp9Δ PaATP9-5* (FG154) with [^{35}S]-(methionine+cysteine) for 20 min. in the presence of cycloheximide to inhibit cytosolic protein synthesis. The total protein extracts from cells were prepared and loaded on 12% urea/glycerol gel and 17.5% SDS polyacrylamide gel (the same amount of radioactivity per each line). After electrophoresis the gel was dried and the proteins were visualized with a Phosphoimager.

GENERAL DISCUSSION

IV.1 YEAST MODELS OF HUMAN DISEASES SHOW INFLUENCE OF MUTATIONS IN ATP6 GENE ON ATP SYNTHASE

In the first part of my work I have analyzed the influence of seven mutations in mitochondrial gene *ATP6* on the ATP synthase: two found in patients with the NARP syndrome and five that were identified in human tumors.

IV.1.1 Consequences of the NARP atp6-S250P and atp6-L252P mutations on yeast ATP synthase

Mutations 9185T>C and 9191T>C of the human *MTATP6* gene found in patients presenting with the NARP syndrome, resulted in a leucine into proline changes at codon positions 220 and 222. These amino acids correspond to serine 250 and leucine 252 into proline changes in yeast Atp6p, respectively. They are located in the last transmembrane segment of Atp6p that is supposed to contact the Atp9p-ring. The *atp6-S250P* mutation caused a 30% drop in the ATP synthesis and affected neither assembly nor stability of the ATP synthase. There was no leak across the inner mitochondrial membrane. Therefore the main effect of this mutation is a partial impairment of proton transport through F_O. Modest impact of the mutation on the enzyme is consistent with the relatively mild clinical phenotype of 9185T>C. The *atp6-L252P* mutation was much more deleterious: ATP synthesis was decreased by more than 95% as compared to the *WT* strain due to a failure in the incorporation of Atp6p into the ATP synthase. It is possible that Atp6p with the L252P mutation cannot interact correctly with the Atp9p-ring to form a proton channel. Another explanation is that the *atp6-L252P* mutation affects the interaction with chaperon Atp10p which supports the assembly of Atp6p. The severe effects on the ATP synthase caused by this mutation are consistent with the severe clinical phenotype of the patients carrying this mutation.

IV.1.2 Yeast-based assay for screening of drugs active against ATP synthase disorders

In the course of preparation of my thesis I have had an opportunity to participate in a project aimed at identification of drugs active against human ATP synthase disorders. In this project we have used yeast models of these diseases. Two positive hits have been identified: chlorhexidine and oleate. For my part, I was testing the ATP synthase stability in the *fmc1Δ* strain in the presence of chlorhexidine. The BN-PAGE analysis demonstrated that the ATP synthase was more stable in the *fmc1Δ* strain in the presence of chlorhexidine. Another

analysis revealed that chlorhexidine attenuates the phenotypes observed in the *fmc1Δ* strain such as lower oxygen consumption, weak energization of the inner mitochondrial membrane, reduced ATP synthase, presence of inclusion bodies in the matrix and almost no *cristae* in the mitochondria. The transcriptional analysis showed that chlorhexidine probably acts by changing the expression of the genes connected with the respiratory chain and retrograde signaling. Chlorhexidine was also active in the NARP-cybrid model. Altogether, the results of this project establish the usefulness of the yeast model for screening of drugs active against ATP synthase disorders and primary clues of their mode of action.

IV.1.3 Influence of the atp6-"cancer" mutations on the ATP synthase

55 mutations were identified in the mitochondrial *MTATP6* gene in various tumors. I introduced in yeast an equivalent of five of these mutations, 8716A>G, 8914C>A, 8932C>T, 8953A>G and 9131T>C, which are in highly conserved positions between humans and yeast. They resulted in the following amino acid changes in yeast Atp6p: *atp6-K90E*, *atp6-P157T*, *atp6-P163S*, *atp6-I170V* and *atp6-L232P*. The respiratory growth of none yeast *atp6* mutant was affected, either at 28°C and 36°C. The *atp6-P163S*, *atp6-K90E* and *atp6-I170V* strains were more resistant *in vivo* to oligomycin, possibly because the mutations compromise the binding of the drug to the ATP synthase. On the contrary, the *atp6-P157T* and *atp6-L232P* strains were more sensitive on the medium supplemented with oligomycin, probably because less drug is needed for the 20% threshold of ATP synthesis below which respiratory growth of yeast is affected (Mukhopadhyay, Uh et al. 1994; Kucharczyk, Ezkurdia et al. 2010). The oxygen consumption in the mitochondria of the *atp6* mutant strains cultured at 28°C was almost normal. Mitochondria from cultures grown at 36°C had a slightly reduced oxygen consumption in the *atp6-P163S* and *atp6-L232P* mutants, whereas respiration in the *atp6-K90E* strain was a little increased. Proportionate decreases and increases in the rate of ATP synthesis were observed. ATP hydrolysis activity was not changed in the *atp6* mutants, with the exception of the *atp6-K90E* strain, in which it was increased *ca.* 50%. All mutants efficiently energized in the inner mitochondrial membrane and normally synthesized the proteins encoded by the mitochondrial DNA.

As described in the Introduction, it has been hypothesized that mutations of the mtDNA found in tumors have impact on their development or/and malignancy by compromising the energy-transduction activity of the mitochondria. However, so far, the biochemical consequences of these mutations have not been characterized. My results show

that ATP synthase is not drastically affected by the *ATP6* mutations found in tumors. Obtained results does not permit to speculate about the role of these mutations in tumorigenesis.

IV.2 REGULATION OF Atp6p AND Atp9p SYNTHESIS IN RELATION TO THEIR ASSEMBLY IN YEAST ATP SYNTHASE

IV.2.1 Atp6p

In the previously analyzed *atp6*-NARP mutants we have found one, *atp6-L183P*, where synthesis of the Atp6 protein was 3 – 4 times faster than in the wild type. The levels of the transcripts were not changed and Atp6p accumulated less at the steady state levels as compared to the *WT*. This means that Atp6 was proteolytically degraded in the mitochondria because the L183P mutation impaired the assembly of Atp6p into the ATP synthase. I found that Atp6p synthesis was also up-regulated in another *atp6* mutant (*atp6-W136R,R179I*) where the assembly of Atp6p was partially compromised. In *atp6* mutants where the assembly of Atp6p was normal, the synthesis of this protein was not increased.

It was shown previously that Atp6p translation is activated by the catalytic head [$(\alpha\beta)_3$] of the ATP synthase, which is believed to provide a means to avoid formation of free F_O particles, *i.e.* not associated to F_1, which would otherwise result in proton leak through the mitochondrial inner membrane (Rak and Tzagoloff 2009a; Rak, Gokova et al. 2011). This was quite a surprising discovery. Indeed, we know that non-assembled Atp6p is very rapidly degraded. Therefore it seems that Atp6p is subject to double control, at the level of synthesis and post-translationally. My results suggest that Atp6p synthesis is up-regulated when its assembly is compromised. Such an effect has never been observed before. Only mutations in Atp6p that affect the Atp6p assembly have the potential to increases its rate of synthesis. In current models, Atp6p is believed to be the last subunit to be incorporated into the ATP synthase, after the assembly of all the other subunits. Thus, we hypothesize that this Atp6p-less intermediate, rather than the sole F_1 component, activates the synthesis of Atp6p.

To test this hypothesis, I have combined the *atp6-L183P* mutation, which causes elevated Atp6p synthesis, with deletions of genes encoding subunits of the ATP synthase or genes encoding proteins that take part in the ATP synthase biogenesis. Consistently with

previous reports (Rak and Tzagoloff 2009a), the deletions of the *ATP1*, *ATP11* or *ATP12* gene, that prevents formation of F_1, completely inhibited the Atp6 synthesis. In the *fmc1Δ* strains there is also a severe, but not total, lack of F_1 catalytic head, but only at an elevated temperature (35-37°C) (Lefebvre-Legendre, Vaillier et al. 2001). In this mutant, Atp6p and Atp8p are almost normally synthesized (Lefebvre-Legendre, Vaillier et al. 2001). The up-regulation of Atp6p synthesis conferred by the *atp6-L183P* mutation was no longer observed, indicating that F_1 is required for its occurrence. To test the influence of the Atp9p-ring on the synthesis of Atp6p, I deleted two genes, *AEP1* and *AEP2*, that are necessary for *ATP9* expression. Again, the up-regulation of Atp6p was lost, indicating that not only F_1, but also the Atp9p-ring influences the Atp6p synthesis.

I next aimed to know whether two proteins, Atp10p and Atp23p, involved in the Atp6p assembly, which are normally not required for At6p synthesis, participate in the up-regulation of Atp6p synthesis in the *atp6-L183P* mutant. After deletion of the *ATP10* or *ATP23* genes, the *atp6-L183P* mutation no longer increased the rate of the Atp6p synthesis. Atp23p has a double function: it cleaves the leader peptide of Atp6p and assist the folding of Atp6p. With a proteolytically inactive version of Atp23p still able to fold Atp6p, the synthesis of Atp6p was still up-regulated in the *atp6-L183P* mutant, indicating that it is the chaperone function of Atp23p that is important for adjustment of the level of Atp6p synthesis. Finally, I have demonstrated that subunits of the central stalk (Atp15p) and the peripheral stalk (Atp7p) are also required for the up-regulation of the Atp6p synthesis in *atp6-L183P* mutant.

Summing up, these results indicate that Atp6p synthesis is modulated by the assembly intermediate that contains all the ATP synthase subunits and into which Atp6p is incorporated. When this intermediate over-accumulates due to a lack of Atp6p, it stimulates Atp6p synthesis. This can be viewed as a mechanism enabling coupling of Atp6p synthesis to its assembly (Fig. 43).

IV.2.2 Atp9p

In the third part of my work I have studied the regulation of expression of Atp9p. There are three known proteins that are necessary for *ATP9* expression: Aep1p, Aep2p and Atp25p. Normally, the loss of one of these proteins strongly destabilizes the mitochondrial genome. This effect could be overcome with the use of the plasmid encoding nuclear *ATP9-5* gene from *Podospora anserina*, which allowed me to analyze the effects of deletions of

AEP1, *AEP2* and *ATP25* in the strains where *ATP9* gene was present or replaced by the *ARG8m* gene.

Strains *aep1Δ* and *aep2Δ* expressing Atp9-5p could grow on glycerol despite their inability to express the native *ATP9* gene, which is consistent with previous reports indicating that these proteins are only required for synthesis of Atp9p. It has been reported that Atp25p is cleaved into two pieces of almost equal length. The N-terminal part plays a role in the oligomerization of the Atp9p-ring and the C-terminal part is needed for the *ATP9* mRNA stability (Zeng, Barros et al. 2008). Strain *atp25Δ* expressing Atp9-5p was thus expected to be unable to grow on glycerol. It turned out that it could, but very slowly, much more slowly compared to strains *aep1Δ* and *aep2Δ* expressing Atp9-5p. Growth of *atp25Δ* expressing Atp9-5p was substantially improved upon addition of the N-terminal domain of Atp25p but not of its C-terminal domain. It can be inferred that the chaperon function of Atp25p is active on Atp9-5p.

Strains *aep1Δ*, *aep2Δ* and *atp25Δ* with the *atp9::ARG8m* mtDNA were unable to grow on plates lacking arginine, showing that the three proteins are absolutely necessary to express *ARG8m* from the *ATP9 locus*. Interestingly, arginine prototrophy was restored in the *atp25Δ* strain after transformation with a plasmid expressing the C-terminal domain of Atp25p, which is consistent with the role of this domain of Atp25 in the expression of the *ATP9 locus.* Taken together, the results show that Aep1p, Aep2p and Atp25p act only in the synthesis and assembly of atp9p and have no additional functions.

Complementation by the C-terminal and N-terminal domains of Atp25p expressed separately was rather inefficient. I found that this was due to poor accumulation of these polypeptides when expressed separately. It is possible that they are unstable and partially degraded in their way to organelle or inside mitochondrial. Why does a proper expression of Atp25p requires this protein to be synthesized in one block and then cleaved into two fragments is an interesting question.

Interestingly, expression of Atp9-5p in wild type yeast resulted in a dramatic increase of Atp9p synthesis in the mitochondria, whereas synthesis of other proteins encoded by mtDNA remained unchanged. At the steady state, the levels of Atp9p were not increased, meaning that the excess of synthesized Atp9p proteins is degraded. This is an interesting observation indicating that Atp9p is subject to post-translation control like many other

subunits of the mitochondrial energy-transducing system. The results suggest also that Atp9p is subject to control at the level of synthesis.

Although synthesis of Atp6p was not modified in the wild type with Atp9-5p, the steady state levels of this protein were substantially decreased (by >50%). We reasoned that this lack of Atp6p could be what provoked the increased synthesis of Atp9p. Consistent with this hypothesis, Atp9p synthesis was also increased in the *atp6Δ* strain. However, synthesis of Atp9p was further stimulated when the *atp6Δ* strain expressed Atp9-5p, indicating that Atp9-5 protein by itself has the capacity to enhance Atp9p synthesis.

As already mentioned, previous work has shown that Atp6p synthesis is strongly down-regulated when the catalytic head of F_1 cannot form. We aimed to determine whether the up-regulation of Atp9p observed in strains expressing Atp9-5 and/or lacking Atp6p, was also dependent upon F_1. Indeed, in strains lacking F_1, Atp9p synthesis was no longer stimulated. We further observed, that the steady state levels of Atp9p were strongly diminished in strains unable to express F_1. Thus, when F_1 is absent, Atp9p can still be synthesized but is largely degraded.

Taken together, these observations allow us to propose a scenario in which Atp9p controls its own synthesis, as a means to adjust the production of this protein relative to its protein partners within the ATP synthase, F_1 and Atp6p. When F_1 is absent, Atp9p is synthesized but is mostly degraded, because it cannot assemble with F_1. An interesting scenario would be that the Atp9p-ring assembles on F_1. If F_1 is absent, Atp9p remains essentially in a monomeric state and Atp9p monomers are unstable and rapidly degraded. Atp6p, which is believed to be the last subunit to be incorporated into the ATP synthase, is not required for the assembly of the Atp9p ring. However, a 'nude' Atp9-ring, *i.e.* not associated to Atp6p, might be unstable and partially dissociates. This results in the accumulation of incomplete Atp9p-rings that are sensed as a signal that more Atp9p proteins are requested to complete the assembly of the ATP synthase (Fig. 43). When the Atp9-ring interacts with Atp6p, it becomes silenced and ceases to activate Atp9p synthesis. This scenario may provide an explanation for the up-regulation of Atp9p by Atp9-5p. Indeed, Atp9-5 possibly interacts less efficiently with Atp6p, which results in an enhanced degradation of Atp6p. As a consequence, incomplete Atp9p-rings accumulate and stimulate Atp9p synthesis. When there is no F_1, incomplete Atp9p-rings do not accumulate. If the assembly of the ring requires the presence of F_1: Atp9p synthesis is no longer stimulated.

Obviously it is too difficult to imagine that Atp9p, or incomplete Atp9p-rings, can activate Atp9p synthesis directly. This control probably involves proteins (Aep1, Aep2, the C-terminal domain of Atp25p) that are required to synthesize Atp9p, as well as the N-terminal domain of Atp25p that facilitates the assembly of the Atp9p-ring (Fig. 43). In future work, it will be interesting to determine how these proteins interact with each other and with *ATP9* mRNA/Atp9p, to understand how synthesis of Atp9p is coupled to its synthesis.

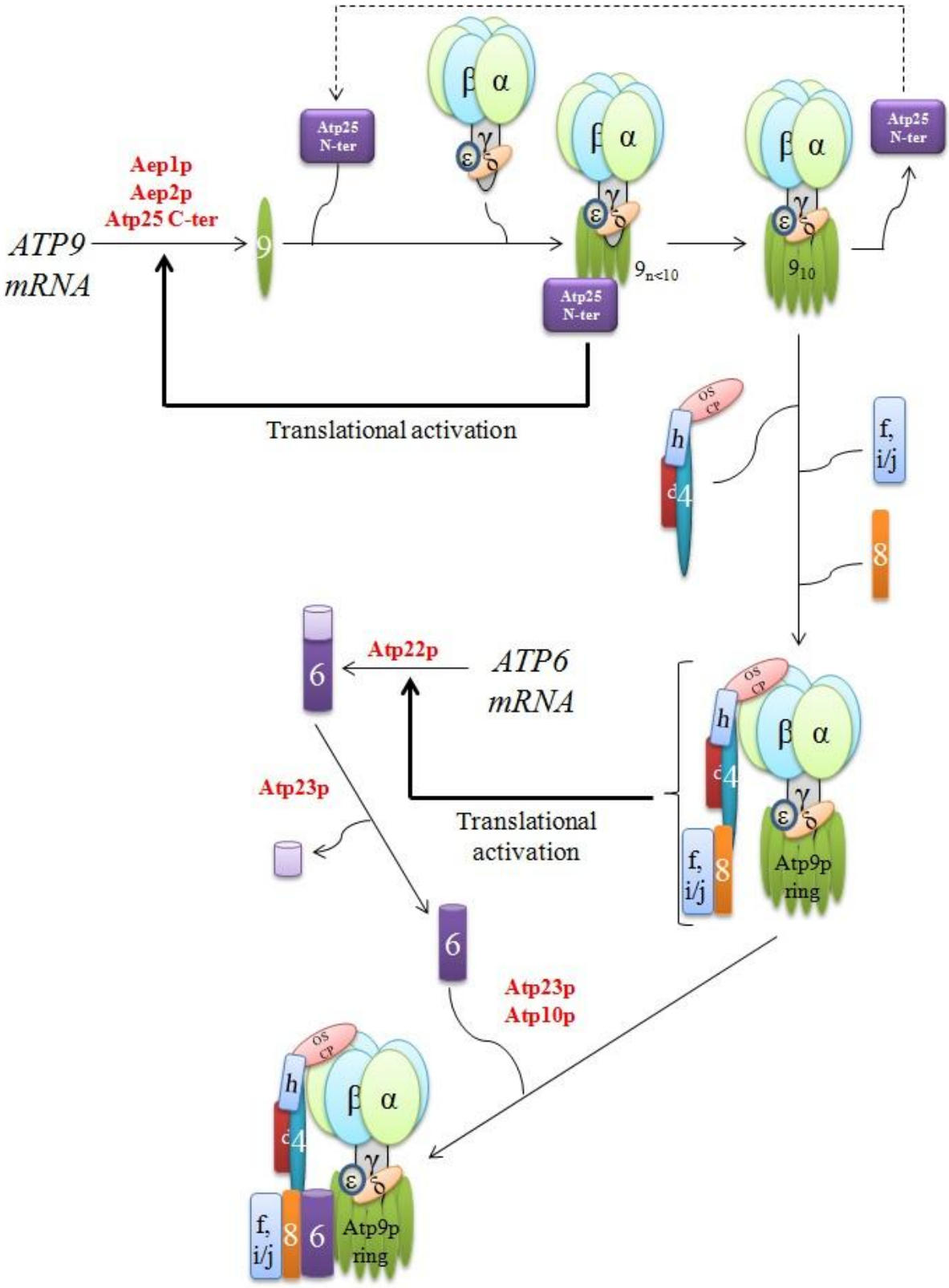

Figure 43 – Model of regulation of Atp6p and Atp9p synthesis in relation to their assembly into yeast ATP synthase. See text for description.

BIBLIOGRAPHY

Abrahams, J. P., A. G. Leslie, et al. (1994). "Structure at 2.8 A resolution of F1-ATPase from bovine heart mitochondria." Nature **370**(6491): 621-628.

Abu-Amero, K. K., A. S. Alzahrani, et al. (2006). "Association of mitochondrial DNA transversion mutations with familial medullary thyroid carcinoma/multiple endocrine neoplasia type 2 syndrome." Oncogene **25**(5): 677-684.

Ackerman, S. H. (2002). "Atp11p and Atp12p are chaperones for F(1)-ATPase biogenesis in mitochondria." Biochim Biophys Acta **1555**(1-3): 101-105.

Ackerman, S. H., D. L. Gatti, et al. (1991). "ATP13, a nuclear gene of Saccharomyces cerevisiae essential for the expression of subunit 9 of the mitochondrial ATPase." FEBS Lett **278**(2): 234-238.

Ackerman, S. H. and A. Tzagoloff (1990a). "Identification of two nuclear genes (ATP11, ATP12) required for assembly of the yeast F1-ATPase." Proc Natl Acad Sci U S A **87**(13): 4986-4990.

Ackerman, S. H. and A. Tzagoloff (1990b). "ATP10, a yeast nuclear gene required for the assembly of the mitochondrial F1-F0 complex." J Biol Chem **265**(17): 9952-9959.

Ackerman, S. H. and A. Tzagoloff (2005). "Function, structure, and biogenesis of mitochondrial ATP synthase." Prog Nucleic Acid Res Mol Biol **80**: 95-133.

Anderson, S., A. T. Bankier, et al. (1981). "Sequence and organization of the human mitochondrial genome." Nature **290**(5806): 457-465.

Atay, Z., A. Bereket, et al. (2013). "A novel homozygous TMEM70 mutation results in congenital cataract and neonatal mitochondrial encephalo-cardiomyopathy." Gene **515**(1): 197-199.

Baracca, A., S. Barogi, et al. (2000). "Catalytic activities of mitochondrial ATP synthase in patients with mitochondrial DNA T8993G mutation in the ATPase 6 gene encoding subunit a." J Biol Chem **275**(6): 4177-4182.

Baracca, A., G. Sgarbi, et al. (2007). "Biochemical phenotypes associated with the mitochondrial ATP6 gene mutations at nt8993." Biochim Biophys Acta **1767**(7): 913-919.

Barrientos, A., D. Korr, et al. (2002). "Shy1p is necessary for full expression of mitochondrial COX1 in the yeast model of Leigh's syndrome." EMBO J **21**(1-2): 43-52.

Becker, T., L. Bottinger, et al. (2012). "Mitochondrial protein import: from transport pathways to an integrated network." Trends Biochem Sci **37**(3): 85-91.

Beilharz, M. W., G. S. Cobon, et al. (1982). "Physiological alteration of the pattern of transcription of the oli2 region of yeast mitochondrial DNA." FEBS Lett **147**(2): 235-238.

Berger, K. H. and M. P. Yaffe (2000). "Mitochondrial DNA inheritance in Saccharomyces cerevisiae." Trends Microbiol **8**(11): 508-513.

Bietenhader, M., A. Martos, et al. (2012). "Experimental relocation of the mitochondrial ATP9 gene to the nucleus reveals forces underlying mitochondrial genome evolution." PLoS Genet **8**(8): e1002876.

Bonnefoy, N., N. Bsat, et al. (2001a). "Mitochondrial translation of Saccharomyces cerevisiae COX2 mRNA is controlled by the nucleotide sequence specifying the pre-Cox2p leader peptide." Mol Cell Biol **21**(7): 2359-2372.

Bonnefoy, N. and T. D. Fox (2001b). "Genetic transformation of Saccharomyces cerevisiae mitochondria." Methods Cell Biol **65**: 381-396.

Boyer, P. D. (1993). "The binding change mechanism for ATP synthase--some probabilities and possibilities." Biochim Biophys Acta **1140**(3): 215-250.

Braig, K., R. I. Menz, et al. (2000). "Structure of bovine mitochondrial F(1)-ATPase inhibited by Mg(2+) ADP and aluminium fluoride." Structure **8**(6): 567-573.

Brandon, M., P. Baldi, et al. (2006). "Mitochondrial mutations in cancer." Oncogene **25**(34): 4647-4662.

Cai, W., Q. Fu, et al. (2008). "Mitochondrial variants may influence the phenotypic manifestation of Leber's hereditary optic neuropathy-associated ND4 G11778A mutation." J Genet Genomics **35**(11): 649-655.

Cameron, J. M., V. Levandovskiy, et al. (2011). "Complex V TMEM70 deficiency results in mitochondrial nucleoid disorganization." Mitochondrion **11**(1): 191-199.

Camougrand, N., P. Pelissier, et al. (1995). "NCA2, a second nuclear gene required for the control of mitochondrial synthesis of subunits 6 and 8 of ATP synthase in Saccharomyces cerevisiae." J Mol Biol **247**(4): 588-596.

Carrozzo, R., J. Murray, et al. (2000). "The T9176G mutation of human mtDNA gives a fully assembled but inactive ATP synthase when modeled in Escherichia coli." FEBS Lett **486**(3): 297-299.

Carrozzo, R., T. Rizza, et al. (2004). "A mitochondrial ATPase 6 mutation is associated with Leigh syndrome in a family and affects proton flow and adenosine triphosphate output when modeled in Escherichia coli." Acta Paediatr Suppl **93**(445): 65-67.

Cavalli, L. R., M. Varella-Garcia, et al. (1997). "Diminished tumorigenic phenotype after depletion of mitochondrial DNA." Cell Growth Differ **8**(11): 1189-1198.

Chen, Y., R. Cairns, et al. (2009). "Oxygen consumption can regulate the growth of tumors, a new perspective on the Warburg effect." PLoS One **4**(9): e7033.

Chinnery, P. F., D. R. Thorburn, et al. (2000). "The inheritance of mitochondrial DNA heteroplasmy: random drift, selection or both?" Trends Genet **16**(11): 500-505.

Christianson, T. and M. Rabinowitz (1983). "Identification of multiple transcriptional initiation sites on the yeast mitochondrial genome by in vitro capping with guanylyltransferase." J Biol Chem **258**(22): 14025-14033.

Cizkova, A., V. Stranecky, et al. (2008). "TMEM70 mutations cause isolated ATP synthase deficiency and neonatal mitochondrial encephalocardiomyopathy." Nat Genet **40**(11): 1288-1290.

Collins, T. J., M. J. Berridge, et al. (2002). "Mitochondria are morphologically and functionally heterogeneous within cells." EMBO J **21**(7): 1616-1627.

Conde, J. and G. R. Fink (1976). "A mutant of Saccharomyces cerevisiae defective for nuclear fusion." Proc Natl Acad Sci U S A **73**(10): 3651-3655.

Contamine, V. and M. Picard (2000). "Maintenance and integrity of the mitochondrial genome: a plethora of nuclear genes in the budding yeast." Microbiol Mol Biol Rev **64**(2): 281-315.

Copeland, W. C., J. T. Wachsman, et al. (2002). "Mitochondrial DNA alterations in cancer." Cancer Invest **20**(4): 557-569.

Cortes-Hernandez, P., M. E. Vazquez-Memije, et al. (2007). "ATP6 homoplasmic mutations inhibit and destabilize the human F1F0-ATP synthase without preventing enzyme assembly and oligomerization." J Biol Chem **282**(2): 1051-1058.

Costa-Guda, J., T. Tokura, et al. (2007). "Mitochondrial DNA mutations in oxyphilic and chief cell parathyroid adenomas." BMC Endocr Disord **7**: 8.

Couplan, E., R. S. Aiyar, et al. (2011). "A yeast-based assay identifies drugs active against human mitochondrial disorders." Proc Natl Acad Sci U S A **108**(29): 11989-11994.

De Meirleir, L., S. Seneca, et al. (2004). "Respiratory chain complex V deficiency due to a mutation in the assembly gene ATP12." J Med Genet **41**(2): 120-124.

De Meirleir, L., S. Seneca, et al. (1995). "Bilateral striatal necrosis with a novel point mutation in the mitochondrial ATPase 6 gene." Pediatr Neurol **13**(3): 242-246.

de Zamaroczy, M. and G. Bernardi (1986). "The primary structure of the mitochondrial genome of Saccharomyces cerevisiae--a review." Gene **47**(2-3): 155-177.

DiMauro, S., M. Hirano, et al. (2006). "Approaches to the treatment of mitochondrial diseases." Muscle Nerve **34**(3): 265-283.

Dionisi-Vici, C., S. Seneca, et al. (1998). "Fulminant Leigh syndrome and sudden unexpected death in a family with the T9176C mutation of the mitochondrial ATPase 6 gene." J Inherit Metab Dis **21**(1): 2-8.

Ellis, T. P., K. G. Helfenbein, et al. (2004). "Aep3p stabilizes the mitochondrial bicistronic mRNA encoding subunits 6 and 8 of the H+-translocating ATP synthase of Saccharomyces cerevisiae." J Biol Chem **279**(16): 15728-15733.

Ellis, T. P., H. B. Lukins, et al. (1999). "Suppression of a nuclear aep2 mutation in Saccharomyces cerevisiae by a base substitution in the 5'-untranslated region of the mitochondrial oli1 gene encoding subunit 9 of ATP synthase." Genetics **151**(4): 1353-1363.

Emaus, R. K., R. Grunwald, et al. (1986). "Rhodamine 123 as a probe of transmembrane potential in isolated rat-liver mitochondria: spectral and metabolic properties." Biochim Biophys Acta **850**(3): 436-448.

Ernster, L. and G. Schatz (1981). "Mitochondria: a historical review." J Cell Biol **91**(3 Pt 2): 227s-255s.

Fagarasanu, A. and R. A. Rachubinski (2007). "Orchestrating organelle inheritance in Saccharomyces cerevisiae." Curr Opin Microbiol **10**(6): 528-538.

Fillingame, R. H., C. M. Angevine, et al. (2002). "Coupling proton movements to c-ring rotation in F(1)F(o) ATP synthase: aqueous access channels and helix rotations at the a-c interface." Biochim Biophys Acta **1555**(1-3): 29-36.

Finnegan, P. M., T. P. Ellis, et al. (1995). "The mature AEP2 gene product of Saccharomyces cerevisiae, required for the expression of subunit 9 of ATP synthase, is a 58 kDa mitochondrial protein." FEBS Lett **368**(3): 505-508.

Finnegan, P. M., M. J. Payne, et al. (1991). "Characterization of a yeast nuclear gene, AEP2, required for accumulation of mitochondrial mRNA encoding subunit 9 of the ATP synthase." Curr Genet **20**(1-2): 53-61.

Foury, F., T. Roganti, et al. (1998). "The complete sequence of the mitochondrial genome of Saccharomyces cerevisiae." FEBS Lett **440**(3): 325-331.

Foury, F. and A. Tzagoloff (1976). "Localization on mitochondrial DNA of mutations leading to a loss of rutamycin-sensitive adenosine triphosphatase." Eur J Biochem **68**(1): 113-119.

Fritz, S., D. Rapaport, et al. (2001). "Connection of the mitochondrial outer and inner membranes by Fzo1 is critical for organellar fusion." J Cell Biol **152**(4): 683-692.

Galluzzi, L., O. Kepp, et al. (2012). "Mitochondrial control of cellular life, stress, and death." Circ Res **111**(9): 1198-1207.

Galluzzi, L., E. Morselli, et al. (2010). "Mitochondrial gateways to cancer." Mol Aspects Med **31**(1): 1-20.

Gao, Y. Q., W. Yang, et al. (2005). "A structure-based model for the synthesis and hydrolysis of ATP by F1-ATPase." Cell **123**(2): 195-205.

Gaude, E. and C. Frezza (2014). "Defects in mitochondrial metabolism and cancer." Cancer Metab **2**: 10.

Gietz, R. D. and R. H. Schiestl (2007). "Quick and easy yeast transformation using the LiAc/SS carrier DNA/PEG method." Nat Protoc **2**(1): 35-37.

Giraud, M. F. and J. Velours (1997). "The absence of the mitochondrial ATP synthase delta subunit promotes a slow growth phenotype of rho- yeast cells by a lack of assembly of the catalytic sector F1." Eur J Biochem **245**(3): 813-818.

Grandier-Vazeille, X. and M. Guerin (1996). "Separation by blue native and colorless native polyacrylamide gel electrophoresis of the oxidative phosphorylation complexes of yeast mitochondria solubilized by different detergents: specific staining of the different complexes." Anal Biochem **242**(2): 248-254.

Gray, M. W. (2012). "Mitochondrial evolution." Cold Spring Harb Perspect Biol **4**(9): a011403.

Groudinsky, O., I. Bousquet, et al. (1993). "The NAM1/MTF2 nuclear gene product is selectively required for the stability and/or processing of mitochondrial transcripts of the atp6 and of the mosaic, cox1 and cytb genes in Saccharomyces cerevisiae." Mol Gen Genet **240**(3): 419-427.

Guerin, B., P. Labbe, et al. (1979). "Preparation of yeast mitochondria (Saccharomyces cerevisiae) with good P/O and respiratory control ratios." Methods Enzymol **55**: 149-159.

Hadikusumo, R. G., S. Meltzer, et al. (1988). "The definition of mitochondrial H+ ATPase assembly defects in mit- mutants of Saccharomyces cerevisiae with a monoclonal antibody to the enzyme complex as an assembly probe." Biochim Biophys Acta **933**(1): 212-222.

Harbauer, A. B., R. P. Zahedi, et al. (2014). "The protein import machinery of mitochondria-a regulatory hub in metabolism, stress, and disease." Cell Metab **19**(3): 357-372.

Helfenbein, K. G., T. P. Ellis, et al. (2003). "ATP22, a nuclear gene required for expression of the F0 sector of mitochondrial ATPase in Saccharomyces cerevisiae." J Biol Chem **278**(22): 19751-19756.

Houstek, J., S. Kmoch, et al. (2009). "TMEM70 protein - a novel ancillary factor of mammalian ATP synthase." Biochim Biophys Acta **1787**(5): 529-532.

Houstek, J., A. Pickova, et al. (2006). "Mitochondrial diseases and genetic defects of ATP synthase." Biochim Biophys Acta **1757**(9-10): 1400-1405.

Ishikawa, K., K. Takenaga, et al. (2008). "ROS-generating mitochondrial DNA mutations can regulate tumor cell metastasis." Science **320**(5876): 661-664.

Jesina, P., M. Tesarova, et al. (2004). "Diminished synthesis of subunit a (ATP6) and altered function of ATP synthase and cytochrome c oxidase due to the mtDNA 2 bp microdeletion of TA at positions 9205 and 9206." Biochem J **383**(Pt. 3): 561-571.

Jia, L., M. K. Dienhart, et al. (2007). "Oxa1 directly interacts with Atp9 and mediates its assembly into the mitochondrial F1Fo-ATP synthase complex." Mol Biol Cell **18**(5): 1897-1908.

John, A. P. (2001). "Dysfunctional mitochondria, not oxygen insufficiency, cause cancer cells to produce inordinate amounts of lactic acid: the impact of this on the treatment of cancer." Med Hypotheses **57**(4): 429-431.

John, U. P. and P. Nagley (1986). "Amino acid substitutions in mitochondrial ATPase subunit 6 of Saccharomyces cerevisiae leading to oligomycin resistance." FEBS Lett **207**(1): 79-83.

Jonckheere, A. I., M. Hogeveen, et al. (2008). "A novel mitochondrial ATP8 gene mutation in a patient with apical hypertrophic cardiomyopathy and neuropathy." J Med Genet **45**(3): 129-133.

Jonckheere, A. I., M. Huigsloot, et al. (2011). "Restoration of complex V deficiency caused by a novel deletion in the human TMEM70 gene normalizes mitochondrial morphology." Mitochondrion **11**(6): 954-963.

Jonckheere, A. I., G. H. Renkema, et al. (2013). "A complex V ATP5A1 defect causes fatal neonatal mitochondrial encephalopathy." Brain **136**(Pt 5): 1544-1554.

Jonckheere, A. I., J. A. Smeitink, et al. (2012). "Mitochondrial ATP synthase: architecture, function and pathology." J Inherit Metab Dis **35**(2): 211-225.

Junge, W., H. Lill, et al. (1997). "ATP synthase: an electrochemical transducer with rotatory mechanics." Trends Biochem Sci **22**(11): 420-423.

Kabala, A. M., J. P. Lasserre, et al. (2014). "Defining the impact on yeast ATP synthase of two pathogenic human mitochondrial DNA mutations, T9185C and T9191C." Biochimie **100**: 200-206.

King, M. P. and G. Attardi (1989). "Human cells lacking mtDNA: repopulation with exogenous mitochondria by complementation." Science **246**(4929): 500-503.

Koonin, E. V. (2010). "The origin and early evolution of eukaryotes in the light of phylogenomics." Genome Biol **11**(5): 209.

Kratochvilova, H., K. Hejzlarova, et al. (2014). "Mitochondrial membrane assembly of TMEM70 protein." Mitochondrion **15**: 1-9.

Kucharczyk, R., N. Ezkurdia, et al. (2010). "Consequences of the pathogenic T9176C mutation of human mitochondrial DNA on yeast mitochondrial ATP synthase." Biochim Biophys Acta **1797**(6-7): 1105-1112.

Kucharczyk, R., M. F. Giraud, et al. (2013). "Defining the pathogenesis of human mtDNA mutations using a yeast model: the case of T8851C." Int J Biochem Cell Biol **45**(1): 130-140.

Kucharczyk, R., M. Rak, et al. (2009a). "Biochemical consequences in yeast of the human mitochondrial DNA 8993T>C mutation in the ATPase6 gene found in NARP/MILS patients." Biochim Biophys Acta **1793**(5): 817-824.

Kucharczyk, R., B. Salin, et al. (2009b). "Introducing the human Leigh syndrome mutation T9176G into Saccharomyces cerevisiae mitochondrial DNA leads to severe defects in the incorporation of Atp6p into the ATP synthase and in the mitochondrial morphology." Hum Mol Genet **18**(15): 2889-2898.

Kucharczyk, R., M. Zick, et al. (2009c). "Mitochondrial ATP synthase disorders: molecular mechanisms and the quest for curative therapeutic approaches." Biochim Biophys Acta **1793**(1): 186-199.

Kun, E., E. Kirsten, et al. (1979). "Stabilization of mitochondrial functions with digitonin." Methods Enzymol **55**: 115-118.

Kunkele, K. P., S. Heins, et al. (1998). "The preprotein translocation channel of the outer membrane of mitochondria." Cell **93**(6): 1009-1019.

Laemmli, U. K. (1970). "Cleavage of structural proteins during the assembly of the head of bacteriophage T4." Nature **227**(5259): 680-685.

Lee, C., A. S. Tibbetts, et al. (2009). "Yeast AEP3p is an accessory factor in initiation of mitochondrial translation." J Biol Chem **284**(49): 34116-34125.

Lefebvre-Legendre, L., A. Balguerie, et al. (2003). "F1-catalysed ATP hydrolysis is required for mitochondrial biogenesis in Saccharomyces cerevisiae growing under conditions where it cannot respire." Mol Microbiol **47**(5): 1329-1339.

Lefebvre-Legendre, L., J. Vaillier, et al. (2001). "Identification of a nuclear gene (FMC1) required for the assembly/stability of yeast mitochondrial F(1)-ATPase in heat stress conditions." J Biol Chem **276**(9): 6789-6796.

Logan, D. C. (2006). "The mitochondrial compartment." J Exp Bot **57**(6): 1225-1243.

Lowry, O. H., N. J. Rosebrough, et al. (1951). "Protein measurement with the Folin phenol reagent." J Biol Chem **193**(1): 265-275.

Lu, J., L. K. Sharma, et al. (2009). "Implications of mitochondrial DNA mutations and mitochondrial dysfunction in tumorigenesis." Cell Res **19**(7): 802-815.

Ludlam, A., J. Brunzelle, et al. (2009). "Chaperones of F1-ATPase." J Biol Chem **284**(25): 17138-17146.

Lytovchenko, O., N. Naumenko, et al. (2014). "The INA complex facilitates assembly of the peripheral stalk of the mitochondrial F1Fo-ATP synthase." EMBO J **33**(15): 1624-1638.

Macino, G. and A. Tzagoloff (1980). "Assembly of the mitochondrial membrane system: sequence analysis of a yeast mitochondrial ATPase gene containing the oli-2 and oli-4 loci." Cell **20**(2): 507-517.

Mattiazzi, M., C. Vijayvergiya, et al. (2004). "The mtDNA T8993G (NARP) mutation results in an impairment of oxidative phosphorylation that can be improved by antioxidants." Hum Mol Genet **13**(8): 869-879.

Maximo, V., P. Soares, et al. (2002). "Mitochondrial DNA somatic mutations (point mutations and large deletions) and mitochondrial DNA variants in human thyroid pathology: a study with emphasis on Hurthle cell tumors." Am J Pathol **160**(5): 1857-1865.

Mayr, J. A., V. Havlickova, et al. (2010). "Mitochondrial ATP synthase deficiency due to a mutation in the ATP5E gene for the F1 epsilon subunit." Hum Mol Genet **19**(17): 3430-3439.

Menz, R. I., J. E. Walker, et al. (2001). "Structure of bovine mitochondrial F(1)-ATPase with nucleotide bound to all three catalytic sites: implications for the mechanism of rotary catalysis." Cell **106**(3): 331-341.

Michon, T., M. Galante, et al. (1988). "NH2-terminal sequence of the isolated yeast ATP synthase subunit 6 reveals post-translational cleavage." Eur J Biochem **172**(3): 621-625.

Mitchell, P. (1961). "Coupling of phosphorylation to electron and hydrogen transfer by a chemi-osmotic type of mechanism." Nature **191**: 144-148.

Mitchell, P. (1967a). "Proton current flow in mitochondrial systems." Nature **214**(5095): 1327-1328.

Mitchell, P. and J. Moyle (1967b). "Chemiosmotic hypothesis of oxidative phosphorylation." Nature **213**(5072): 137-139.

Mkaouar-Rebai, E., F. Kammoun, et al. (2010). "A de novo mutation in the adenosine triphosphatase (ATPase) 8 gene in a patient with mitochondrial disorder." J Child Neurol **25**(6): 770-775.

Morais, R., K. Zinkewich-Peotti, et al. (1994). "Tumor-forming ability in athymic nude mice of human cell lines devoid of mitochondrial DNA." Cancer Res **54**(14): 3889-3896.

Morava, E., R. J. Rodenburg, et al. (2006). "Clinical and biochemical characteristics in patients with a high mutant load of the mitochondrial T8993G/C mutations." Am J Med Genet A **140**(8): 863-868.

Moslemi, A. R., N. Darin, et al. (2005). "Two new mutations in the MTATP6 gene associated with Leigh syndrome." Neuropediatrics **36**(5): 314-318.

Mukhopadhyay, A., M. Uh, et al. (1994). "Level of ATP synthase activity required for yeast Saccharomyces cerevisiae to grow on glycerol media." FEBS Lett **343**(2): 160-164.

Nakagawa, K., N. Morishima, et al. (1991). "A maturase-like subunit of the sequence-specific endonuclease endo.SceI from yeast mitochondria." J Biol Chem **266**(3): 1977-1984.

Nicholls, D. G. and S. Chalmers (2004). "The integration of mitochondrial calcium transport and storage." J Bioenerg Biomembr **36**(4): 277-281.

Okamoto, K., P. S. Perlman, et al. (1998). "The sorting of mitochondrial DNA and mitochondrial proteins in zygotes: preferential transmission of mitochondrial DNA to the medial bud." J Cell Biol **142**(3): 613-623.

Okamoto, K. and J. M. Shaw (2005). "Mitochondrial morphology and dynamics in yeast and multicellular eukaryotes." Annu Rev Genet **39**: 503-536.

Osman, C., C. Wilmes, et al. (2007). "Prohibitins interact genetically with Atp23, a novel processing peptidase and chaperone for the F1Fo-ATP synthase." Mol Biol Cell **18**(2): 627-635.

Park, J. S., L. K. Sharma, et al. (2009). "A heteroplasmic, not homoplasmic, mitochondrial DNA mutation promotes tumorigenesis via alteration in reactive oxygen species generation and apoptosis." Hum Mol Genet **18**(9): 1578-1589.

Partikian, A., B. Olveczky, et al. (1998). "Rapid diffusion of green fluorescent protein in the mitochondrial matrix." J Cell Biol **140**(4): 821-829.

Paul, M. F., S. Ackerman, et al. (1994). "Cloning of the yeast ATP3 gene coding for the gamma-subunit of F1 and characterization of atp3 mutants." J Biol Chem **269**(42): 26158-26164.

Paul, M. F., A. Barrientos, et al. (2000). "A single amino acid change in subunit 6 of the yeast mitochondrial ATPase suppresses a null mutation in ATP10." J Biol Chem **275**(38): 29238-29243.

Payne, M. J., P. M. Finnegan, et al. (1993). "Characterization of a second nuclear gene, AEP1, required for expression of the mitochondrial OLI1 gene in Saccharomyces cerevisiae." Curr Genet **24**(1-2): 126-135.

Payne, M. J., E. Schweizer, et al. (1991). "Properties of two nuclear pet mutants affecting expression of the mitochondrial oli1 gene of Saccharomyces cerevisiae." Curr Genet **19**(5): 343-351.

Pelissier, P., N. Camougrand, et al. (1995). "NCA3, a nuclear gene involved in the mitochondrial expression of subunits 6 and 8 of the Fo-F1 ATP synthase of S. cerevisiae." Curr Genet **27**(5): 409-416.

Pelissier, P. P., N. M. Camougrand, et al. (1992). "Regulation by nuclear genes of the mitochondrial synthesis of subunits 6 and 8 of the ATP synthase of Saccharomyces cerevisiae." J Biol Chem **267**(4): 2467-2473.

Petros, J. A., A. K. Baumann, et al. (2005). "mtDNA mutations increase tumorigenicity in prostate cancer." Proc Natl Acad Sci U S A **102**(3): 719-724.

Pozzan, T., P. Magalhaes, et al. (2000). "The comeback of mitochondria to calcium signalling." Cell Calcium **28**(5-6): 279-283.

Rak, M., S. Gokova, et al. (2011). "Modular assembly of yeast mitochondrial ATP synthase." EMBO J **30**(5): 920-930.

Rak, M., E. Tetaud, et al. (2007a). "A yeast model of the neurogenic ataxia retinitis pigmentosa (NARP) T8993G mutation in the mitochondrial ATP synthase-6 gene." J Biol Chem **282**(47): 34039-34047.

Rak, M., E. Tetaud, et al. (2007b). "Yeast cells lacking the mitochondrial gene encoding the ATP synthase subunit 6 exhibit a selective loss of complex IV and unusual mitochondrial morphology." J Biol Chem **282**(15): 10853-10864.

Rak, M. and A. Tzagoloff (2009a). "F1-dependent translation of mitochondrially encoded Atp6p and Atp8p subunits of yeast ATP synthase." Proc Natl Acad Sci U S A **106**(44): 18509-18514.

Rak, M., X. Zeng, et al. (2009b). "Assembly of F0 in Saccharomyces cerevisiae." Biochim Biophys Acta **1793**(1): 108-116.

Ramanathan, A., C. Wang, et al. (2005). "Perturbational profiling of a cell-line model of tumorigenesis by using metabolic measurements." Proc Natl Acad Sci U S A **102**(17): 5992-5997.

Reichert, A. S. and W. Neupert (2004). "Mitochondriomics or what makes us breathe." Trends Genet **20**(11): 555-562.

Rigoulet, M., A. Mourier, et al. (2010). "Electron competition process in respiratory chain: regulatory mechanisms and physiological functions." Biochim Biophys Acta **1797**(6-7): 671-677.

Robinson, G. C., J. V. Bason, et al. (2013). "The structure of F(1)-ATPase from Saccharomyces cerevisiae inhibited by its regulatory protein IF(1)." Open Biol **3**(2): 120164.

Rodeheffer, M. S., B. E. Boone, et al. (2001). "Nam1p, a protein involved in RNA processing and translation, is coupled to transcription through an interaction with yeast mitochondrial RNA polymerase." J Biol Chem **276**(11): 8616-8622.

Schagger, H. and G. von Jagow (1987). "Tricine-sodium dodecyl sulfate-polyacrylamide gel electrophoresis for the separation of proteins in the range from 1 to 100 kDa." Anal Biochem **166**(2): 368-379.

Schagger, H. and G. von Jagow (1991). "Blue native electrophoresis for isolation of membrane protein complexes in enzymatically active form." Anal Biochem **199**(2): 223-231.

Scheffler, I. E. (2008). Mitochondria, 2nd ed, Hoboken, NJ USA: John Wiley & Sons.

Schwerzmann, K. and P. L. Pedersen (1986). "Regulation of the mitochondrial ATP synthase/ATPase complex." Arch Biochem Biophys **250**(1): 1-18.

Seneca, S., M. Abramowicz, et al. (1996). "A mitochondrial DNA microdeletion in a newborn girl with transient lactic acidosis." J Inherit Metab Dis **19**(2): 115-118.

Shchelochkov, O. A., F. Y. Li, et al. (2010). "Milder clinical course of Type IV 3-methylglutaconic aciduria due to a novel mutation in TMEM70." Mol Genet Metab **101**(2-3): 282-285.

Shidara, Y., K. Yamagata, et al. (2005). "Positive contribution of pathogenic mutations in the mitochondrial genome to the promotion of cancer by prevention from apoptosis." Cancer Res **65**(5): 1655-1663.

Simon, M. and G. Faye (1984). "Organization and processing of the mitochondrial oxi3/oli2 multigenic transcript in yeast." Mol Gen Genet **196**(2): 266-274.

Somlo, M. (1968). "Induction and repression of mitochondrial ATPase in yeast." Eur J Biochem **5**(2): 276-284.

Soto, I. C., F. Fontanesi, et al. (2009). "Synthesis of cytochrome c oxidase subunit 1 is translationally downregulated in the absence of functional F1F0-ATP synthase." Biochim Biophys Acta **1793**(11): 1776-1786.

Spiegel, R., M. Khayat, et al. (2011). "TMEM70 mutations are a common cause of nuclear encoded ATP synthase assembly defect: further delineation of a new syndrome." J Med Genet **48**(3): 177-182.

Steele, D. F., C. A. Butler, et al. (1996). "Expression of a recoded nuclear gene inserted into yeast mitochondrial DNA is limited by mRNA-specific translational activation." Proc Natl Acad Sci U S A **93**(11): 5253-5257.

Stock, D., C. Gibbons, et al. (2000). "The rotary mechanism of ATP synthase." Curr Opin Struct Biol **10**(6): 672-679.

Stock, D., A. G. Leslie, et al. (1999). "Molecular architecture of the rotary motor in ATP synthase." Science **286**(5445): 1700-1705.

Swalwell, H., E. L. Blakely, et al. (2008). "A homoplasmic mtDNA variant can influence the phenotype of the pathogenic m.7472Cins MTTS1 mutation: are two mutations better than one?" Eur J Hum Genet **16**(10): 1265-1274.

Tan, D. J., R. K. Bai, et al. (2002). "Comprehensive scanning of somatic mitochondrial DNA mutations in breast cancer." Cancer Res **62**(4): 972-976.

Tautz, D. and M. Renz (1983). "An optimized freeze-squeeze method for the recovery of DNA fragments from agarose gels." Anal Biochem **132**(1): 14-19.

Tibbetts, A. S., Y. Sun, et al. (2002). "Yeast mitochondrial oxodicarboxylate transporters are important for growth on oleic acid." Arch Biochem Biophys **406**(1): 96-104.

Torraco, A., D. Verrigni, et al. (2012). "TMEM70: a mutational hot spot in nuclear ATP synthase deficiency with a pivotal role in complex V biogenesis." Neurogenetics **13**(4): 375-386.

Tort, F., M. Del Toro, et al. (2011). "Screening for nuclear genetic defects in the ATP synthase-associated genes TMEM70, ATP12 and ATP5E in patients with 3-methylglutaconic aciduria." Clin Genet **80**(3): 297-300.

Tzagoloff, A., A. Barrientos, et al. (2004). "Atp10p assists assembly of Atp6p into the F0 unit of the yeast mitochondrial ATPase." J Biol Chem **279**(19): 19775-19780.

Walker, J. E. (2013). "The ATP synthase: the understood, the uncertain and the unknown." Biochem Soc Trans **41**(1): 1-16.

Walker, J. E. and V. K. Dickson (2006). "The peripheral stalk of the mitochondrial ATP synthase." Biochim Biophys Acta **1757**(5-6): 286-296.

Wallace, D. C. (2012). "Mitochondria and cancer." Nat Rev Cancer **12**(10): 685-698.

Wallis, M. G., O. Groudinsky, et al. (1994). "The NAM1 protein (NAM1p), which is selectively required for cox1, cytb and atp6 transcript processing/stabilisation, is located in the yeast mitochondrial matrix." Eur J Biochem **222**(1): 27-32.

Wang, Z. G. and S. H. Ackerman (2000a). "The assembly factor Atp11p binds to the beta-subunit of the mitochondrial F(1)-ATPase." J Biol Chem **275**(8): 5767-5772.

Wang, Z. G., D. Sheluho, et al. (2000b). "The alpha-subunit of the mitochondrial F(1) ATPase interacts directly with the assembly factor Atp12p." EMBO J **19**(7): 1486-1493.

Warburg, O. (1956a). "On respiratory impairment in cancer cells." Science **124**(3215): 269-270.

Warburg, O. (1956b). "On the origin of cancer cells." Science **123**(3191): 309-314.

Ware, S. M., N. El-Hassan, et al. (2009). "Infantile cardiomyopathy caused by a mutation in the overlapping region of mitochondrial ATPase 6 and 8 genes." J Med Genet **46**(5): 308-314.

Westermann, B. (2010). "Mitochondrial dynamics in model organisms: what yeasts, worms and flies have taught us about fusion and fission of mitochondria." Semin Cell Dev Biol **21**(6): 542-549.

Westermann, B. and W. Neupert (2000). "Mitochondria-targeted green fluorescent proteins: convenient tools for the study of organelle biogenesis in Saccharomyces cerevisiae." Yeast **16**(15): 1421-1427.

Zassenhaus, H. P., N. C. Martin, et al. (1984). "Origins of transcripts of the yeast mitochondrial var 1 gene." J Biol Chem **259**(9): 6019-6027.

Zeng, X., M. H. Barros, et al. (2008). "ATP25, a new nuclear gene of Saccharomyces cerevisiae required for expression and assembly of the Atp9p subunit of mitochondrial ATPase." Mol Biol Cell **19**(4): 1366-1377.

Zeng, X., A. Hourset, et al. (2007a). "The Saccharomyces cerevisiae ATP22 gene codes for the mitochondrial ATPase subunit 6-specific translation factor." Genetics **175**(1): 55-63.

Zeng, X., R. Kucharczyk, et al. (2007b). "The leader peptide of yeast Atp6p is required for efficient interaction with the Atp9p ring of the mitochondrial ATPase." J Biol Chem **282**(50): 36167-36176.

Zeng, X., W. Neupert, et al. (2007c). "The metalloprotease encoded by ATP23 has a dual function in processing and assembly of subunit 6 of mitochondrial ATPase." Mol Biol Cell **18**(2): 617-626.

Zeviani, M. and S. Di Donato (2004). "Mitochondrial disorders." Brain **127**(Pt 10): 2153-2172.

Zhao, J., U. Lendahl, et al. (2013). "Regulation of mitochondrial dynamics: convergences and divergences between yeast and vertebrates." Cell Mol Life Sci **70**(6): 951-976.

Ziaja, K., G. Michaelis, et al. (1993). "Nuclear control of the messenger RNA expression for mitochondrial ATPase subunit 9 in a new yeast mutant." J Mol Biol **229**(4): 909-916.

Biogenèse de l'ATP synthase mitochondriale et des dysfonctions générant des maladies

L'ATP synthase mitochondriale est une enzyme ancrée dans la membrane interne de la mitochondrie. Sa structure d'enzyme est conservée entre différentes espèces, c'est un complexe multi-protéique.

Chez la levure *Saccharomyces cerevisiae,* trois sous-unités sont codées dans le génome mitochondrial (deux chez les vertébrés). Les autres sous-unités et les protéines nécessaires à l'assemblage de l'ATP synthase, sont codées dans le génome nucléaire.

L'ATP synthase contient deux domaines :

- le domaine hydrophobe F_O qui est composé du canal à protons et du pied périphérique,
- le domaine hydrophile F_1, qui est composé du centre catalytique et de la tige centrale.

L'ATP synthase mitochondriale produit la majorité de l'énergie cellulaire chez les eucaryotes aérobes sous forme d'ATP par le processus d'oxydation phosphorylante.

La biogenèse d'enzyme est un processus compliqué car il demande la coordination d'expression des gènes à partir de deux génomes. Aujourd'hui, le modèle d'assemblage d'ATP synthase présente que le centre catalytique, la tige centrale et l'anneau de sous-unités 9 de domaine F_O et sont formes indépendamment.

Après leur assemblage, le pied périphérique est attaché et les dernières sous-unités 8 et 6 du domaine F_O sont assemblées.

Les mutations causant les dysfonctionnements de l'ATP synthase ont été identifié dans :

- plusieurs maladies neurodégénératives (par exemple : la maladie de Parkinson ou la maladie d'Alzheimer),
- des maladies mitochondriales (par exemple : le syndrome NARP, LHON, MELAS),
- le diabète et les tumeurs.

Ma thèse concerne deux sujets :

1. La construction des modèles de levure *S. cerevisiae* de mutations du gène mitochondrial *ATP6* de l'ATP synthase découvertes chez des patients atteints de maladies neurologiques ou dans des tumeurs et analyser les effets biochimiques de ces mutations.
2. L'analyse de la régulation de la synthèse des sous-unités 6 et 9 dans les mitochondries de levure *S. cerevisiae*.

Ad.1

Dans notre laboratoire, la levure *S. cerevisiae* était utilisée avec succès pour analyser des effets de mutations du gène mitochondrial *ATP6* de l'ATP synthase découvertes chez des patients atteints du syndrome NARP.

Le gène *ATP6* code la sous-unite 6 (Atp6p) de l'ATP synthase. L'Atp6p avec l'anneau de sous-unités 9 forment le canal à protons dans la membrane interne de la mitochondrie. Dans la première partie de ce travail, j'ai construit des modèles de levure de deux nouvelles mutations du gène mitochondrial *ATP6* découvertes chez des patients atteints du syndrome NARP (9185T>C and 9191T>C) et cinq mutations dans ce gène identifiées dans des tumeurs (8716A>G, 8914C>A, 8932C>T, 8953A>G et 9131T>C).

L'effet majeur de la mutation 9185T>C était une diminution de la vitesse de synthèse d'ATP d'environ 30%. A cause du dysfonctionnement partiel du domaine F_O. La mutation 9191T>C menait à une diminution de la vitesse de synthèse d'ATP d'environ 95%.

Dans la souche avec cette mutation, la protéine synthétisée Atp6 était vite dégradée et le domaine F_1 libre était present : ce qui indiquent que la mutation empêche presque entièrement l'incorporation de la sous-unité 6 dans l'ATP synthase.

Les effets de ces mutations dans les modèles de levure correspondent aux phénotypes chez les patients où la mutation 9185T>C donnait la forme aténuée du syndrome NARP. Par contre le patient avec la mutation 9191T>C mourait quelques heures aprés la naissance. Encore une fois, des résultats montraient que la levure *S. cerevisiae* est un bon modèle pour analyser des effets moléculaire et biochimique des mutations du gène mitochondrial *ATP6*.

Les mutations du gène mitochondrial *ATP6* identifiées dans des tumeurs introduites dans le génome mitochondrial de la levure, n'ont pas influencé le fonctionnement de la chaîne

respiratoire et l'ATP synthase à 28ºC (température optimale pour la croissance de *S. cerevisiae)*.

A une température plus élevée (36ºC), une mutation (8932C>T) conduisait à une diminution de la vitesse de synthèse d'ATP d'environ 60%. Dans les souches modèles d'autres mutations, je n'observais pas de changements de fonctionnement de la chaîne respiratoire et l'ATP synthase.

Les resultats indiquent que les mutations analysées dans cette étude ont une influence mineur sur l'ATP synthase de la levure *S. cerevisiae*. Il n'est pas possible de constater clairement si des mutations du gène mitochondrial *ATP6* influencent le développement ou la malignité des tumeurs chez les humaines.

Des modèles de levure *S. cereivsiae* des maladies mitochondriales peuvent être utilisées pour chercher des nouvelles molécules actives contre ces maladies parmi celles déjà utilisées comme médicaments.

Une molécule active : la chlorhexidine, était analysée. Chez les humains, des mutations dans des gènes nucléaires *ATP12* et *TMEM70* causent des maladies mitochondriales qui sont modélisées chez la levure *S. cerevisiae* par la délétion du gène *FMC1*.

Dans cette souche, nous observions

- une diminution de la consommation d'oxygène par des complexes de la chaîne respiratoire,
- le potentiel faible de la membrane interne de la mitochondrie,
- une diminution de la vitesse de synthèse d'ATP,
- une présence des corps d'inclusion dans la mitochondrie,
- une absence casi-complète de *cristae*.

La présence de chlorhexidine dans le milieu améliore tous ces phénotypes observés.

Ad.2

Dans notre laboratoire, sur deux souches modèles de mutation du gène mitochondrial *ATP6* (*atp6-L183P* et *atp6-W136R, R179I*) nous observions que le niveau de synthèse d'Atp6p était élevé mais que le niveau de transcrit ne changeait pas. Par contre le niveau d'accumulation d'Atp6p dans la mitochondrie était diminué, de plus, l'anneau de sous-unités

9 s'accumulait dans les deux souches : ce qui indique une dysfonction d'assemblage d'ATP synthase.

Sachant que la sous-unité 6 est assemblée comme la dernière, il est possible qu'un complexe où il manque la sous-unité 6 soit présent dans la mitochondrie. Ce sous-complexe peut être un signal pour la synthèse d'Atp6p, donc la synthèse d'Atp6p est augmentée dans les deux souches analysées.

Pour prouver cette hypothèse, j'ai construit une collection de souches où j'avais deleté les gènes codants les sous-unités d'ATP synthase (*ATP1, ATP7, ATP15*) et les gènes codants les protéines nécessaires à l'expression des gènes mitochondriaux ou l'assemblage d'ATP synthase (*ATP10, ATP11, ATP12, FMC1, ATP23, AEP1, AEP2*).

J'ai analysé l'influence de ces deletions au niveau de la synthèse d'Atp6p par analyse du niveau de synthèse de protéines mitochondriales dans les souches de ma collection en comparaison avec la souche sauvage et la souche *atp6-L183P*.

Les résultats obtenus ont montré que dans les souches de ma collection il n'y avait pas d'effets d'augmentation de la synthèse d'Atp6p même si la mutation *atp6-L183P* était présente. Ces résultats ont confirmé l'hypothèse.

L'expression du gène mitochondrial *ATP9* est régulée par trois protéines : Aep1p, Aep2p et Atp25p.

Des données de la littérature montrent que l'Aep1p et l'Aep2p sont nécessaires pour la traduction de mRNA *ATP9* par son 5'UTR. L'Aep2p participe aussi en maturation de mRNA *ATP9*, sa stabilité et/ou l'initiation de traduction.

L'Atp25p est coupée dans la mitochondrie en deux morceaux :

- La partie C-terminal d'Atp25p est necessaire pour la stabilisation de mRNA *ATP9*.
- La partie N-terminal d'Atp25p est responsable d'oligomerisation d'anneau des sous-unitès 9.

L'analyse détaillée des fonctions de ces trois protéines dans la regulation d'expression du gène *ATP9* était, jusqu'à maintenant, très difficile à cause de l'instabilité du génome mitochondrial dans des souches ou les gènes *AEP1, AEP2* et *ATP25* étaient deletés.

Dans le laboratoire de Jean-Paul di Rago, un plasmide qui code le gène *ATP9-5* de *Podospora anserina* était construit. Ce plasmide a stabilisé le génome mitochondrial dans la souche de *S. cerevisiae* où le gène *ATP9* était remplacé par le gène *ARG8m*.

En conséquence, j'ai deleté les gènes nucleaires *AEP1, AEP2* et *ATP25* en présence de plasmide avec *ATP9-5* dans des souches avec du génome mitochondrial sauvage et avec le gène *ATP9* remplacé par *ARG8m*.

L'analyse de ces souches a montré que :

- les protéines Aep1, Aep2 et Atp25 sont nécessaires que pour l'expression de *locus ATP9*,
- la presence de la protéine Atp9-5 stimule la synthèse de *locus ATP9*,
- la synthèse d'Atp9p était augmentée dans la souche où le gène *ATP6* était deleté.

Ces resultas ont suggéré que la protéine Atp9 stimule sa propre synthèse. Des analyses supplémentaires ont montré que la protéine Atp9p est dégradée par la protéolyse, sa synthèse augmentée et sa stabilité sont dependente de la presence de le domaine F_1.

Les résultats de la deuxième partie de ma thèse ont permis une proposition de modèle où la synthèse de sous-unités 9 et 6 dépendent de leur assemblage dans le complexe d'ATP synthase.